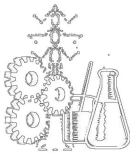




UNIVERSITÀ DEGLI STUDI DI CAGLIARI



DOTTORATO DI RICERCA
INGEGNERIA INDUSTRIALE
CICLO XXVI



TITOLO TESI

Robust Observation and Control of Complex Networks

Presentata da: Alessandro Pilloni

Coordinatore Dottorato: Prof. Roberto Baratti

Tutor/Relatore: Prof. Elio Usai

Settore/i scientifico disciplinari di afferenza
ING-INF/04 AUTOMATICA

Esame finale anno accademico 2012 - 2013

Questa Tesi può essere utilizzata, nei limiti stabiliti dalla normativa vigente sul Diritto d'Autore (Legge 22 Aprile 1941 n. 633 e successive modificazioni e articoli da 2575 a 2583 del Codice civile) ed esclusivamente per scopi didattici e di ricerca; vietato qualsiasi utilizzo per fini commerciali. In ogni caso tutti gli utilizzi devono riportare la corretta citazione delle fonti. La traduzione, l'adattamento totale e parziale, sono riservati per tutti i Paesi. I documenti depositati sono sottoposti alla legislazione italiana in vigore nel rispetto del Diritto di Autore, da qualunque luogo essi siano fruiti.

Alla mia famiglia

Abstract

The problem of understanding when individual actions of interacting agents display to a coordinated collective behavior has receiving a considerable attention in many research fields. Especially in control engineering, distributed applications in cooperative environments are achieving resounding success, due to the large number of relevant applications, such as formation control, attitude synchronization tasks and cooperative applications in large-scale systems.

Although those problems have been extensively studied in Literature, the most of classic approaches use to consider the unrealistic scenario in which networks always consist of identical, linear, time-invariant entities. It's clear that this assumption strongly approximates the effective behavior of a network. In fact agents can be subjected to parameter uncertainties, unmodeled dynamics or simply characterized by proper nonlinear dynamics.

Therefore, motivated by those practical problems, the present Thesis proposes various approaches for dealing with the problem of observation and control in both the framework of multi-agents and complex interconnected systems. The main contributions of this Thesis consist on the development of several algorithms based on concepts of discontinuous sliding-mode control. This techniques can be employed for solving in finite-time problems of robust state estimation and consensus-based synchronization in network of heterogenous nonlinear systems subjected to unknown but bounded disturbances and sudden topological changes. Both directed and undirected topologies have been taken into account. It is worth to mention also the extension of the consensus problem to networks of agents governed by a class parabolic partial differential equation, for which, for the first time, a boundary-based robust local interaction protocol has been presented.

Acknowledgement

Foremost, I would like to express my sincere gratitude to my advisor Prof. Elio Usai for the continuous support of my Ph.D study and research, for his patience, motivation, enthusiasm, and immense knowledge. His guidance helped me in all the time of research and writing of this thesis. I could not have imagined having a better advisor and mentor for my Ph.D study.

Particular thanks to Professor Alessandro Pisano who have guided me in my research activity, giving me confidence and transmitting his fondness for this discipline.

My sincere thanks also goes to Dr. Chistopher Edwards from University of Exeter for offering me an internship opportunities in their groups and supporting my activity.

I thank my fellow labmates in Automatic Control Group of Cagliari: Daniele Rosa, Stefano Scodina, Mehran Zareh, Siro Pillosu and Antonello Baccoli for the stimulating discussions, and for all the fun we have had in the last years. Also I thank my friends and cohautors: Rubèn Puche Panadero, Manuel Pineda-Sanchez and Alejandro Vignoni from the Universidad Politécnica de Valencia (Spain), Ijaz Kazmi from the Mohammad Ali Jinnah University (Pakistan) and Mehdi Rakhtal from the Golestan University (Iran).

Last but not the least, I would like to thank my parents for their support and my girlfriend for her encouragement, understanding, and patience even during hard times of this study.

Contents

List of Figures	x
Introduction	1
Motivations	1
Thesis' Overview	3
Author's Publications	5
I State of the Art	8
1 Digraph and Matrices	9
1.1 Notions of graphs	9
1.1.1 Directed Graph	9
1.1.2 Undirected Graph	10
1.1.3 Weighted graphs	11
1.2 Notions of connectedness	11
1.3 Graph Theory and Matrices	13
1.3.1 Adjacency Matrices and digraphs	14
1.4 The Laplacian Matrix	14
1.5 Conclusion	16
2 Mathematical modeling of Complex Systems	17

2.1	Graph Theory and Dynamical Systems	18
2.1.1	Modeling Dynamical Systems as digraphs	18
2.1.2	Input and Output Reachability	20
2.2	Scale-free dynamical networks	23
2.2.1	Complex network Preliminaries	23
2.2.2	The scale-free network model	24
2.2.3	Scale-free Dynamical Network Model	25
2.3	Consensus Problem and Cooperative Control	27
2.3.1	Cooperative Control Preliminaries	27
2.3.2	Multi-Agents Systems	28
2.3.3	Fundamental Consensus Algorithms	29
2.3.4	Nonlinear Consensus Algorithms	32
2.4	Conclusion	33
3	Strong observability of MIMO Systems	34
3.1	Introduction	34
3.2	Notion of Strong Observability for LTI MIMO Systems	35
3.2.1	State of Art of Strong Observability in MIMO LTI Systems	35
3.2.2	Strong Observability Conditions for Non-Square LTI MIMO Systems	37
3.2.3	Extension for a generic Non-Square MIMO Nonlinear Systems . . .	39
3.3	Conclusion	40
4	Sliding Mode Control	41
4.1	Introduction	41
4.2	Sliding modes in discontinuous control systems	42
4.3	First Order Sliding Mode	45

4.3.1	Filippov Continuation and Equivalent Control	46
4.4	Higher-order sliding mode control	48
4.4.1	Second-order sliding mode control	50
4.4.2	The Generalized Sub-Optimal controller	50
4.4.3	The Super-Twisting controller	51
4.4.4	Arbitrary order sliding mode controllers	51
4.5	Chattering Analysis in High-Order Sliding Mode	53
4.5.1	Describing-function analysis of the generalized sub-optimal algorithm	54
4.6	Conclusion	55
 II Author's Contributions		57
 5 Chattering adjustment and Tuning of the Super-Twisting Algorithm		58
5.1	Introduction	58
5.2	Motivations	59
5.3	Super-Twisting Algorithm and its DF Analysis	61
5.3.1	Existence of the Periodic Solution	62
5.4	Problem Formulation and Proposed Tuning Procedure	64
5.4.1	Problem Formulation	64
5.4.2	Proposed Tuning Procedure	66
5.5	Simulation Results	66
5.6	Experimental Results	67
5.7	Conclusions and Future Works	68
 6 Decentralized Estimation in Complex Network		70
6.1	Introduction	70

6.2	The Scale-Free Dynamical Network Model	71
6.3	Strong Observability and Unknown Input Reconstruction	72
6.4	Local Network Observer design	75
6.5	Numerical Example	78
6.5.1	Observer design	78
6.5.2	Observer design for agents networks	79
6.6	Conclusion	82
7	Sliding Mode Strong Observer as a tool for FDI: An application to Induction Motor	84
7.1	Motivations	84
7.2	Faulty SCIM Model	86
7.2.1	Air-Gap Eccentricity Fault	88
7.2.2	Broken Bars Fault	88
7.2.3	Faulty machine model	88
7.3	Second order sliding mode FDI observer for SCIMs	89
7.3.1	Residual Generation	89
7.3.2	Residual Evaluation	92
7.4	Experimental Results	93
7.5	Conclusions and Future Works	96
8	Robust Consensus Algorithms for First-integrator Dynamics	97
8.1	Introduction	97
8.2	Preliminaries and Problem Statement	99
8.3	Main result and Convergence Analysis	100
8.4	Numerical Simulations	105

8.5	Conclusion and Future Works	107
9	Robust Consensus Algorithms for Double-integrator Dynamics	110
9.1	Introduction	110
9.2	Preliminaries and Notation	111
9.3	Problem Statement	112
9.4	Convergence Analysis	113
9.5	Numerical Simulations	120
9.6	Conclusion and Future Works	120
10	Robust Consensus Algorithms in Infinite-Dimensional Networked Systems	123
10.1	Introduction	123
10.2	Mathematical Preliminaries and Notations	125
10.2.1	Useful Norm Properties	125
10.3	Problem Statements	126
10.4	Convergence Analysis	129
10.5	Simulation Results	136
10.6	Conclusion	138
11	Conclusion	140
	Bibliography	142

List of Figures

1.1	Digraphs.	9
1.2	An undirected digraphs and bidirectional digraph.	10
1.3	Digraphs with different connectedness properties.	13
2.1	Pendulum.	19
2.2	Directed graph associated to the pendulum system.	20
2.3	Input and output unreachable digraph.	22
4.1	Filippov's continuation method.	46
4.2	DF-analysis in the complex plane.	54
4.3	Level sets of (continuous lines) and MU/a_y (dotted lines) in the (β, α^*) plane.	55
5.1	Block diagram of a linear plant with the Super-Twisting Algorithm.	60
5.2	Architecture Comparison between linear (left) and nonlinear PI.	60
5.3	Decomposition of the arbitrary relative degree plant $W(s)$	61
5.4	Plots of the negative reciprocal DF (5.12) for different values of ω	63
5.5	Level sets of the right-hand of (5.20) for different values of a_y	65
5.6	Step response of the plant $W(s)$ in closed-loop with STW parameters $\lambda = 5.0119, \gamma = 18.3575$	67
5.7	Experimental set-up with FAULHABER [®] DC Micromotor Series 3557 024 CS.	68

5.8	Example of abacus utilization for the system $W(s)$ (5.27).	68
5.9	Experimental step response of the DC-Motor in closed-loop with $\lambda = 18.64$, $\gamma = 159.99$	69
5.10	Experimental step response of the DC-Motor in closed-loop with $\lambda = 20.05$, $\gamma = 223.99$	69
6.1	Estimation errors and UIR after proper filtering.	79
6.2	Time-Varying network topology.	81
6.3	State reconstruction process in Σ_1 (top) and Σ_4 (down).	82
6.4	Convergence to the references trajectory and UIR.	83
7.1	Experimental set-up (left) and a drilled rotor cage bar (right).	93
7.2	Residuals and chosen threshold (upper plot) and diagnosis signal (lower plot) for the broken bar tests.	94
7.3	Residuals and chosen threshold (upper plot) and diagnosis signal (lower plot) for the eccentricity tests.	95
7.4	Comparison between the normalized spectra of the faulty motor stator cur- rents (left plot) and that of the observer injection signal v_2 (right plot) for the broken bar test.	95
7.5	Comparison between the normalized spectra of the faulty motor stator cur- rents (left plot) and that of the observer injection signal v_2 (right plot) for the eccentricity test.	96
8.1	Changes in network topology and communication constraints.	101
8.2	Actual and majorant curves of $V(t)$	106
8.3	Time evolution of the clock variables for TEST1-3 (right).	107
8.4	Transient evolution (left) and steady state accuracy (right) of the Lyapunov function $V(t)$	108
8.5	Transient evolution of the agent states in TEST2 and TEST4.	108

8.6	Transient evolution (left) and steady state accuracy (right) of the Lyapunov function $V(t)$ in TEST 5.	109
9.1	Communication topologies respectively for the second-order consensus task (left) and the distributed-tracking task (right).	120
9.2	Trajectories of the disagreement vectors $\delta_1(t)$ and $\delta_2(t)$	121
9.3	Transient evolution of the Lyapunov Function $V_R(t)$	121
9.4	Transient evolution of the state-space vectors $X_1(t)$ and $X_2(t)$ for the distributed tracking task.	122
10.1	Graph representation $\mathcal{G} = (\mathcal{V}, \mathcal{E})$ of the network under test.	136
10.2	Spatial distribution of temperature of the 5-st Rod $Q^5(\zeta, t)$	137
10.3	Spatial distribution of temperature of the 10-th Rod $Q^{10}(\zeta, t)$	137
10.4	Spatial distribution of temperature disagreement vector $\delta_1(\zeta, t)$ computed for all the 30 discretization's nodes.	138
10.5	Temperature disagreement vector $\delta_1(\zeta, t)$ behavior computed at boundaries $\zeta = 1$, $\zeta = 0$ and in the middle node of the spatial discretization $\zeta = 0.4828$	138

Introduction

This introductory Chapter is intended to present the motivations behind the development of this Thesis along with a brief description of the Thesis' structure. Finally, a list of the Author's publications derived from the present work are listed.

Motivations

The problem of understanding when individual actions of interacting agents display to a coordinated collective behavior has receiving a considerably attention in many research fields, starting from system biology [[Rosenfeld, 2013](#)] up to engineering science like computer graphics [[Yang et al., 2003](#)] or sensors network [[Schenato & Fiorentin, 2009](#)]. Especially in control engineering, distributed applications in cooperative environments are achieving resounding success, due to the large number of relevant applications, such as formation control [[Fax & Murray, 2004](#), [Ren, 2007](#)], attitude synchronization tasks [[Fadakar et al., 2013](#)] and cooperative applications in large-scale systems [[Pilloni et al., 2013a](#)].

There are many reasons for the current intensity of interest in coordination applications, but certainly the winning one comes from the flexibility, scalability and reconfigurability to sudden environmental changes [[Raudys & Mitasiunas, 2007](#)]. Infact this paradigm uses to model each entity of the network as a smart, active autonomous system, capable of interacting with other agents in order to satisfy its design objectives.

One of the key components of this research area is to gain a better understanding of how the underlying connection topology directly affects certain properties of the entire system [[Chang et al., 2003](#)].

An overview of the recent research trends in cooperative control and multi-agent systems (MAS) can be found in [[Zampieri, 2008](#), [Garin & Schenato, 2011](#)]. The reader is referred to [[Ren et al., 2007a](#), [Olfati-Saber et al., 2007](#)] for a tutorial overview of information in cooperative consensus-based control.

Although those problems have been extensively studied in Literature, the most of classic approaches use to consider the unrealistic scenario in which networks always consist of identical, linear, time-invariant entities [Olfati-Saber et al., 2007, Šiljak, 1991, Ren & Beard, 2008, Ni et al., 2013].

It's clear that this assumption strongly approximates the effective behavior of a network [Wang & Wen, 2008]. In fact agents can be subjected to parameter uncertainties, unmodeled dynamics or simply characterized by proper nonlinear dynamics [Pilloni et al., 2013a, Edwards & Menon, 2008].

Therefore, motivated by those practical problems, the present Thesis proposes various approaches for dealing with the problem of observation and control in both the framework of multi-agents systems (MAS) and complex interconnected systems. The main contributions of this Thesis consist on the development of several algorithms based on concepts of discontinuous sliding-mode-based control [Utkin & Guldner, 1999, Orlov, 2008, Bartolini et al., 2003, Pisano & Usai, 2011]. These approaches can be employed for solving in finite-time problems of robust state estimation [Pilloni et al., 2013a, Edwards & Menon, 2008] and consensus-based synchronization [Franceschelli et al., 2013b, Franceschelli et al., 2013a, Franceschelli et al., 2012a] in network of heterogenous nonlinear systems subjected to unknown but bounded disturbances and sudden topological changes. Both directed and undirected topologies have been taken into account.

In particular with regards to the problem of robust state estimation in connected systems, it is worth to mention the work [Pilloni et al., 2013a] in which a new approach for designing strong observers which result totally independent to the network configuration or to the number of nodes is presented; whereas with regards to the problem of consensus-based network synchronization, in [Franceschelli et al., 2013b] and [Pilloni et al., 2013b] respectively, two novel local interaction protocols for network consisting of first and second order perturbed dynamics are discussed.

It is worth to mention also the extension of the consensus problem to networks of agents governed by a class parabolic partial differential equation, for which, for the first time, a boundary-based robust local interaction protocol has been presented [Pilloni et al., 2014b].

Thesis' Overview

The Thesis is organized into two distinct parts. The first one, namely *State of the Art* which provide a brief summary of the necessary theoretical notions useful for understanding the remainder the Thesis, and the second one, namely *Author's contribution* in which all the Author's works, developed during this research, are deeply discussed. A brief overview of each Chapter of the Thesis is reported below.

Part I. State of the Art:

- **Chapter 1. Digraph and Matrices:** This Chapter provides some notions on graph theory along with some mandatory results about connectivity properties of directed graphs. Furthermore the relations between graphs and non-negative matrices are taken into account;
- **Chapter 2. Mathematical modeling of Complex Systems:** This Chapter provided some preliminary notion of the mathematical modelization of connected systems. Particular emphasis has been given to the modelization of distributed systems and Large-scale Dynamical Networks. Finally concepts of decision-making in the framework of multi-agents systems has been discussed;
- **Chapter 3. Strong observability of MIMO Systems:** Since, every complex system can be represented as an interconnection of subsystems or equivalently with a multi-input-multi-output (MIMO) representation, in this Chapter some theoretical definition on strong observability are provided;
- **Chapter 4. Sliding Mode Control:** Due to the extensively use of Sliding Mode concepts in all the Author's contributions presented in this Thesis, this Chapter provides a brief survey on Sliding Mode Control (SMC) Theory with particular emphasis to the so-called High Order Sliding Modes algorithms.

Part II. State of the Art:

- **Chapter 5. Chattering adjustment and Tuning of the Super-Twisting Algorithm:** Based on the works [Pilloni et al., 2012a, Pilloni et al., 2012b], the present Chapter illustrates a systematic procedure for tuning the parameters of the Super-Twisting HOSM Algorithm when unmodeled parasitic

dynamics appears in the plant model. For example when actuators dynamics are neglected. Although the topic of this Chapter is not strictly related to the framework of distributed systems, it is reasonable thinking that when discontinuous control action are applied for controlling real network of systems, due to the unavoidable presence of parasitic dynamics, complex phenomenon such as chattering can appear. This Chapter is based on the Author's work [Pilloni et al., 2012a, Pilloni et al., 2012b];

- **Chapter 6. Decentralized Estimation in Complex Network:** Based on the work [Pilloni et al., 2013a], this Chapter provides a new approach for designing local robust observers for a network of perturbed, diffusively coupled heterogeneous MIMO systems. Worth of noting that the proposed approach result inherently robust and totally independent to the network configuration or to the number of nodes;
- **Chapter 7. Sliding Mode Strong Observer as a tool for FDI: An application to Induction Motor:** Strictly related to the task of designing strong observers in MIMO systems, in this Chapter High-Order Sliding Mode observers are employed as a tool for detecting certain abnormal operating conditions in squirrel cage induction motors (SCIMs). The Chapter is based on the works [Pilloni et al., 2013c, Pilloni et al., 2012c, Pilloni et al., 2012d]. Through the Chapter the effectiveness of proposed scheme has been theoretically demonstrated and verified by real tests carried out using measurements taken from intentionally damaged commercial three-phase motors;
- **Chapter 8. Robust Consensus Algorithms for First-integrator Dynamics:** Based on the work [Franceschelli et al., 2013b], in this Chapter is proposed a novel decentralized consensus algorithm for a network of continuous-time integrators subject to persistent disturbances and communication changes. Notice that, although the network during its evolution is not always connected, it is proved that under certain restrictions on the directed switching policy, after a finite transient time, the agents achieve an approximated consensus condition by attenuating the destabilizing effect of the disturbances. A Lyapunov-based analysis confirm the effectiveness of the suggested algorithm;
- **Chapter 9. Robust Consensus Algorithms for Double-integrator Dynamics:** Based on the work [Pilloni et al., 2013b], in this Chapter a novel

robust local interaction rule for achieving finite-time consensus in a network of double integrators agents affected by bounded disturbances is presented. Agents' are supposed to interact through an undirected, static and connected, communication topology. A Lyapunov-Based analysis confirm the effectiveness of the proposed and provides a very simple tuning rules for achieving the complete disturbance rejection. The proposed algorithm is then presented as a valiant solution for solving problem of distributed leader-tracking in multi-robot networks [Pilloni et al., 2014a, Pilloni et al., 2014c];

- **Chapter 10. Robust Consensus Algorithms in Infinite-Dimensional Networked Systems:** Based on the work [Pilloni et al., 2013b], in this Chapter is considered the problem of driving a group of perturbed infinite-dimensional agents communicating through an undirected topology towards a common temperature's consensus value. Performances of the proposed local interaction rule in terms of robustness and rate of convergence are investigate by Lyapunov-Based approach from which simple tuning rules for achieving the consensus condition are developed;
- **Chapter 11.** In this Chapter, a summary of the main part of the text along with deductions and personal opinions about the developed work are provided. Furthermore, some comments and recommendations about the potential future research directions of those topics are discussed.

Acknowledgement

Alessandro Pilloni gratefully acknowledges Sardinia Regional Government for the financial support of his PhD scholarship (P.O.R. Sardegna F.S.E. Operational Programme of the Autonomous Region of Sardinia, European Social Fund 2007-2013 - Axis IV Human Resources, Objective 1.3, Line of Activity 1.3.1.).

Author's Publications

- [Pilloni et al., 2014a] Pilloni, A., Pisano, A., Franceschelli, M., and Usai, E. (2014). *Distributed tracking for a network of perturbed double integrators by second-order sliding mode technique*. Under revision for submission on: Automatic Control, IEEE Transactions on.

- **[Pilloni et al., 2014b]** Pilloni, A., Pisano, A., Orlov, Y., and Usai, E. (2014). *On boundary consensus protocol for a network of perturbed parabolic infinite dimensional processes*. (2014) Under revision for submission on: Automatic Control, IEEE Transactions on.
- **[Pilloni et al., 2014c]** Pilloni, A., Pisano, A., Franceschelli, M., and Usai, E. (2014). *Recent advances in sliding-mode based consensus strategies*. Under revision for proceeding on: Variable Structure Systems (VSS), 13th International Workshop on.: IEEE.
- **[Franceschelli et al., 2013b]** Franceschelli, M., Pilloni, A., Pisano, A., Giua, A., and Usai, E. *Finite-time consensus with disturbance attenuation for directed switching network topologies by discontinuous local interactions*. In Decision and Control (CDC), 2013 IEEE 52nd Annual Conference on: IEEE.
- **[Pilloni et al., 2013a]** Pilloni, A., Pisano, A., Usai, E., Edwards, C., and Menon, P. *Decentralized state estimation in connected systems*. In Proc. 5th IFAC Symposium on Systems, Structure and Control SSC 2013, Grenoble, France.
- **[Pilloni et al., 2013b]** Pilloni, A., Pisano, A., Franceschelli, M., and Usai, E. *Finite-time consensus for a network of perturbed double integrators by second-order sliding mode technique*. 2013 In IEEE Conference on Decision and Control.
- **[Pilloni et al., 2013c]** Pilloni, A., Pisano, A., Riera-Guasp, M., Puche-Panadero, R., and Pineda-Sanchez, M. *Chapter 14. Fault detection in induction motors*. 2013, AC Electric Motors Control: Advanced Design Techniques and Applications, (pp. 275-309).
- **[Pilloni et al., 2012a]** Pilloni, A., Pisano, A., and Usai, E. *Oscillation shaping in uncertain linear plants with nonlinear pi control: Analysis and experimental results*. 2012, In Advances in PID Control, volume 2 (pp. 116-121).
- **[Pilloni et al., 2012b]** Pilloni, A., Pisano, A., and Usai, E. *Parameter tuning and chattering adjustment of Super-Twisting sliding mode control system for linear plants*. In Variable Structure Systems (VSS), 2012 12th International Workshop on (pp. 479-484): IEEE.
- **[Pilloni et al., 2012c]** Pilloni, A., Pisano, A., and Usai, E. *Robust fdi in induction motors via second order sliding mode technique*. In Variable Structure Systems (VSS), 2012 12th International Workshop on (pp. 467-472): IEEE.

- **[Pilloni et al., 2012d]** Pilloni, A., Pisano, A., Usai, E., and Puche-Panadero, R. *Detection of rotor broken bar and eccentricity faults in induction motors via second order sliding mode observer*. In Decision and Control (CDC), 2012 IEEE 51st Annual Conference on (pp. 7614-7619).: IEEE.

Part I

State of the Art

Chapter 1

Digraph and Matrices

In this Chapter basic definitions about graph theory along with some mandatory results about connectivity properties of directed graphs, following the treatments in the literature, see for example [Godsil et al., 2001, Lin, 2006, Diestel, 1997, Biggs, 1993], will be discussed. Furthermore the relations between graphs and non-negative matrices will be taken into account. For rigor in presentation, the applicability of those concepts in the real world will be postponed in the reminder of the thesis.

1.1 Notions of graphs

1.1.1 Directed Graph

A directed graph (or just *digraph*) of order n is a pair $\mathcal{G}(\mathcal{V}, \mathcal{E})$, where \mathcal{V} is a set of n elements called *vertices* (or nodes) and $\mathcal{E} \subseteq \mathcal{V} \times \mathcal{V}$ is a set of ordered pairs of nodes called *edges* (or arcs). In Figure 1.1 few examples of directed graph are shown. It is common to refer to \mathcal{V} and \mathcal{E} as the *vertex-set* and *edge-set*, respectively. For $v_i, v_j \in \mathcal{V}$, the ordered pair (v_i, v_j) denotes an edge from v_i to v_j , where v_i is called *tail* and v_j *head* of the considered edge.

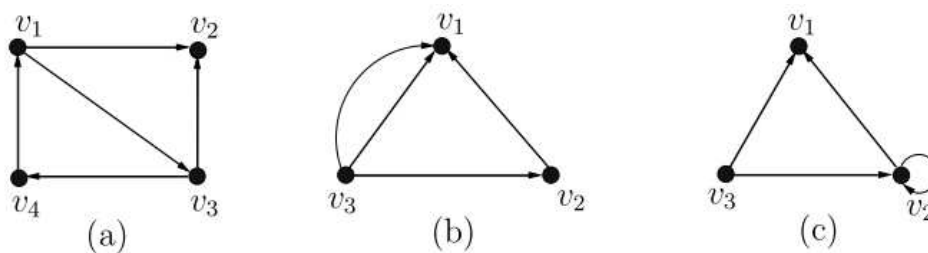


Figure 1.1: Digraphs.



Figure 1.2: An undirected digraphs and bidirectional digraph.

As a definition, a *loop* is an edge whose vertices are the same node and an edge is said to be *multiple* if there is another edge with the same vertices.

A digraph is said to be *simple* if it has not multiple edges or loops. As a consequence the digraph in Figure 1.1.(a) is simple; the digraph in Figure 1.1.(b) has multiple arcs, namely, (v_3, v_1) ; and the digraph in Figure 1.1.(c) has a loop, namely, (v_2, v_2) . In the following, *simple digraph* $\mathcal{G} = (\mathcal{V}, \mathcal{E})$ will be considered.

It should be clear that the local structure of a digraph is described by the neighborhoods and the degrees of its nodes.

Starting from this point, for a digraph $\mathcal{G}(\mathcal{V}, \mathcal{E})$, it can be defined the following notation:

$$\mathcal{N}_i^+ = \{v_j \in \mathcal{V} / \{v_i\} : (v_i, v_j) \in \mathcal{E}\} \subseteq \mathcal{V} \quad , \quad \mathcal{N}_i^- = \{j \in \mathcal{V} / \{i\} : (v_j, v_i) \in \mathcal{E}\} \subseteq \mathcal{V} \quad (1.1)$$

where the sets \mathcal{N}_i^+ and \mathcal{N}_i^- are known respectively as the *out-neighborhood* and *in-neighborhood* of the node v_i . As a consequence, the vertices belonging to \mathcal{N}_i^+ or \mathcal{N}_i^- respectively, can be called the out-neighbors and in-neighbors of v_i .

It can be also defined the *out-degree* d_i^+ and the *in-degree* d_i^- of a node v_i the cardinality of the corresponding neighbor-set. For example, it is trivial to note that the node v_1 in Figure 1.1.(a) has respectively:

$$\mathcal{N}_1^+ = \{v_2, v_3\} \quad , \quad \mathcal{N}_1^- = \{v_4\} \quad , \quad d_1^+ = 2 \quad , \quad d_1^- = 1 \quad (1.2)$$

1.1.2 Undirected Graph

An undirected graph (or symmetric digraphs) $\mathcal{G} = (\mathcal{V}, \mathcal{E})$ can be considered as a special class of digraph where the edge set $\mathcal{E} \subseteq \mathcal{V} \times \mathcal{V}$ consists of unordered pairs of nodes. This means that if $(v_i, v_j) \in \mathcal{E}$, then also its complementary (v_j, v_i) belongs to \mathcal{E} .

Hence problems that can be formulated for both directed and undirected graphs are often easier for the latter. Notice that an undirected graph can be easily treated as a bidirectional digraph by replacing each edge $(v_i, v_j) \in \mathcal{E}$ with the pair of edges (v_i, v_j) and (v_j, v_i) . A simple example is shown in Figure 1.2.

1.1.3 Weighted graphs

A *weighted graph* $\mathcal{G} = (\mathcal{V}, \mathcal{E})$ is a digraph with a label (*weight*) associates to every edge. Weights are usually positive real numbers, but in some application the can be complex. It is worth to mentioning that, weights do not change the topological structure of graphs, but affect just the algebraic properties of graphs.

1.2 Notions of connectedness

Let us now review some basic connectivity notions for directed graphs. The reader is referred to the related literature for a more comprehensive account of the following notion [[Godsil et al., 2001](#), [Lin, 2006](#), [Diestel, 1997](#), [Bullo et al., 2009](#)]:

- A *walk* in a digraph $\mathcal{G}(\mathcal{V}, \mathcal{E})$ is an alternating sequence

$$\mathcal{W} : v_1 e_1 v_2 e_2 \cdots e_{k-1} v_k$$

of nodes v_i such that each edges $e_i = (v_i, v_{i+1})$ belongs to \mathcal{E} for every $i = 1, 2, \dots, k-1$;

- The *length of a walk* is the number of its arcs. Hence the walk \mathcal{W} above has length $k-1$;
- A *semiwalk* in a digraph $\mathcal{G}(\mathcal{V}, \mathcal{E})$ is an alternating sequence

$$\bar{\mathcal{W}} : v_1 e_1 v_2 e_2 \cdots e_{k-1} v_k$$

of nodes v_i such that each edges $e_i = (v_i, v_{i+1})$ or $e_i = (v_i + 1, v_i)$ belongs to \mathcal{E} for every $i = 1, 2, \dots, k-1$;

- A *path* in a digraph $\mathcal{G}(\mathcal{V}, \mathcal{E})$ is a particular class of *walk* such that all the nodes in \mathcal{W} are distinct;
- A *cycle* in a digraph $\mathcal{G}(\mathcal{V}, \mathcal{E})$ is a particular class of *walk* such that all the nodes $v_1, \dots, v_{k-1} \in \mathcal{W}$ are distinct and $v_1 = v_k$. A digraph without cycles is said to be *acyclic*;
- A *successor* of a vertex $v_i \in \mathcal{V}$ is any other node $v_j \in \mathcal{V}/\{v_i\}$ that can be reached with a directed path starting at v_i ;
- A *predecessor* of a vertex $v_i \in \mathcal{V}$ is any other node $v_j \in \mathcal{V}/\{v_i\}$ such that a directed path exists starting at it and reaching v_j ;

- A directed tree (or *rooted tree*) is an acyclic digraph where there exists a vertex $v_i \in \mathcal{V}$, called *root*, such that any other vertex in $\mathcal{G}(\mathcal{V}, \mathcal{E})$ can be reached by one and only one directed path starting at the root;
- A directed spanning tree (or *spanning tree*), is a spanning tree in which no two arcs share their tails. Each vertex is the tail of exactly one arc of the directed spanning tree except for a special vertex v_r called *root of the spanning tree*.

It is worth to mention that, if a digraph $\mathcal{G}(\mathcal{V}, \mathcal{E})$ is not acyclic, the *period* d of $\mathcal{G}(\mathcal{V}, \mathcal{E})$ can be evaluated as the greatest common divisor of all the lengths of cycles in $\mathcal{G}(\mathcal{V}, \mathcal{E})$. The digraph is said to be *d-periodic* if $d > 1$ and *aperiodic* if $d = 1$.

As a consequence, for each node $v_i \in \mathcal{G}$, it can be defined its period as follows

$$d_i = \text{g.c.d.}_{m_i^k \in \mathcal{S}_i} \{m_i^k\} \quad (1.3)$$

where \mathcal{S}_i is the set of all the lengths of cycles in $\mathcal{G}(\mathcal{V}, \mathcal{E})$, m_i^k , of walks from v_i to itself.

After having introduced the previous instrumental concepts, the following notions of connectedness for a digraph can be defined.

Definition 1.1. Reachability: A node $v_i \in \mathcal{V}$ is said to be reachable from another node $v_j \in \mathcal{V}$

$$v_i \rightarrow v_j \quad (1.4)$$

if and only if exist a walk \mathcal{W} from v_j to v_i ; if not v_i is said to be not reachable from v_j ($v_i \nrightarrow v_j$). A node v_i is always reachable from itself by a trivial walk of length $k = 0$. ■

Definition 1.2. Global Reachability: A node $v_i \in \mathcal{V}$ is said to be globally reachable if and only if it is reachable from every node of the digraph $\mathcal{G}(\mathcal{V}, \mathcal{E})$. ■

Definition 1.3. Center Node: A node $v_i \in \mathcal{V}$ is called a center node of the digraph $\mathcal{G}(\mathcal{V}, \mathcal{E})$ if from it every node $v_j \in \mathcal{V}$ is reachable. ■

Definition 1.4. Fully Connectedness: A digraph $\mathcal{G}(\mathcal{V}, \mathcal{E})$ is said to be fully connected if for every pair of nodes v_i and $v_j \in \mathcal{V}$ exist a bidirectional edge which from v_i to v_j and v_j to v_i . ■

Definition 1.5. Unilaterally Connectedness: A digraph $\mathcal{G}(\mathcal{V}, \mathcal{E})$ is said to be unilaterally connected if for every two nodes v_i and $v_j \in \mathcal{V}$ at least one of them is reachable from the other. ■

Definition 1.6. Quasi-Strongly Connectedness: A digraph $\mathcal{G}(\mathcal{V}, \mathcal{E})$ is said to be quasi-strongly connected if for every two nodes v_i and $v_j \in \mathcal{V}$ there is a node $v_k \in \mathcal{V}$ from which v_i and v_j are reachable. ■

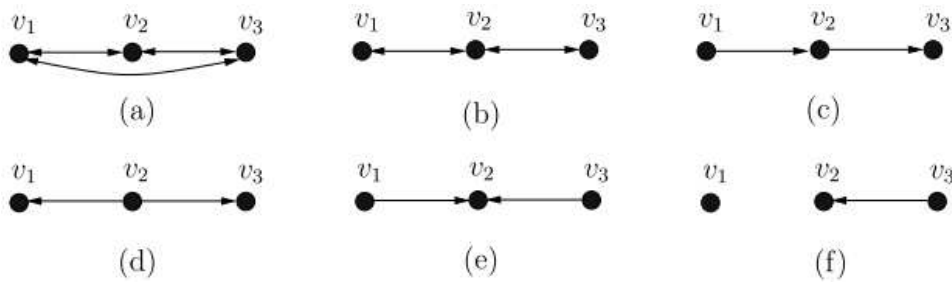


Figure 1.3: Digraphs with different connectedness properties.

Definition 1.7. Weakly connectedness: A digraph $\mathcal{G}(\mathcal{V}, \mathcal{E})$ is said to be weakly connected if every pair of nodes v_i and $v_j \in \mathcal{V}$ are connected by a semiwalk (disregarding the orientation of each arc). ■

Definition 1.8. Disconnectedness: A digraph $\mathcal{G}(\mathcal{V}, \mathcal{E})$ is said to be disconnected if it is not even weakly connected. ■

In Figure 1.3 some digraphs with different connectedness properties are shown. In particular, it results respectively in (a) a fully connected digraph, (b) a strongly connected digraph, (c) an unilaterally connected digraph, (d) a quasi-strongly connected digraph, (e) a weakly connected digraph, (f) a disconnected digraph.

By the previous definitions, it should be clear that those kinds of connectedness properties tends to overlap. Indeed, for example, every fully connected digraph is strongly connected; every strongly connected digraph is also unilaterally connected; every unilaterally connected digraph is quasi-strongly connected and concluding every quasi-strongly connected digraph is weakly connected, but the converses of these statements are not true in general.

Furthermore, it is worth to pointing out that for an undirected graph, the first four kinds of connectedness properties, respectively, *strongly connected*, *unilaterally connected*, *quasi-strongly connected*, and *weakly connected*, are equivalent. In the contest of undirected graphs it is common referring to these properties as *connected*.

1.3 Graph Theory and Matrices

In this section the relations between digraphs and matrices are discussed. In particular it will be shown how all the topological information associated to a graph and discussed in the sections above can be easily encoded in term of Adjacency Matrix, Degree Matrix and Laplacian Matrix.

1.3.1 Adjacency Matrices and digraphs

The Adjacency Matrix associated to a digraph $\mathcal{G}(\mathcal{V}, \mathcal{E})$ is an $n \times n$ binary matrix denoted as $\mathcal{A} = [a_{ij}]$ where each entry is defined as follows:

$$a_{ij} : \begin{cases} 1 & \text{if } (v_i, v_j) \in \mathcal{E} \\ 0 & \text{otherwise} \end{cases} \quad (1.5)$$

It should be clear that this matrix is able to give information about the topological structure of the associated digraph $\mathcal{G}(\mathcal{V}, \mathcal{E})$. For the undirected case, \mathcal{A} is always symmetric. Since by definition (1.5) all the entries of \mathcal{A} are nonnegative, it belongs to the class of *non-negative matrices*. Among the multiple information encoded in \mathcal{A} , hereinafter some of them are listed:

- the sum of the entries in the row i of \mathcal{A} is equal to the *in-degree* d_i^- of v_i ;
- the sum of the entries in column j of \mathcal{A} is equal to the *out-degree* d_j^+ of v_j .

Theorem 1.1. See *Gershgorin Theorem [Bhatia, 1997]*. Every eigenvalue of \mathcal{A} lies in a Gershgorin disc. ■

Theorem 1.2. See *[Berman & Plemmons, 1979]*. An $n \times n$ nonnegative matrix \mathcal{A} is said to be irreducible if and only if $\mathcal{G}(\mathcal{V}, \mathcal{E})$ is strongly connected. ■

Definition 1.9. A matrix \mathcal{A} is irreducible if it does not exist a permutation matrix P such that

$$P^T \mathcal{A} P = \begin{bmatrix} B_{11} & B_{12} \\ \mathbf{0} & B_{22} \end{bmatrix} \quad (1.6)$$

with B_{11} and B_{22} square nonsingular matrices. ■

1.4 The Laplacian Matrix

In this section the well-known Laplacian Matrix is presented. The Laplacian belongs a special class of Metzler matrices where their row-sums are equal to zero.

Definition 1.10. *[Lin, 2006]* A square real matrix \mathcal{A} whose off-diagonal entries are nonnegative is called a Metzler matrix. ■

Given a digraph $\mathcal{G}(\mathcal{V}, \mathcal{E})$, let \mathcal{D} be the so-called *degree matrix* of \mathcal{G} , i.e., a diagonal matrix with the in-degree of each node along its diagonal. The Laplacian of the digraph $\mathcal{G}(\mathcal{V}, \mathcal{G})$ is a square matrix defined as follows:

$$\mathcal{L} = [\mathcal{L}_{ij}] = \mathcal{D} - \mathcal{A} \quad (1.7)$$

with

$$\mathcal{L}_{ij} := \begin{cases} d_i^- & \text{if } i = j \\ -1 & \text{if } (v_i, v_j) \in \mathcal{E} \\ 0 & \text{otherwise} \end{cases} \quad (1.8)$$

It is worth to mention that according to Gershgorin theorem [Olfati-Saber et al., 2007], all eigenvalues of \mathcal{L} are located in a circle centered in the complex plane at $d_m + j0$ with a radius $d_m = \max_{v_i \in \mathcal{V}} d_i^-$, i.e., the maximum degree of a graph. Furthermore for undirected graphs, \mathcal{L} is symmetric and positive semi-definite [Garin & Schenato, 2011, Olfati-Saber et al., 2007] with real eigenvalues ordered sequentially as follows:

$$0 = \lambda_1 \leq \dots \leq \lambda_n \leq 2 \cdot d_m \quad (1.9)$$

Theorem 1.3. See [Lin, 2006]. *The zero eigenvalue of \mathcal{L} has algebraic multiplicity one if and only if the corresponding digraph \mathcal{G} has a directed spanning-tree.* ■

Some important features of \mathcal{L} appears in the undirected framework. For example, if \mathcal{G} is connected, all row and column sums of \mathcal{L} are zero

$$\mathcal{L} \cdot \mathbf{1}_N = \mathbf{0}_N \quad , \quad \mathbf{1}_N^T \cdot \mathcal{L} = \mathbf{0}_N^T \quad (1.10)$$

and thus the column vector $\mathbf{1}_N = \text{col}(1, \dots, 1) \in \mathbb{R}^N$ and its transpose $\mathbf{1}_N^T$ are respectively the left and right eigenvectors associated with the zero eigenvalue $\lambda_1 = 0$.

In addition if $\lambda_2 \neq 0$, the next useful property holds [Horn & Johnson, 1990]

$$\|\mathcal{L}\delta\|_1 \geq \|\mathcal{L}\delta\|_2 = \sqrt{\delta^T \mathcal{L}^2 \delta} \geq \lambda_2 \cdot \|\delta\|_2 \quad (1.11)$$

where λ_2 is the smallest nonzero eigenvalue of \mathcal{L} , known as *algebraic connectivity* [Pereira, 2011], and $\delta \in \mathbb{R}^N$ is any vector with zero column sum $\mathbf{1}_N^T \cdot \delta = 0$. It is worth mentioning that the magnitude of λ_2 reflects information about how well connected the overall graph is, and has been used in analyzing the robustness and synchronizability of networks [Olfati-Saber & Murray, 2004].

Remark 1.1. *The algebraic connectivity of a graph \mathcal{G} with n vertices is greater than 0 if and only if \mathcal{G} is connected. Furthermore the algebraic connectivity of a connected network always satisfies the next constraint [Fax & Murray, 2004]:*

$$0 < \lambda_2 \leq n \quad (1.12)$$

In particular $\lambda_2 = n$ is the graph is fully connected. ■

1.5 Conclusion

In this Chapter a brief overview on Graphs Theory with particular emphasis to directed and undirected graph and their connectedness properties has been presented. Concepts these, that will be extensively used in the rest of the thesis. Furthermore it has been shown how all the topological information associated to a graph could be easily encoded in term of Adjacency Matrix, Degree Matrix or by the Laplacian Matrix.

Chapter 2

Mathematical modeling of Complex Systems

In this Chapter a survey of the existing literature related to the mathematical modeling of connected systems from the point of view of dynamical systems, which means differential equations, is presented.

In particular, it will be shown how different classes of dynamical problems could be easily represented and well described by combining the notions of Graph Theory discussed in Chapter 1 along with the well-known concept of System Theory [Khalil, 2002].

In particular, throughout the Chapter, three main sections are included. The first one presents how complex systems, not necessarily distributed in space, can be represented as an interconnection of subsystems, in order to reduce the complexity of the system. In particular, each subsystem may be identified as a physical entity, or also as a purely mathematical partition of the whole system dynamics, independently from the others and then the complexity of the overall problem is simplified by using a decentralized approach.

Section 2, is inspired to the fact that many real-world complex networks are neither completely regular nor completely random; examples are Internet [Siganos et al., 2003], metabolic networks [Jeong et al., 2000] or social networks [Wasserman, 1994, Barabási et al., 2002]. Therefore, in this section some notion of Large-Scale Systems and possible models that can capture how this complex networks can evolve in time is presented.

Last but not least, in the third section, due to the strictly connections between networked system and multi-agent systems, some concepts about decision-making for network of dynamical systems are introduced with particular emphases to the so-called *consensus problems*.

2.1 Graph Theory and Dynamical Systems

2.1.1 Modeling Dynamical Systems as digraphs

Let us consider a linear dynamic system described by the equations

$$\Sigma: \begin{cases} \dot{\mathbf{x}}(t) = \mathbf{A}\mathbf{x}(t) + \mathbf{B}\mathbf{u}(t) \\ \mathbf{y}(t) = \mathbf{C}\mathbf{x}(t) \end{cases} \quad (2.1)$$

where $\mathbf{x}(t) \in \mathbb{R}^n$ is the state, $\mathbf{u}(t) \in \mathbb{R}^m$ is the input, and $\mathbf{y}(t) \in \mathbb{R}^p$ is the output vector of Σ at time $t \in \mathbb{R}$ and $\mathbf{A} = [a_{ij}]$, $\mathbf{B} = [b_{ij}]$, and $\mathbf{C} = [c_{ij}]$ are constant matrices of proper dimension.

As shown in [Šiljak, 1991], the structure of Σ can be represented by means of the concepts of Graph Theory. In particular, recalling the concepts provided in Section 1.3.1, it can be defined the so-called *adjacency matrix* associated to a dynamical systems as follows:

Definition 2.1. *The adjacency matrix $\mathcal{A} = [a_{ij}]$ associated to the dynamical system Σ in (2.1) is a square binary matrix defined as follows:*

$$\mathcal{A} = \begin{bmatrix} \bar{\mathbf{A}} & \bar{\mathbf{B}} & \bar{\mathbf{0}} \\ \bar{\mathbf{0}} & \bar{\mathbf{0}} & \bar{\mathbf{0}} \\ \bar{\mathbf{C}} & \bar{\mathbf{0}} & \bar{\mathbf{0}} \end{bmatrix} \in \mathbb{R}^{(n+m+p) \times (n+m+p)} \quad (2.2)$$

where $\bar{\mathbf{0}}$ are matrices of zero-entries and the sub-matrices $\bar{\mathbf{A}} = [\bar{a}_{ij}]$, $\bar{\mathbf{B}} = [\bar{b}_{ij}]$, $\bar{\mathbf{C}} = [\bar{c}_{ij}]$ of \mathcal{A} are Boolean representations of the original system matrices \mathbf{A} , \mathbf{B} , \mathbf{C} with entries defined as follows:

$$\bar{a}_{ij} : \begin{cases} 1 & , & a_{ij} \neq 0 \\ 0 & , & a_{ij} = 0 \end{cases} \quad , \quad \bar{b}_{ij} : \begin{cases} 1 & , & b_{ij} \neq 0 \\ 0 & , & b_{ij} = 0 \end{cases} \quad , \quad \bar{c}_{ij} : \begin{cases} 1 & , & c_{ij} \neq 0 \\ 0 & , & c_{ij} = 0 \end{cases} \quad (2.3)$$

■

Obviously as shown in the previous Chapter, at each adjacency matrix is associated a directed graph. Therefore, recalling Definition 2.1, the following statement can be formulated:

Definition 2.2. *The directed graph (digraph) $\mathcal{G} = (\mathcal{V}, \mathcal{E})$ of a system Σ has the vertex set $\mathcal{V} = X \cup U \cup Y$, where $U = \{u_1, u_2, \dots, u_m\}$, $X = \{x_1, x_2, \dots, x_n\}$, and $Y = \{y_1, y_2, \dots, y_p\}$ are nonempty sets of input, state, and output vertices of \mathcal{V} and \mathcal{E} is the edge set defined as follows: $(v_j, v_i) \in \mathcal{E}$ if and only if $a_{ij} = 1$.*

■

It is worth to mentioning that, since there are no connections among inputs, outputs and between inputs and outputs in (2.1), then the digraph \mathcal{G} of Σ contains only the edges (u_j, x_i) , (x_j, x_i) , and (x_j, y_i) , which reflects the basic assumption about the system Σ (2.1).

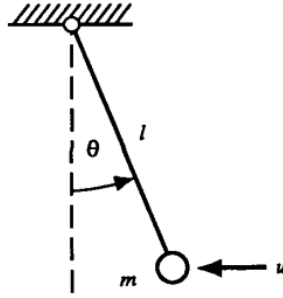


Figure 2.1: Pendulum.

Remark 2.1. *It is worth to note that, this conversion of matrix's entries to binary values makes the adjacency matrix \mathcal{A} an useful modeling tool for study the qualitative properties of the system Σ , independently to the specific numerical values of the matrices representative of the system dynamic. Indeed, in this way it is possible to handle, for example, parameter uncertainties caused by modeling errors or operating failures in the system.*

Furthermore, the adjacency matrix \mathcal{A} give us also qualitative information regarding the structural properties of the system Σ in terms of graph representation. The reader is referred to Chapter 1 for a tutorial overview of information in Graph Theory. ■

To illustrate how graphs can be associated to dynamical systems, in the following it is presented the following illustrative example [Šiljak, 1991].

Example 2.1. *Consider linearized model of a frictionless pendulum shown in Figure 2.1*

$$ml \cdot \ddot{\theta} + mg \cdot \theta = u \quad (2.4)$$

where $\theta(t)$ is the angular position of the bod at time t , $\ddot{\theta}(t)$ is its second derivative, l is the length of the rod (supposed to be rigid and without mass), and m is the mass of the bob subject to a force (input) $u(t)$. Defined $\mathbf{x} = [x_1, x_2]^T = [\theta, \dot{\theta}]^T$ as state vector, the following linearized representation for the pendulum's dynamic results:

$$\Sigma : \begin{cases} \dot{\mathbf{x}} = \begin{bmatrix} 0 & 1 \\ -g/l & 0 \end{bmatrix} \mathbf{x} + \begin{bmatrix} 0 \\ 1/(m \cdot l) \end{bmatrix} \mathbf{u} \\ \mathbf{y} = \begin{bmatrix} 1 & 0 \end{bmatrix} \mathbf{x} \end{cases} \quad (2.5)$$

Then substituting the dynamic's matrices of system (2.5) in the adjacency matrix definition (2.2) the next interconnection matrix takes place:

$$\mathcal{A} = \begin{bmatrix} 0 & 1 & 0 & 0 \\ 1 & 0 & 1 & 0 \\ 0 & 0 & 0 & 0 \\ 1 & 0 & 0 & 0 \end{bmatrix} \quad (2.6)$$

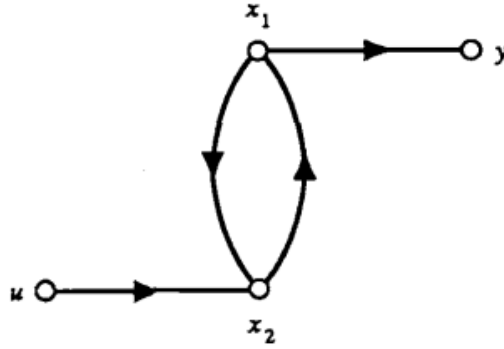


Figure 2.2: Directed graph associated to the pendulum system.

where dashed lines delineate the matrices \bar{A} , \bar{B} , and \bar{C} . As a conclusion in Figure 2.2 is reported the digraph of Σ corresponding to the matrix (2.6). ■

Notice that the properties of a system Σ established by its interconnection matrix \mathcal{A} or digraph \mathcal{G} are at the same time valid for systems *structurally equivalent* to Σ .

Definition 2.3. Two systems Σ_1 and Σ_2 are said to be *structurally equivalent* if there exist nonsingular permutation matrices P_A , P_B , and P_C such that:

$$\bar{A}_2 = P_A \bar{A}_1 P_A^T, \quad \bar{B}_2 = P_B \bar{B}_1 P_B^T, \quad \bar{C}_2 = P_C \bar{C}_1 P_C^T \quad (2.7)$$

■
Remark 2.2. An interesting aspect of structural modeling of complex systems is that the binary nature of the interconnection matrices allows to formulate well-posed numerical problem and robust with respect to parameter variations. ■

2.1.2 Input and Output Reachability

As well-known, the existence of control laws for a dynamic system depend crucially upon the well-known fundamental properties of complete controllability and observability [Khalil, 2002]. Complete controllability means that any initial state of a given dynamical system can be transferred to the zero state by a suitable input. Standard test for analyze this property is to check the rank of the so-called controllability matrix, defined as follows:

$$\mathcal{C} = \begin{bmatrix} B & AB & A^2B & \dots & A^{n-1}B \end{bmatrix}, \quad \text{rank}\{\mathcal{C}\} = n \quad (2.8)$$

which must be equal to the order of the system.

With the same spirit, a system is said to be completely observable if any state of the system can be determined in from subsequent inputs and outputs. Standard test for analyze this

property is to check the rank of the so-called observability matrix, defined as follows:

$$\mathcal{O} = \begin{bmatrix} C^T & (CA)^T & (CA^2)^T & \dots & (CA^{n-1})^T \end{bmatrix}^T, \quad \text{rank}\{\mathcal{O}\} = n \quad (2.9)$$

which must be equal to the order of the system. Anyway in systems of large dimensions, computing the rank conditions can be an hard task due numerical issues [Hansen, 1998]. For these reasons, as shown in [Šiljak, 1991] controllability and observability properties can also be established by studying problems of input reachability and output reachability respectively, in a digraph, or more formally by binary computations alone by using the adjacency matrix defined in (2.2).

In order to evaluate input and output reachability of a given system Σ , recalling [Barnes & Harary, 1983], it results that the reachability matrix $\mathcal{R} = [r_{ij}]$ of a digraph $\mathcal{G}(\mathcal{V}, \mathcal{E})$ is defined as follows:

$$r_{ij} : \begin{cases} 1 & , \text{ if } v_i \text{ is reachable from } v_j \text{ } (v_i \rightarrow v_j) \\ 0 & , \text{ } v_i \not\rightarrow v_j \end{cases} \quad (2.10)$$

To determine the reachability matrix for a given digraph, by citing [Šiljak, 1991], it results:

$$\mathcal{R} = \mathcal{A} \vee \mathcal{A}^2 \vee \dots \vee \mathcal{A}^s \quad (2.11)$$

where $\mathcal{A}^k = \mathcal{A}^{k-1} \wedge \mathcal{A}$ with \vee and \wedge respectively the OR and AND boolean operators and $s = n + m + p$.

A more efficient Boolean-type algorithm for computing the matrix exponentiation of \mathcal{A} was proposed by Warshall in [Warshall, 1962], where:

$$\mathcal{A}^k = \begin{bmatrix} \bar{A}^k & \bar{A}^{k-1} \bar{B} & \bar{0} \\ \bar{0} & \bar{0} & \bar{0} \\ \bar{C} \bar{A}^{k-1} & \bar{C} \bar{A}^{k-2} \bar{B} & \bar{0} \end{bmatrix} \in \mathbb{R}^{(n+m+p) \times (n+m+p)} \quad (2.12)$$

from which, combining with (2.11) one gets the reachability matrix as:

$$\mathcal{R} = \begin{bmatrix} F & G & 0 \\ 0 & 0 & 0 \\ H & \theta & 0 \end{bmatrix} \quad (2.13)$$

where the binary matrices F , G , H , and θ have proper dimensions according to (2.12). From (2.13), the following result is obvious:

Theorem 2.1. *A system Σ is input reachable if and only if matrix G has no zero rows, and it is output reachable if and only if matrix H has no zero columns.* ■

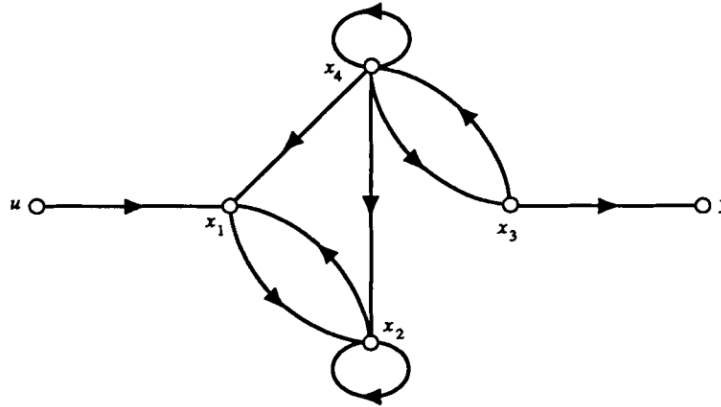


Figure 2.3: Input and output unreachable digraph.

It is worth to note that the system is said to be *input-output reachable* if and only if matrix θ has neither zero rows nor zero columns. Which means that the set of output Y is a reachable from set of input U , and U is an antecedent set of Y .

The following example illustrate the application of Theorem 2.1.

Example 2.2. Consider the digraph in Figure 2.3, which is clearly input and output unreachable because there are no directed walks from u to x_3 or x_4 , and at the same manner y is unreachable from x_1 and x_2 . Computing the adjacency matrix of digraph in Figure 2.3, it results

$$\mathcal{A} = \begin{bmatrix} 0 & 1 & 0 & 1 & 0 & 0 \\ 1 & 1 & 0 & 1 & 0 & 0 \\ 0 & 0 & 0 & 1 & 0 & 0 \\ 0 & 0 & 1 & 1 & 0 & 0 \\ \hline 0 & 0 & 0 & 0 & 0 & 0 \\ \hline 0 & 0 & 1 & 0 & 0 & 0 \end{bmatrix} \quad (2.14)$$

then by (2.13) and (2.12), the corresponding reachability matrix is:

$$\mathcal{R} = \begin{bmatrix} 1 & 1 & 1 & 1 & 1 & 0 \\ 1 & 1 & 1 & 1 & 1 & 0 \\ 0 & 0 & 1 & 1 & 0 & 0 \\ 0 & 0 & 1 & 1 & 0 & 0 \\ \hline 0 & 0 & 0 & 0 & 0 & 0 \\ \hline 0 & 0 & 1 & 1 & 0 & 0 \end{bmatrix} \quad (2.15)$$

which, as discussed in Theorem 2.1 confirms that $\mathcal{G}(\mathcal{V}, \mathcal{U})$ is unreachable. ■

2.2 Scale-free dynamical networks

In this Section inspired to the fact that many real-world complex networks are neither completely regular nor completely random, some notion of Large-Scale Systems and a possible model that can capture how this complex networks can evolve in time is presented.

2.2.1 Complex network Preliminaries

Complex networks are usually characterized by several distinctive properties including complexity, topological structure, dynamical evolution, time-varying coupling strengths and interactions between nodes. Traditionally, the first model of networks was proposed in [Erdős & Rényi, 1960], also known as Erdos-Rényi model (or just ER-Model). In that model each pair of elements was randomly connected with the same probability. As an example, let $\mathcal{G}(\mathcal{V}, \mathcal{E})$ be a digraph on n vertices and $M = \text{card}\{\mathcal{E}\}$ edges, pursuant to the ER-Model, all graphs with n nodes and M edges have equal probability to exist. Formally this probability results equal to:

$$p^M \cdot (1 - p)^{\binom{n}{2} - M} \quad (2.16)$$

where the probability p can be thought of as a weighting function; as p increases from 0 to 1, the model becomes more and more likely to include graphs with more edges and less and less likely to include graphs with fewer edges. In particular, the case $p = 0.5$ corresponds to the case where all graphs on n vertices are chosen with equal probability.

However in the real world, connectivity between each element is neither completely regular nor completely random. Therefore, thanks to Watts and Strogatzs (WS-Model) a more realistic representation has been given. In particular, the Watts-Strogatz model is still a random graph generation model, but concepts as *short average path lengths*, *high clustering* and *degree distribution* have been introduced [Watts & Strogatz, 1998].

The main difference between the ER-Model is that the degree distribution converges is a power law instead of a Poisson distribution. As a limitation, the WR-model produces an unrealistic degree distribution in contrast with real networks that are often scale-free networks and inhomogeneous in degree [Barrat & Weigt, 2000]. Indeed, the WR-Model produces a locally clustered network, and the random links dramatically reduce the *average path lengths*¹.

¹Average path length is a concept in network topology that is defined as the average number of steps along the shortest paths for all possible pairs of network nodes. It is a measure of the efficiency of information or mass transport on a network.

In particular, let n be the desired number of nodes, d the average-degree of a node, and β a parameter satisfying $0 \leq \beta \leq 1$ with $n \gg K \gg \ln(N) \gg 1$, where N is the desired number of nodes and K the mean degree (assumed to be an even integer). The algorithm starts generating an underlying regular lattice structure with $(nd)/2$ arcs and then randomly, introduces about $(\beta nd)/2$ non-lattice edges.

Finally, another significant development in the field of complex networks has been proposed by Barabási and Albert in [Barabási et al., 1999]. They observed that a number of large-scale and complex networks are *scale-free*² [Albert & Barabási, 2000]. The Barabási-Albert (BA-Model) is an algorithm for generating random scale-free networks using a preferential attachment mechanism. Thanks to this more sophisticated approach for modeling complex systems topologies, systems like Internet [Siganos et al., 2003], metabolic networks [Jeong et al., 2000] or social networks [Wasserman, 1994, Barabási et al., 2002] have been modeled.

2.2.2 The scale-free network model

The Barabási-Albert Model incorporates two important general concepts:

- *growth*: which means that the number of nodes in the network can increase over time;
- *preferential attachment*: which means that the more connected node is, likely, the one who will receive a new link.

As a consequence, nodes with higher degree have stronger ability to grab links added to the network. Intuitively, the preferential attachment can be understood as follows: for example, thinking in terms of social networks, it's common to have that more popular people have more chance to know new people with respect to an anonymous person, i.e. *the rich get richer* phenomenon.

Starting for these two ingredients, Barabasi and Albert proposed a simple scale-free model which, starting with m_0 nodes, at every time step, a new node is introduced. Each new node is connected to $m \leq m_0$ existing nodes with a probability that is proportional to the number of links that the existing nodes already have. More formally

$$p_i = \frac{d_i}{\sum_j d_j} \quad (2.17)$$

²A *scale-free* network is inhomogeneous in nature, which means that most nodes have very few connections and a few nodes have many connections.

where d_i is the degree of node v_i and the summation is made over all the pre-existing nodes v_j (i.e. the denominator results in the current number of edges in the network).

It has been shown that, for a large time constant, the degree distribution resulting from the BA-Model is scale-free. In particular, the probability that a network's node is connected to k other nodes decays as a power-law

$$P(k) = 2 \cdot \frac{m^2}{k^3} \quad (2.18)$$

More recently the BA-Model has been improved by the authors in order to taking into account the additions of new nodes, new links, and the rewiring of links (see [Albert & Barabási, 2000]).

2.2.3 Scale-free Dynamical Network Model

During the decades a great deal of attention has been paid to networks of coupled dynamical systems, in particular from the nonlinear dynamics community. Reasons are that, those networks can exhibit many complex and interesting dynamical phenomena, such as *Turing patterns*, *auto-waves*, *spiral waves*, and *spatiotemporal chaos* [Wang & Chen, 2003].

For the same reason, many scientists have started to consider the synchronization phenomenon in large-scale networks of coupled chaotic oscillators [Chua, 1998, Wang & Chen, 2002a, Edwards & Menon, 2008, Piloni et al., 2013a] due to the fact that they allow to focus on the complexity caused by the nonlinear dynamics of each nodes without worrying about additional complexity in the network topologies.

A common accepted representation of a dynamical network consisting of N heterogeneous, dynamical, linearly and diffusively coupled nodes (e.g., a chaotic system), has been shown in [Wang & Chen, 2002a], where the state equations of the network are described by

$$\dot{\mathbf{x}}_i(t) = \mathbf{f}_i(\mathbf{x}_i) + c \cdot \sum_{j=1}^N \mathcal{L}_{ij} \Gamma_{ij} \mathbf{x}_j \quad , \quad i = 1, \dots, N \quad (2.19)$$

with $\mathbf{x}_i \in \mathbb{R}^{n_i}$ is the state vector of i -th node, $c \in \mathbb{R}^+$ represents the coupling strength, and $\Gamma_{ij} \in \mathbb{R}^{n_i \times n_j}$ is a binary matrix of suitable dimensions which represents the *node-to-node* coupling configuration among the i -th and j -th node. The entries of Γ_{ij} are nonzero if and only if a communication channel among different states of neighbors nodes exist. Whereas \mathcal{L}_{ij} represents the (i, j) entry of the Laplacian Matrix associated to the actual configuration of the network at time t .

It is worth to noticed how those network configuration results to be described by a switching topology characterized by a time-varying graph $\hat{\mathcal{G}}(t)(\mathcal{V}, \mathcal{E}(t) \subseteq \mathcal{E})$, where $\mathcal{E}(t)$ is the subset of active edges at time t , whereas \mathcal{E} is the set of the whole available communication edges in $\mathcal{G}(\mathcal{V}, \mathcal{E})$.

Furthermore, with reference to the synchronization phenomenon in large-scale networks; under the assumption that each heterogeneous node has the same dimension $n_i = n_j = n$; it results that a dynamical network (2.19) is said to be (asymptotically) synchronized if

$$\mathbf{x}_1(t) = \mathbf{x}_2(t) = \dots = \mathbf{x}_N(t) = \mathbf{s}(t) \quad , \quad \text{as } t \rightarrow \infty \quad (2.20)$$

where $\mathbf{s}(t) \in \mathbb{R}^n$ can be, for example, an equilibrium point, a defined periodic orbit, or a chaotic attractor, depending on the interest of the study.

As proved in [Lago-Fernández et al., 2000, Wang & Chen, 2002b], a connected network, in the sense that there are no isolated clusters of nodes (see Section 1.2), can achieve state synchronization (2.20) with exponential rate if

$$c > \left| \frac{\bar{d}}{\lambda_2} \right| \quad (2.21)$$

where $\bar{d} < 0$ is a constant determined by the dynamics of an isolated node and the inner linking structural matrix Γ . More precisely \bar{d} depends by the Lyapunov exponents of the network [Li & Chen, 2003]. Whereas λ_2 is the *algebraic connectivity* of the Laplacian Matrix of the network, which gives information about the connectedness of the network.

Remark 2.3. Notice that, since the algebraic connectivity for a connected network satisfy the next constraint:

$$0 < \lambda_2 \leq N \quad (2.22)$$

this implies that for any given and fixed nonzero coupling strength c , the network will synchronize as long as its size increase. As a limit case, supposed the network fully connected ($\lambda_2 = N$) and N large enough (i.e $N \rightarrow \infty$); by (2.21) it is possible to note that for any given and fixed nonzero coupling strength $c \geq \varepsilon > 0$, the network can achieve synchronization for sufficiently large networks. ■

In literature, different control strategies are taken into account to realize control and synchronization of complex dynamical networks. Among the varius aproaches pinning control have received many attention because it is easily achieve synchronization by controlling just a part of the nodes instead of all nodes in the network [Wang & Wen, 2008].

It is worth to mentions that the only commonly accepted requirements for achieving the

synchronization of a complex network is that it has a directed spanning tree interaction graph [Wu, 2008].

2.3 Consensus Problem and Cooperative Control

2.3.1 Cooperative Control Preliminaries

Control applications in distributed and cooperative environments are studied with growing interest in recent years. The success of this paradigm can be attributed to the fact that many complex systems are naturally represented by a network of interacting subsystems or “agents”. Transportation networks, power grids, networks of mobile robots and localization systems are just few examples of engineering applications of networked systems [Zampieri, 2008, Piloni et al., 2013a, Frew et al., 2005a]. The winning features of networked structured applications comes from their reduced cost, flexibility, scalability/reconfigurability and robustness to failures. An overview of the recent research trends in cooperative control can be found in [Zampieri, 2008, Ren et al., 2007a, Garin & Schenato, 2011, Ren & Beard, 2008]

In particular, *Multi-Agent Systems* deal with the analysis of how distributed interaction architectures affect the achievement of a collective behavior through only local interaction [Cao & Ren, 2012]. A crucial problem in cooperative control is to achieve a distributed agreement on parts of the networked system’s state (i.e. barycenter, average phase, a common attitude) exploiting only local interaction and information exchange.

This problem, known to as *consensus*, has been widely studied in literature especially with reference to single and double integrators agents’ dynamics [Cao & Ren, 2012, Bullo et al., 2009, Olfati-Saber & Murray, 2004, Ren & Beard, 2008, Olfati-Saber & Shamma, 2005, Fax & Murray, 2004, Piloni et al., 2013b, Cortes, 2008]. Anyway, although in practical application disturbances and unmodeled dynamic are unavoidable, in much of the current literature on cooperative control, the consensus problem is often studied in the presence of identical homogeneous agents and/or under the assumption of full and reliable communication [Ren & Beard, 2008].

In the following a brief literature review on consensus algorithms on network of multi-agent systems is provided.

2.3.2 Multi-Agents Systems

A networked multi-agent system can be thought as a collection of individual, but coupled, dynamical systems. Where the coupling structure can be static or dynamic when communications links are established or dropped over time. Some common feature of every Multi-Agents Systems are:

- local interaction: agents can interact each other only using relative information from their neighbors;
- lack of a common reference frame in both space, time or states;
- complete absence of a centralized supervisor;
- scalability, which means that when the network's size changes, the local strategy remain the same for every agent and the same group behavior still emerges.

After those considerations, it is now possible to present how to model a multi-agent system. Since multi-agent system are described by a finite number of entities operating over a network, by using concept of Graph Theory, the network topology can be represented as a digraph $\mathcal{G}(\mathcal{V}, \mathcal{E})$ where $\mathcal{V} = \{1, 2, \dots, N\}$ is the set of agents, represented by nodes in the graph and $\mathcal{E} \subseteq \mathcal{V} \times \mathcal{V}$ is the set of edges. An edge (i, j) exists if agent i interacts with agent j . The neighborhood of each agent i is defined as $\mathcal{N}_i^- = \{j \in \mathcal{V} / \{i\} : (i, j) \in \mathcal{E}\}$ which represents the set of agents which directly interact with it. Furthermore, as discussed in Section 1.4, topological information associated to a graph \mathcal{G} can be encoded by the well-known *Laplacian Matrix* $\mathcal{L} = [\mathcal{L}_{ij}] \in \mathbb{R}^{N \times N}$ defined, accordingly with the previous treatment as follows:

$$\mathcal{L}_{ij} := \begin{cases} |\mathcal{N}_i^-| & \text{if } i = j \\ -1 & \text{if } (i, j) \in \mathcal{E} \\ 0 & \text{otherwise} \end{cases} \quad (2.23)$$

where $|\mathcal{N}_i^-|$ is the cardinality of the i -th agent's neighbor set. Whereas the agent's dynamic is generally described as follows:

$$\dot{\mathbf{x}}_i = \mathbf{f}_i(\mathbf{x}_i, \mathbf{u}_i) \quad (2.24)$$

where $\mathbf{x}_i \in \mathbb{R}^n$ is the agent's state and $\mathbf{u}_i \in \mathbb{R}^m$ is the vector of inputs. Whereas the local interaction protocol for agent i can be defined, accordingly to the considered task as follows:

$$\mathbf{u}_i = \mathbf{u}(\mathbf{x}_j : j \in \mathcal{N}_i^-) \quad (2.25)$$

Therefore, a typical autonomous multi-agent system is thus completely defined by the network topology \mathcal{G} , the agents' dynamics and the defined local interaction protocol.

2.3.3 Fundamental Consensus Algorithms

Consensus algorithms have a historical perspective in [Borkar & Varaiya, 1982, Chatterjee & Seneta, 1977, DeGroot, 1974], and, as discussed in the previous section, they have been recently brought up again in the context of cooperative control. The basic idea in *consensus* is to impose, using information coming from the agent's neighborhoods, a similar dynamics to all the agents operating over a network. More formally, a consensus problem can be defined as follows:

Definition 2.4. Consider a multi-agent system defined by the network topology $\mathcal{G}(\mathcal{V}, \mathcal{E})$ and the agents' dynamics $\dot{\mathbf{x}}_i = \mathbf{f}(\mathbf{x}_i, \mathbf{u}_i)$ with $\mathbf{x}_i \in \mathbb{R}^n$. A consensus problem consists in the design of a local interaction protocol $\mathbf{u}(\mathbf{x}_j : j \in \mathcal{N}_i^-)$ such that:

$$\forall i, j \in \mathcal{V}, \quad \lim_{t \rightarrow \infty} \|\mathbf{x}_i - \mathbf{x}_j\| = 0 \quad (2.26)$$

■

In the following subsections several frameworks for modeling multi-agent systems will be presented, each differing in interaction protocols adopted, agents model and network topology.

First-Order Consensus Algorithm

The most common continuous-time consensus algorithm [Fax & Murray, 2004, Jadbabaie et al., 2003, Olfati-Saber & Murray, 2004, Lin et al., 2004] assume that each agent is a single continuous-time integrator with dynamics:

$$\dot{x}_i(t) = u_i(t) \quad , \quad x_i, u_i \in \mathbb{R} \quad (2.27)$$

with local interaction protocol defined as follows

$$u_i(t) = - \sum_{j \in \mathcal{N}_i^-} (x_i(t) - x_j(t)) \quad (2.28)$$

From (2.28), it is easy to see that the information state $x_i(t)$ of agent i is driven toward the information states of its neighbors. By substituting (2.28) into (2.27), the resulting global system dynamics can be rewritten at the network level in the following compact form:

$$\dot{\mathbf{x}}(t) = -\mathcal{L} \cdot \mathbf{x}(t) \quad (2.29)$$

with $\mathbf{x} = [x_1, x_2, \dots, x_n] \in \mathbb{R}^N$ and \mathcal{L} defined as in (2.23).

At this point, a critical question is to understand if the network is really converging towards a common consensus value or not.

A well-known approach adopted to deal with this problem in network of simple integrator is to study the convergence to zero of the so-called *disagreement vector dynamics* [Olfati-Saber et al., 2007] defined as follows:

$$\dot{\delta}(t) = -\mathcal{L} \cdot \delta(t) \quad , \quad \text{with} \quad \delta(t) = \mathbf{x}(t) - \frac{\mathbf{1}_N^T \cdot \mathbf{1}_N}{N} \cdot \mathbf{x}(t) \quad (2.30)$$

In particular, for the case of an undirected connected topology ($\lambda_2 > 0$), recalling the Laplacian's property reported in (1.11)

$$\|\mathcal{L}\delta(t)\|_2^2 = \delta(t)^T \mathcal{L}^2 \delta(t) \geq \lambda_2 \cdot \|\delta(t)\|_2^2 \quad (2.31)$$

it is easy to show that the annihilation of the disagreement vector implies the convergence towards a common value of the agents dynamics by the following simple Lyapunov-Based analysis. Let's consider the following sum-of-squares positive definite function:

$$V(t) = \frac{1}{2} \delta(t)^T \mathcal{L} \delta(t) \quad (2.32)$$

Differentiating $V(t)$, it results:

$$\dot{V}(t) = -\delta(t)^T \mathcal{L}^2 \delta(t) \leq -\lambda_2 \|\delta(t)\|_2^2 \quad (2.33)$$

which implies the exponential convergence to zero of the disagreement vector dynamics and then the achievement of the consensus condition (2.26).

Whereas if the consensus problem (2.29) for a network with a directed topology is considered, the proof is slightly different but the only requirement is that the network has a directed spanning tree. The proof follows from [Olfati-Saber et al., 2007] and can be derived as next.

Since the graph is supposed to has a directed spanning tree, \mathcal{G} has a single null eigenvalue to which corresponds the right eigenvector $\mathbf{1}_N = \text{col}(1, \dots, 1) \in \mathbb{R}^N$, therefore the dynamic (2.29) is marginally stable and converges inside an invariant subspace defined as follows:

$$\mathcal{S} = \{ \mathbf{x} \in \mathbb{R}^N \quad : \quad \mathbf{x} = \alpha \cdot \mathbf{1}_N \quad \text{with} \quad \alpha \in \mathbb{R} \} \quad (2.34)$$

Let η^T be a left-eigenvector of \mathcal{L} corresponding to the zero eigenvalue. Defined a new variable $\mathbf{y} = \eta^T \cdot \mathbf{x}$, it results:

$$\dot{\mathbf{y}} = \eta^T \dot{\mathbf{x}} = \eta^T \mathcal{L} \mathbf{x} = 0 \quad \Rightarrow \quad \mathbf{y}(t) = \mathbf{y}(0) \quad \forall \quad t \geq 0 \quad (2.35)$$

which implies

$$\lim_{t \rightarrow \infty} \mathbf{y}(t) = \mathbf{y}(0) = \boldsymbol{\eta}^T \mathbf{x}(0) = \boldsymbol{\eta}^T \mathbf{x}(0) = \boldsymbol{\eta}^T \boldsymbol{\alpha} \mathbf{1}_N \quad \Rightarrow \quad \boldsymbol{\alpha} = \frac{\boldsymbol{\eta}^T \cdot \mathbf{x}(0)}{\boldsymbol{\eta}^T \cdot \mathbf{1}_N} \quad (2.36)$$

Hence, the agents' state converges toward the weighted average of their initial condition:

$$\lim_{t \rightarrow \infty} \mathbf{x}(t) = \left(\frac{\boldsymbol{\eta}^T \cdot \mathbf{x}(0)}{\boldsymbol{\eta}^T \cdot \mathbf{1}_N} \right) \mathbf{1}_N \quad (2.37)$$

As shown in [Ren & Beard, 2005], the previous treatment can be easily extended also for directed switching topology under the same assumption that each network's configuration always has a directed spanning tree.

Analogous consideration can be extended when communication among agents occurs at discrete instants. In such case the network's dynamics can be represented as follows:

$$\mathbf{x}[k+1] = \mathcal{D}[k] \cdot \mathbf{x}[k] \quad (2.38)$$

where $\mathcal{D} = [d_{ij}] \in \mathbb{R}^{N \times N}$ is a row-stochastic matrix at the discrete-time index k such that $d_{ij}[k] > 0$ if $(i, j) \in \mathcal{E}$ and $d_{ij}[k] = 0$ otherwise. At discrete-time a slightly similar stability analysis can prove the convergence towards a consensus value of dynamic (2.38). Anyway, since in this thesis only continuous-time algorithm will be discussed, the readers is referred to [Olfati-Saber et al., 2007, Ren & Beard, 2008] for further details.

Second-Order Consensus Algorithm

The single-integrator consensus algorithm in (2.29) has been also extended to double-integrator dynamics (see for example [Hargrove et al., 2000, Ren & Atkins, 2007, Piloni et al., 2013b] and references therein) for modeling more naturally the evolution of physical phenomena, such as for example, formation control and flocking which can be controlled through gentle maneuvers with a decoupled double-integrator model.

For double-integrator dynamics, the classic consensus algorithm is given by

$$\ddot{x}_i(t) = - \sum_{j=1}^N [(x_i(t) - x_j(t)) + \gamma \cdot (\dot{x}_i(t) - \dot{x}_j(t))] \quad (2.39)$$

where $\gamma > 0$ denotes the coupling strength between the information state derivatives and both x_i and \dot{x}_i are transmitted between team members. In [Ren & Atkins, 2007] it has been proved that the achievement of consensus, in the general directed framework, must requires a directed spanning tree and γ must be sufficiently large. See [Ren et al., 2007b] for extension to higher-order dynamics.

2.3.4 Nonlinear Consensus Algorithms

In this Subsection some notion about nonlinearities in consensus problems will be addressed along with some motivations about this reasonable extension.

As well-known real systems are not modeled in general by simple LTI systems. Let's try to think about a simple pendulum, or for example to the dynamic of a cart; or with reference to a multi-agent scenario, the realistic case in which disturbances in the communication protocol appears, or when the objective task is to reach a formation by maneuvering a group of robot with strongly nonlinear dynamics.

Well, in these cases every consensus protocol discussed above can not achieve good performance in terms of consensus due to the fact that concepts like robustness or disturbance rejection are not taken into account. Due to this practical necessity, recently a new area in the field of network coordination was born: the area of nonlinear robust consensus.

In literature examples of consensus of agents with nonlinearities have already been treated. A classical example is the synchronization of coupled Kuramoto oscillators [Kuramoto, 2003]. The Kuramoto model describes the dynamics of a set of N phase oscillators with dynamic defined as follows:

$$\dot{\theta}_i(t) = \omega_i(t) + k \sum_{j=1}^N \sin(\theta_j(t) - \theta_i(t)) \quad (2.40)$$

where $\theta_i(t)$ is the oscillator's phase, $\omega_i(t)$ the natural frequencies and k is the coupling strength. Synchronization of coupled oscillators with other nonlinear dynamics is also studied in the literature. As an example, consider a network of N vehicles with information dynamics given by

$$\dot{\mathbf{x}}_i(t) = \mathbf{f}_i(\mathbf{x}_i, t) + \gamma \cdot \sum_{j=1}^N (\mathbf{x}_j(t) - \mathbf{x}_i(t)) \quad (2.41)$$

where $\mathbf{x}_i \in \mathbb{R}^n$ and $\gamma > 0$ denotes the global coupling strength parameter. Therefore, although nonlinearities in general could complicate the agents dynamics and sometimes give arise undesired complex phenomenon such as limit-cycles or instability, they are able, if properly injected in the consensus algorithm, to introduce properties in terms of robustness or disturbance rejection impossible to achieve in the linear framework, even in the presence of a non-persistent spanning-tree network topology (see Chapter 8).

In the reminder of the Thesis, in particular in Chapters 8, 9 and 10 some of the recent improvement in the field of robust consensus will be addressed with reference to discontinuous sliding-mode-based consensus algorithm in both both the finite and infinite di-

mensional space agents' framework (see also [Franceschelli et al., 2013b, Piloni et al., 2013b, Demetriou, 2009]).

2.4 Conclusion

In this Chapter a survey of the existing literature related to the mathematical modeling of connected systems from the point of view of dynamical systems has been presented.

In particular, throughout the Chapter the following problems: first how to model a complex systems, not necessarily distributed in space, as interconnected subsystems, in order to reduce the complexity of the whole dynamics have been treated. Secondly, inspired to the fact that many real-world complex networks are neither completely regular nor completely random, notions of Large-Scale Dynamical Network are presented. Last but not least, in the third part of the Chapter, due to the strictly connections between networked systems and multi-agent systems, concepts of decision-making for network of dynamical systems have been introduced with particular emphases to the so-called *consensus problems*.

Chapter 3

Strong observability of MIMO Systems

The task of reconstructing the state of a large-scale system or more generally of a complex system has been largely studied in the last decades [[Šiljak, 1991](#), [Stankovic et al., 2009](#), [Stankovic et al., 2011](#), [Edwards & Menon, 2008](#), [Pillosu et al., 2011](#), [Pilloni et al., 2013a](#), [Trentelman et al., 2001](#), [Fridman et al., 2007b](#)]

Since, as shown in [Chapter 2](#), every complex system can be represented as an interconnection of subsystems or equivalently with a multi-input-multi-output (MIMO) representation, in the following some notions of observability for this class of systems will be discussed in order to provide to the reader the necessary notion for understanding the treatment presented in [Chapter 6](#) where a new approach for state estimation and unknown input reconstruction of a class of connected heterogeneous LTI MIMO systems is presented.

The Chapter is organized as follows. After a very short introduction about the problem of *Strong Observability* in [Section 3.1](#), in [Section 3.2](#) the main notions of Strong Observability in the framework of MIMO LTI systems are discussed. In particular, firstly standard condition for evaluating the strong observability properties of a MIMO system has been presented, then in the second and third part of the section some recent development of the Author [[Pilloni et al., 2013a](#)] for evaluating those properties for non-square MIMO systems are provided.

3.1 Introduction

Observation of system states in the presence of unknown inputs, as well as to determine observability and detectability properties of a system in order to assess the possibility of constructing observers, are some of the most important problems in the modern control

theory [Fridman et al., 2007b]. For linear and nonlinear systems this task can be solved by well-known techniques, for the case without perturbations. However, in presence of unknown inputs and/or nonvanishing perturbations this study has still some obscure points [Fridman et al., 2007b, Pilloni et al., 2013a].

In the following, some literature results regarding structural conditions [Trentelman et al., 2001, Hautus, 1983, Molinari, 1976, Fridman et al., 2007b] and the more recent development of the Author [Pilloni et al., 2013a] for evaluating those properties in both the linear and nonlinear framework are provided.

3.2 Notion of Strong Observability for LTI MIMO Systems

3.2.1 State of Art of Strong Observability in MIMO LTI Systems

Consider a LTI system Σ :

$$\dot{\mathbf{x}}(t) = \mathbf{A}\mathbf{x}(t) + \mathbf{D}\mathbf{f}(t) \quad (3.1)$$

$$\mathbf{y}(t) = \mathbf{C}\mathbf{x}(t) \quad (3.2)$$

where $\mathbf{x} \in \mathbb{R}^n$, $\mathbf{y} \in \mathbb{R}^p$, $\mathbf{u} \in \mathbb{R}^m$ and $\mathbf{f} \in \mathbb{R}^q$ are vectors which represent the state, the output and the unknown input.

Conditions for observability and detectability of LTI systems with unknown inputs are studied in literature, for example, in [Trentelman et al., 2001, Hautus, 1983, Molinari, 1976]. Hereinafter, some necessary and sufficient conditions for strong observability and strong detectability are recalled.

Definition 3.1. $s_0 \in \mathbb{C}$ is called an Invariant Zero of the triplet $(\mathbf{A}, \mathbf{D}, \mathbf{C})$ if $\text{rank}\{\mathbf{R}(s_0)\} < n + \text{rank}\{\mathbf{D}\}$, where \mathbf{R} is the Rosembrock matrix of Σ .

$$\mathbf{R}(s) = \begin{pmatrix} s\mathcal{I} - \mathbf{A} & -\mathbf{D} \\ \mathbf{C} & \mathbf{0} \end{pmatrix} \quad (3.3)$$

■

Definition 3.2. Σ is called (strongly) observable if for any initial condition $\mathbf{x}(0)$ and $\mathbf{f} = \mathbf{0}$ (any input \mathbf{f}), the following holds: $\mathbf{y}(t, \mathbf{x}(0)) \equiv \mathbf{0}$ for all $t \geq 0$ implies $\mathbf{x} \equiv \mathbf{0}$. The following statements are equivalent (see [Trentelman et al., 2001]):

- i) Σ is strongly observable;

- ii) The triple $(\mathbf{A}, \mathbf{C}, \mathbf{D})$ has no invariant zeros;
- iii) The Smith form of \mathbf{R} , \mathbf{R}_S is equal to the constant matrix

$$\mathbf{R}_S(s) = \begin{pmatrix} \mathcal{I}_{(n+q)} & \mathbf{0} \\ \mathbf{0} & \mathbf{0} \end{pmatrix} \quad (3.4)$$

■

Definition 3.3. The system is strongly detectable, if for any $\mathbf{f}(t)$ and $\mathbf{x}(0)$ it follows from $\mathbf{y}(t) \equiv \mathbf{0}$ with $\forall t \geq 0$ that $\mathbf{x} \rightarrow \mathbf{0}$ with $t \rightarrow \infty$ [Hautus, 1983]. The following statements are equivalent:

- i) Σ is strongly observable;
- ii) The system Σ is minimum phase (i.e. the invariant zeroes of the triple $(\mathbf{A}, \mathbf{C}, \mathbf{D})$ satisfy $\Re(s) < 0$).

■

Note that in the absence of the unknown input ($\mathbf{D} = \mathbf{0}$) the notions of strong observability coincide with the concept of observability. Thus, let \mathcal{O} be the observability matrix of the generic system Σ

$$\mathcal{O} = \begin{pmatrix} \mathbf{C} \\ \mathbf{C}\mathbf{A} \\ \vdots \\ \mathbf{C}\mathbf{A}^{n-1} \end{pmatrix} \in \mathbb{R}^{n \times p \times n} \quad (3.5)$$

then the system is observable if and only if $n_o = \text{rank}\{\mathcal{O}\} = n$. In this case any spectrum can be assigned to the matrix $\mathbf{A} - \mathbf{L}\mathbf{C}$, by choosing an appropriate matrix \mathbf{L} .

In [Fridman et al., 2007b] conditions necessary for strong observability with respect to the unknown input \mathbf{f} , under the assumption that $q = p$, has been given.

Let \mathbf{c}_i and \mathbf{d}_j be the rows of \mathbf{C} and the columns of \mathbf{D} . The output $\mathbf{y} = \mathbf{C}\mathbf{x}$ is said to have vector relative degree $\mathbf{r} = (r_1, \dots, r_p)$ with respect to the unknown input \mathbf{f} if

$$\begin{aligned} \mathbf{c}_i \mathbf{A}^l \mathbf{D} &= \mathbf{0}_{(1 \times q)} \\ \mathbf{c}_i \mathbf{A}^{r_i-1} \mathbf{D} &\neq \mathbf{0}_{(1 \times q)} \end{aligned} \quad \text{with} \quad \begin{cases} i = 1, 2, \dots, p \\ l = 0, 1, \dots, r_i - 2 \end{cases} \quad (3.6)$$

and

$$\det(\mathbf{Q}) \neq 0 \quad \text{with} \quad \mathbf{Q} = \begin{pmatrix} \mathbf{c}_1 \mathbf{A}^{r_1-1} \mathbf{d}_1 & \dots & \mathbf{c}_1 \mathbf{A}^{r_1-1} \mathbf{d}_q \\ \vdots & & \vdots \\ \mathbf{c}_p \mathbf{A}^{r_p-1} \mathbf{d}_1 & \dots & \mathbf{c}_p \mathbf{A}^{r_p-1} \mathbf{d}_q \end{pmatrix} \quad (3.7)$$

The following lemma asserts the strongly observability properties for the systems (3.1)-(3.2):

Lemma 3.1. *Let the output \mathbf{y} of Σ have vector relative degree \mathbf{r} . Then the vectors*

$$\mathbf{c}_1, \dots, \mathbf{c}_1 \mathbf{A}^{r_1-1}, \dots, \mathbf{c}_p, \dots, \mathbf{c}_p \mathbf{A}^{r_p-1} \quad (3.8)$$

are linearly independent. The system is strongly observable if the total relative degree of the system $\bar{\mathbf{r}} = \sum_k r_k$ with $k = 1, \dots, p$ is equal to $n_o = n$. ■

Remark 3.1. *Generalizing Lemma 3.1 to the case of rectangular systems when ($q < p$), it is obvious that $\mathbf{c}_1, \dots, \mathbf{c}_1 \mathbf{A}^{r_1-1}, \dots, \mathbf{c}_p, \dots, \mathbf{c}_p \mathbf{A}^{r_p-1}$ can not be linearly independent even if the system is strongly observable. This assertion can be easily proved applying the same procedure shown in [Fridman et al., 2007b] because \mathbf{Q} is a non-square matrix. ■*

Currently the concept of strong observability with respect to the unknown input for non-square LTI systems ($q < p$) is not well defined and remains an open problem in the field of estimation and control.

In the next subsection I revert to the concept of *observability indices* in order to define a possible approach for non-square systems. The following treatment is based on the Author's work [Pilloni et al., 2013a].

3.2.2 Strong Observability Conditions for Non-Square LTI MIMO Systems

Consider the system Σ in (3.1)-(3.2), the concept of *observability index* for each i -th output of the system are first introduced:

Definition 3.4. *The maximum number v_i of successive linearly independent derivatives of the i -th output of Σ , which represents the number of system state which can be reconstructed from y_i , is called the observability index for the i -th output. ■*

The set $V = \{v_1, \dots, v_p\}$ is called the *observability indices of the pair (\mathbf{A}, \mathbf{C})* . It is obvious that each v_i can not be greater then the order of the system n . Then, recalling the definition of relative degree r_i of the i -th output of the system with respect to an unknown input \mathbf{f} in (3.6), it can be asserted that if the following lemma holds, the system Σ is strongly observable and then the unknown input reconstruction (UIR) is practicable.

Lemma 3.2. *The system Σ is strongly observable if it is possible to define a set of positive integers $\mathcal{U} := \{\mu_1, \dots, \mu_h\}$ with $h \leq p$, in which each of element is associated with one output's component, such that the following conditions are satisfied:*

$$\begin{cases} \mu_i \leq v_i \\ \mu_i \leq r_i \end{cases}, \quad \mu_1 + \mu_2 + \dots + \mu_h = n \quad \text{with } i = 1, 2, \dots, h \quad (3.9)$$

$$\det \{M\} \neq 0, \quad M = \begin{pmatrix} M_1 \\ \vdots \\ M_i \\ \vdots \\ M_h \end{pmatrix}, \quad M_i = \begin{pmatrix} \mathbf{c}_i \\ \mathbf{c}_i \mathbf{A} \\ \mathbf{c}_i \mathbf{A}^2 \\ \vdots \\ \mathbf{c}_i \mathbf{A}^{\mu_i-1} \end{pmatrix} \in \mathbb{R}^{\mu_i \times n} \quad (3.10)$$

■

Proof. Suppose the pair (\mathbf{A}, \mathbf{C}) is observable, \mathcal{O} has n linearly independent rows. After choosing a set \mathcal{U} which satisfies the conditions (3.22)-(3.23), it is obvious that the matrix \mathbf{M} is full-rank because it is obtained combining linear independent block like $\mathbf{c}_i, \mathbf{c}_i \mathbf{A}, \dots, \mathbf{c}_i \mathbf{A}^{\mu_i-1}$ linearly independent each other. Then, applying the following bijection mapping $\mathbf{x} = \mathbf{M} \mathbf{x}_o$ the following canonical observable representation is obtained:

$$\begin{aligned}\dot{\mathbf{x}}_o &= \mathbf{A}_o \mathbf{x}_o + \mathbf{D}_o \mathbf{f} \\ \mathbf{y}_o &= \mathbf{C}_o \mathbf{x}_o\end{aligned}\quad (3.11)$$

where

$$\mathbf{A}_o = \begin{pmatrix} \mathbf{A}_{11} & \cdots & \mathbf{A}_{1h} \\ \vdots & \ddots & \vdots \\ \mathbf{A}_{h1} & \cdots & \mathbf{A}_{hh} \end{pmatrix}, \quad \mathbf{C}_o = \begin{pmatrix} \mathbf{c}_{11} & \cdots & \mathbf{c}_{1h} \\ \vdots & \ddots & \vdots \\ \mathbf{c}_{h1} & \cdots & \mathbf{c}_{hh} \end{pmatrix}\quad (3.12)$$

$$\mathbf{A}_{ii} = \begin{pmatrix} 0 & 1 & \cdots & 0 \\ \vdots & \vdots & \ddots & \vdots \\ 0 & 0 & \cdots & 1 \\ a_{ii,1} & a_{ii,2} & \cdots & a_{ii,\mu_i} \end{pmatrix}, \quad \mathbf{A}_{ij} = \begin{pmatrix} 0 & \cdots & 0 \\ \vdots & & \vdots \\ 0 & \cdots & 0 \\ a_{ij,1} & \cdots & a_{ij,\mu_j} \end{pmatrix}\quad (3.13)$$

$$\mathbf{D}_o = \mathbf{M} \mathbf{D} = \begin{pmatrix} \delta_1 \\ \vdots \\ \delta_h \end{pmatrix}, \quad \delta_i = \begin{pmatrix} 0 \\ \vdots \\ 0 \\ \mathbf{c}_i \mathbf{A}^{\mu_i-1} \mathbf{D} \end{pmatrix} \in \mathbb{R}^{\mu_i \times q}\quad (3.14)$$

$$\mathbf{c}_{ii} = \begin{pmatrix} 1 & 0 & \cdots & 0 \end{pmatrix} \in \mathbb{R}^{1 \times \mu_i}, \quad \mathbf{c}_{ij} = \begin{pmatrix} 0 & \cdots & 0 \end{pmatrix} \in \mathbb{R}^{1 \times \mu_j}\quad (3.15)$$

Note that the previous mapping emphasized the strong observability property of Σ . It is easy to see that the condition $\mathbf{y} \equiv \mathbf{0}$ implies $\mathbf{x} = \mathbf{0}$ for any unknown input \mathbf{f} . Note that if μ_i is chosen lower than r_i the entries $\mathbf{c}_i \mathbf{A}^{\mu_i-1} \mathbf{D}$ in δ_i are zero, then \mathbf{f} has no effect on the linear combination \mathbf{M}_i obtained by the i -th component of \mathbf{y} . ■

Corollary 3.1. If Lemma 3.2 is satisfied and

$$\text{rank} \left\{ (\mathbf{D}^T \mathbf{D})^{-1} \mathbf{D}^T \mathbf{M}^{-1} \mathbf{T} \right\} = q\quad (3.16)$$

with $\mathbf{T} = \text{diag}(\mathbf{t}_1, \dots, \mathbf{t}_i, \dots, \mathbf{t}_h)$ and $\mathbf{t}_i = \begin{pmatrix} 0 & \cdots & 0 & 1 \end{pmatrix}^T \in \mathbb{R}^{\mu_i \times 1}$, it is possible to reconstruct completely the unknown vector $\mathbf{f} = [f_1, \dots, f_q]^T$ by a suitable robust observer. ■

Proof. Consider the system (3.11) and the following observer:

$$\begin{aligned}\dot{\hat{\mathbf{x}}}_o &= \mathbf{A}_o \hat{\mathbf{x}}_o + \mathbf{T} \zeta \\ \hat{\mathbf{y}}_o &= \mathbf{C}_o \hat{\mathbf{x}}_o\end{aligned}\quad (3.17)$$

where $\hat{\mathbf{x}}_o$, $\hat{\mathbf{y}}_o$ and ζ represent the estimated states, the observed output of the node and the injection term. If condition (3.16) holds, it is obvious that the mapping $\mathbf{x} = \mathbf{M} \mathbf{x}_o$ implies that the matrix $\text{rank}\{\mathbf{D}_o\} = \text{rank}\{\mathbf{D}\} = q$. Let $\mathbf{e}_o = \hat{\mathbf{x}}_o - \mathbf{x}_o$ be the state observation error, its dynamic takes the following form:

$$\dot{\mathbf{e}}_o = \mathbf{A}_o \mathbf{e}_o + \mathbf{T} \zeta - \mathbf{D}_o \mathbf{f}\quad (3.18)$$

Let $\mathbf{F} = [F_1, \dots, F_q]^T$ be a constant vector which constitutes an upper bound on the input \mathbf{f} so that $|f_i| < F_i$, then it can be designed an algorithm which drives to zero the observation error dynamic $(\mathbf{e}, \dot{\mathbf{e}}) \rightarrow (\mathbf{0}, \mathbf{0})$, and then reconstructs \mathbf{f} as follows:

$$\mathbf{f} = D_o^+ \mathbf{T} \zeta = D^+ M^{-1} \mathbf{T} \zeta \quad (3.19)$$

where the index $+$ indicates the Moore-Penrose pseudo-inverse of the matrix. It is obvious that by construction, the solution of system (3.18)-(3.19) gives an unique solution with respect to the unknown input \mathbf{f} if and only if the condition (3.16) is satisfied. ■

Remark 3.2. Consider the observer structure (3.17). Applying the inverse mapping $\mathbf{x}_o = M^{-1} \mathbf{x}$, it can be obtained a completely equivalent representation for the observer (3.17) which dispenses with the need to work in a transformed domain. ■

3.2.3 Extension for a generic Non-Square MIMO Nonlinear Systems

It is worth to note that, following from the result discussed above, a more generic treatment for Non-Square MIMO Nonlinear System can be easily derived by recalling concepts of *Lie Algebras* for understanding the structure of nonlinear partial differential equations useful for generating integrable equations (see i.e. [Slotine et al., 1991]). In particular the following Non-Square MIMO Nonlinear System defined as follows

$$\Sigma_{NL} \quad : \quad \begin{cases} \dot{\mathbf{x}} = \mathbf{g}(\mathbf{x}) + \mathbf{f} \\ \mathbf{y} = \mathbf{h}(\mathbf{x}) \end{cases} \quad (3.20)$$

where $\mathbf{x} \in \mathbb{R}^n$ is the state vector, $\mathbf{y} = [y_1, \dots, y_p]^T \in \mathbb{R}^p$ the output vector, $\mathbf{g}(\mathbf{x})$ is the nominal autonomous dynamics and \mathbf{f} is an unknown vector function.

Then, under the assumption that the autonomous system dynamics of Σ_{NL} is **sufficiently smooth and observable**, by analogous consideration as the one for the linear case, it can be defined a **non-singular** state-dependent matrix (i.e. *it has n independent rows*) which has the same meaning of the Observability Matrix in (3.5). For the nonlinear case $\mathcal{O}(\mathbf{x})$ can be defined as follows:

$$\mathcal{O}(\mathbf{x}) = \begin{pmatrix} \frac{\partial L_g^0 \mathbf{h}(\mathbf{x})}{\partial \mathbf{x}} \\ \frac{\partial L_g^1 \mathbf{h}(\mathbf{x})}{\partial \mathbf{x}} \\ \frac{\partial L_g^2 \mathbf{h}(\mathbf{x})}{\partial \mathbf{x}} \\ \vdots \\ \frac{\partial L_g^{n-1} \mathbf{h}(\mathbf{x})}{\partial \mathbf{x}} \end{pmatrix} \in \mathbb{R}^{p \cdot n \times n} \quad (3.21)$$

After those considerations, the extension of Lemma 3.2 for the nonlinear case of the previous treatment can be presented. Let's defined, according to Lemma 3.2, the positive integers v_i and r_i as the maximum number of successive linearly independent derivatives of the i -th output of Σ_{NL} and the relative degree of the i -th output of the system with respect to the unknown input vector \mathbf{f} , respectively. A nonlinear system Σ_{NL} is said to be strongly Observable is the following Lemma is satisfied:

Lemma 3.3. *The nonlinear system Σ_{NL} is strongly observable if it is possible to define a set of positive integers $\mathcal{U} := \{\mu_1, \dots, \mu_h\}$ with $h \leq p$, in which each element is associated with one output's component, such that the following conditions are satisfied:*

$$\begin{cases} \mu_i \leq v_i \\ \mu_i \leq r_i \end{cases}, \quad \mu_1 + \mu_2 + \dots + \mu_h = n \quad \text{with } i = 1, 2, \dots, h \quad (3.22)$$

$$\det \{M\} \neq 0, \quad M = \begin{pmatrix} M_1 \\ \vdots \\ M_i \\ \vdots \\ M_h \end{pmatrix}, \quad M_i = \begin{pmatrix} \frac{\partial L_g^0 y_i(\mathbf{x})}{\partial \mathbf{x}} \\ \frac{\partial L_g^1 y_i(\mathbf{x})}{\partial \mathbf{x}} \\ \frac{\partial L_g^2 y_i(\mathbf{x})}{\partial \mathbf{x}} \\ \vdots \\ \frac{\partial L_g^{\mu_i-1} y_i(\mathbf{x})}{\partial \mathbf{x}} \end{pmatrix} \in \mathbb{R}^{\mu_i \times n} \quad (3.23)$$

■

Since this extension straight derives from an analogous treatment as the one presented in Proof 3.2.2, and because in rest of the Thesis only systems in a *Luré Form* will be considered, for the sake of brevity, the previous Lemma is provided without any proof.

3.3 Conclusion

Since, as shown in Chapter 2, every complex system can be represented as an interconnection of subsystems or equivalently with a multi-input-multi-output (MIMO) representation in this Chapter some notion of observability in MIMO systems has been presented in order to provide to the reader the necessary notion for understanding the treatment presented in Chapter 6 where a new approach for state estimation and unknown input reconstruction of a class of connected heterogeneous LTI MIMO systems is presented.

In particular, some literature results and the recent Author's work presented in [Pilloni et al., 2013a], for evaluating the strong observability properties of MIMO System subjected to unknown input and achieve the complete unknown input reconstruction has been discussed.

Chapter 4

Sliding Mode Control

Due to the extensively use of Sliding Mode concepts in the second part of this Thesis (see Part II), in which all the Author's contributions related to this work are presented, in this Chapter a brief survey on Sliding Mode Control (SMC) Theory, to provide to the reader the necessary notions for understanding the treatment presented in the remainder of the Thesis is presented.

This Chapter is organized as follows: starting from a general case of sliding mode in dynamical systems with discontinuous right-hand side, the classic approaches to sliding mode control systems are considered. Then, Higher-Order Sliding Modes are presented as a tool to remove discontinuity from the control action, and to deal with higher relative degree systems.

Furthermore some techniques for chattering analysis are discussed with particular emphasis to the *Describing Function* approach [Vander Velde, 1968]. As a conclusion a procedure for chattering attenuation by choosing properly the control parameters is considered for a particular class of second order sliding mode (2-SM) control algorithm.

4.1 Introduction

The control of dynamical systems in the presence of parameter uncertainties or unmodeled dynamics is a common problem to deal with in real applications. For these reason the problem of controlling uncertain systems has attracted great interest in the research community [Corless & Leitmann, 1981, Oh & Khalil, 1997, Young et al., 1996, Bartolini et al., 2003]. Among existing methodologies, one of the most renowned, due to its high simplicity it is for sure the sliding mode control (SMC) technique [Utkin, 1992, Slotine et al., 1991, Edwards & Spurgeon, 1998] which is a special class of variable-structure systems (VSSs) [Emelyanov, 1959, Utkin, 1977].

The main idea behinds SMC techniques is to design a sliding surface under onto the controlled system trajectories are constrained, by applying a discontinuous control action. The latter forces the system to *slide* along the designed surface on which the behavior of the system is the expected one [Utkin, 1992]. Notice that, in order to guarantee the control aims the control must be designed with a sufficient authority to dominate the uncertainties and the disturbances acting on the system. In particular the control action must promptly react

to any deviation, from the prescribed behavior and then, steer the system back to the sliding surface. The main advantage of this approach is that the sliding behavior does not depend to model uncertainties or disturbances if the *control strength* is larger enough to dominate all the system's uncertainties [Bartolini et al., 1999, Bartolini et al., 2003, Slotine et al., 1991].

Although the claimed robustness properties, real SMC implementation has a major drawback. Indeed, theoretically, the control action should switch with infinite frequency to provide total uncertainty's rejection, but due to the limited bandwidth of real control devices (i.e. electronic converters) which perform a finite switching frequency, high-frequency components appear in the control signal, which, propagating along the control loop, may excite parasitic resonant modes of the plant (i.e. unmodeled dynamics). Therefore, at steady-state the system trajectory rapidly oscillates around the sliding surface [Bartolini, 1989]. This phenomenon is known as *chattering* [Boiko et al., 2006, Pilloni et al., 2012a].

Chattering, along with the necessity of discontinuous control action, constitute two of the main criticisms of Variable Structure Systems (VSS) with sliding modes, and these drawbacks are much more evident when dealing with mechanical systems in which, rapidly changing in the control actions can induce fatigue and damaging in a short time [Utkin & Guldner, 1999].

The most common approach to avoid chattering is to approximate the sign function of the discontinuous control by the saturation function. Anyway in this case, the system motion is confined within a boundary layer of the sliding manifold, the robustness' the properties are not preserved and oscillation can appear as well.

More recently a different approach to avoid chattering has been developed. The idea is to augment the controlled system dynamics, by adding integrators at the input side, so as to obtain a higher-order system in which the actual control signal and its derivatives explicitly appear. If the discontinuous signal coincides with the highest derivative of the actual plant control, the latter results to be continuous with a smoothness degree depending on the considered derivative order. This procedure refers to higher order SM (HOSM) [Levant, 1993a, Bartolini et al., 1998a] and will be shortly discussed in the following along with some approaches for chattering analysis.

Finally, it is worth to mention that those phenomenon are less significant in software-based applications such as for example estimation problems, in which chattering can be filtered and then neglected without significant loss in performance. For these reasons, SMC algorithm in the last decades, has also found a rich soil in the area of robust state-estimation and fault detection isolation (see for example [Spurgeon, 2008] and references therein). In the following a brief overview of all the aspects cited above will be provided.

4.2 Sliding modes in discontinuous control systems

Consider a general nonlinear dynamic defined as follows:

$$\dot{\mathbf{x}}(t) = \mathbf{f}(\mathbf{x}(t), \mathbf{u}(t), t) \quad (4.1)$$

where $\mathbf{x} \in \mathbb{R}^n$ is the state vector, $\mathbf{u} \in \mathbb{R}^q$ is the control input vector, t is time, and $\mathbf{f} : \mathbb{R}^n \times \mathbb{R}^q \times \mathbb{R}^+ \rightarrow \mathbb{R}^n$ is a vector field in the state space. Assume that the state space is divided into

2^q subspaces S_k with $k = 1, 2, \dots, 2^q$, by the guard

$$\mathfrak{G} = \{\mathbf{x} \quad : \quad \sigma(\mathbf{x}) = 0\} \quad (4.2)$$

where $\sigma : \mathbb{R}^n \rightarrow \mathbb{R}^q$ is a sufficiently smooth vector function. Its ε -vicinity is defined as follows

$$\mathfrak{V}_\varepsilon = \{\mathbf{x} \in \mathbb{R}^n \quad : \quad \|\sigma(\mathbf{x})\| \leq \varepsilon; \quad \varepsilon > 0\} \quad (4.3)$$

Define the control vector by a state feedback law such that

$$\mathbf{u}(t) = \mathbf{u}_k(\mathbf{x}) \quad \text{if} \quad \mathbf{x} \in S_k \quad \text{with} \quad k \in \{1, 2, \dots, 2^q\} \quad (4.4)$$

then the following theorem holds:

Theorem 4.1. *Consider the nonlinear dynamics (4.1) and let $\mathbf{J}_x^\sigma(\mathbf{x}(t)) = \partial\sigma(\mathbf{x})/\partial\mathbf{x}$ be the Jacobian Matrix of σ with respect to \mathbf{x} ; if a proper ε defining (4.3) exists such that the control vector (4.4) satisfies the conditions:*

$$\text{sign}(\mathbf{J}_x^\sigma(\mathbf{x}(t)) \cdot \mathbf{f}(\mathbf{x}(t), \mathbf{u}(t), t)) = -\text{sign}(\sigma) \quad \forall \quad \mathbf{x} \in V_\varepsilon \quad (4.5)$$

then the guard \mathfrak{G} in (4.3) is an invariant set in the state space and a sliding mode occurs on it.

■

Proof. Consider the q -dimensional vector

$$\mathbf{s} = \sigma(\mathbf{x}) \quad (4.6)$$

usually named sliding variables vector, and define the positive definite function

$$V(\mathbf{s}) = \frac{1}{2} \cdot \|\mathbf{s}\|_2^2 \quad (4.7)$$

The total time derivative of V is

$$\dot{V}(\mathbf{s}) = \mathbf{s}^T \dot{\mathbf{s}} = \mathbf{s}^T \cdot \text{diag}\{\text{sign}(\dot{s}_i)\} \cdot |\dot{\mathbf{s}}| \quad (4.8)$$

Taking into account the implicit function theorem, (4.1), (4.4) and (4.5) then (4.8) results into

$$\dot{V}(\mathbf{s}) = -\mathbf{s}^T \cdot \text{diag}\{\text{sign}(s_i)\} \cdot |\dot{\mathbf{s}}| = -|\mathbf{s}|^T \cdot |\dot{\mathbf{s}}| \quad (4.9)$$

Therefore $V(\mathbf{s})$ is a Lyapunov function and the origin of the q -dimensional space of variables \mathbf{s} is an asymptotically stable equilibrium point.

■

Remark 4.1. Notice that, as discussed in [Utkin, 1992], from a geometrical point of view, condition (4.5) implies that within the neighborhood \mathfrak{V}_ε of \mathfrak{G} the vector field defining the state dynamics (4.1) is always directed towards \mathfrak{G} itself. Furthermore, if the magnitude of the control vector \mathbf{u} components is sufficiently large so that

$$|s_i| \geq \eta \quad \text{with} \quad i = 1, 2, \dots, q \quad (4.10)$$

condition (4.9) satisfies the classical well-known reaching condition

$$\frac{1}{2} \frac{d}{dt} \mathbf{s}^T \cdot \mathbf{s} \leq -\eta |\mathbf{s}|, \quad \eta > 0 \quad (4.11)$$

As a consequence, the invariant set \mathfrak{G} is reached in a finite time

$$T_r = t_0 + \frac{|\mathbf{s}(t_0)|}{\eta} \quad (4.12)$$

where $\mathbf{s}(t_0)$, with $|\mathbf{s}(t_0)| = \xi(\varepsilon) < \varepsilon$ is known as the sliding variables vector at initial time t_0 . ■

Remark 4.2. From the definition of control \mathbf{u} in (4.4), and taking into account condition (4.5), it is apparent that the vector field \mathbf{f} defining the system dynamics (4.1) is discontinuous across the boundaries of the guard \mathfrak{G} . Therefore, function $\mathbf{f}(\mathbf{x}(t), \mathbf{u}(t), t)$ has to be Lebesgue integrable on time and solution of (4.1) exists in the Filippov sense [Filippov, 1988]. Control \mathbf{u} switches at infinite frequency when the system performs a sliding mode on \mathfrak{G} , which is usually named sliding surface [Utkin, 1992]. ■

Following from those considerations, it is interesting to analyze the state trajectory when system (4.1) is constrained on \mathfrak{G} . A simple approach to the problem is to consider the variable \mathbf{s} defined by (4.6) as the output of the dynamical system (4.1), in which function $\mathbf{s} : \mathbb{R}^n \rightarrow \mathbb{R}^q$ represents the so-called output transformation. In classic sliding mode control usually condition (4.5) is assured by a proper choice of the control variables \mathbf{u} so that matrix $\partial \dot{\mathbf{s}} / \partial \mathbf{u}$ has full rank in \mathfrak{V}_ε . Then the overall system dynamics can be split into the input-output dynamics

$$\dot{\mathbf{s}} = \mathbf{J}_x^\sigma(\mathbf{x}(t), \mathbf{u}(t), t) = \phi(\mathbf{x}(t), \mathbf{u}(t), t) \quad (4.13)$$

and the internal dynamics

$$\dot{\mathbf{w}} = \psi(\mathbf{x}(t), \mathbf{u}(t), t) \quad (4.14)$$

where $\mathbf{w} \in \mathbb{R}^{n-q}$ is named internal state and $\psi : \mathbb{R}^n \times \mathbb{R}^+ \rightarrow \mathbb{R}^{n-q}$ is a sufficiently smooth vector function. The relationship between the vector state \mathbf{x} and the new state variables \mathbf{s} and \mathbf{w} is defined by a diffeomorphism $\Phi : \mathbb{R}^n \rightarrow \mathbb{R}^n$ preserving the origin and defined as follows in a vicinity of the guard \mathfrak{G} [Isidori, 1995, Slotine et al., 1991]:

$$[\mathbf{s}^T, \mathbf{w}^T]^T = \Phi(\mathbf{x}) \quad : \quad \Phi(\mathbf{0}) = \mathbf{0} \quad \forall \quad \mathbf{x} \in \mathfrak{V}_\varepsilon \quad (4.15)$$

From this statement, it can be presented the following result [Pisano & Usai, 2011]:

Theorem 4.2. Assume that the diffeomorphic transformation (4.15) holds in the vicinity \mathfrak{V}_ε of the sliding manifold. Then system (4.1), (4.6) is stabilizable if a unique control \mathbf{u} exists such that conditions of Theorem 4.1 are satisfied, the internal dynamics (4.14) is Bounded-Input Bounded-State (BIBS) stable and the zero dynamics

$$\dot{\mathbf{w}} = \psi(\mathbf{w}(t), \mathbf{0}, t) \quad (4.16)$$

is stable in the Lyapunov sense. ■

Proof. The proof straightforwardly derives from results of Theorem 4.1 and the stability of the internal dynamics when the system is constrained onto \mathfrak{G} .

When the state is constrained onto the sliding surface \mathfrak{S} , the system behavior is completely defined by the zero dynamics (4.16) [Isidori, 1995], taking into account the invertible relationship (4.15). That is, only a reduced order dynamics has to be considered during the sliding motion [Utkin, 1992]. This *order reduction* property is a peculiar phenomenon in variable structure systems with sliding modes. ■

4.3 First Order Sliding Mode

Finding a feedback control (4.4) such that Theorem 4.1 holds is quite hard in the general case. Therefore, Sliding Mode Control (SMC) of uncertain systems usually refers to systems whose dynamics is affine with respect to control [Edwards & Spurgeon, 1998][Utkin, 1992] as follows:

$$\dot{\mathbf{x}}(t) = \mathbf{A}(\mathbf{x}(t), t) + \mathbf{B}(\mathbf{x}(t), t)\mathbf{u}(t) \quad (4.17)$$

where $\mathbf{A} : \mathbb{R}^n \times \mathbb{R}^+ \rightarrow \mathbb{R}^n$ is a vector field in the state space, possibly uncertain, and \mathbf{B} is a $n \times q$ matrix of functions $b_{ij}(\mathbf{x}(t), t) : \mathbb{R}^n \times \mathbb{R}^+ \rightarrow \mathbb{R}$.

When the SMC approach is implemented, the first step of the design procedure is to define a proper system output \mathbf{s} , as in (4.6), such that the resulting internal dynamics is BIBS stable and, possibly, its zero dynamics is asymptotically stable. Then the control \mathbf{u} is designed such that $\|\mathbf{s}\|$ goes to zero in a finite time in spite of possible uncertainties.

Theorem 4.3. Consider system (4.17), (4.6). Assume that the corresponding internal dynamics is BIBS stable, that the norm of its uncertain drift term $\mathbf{A}(\mathbf{x}(t), t)$ is upper bounded by a known function $F : \mathbb{R}^n \rightarrow \mathbb{R}^+$, such that

$$\|\mathbf{A}(\mathbf{x}(t), t)\| \leq F(\mathbf{x}) \quad (4.18)$$

and that the known square matrix $\mathbf{G}(\mathbf{x}, t) = \mathbf{J}_x^\sigma(\mathbf{x}) \cdot \mathbf{B}(\mathbf{x}, t) \in \mathbb{R}^{q \times q}$ is non singular $\forall \mathbf{x} \in \mathfrak{X}_\varepsilon$, uniformly in time. Then, the set \mathfrak{S} in (4.2) is made finite time stable by means of the control law

$$\mathbf{u}(t) = -(F(\mathbf{x})\|\mathbf{J}_x^\sigma\| + \eta) \cdot [\mathbf{G}(\mathbf{x})]^{-1} \text{sign}(\mathbf{s}) \quad \text{with} \quad \eta > 0 \quad (4.19)$$

Proof. The input-output dynamics of system (4.17), (4.6) is ■

$$\dot{\mathbf{s}}(t) = \mathbf{J}_x^\sigma(\mathbf{x}) \cdot \mathbf{A}(\mathbf{x}, t) + \mathbf{G}(\mathbf{x}, t)\mathbf{u}(t) \quad (4.20)$$

Consider the positive definite function (4.7). Considering the time derivative of V along the trajectories of system (4.20), and taking into account (4.19), (4.8) yields

$$\begin{aligned} \dot{V}(\mathbf{s}) &= \mathbf{s}^T \cdot (\mathbf{J}_x^\sigma(\mathbf{x}) \cdot \mathbf{A}(\mathbf{x}, t) - (F(\mathbf{x})\|\mathbf{J}_x^\sigma\| + \eta) \cdot \text{sign}(\mathbf{s})) = \\ &= -\eta \cdot \mathbf{s}^T \text{sign}(\mathbf{s}) = -\eta \cdot \|\mathbf{s}\|_1 < -\eta \|\mathbf{s}\|_2 < 0 \end{aligned} \quad (4.21)$$

Notice that, when the matrix control gain $\mathbf{B}(\mathbf{x}, t)$ is uncertain, a similar theorem can be proved if some condition about \mathbf{B} is met. ■

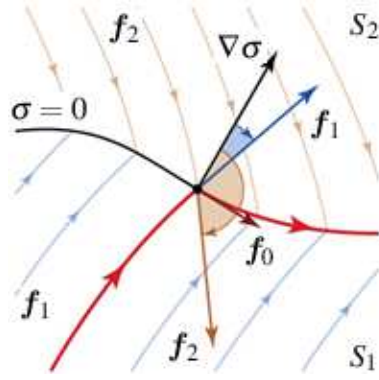


Figure 4.1: Filippov's continuation method.

Theorem 4.4. Consider system (4.17), (4.6) and satisfying (4.18). Assume that the corresponding internal dynamics is BIBS stable, that the uncertain gain matrix $\mathbf{B}(\mathbf{x}, t)$ and the guard \mathfrak{G} are such that the square matrix $\mathbf{G}(\mathbf{x}, t) = \mathbf{J}_x^\sigma(\mathbf{x}) \cdot \mathbf{B}(\mathbf{x}, t)$ is positive definite and a known bound $\Lambda_m > 0$ exists such that

$$\Lambda_m \leq \min \left\{ \lambda_i^{\mathbf{G}}(\mathbf{x}, t); i = 1, 2, \dots, q \right\} \quad \forall \mathbf{x} \in \mathfrak{X}_\varepsilon, \quad \forall t \in \mathbb{R}^+ \quad (4.22)$$

where $\lambda_i^{\mathbf{G}}(\mathbf{x}, t)$ with $i = 1, 2, \dots, q$ are the eigenvalues of matrix $\mathbf{G}(\mathbf{x}, t)$. Then, the guard \mathfrak{G} in (4.2) is made finite time stable by means of the control law

$$u(t) = -\frac{F(\mathbf{x}) \|\mathbf{J}_x^\sigma(\mathbf{x})\| + \eta}{\Lambda_m} \cdot \frac{\mathbf{s}}{\|\mathbf{s}\|_2} \quad \text{with } \eta > 0 \quad (4.23)$$

■

Proof. The proof follows the same steps than previous Theorem 4.3. Define function $V(\mathbf{s})$ as in (4.7) and consider (4.20) and (4.23) into its time derivative (4.8). By (4.22) it results

$$\begin{aligned} \dot{V}(\mathbf{s}) &= \mathbf{s}^T \cdot \left(\mathbf{J}_x^\sigma(\mathbf{x}) \cdot \mathbf{A}(\mathbf{x}, t) - \frac{F(\mathbf{x}) \|\mathbf{J}_x^\sigma(\mathbf{x})\| + \eta}{\Lambda_m} \mathbf{G}(\mathbf{x}, t) \frac{\mathbf{s}}{\|\mathbf{s}\|_2} \right) \leq \\ &\leq -\frac{\eta}{\Lambda_m \|\mathbf{s}\|_2} \cdot \mathbf{s}^T \mathbf{G}(\mathbf{x}, t) \mathbf{s} \leq -\eta \|\mathbf{s}\|_2 < 0 \end{aligned} \quad (4.24)$$

■

Notice that to overcome the presence of uncertain terms in the system model the control's magnitude must be sufficiently large. The positive parameter $\eta > 0$ is a design parameter which guarantees the above mentioned reaching condition. In literature, several design methods can be found [Utkin, 1992, Edwards & Spurgeon, 1998, Young et al., 1996, Bartolini et al., 2008].

4.3.1 Filippov Continuation and Equivalent Control

When the system exhibits a sliding-mode behavior, the discontinuous control (4.19), or (4.23), undergoes infinite-frequency switchings. The effect of the discontinuous and infinite-frequency switching control on the system dynamics is the same as that of the continuous

control which allows the state trajectory to remain on the sliding surface [Slotine et al., 1991, Filippov, 1988, Utkin, 1992]. Considering the non linear system (4.1) with a scalar input (for example $q = 1$), in [Filippov,] it was shown that such a continuous dynamics is a convex combination of the two vector fields

$$\mathbf{f}_1 = \mathbf{f}(\mathbf{x}, \mathbf{u}_1, t) \quad , \quad \mathbf{f}_2 = \mathbf{f}(\mathbf{x}, \mathbf{u}_2, t) \quad (4.25)$$

defined on partition S_1 and S_2 , such that:

$$\dot{\mathbf{x}}(t) = \mathbf{f}_0(\mathbf{x}, t) \quad (4.26)$$

with

$$\mathbf{f}_0 = \alpha \cdot \mathbf{f}_1 + (1 - \alpha) \cdot \mathbf{f}_2 \quad \text{with} \quad \alpha = \frac{\nabla \sigma \cdot \mathbf{f}_2}{\nabla \sigma \cdot (\mathbf{f}_2 - \mathbf{f}_1)} \sigma = 0 \quad (4.27)$$

The above approach to regularize differential equations with discontinuous right-hand side is called the Filippov's continuation method. A geometrical representation of this continuation is shown in Figure 4.1 where the discontinuity surface is defined by $\sigma = 0$ and the vector fields for S_1 (i.e. $\sigma > 0$) and S_2 (i.e. $\sigma < 0$) are \mathbf{f}_1 and \mathbf{f}_2 , respectively.

Extending those concepts to a generic control vector $\mathbf{u} \in \mathbb{R}^q$ the continuous vector field \mathbf{f}_0 allowing the continuation of the state trajectory on \mathcal{G} is still a convex combination of the 2^q vector fields $\mathbf{f}_k = \mathbf{f}(\mathbf{x}, \mathbf{u}_k, t)$ with $k = 1, 2, \dots, 2^q$ as in (4.26) where:

$$\mathbf{f}_0 = \sum_{k=1}^{2^q} \alpha_k \cdot \mathbf{f}_k \quad \text{with} \quad \sum_{k=1}^{2^q} \alpha_k = 1 \quad (4.28)$$

As a remark, if the discontinuous right-hand-side of the differential equation defining the system dynamics satisfies some geometric conditions, the Filippov's continuation method can be unambiguously defined on \mathcal{G} [Bartolini et al., 2004]. Furthermore, recently explicit formulas for the computation of coefficients α_k has been presented [Dieci & Lopez, 2009]. Those concepts are discussed with greater length in [Utkin, 1992]. Anyway the most intuitively and appealing approach capable to described the behavior of the system along the sliding surface is the the method of *equivalent control* proposed in [Utkin, 1977]. In a few words, the equivalent control is the control action necessary to maintain an ideal sliding motion by nullifying $\dot{\sigma}$; more formally:

$$\dot{\mathbf{x}}(t) = \mathbf{f}(\mathbf{x}, \mathbf{u}_{eq}, t) \quad (4.29)$$

$$\dot{\sigma} = \frac{\partial}{\partial \mathbf{x}} \sigma(\mathbf{x}, \mathbf{u}_{eq}, t) \cdot \mathbf{f}(\mathbf{x}, \mathbf{u}_{eq}, t) = 0 \quad (4.30)$$

With reference to affine systems in (4.17), by nullifying (4.20), the equivalent control takes the following expression

$$\mathbf{u}_{eq}(t) = -[\mathbf{G}(\mathbf{x}, t)]^{-1} \mathbf{J}_x^\sigma(\mathbf{x}) \cdot \mathbf{A}(\mathbf{x}, t) \quad (4.31)$$

Remark 4.3. *It is worth to underline how the equivalent control approach and the Filippov's continuation method give the same results only for affine scalar control [Utkin, 1992] and for a limited class of nonlinear systems[Bartolini & Zolezzi, 1985]. More recently in [Levaggi & Villa, 2007, Bartolini et al., 2007b] has been proposed regularization approaches for wider classes of nonlinear systems. ■*

Notice that the non-singularity condition for the q -dimensional square matrix $\mathbf{G}(\mathbf{x}, t)$ implies that the sliding variable vector \mathbf{s} has relative degree vector $\mathbf{r} = (1, \dots, 1)$ with respect to the control input \mathbf{u} (see i.e. Equation (6.5) in Chapter 3). In other words, this means that \mathbf{u} explicitly appears at the first derivative of \mathbf{s} . This condition can be thought as a kind of controllability condition [Slotine et al., 1991, Pisano & Usai, 2011].

It is worth to mention that if such a condition is not satisfied, then the control input \mathbf{u} could have relative degree higher than one. In literature, it is common to referred to this kind of sliding mode algorithm to as Higher Order Sliding Mode (HOSM) [Emelyanov, 1959, Fridman & Levant, 1996, Levant, 1993a, Bartolini et al., 1998a, Bartolini et al., 2008]. In the next section those algorithm will be briefly discussed.

4.4 Higher-order sliding mode control

With reference to HOSM, a second order sliding mode (2-SM) appears when the differential inclusion $V(\mathbf{x}, t)$ defining the closed loop dynamics (4.1),(4.4) belongs to the tangential space of the sliding manifold \mathfrak{G} defined accordingly to (4.2) as follows [Levant, 1993a]:

$$\mathfrak{G}_2 = \{\mathbf{x} \quad : \quad \dot{\sigma}(\mathbf{x}) = \sigma(\mathbf{x}) = 0\} \quad (4.32)$$

Therefore, extending this definition an r -SM behavior appears when the closed loop dynamic are confined to the following manifold

$$\mathfrak{G}_r = \left\{ \mathbf{x} \quad : \quad \frac{d^{r-1}}{dt} \sigma(\mathbf{x}) = \dots = \dot{\sigma}(\mathbf{x}) = \sigma(\mathbf{x}) = 0 \right\} \quad (4.33)$$

where $\sigma : \mathbb{R}^n \rightarrow \mathbb{R}^q$ is, again, a sufficiently smooth vector function and r represents the order of the so-called sliding set. The following definition can be now presented:

Definition 4.1. [Levant, 1993a] *Let the r -sliding set (4.33) be non-empty and assume that it is locally an integral set in Filippov's sense. Then the corresponding motion satisfying (4.33) is called r -SM with respect to the constraint function σ .* ■

Remark 4.4. *Notice that HOSMC are difficult to design with respect to a general nonlinear systems (4.1) because extends the sliding manifold (4.2) by using (4.33) for a generic order r is not a trivial task, because, supposed q control variables available (i.e. $\mathbf{u} \in \mathbb{R}^q$), it should results that condition (4.5) should be guaranteed with respect to the whole resulting rq variables $\sigma, \dot{\sigma}, \dots, \sigma^r$, which is impossible for a generic scenario.* ■

An affine time-independent structure for the nonlinear dynamics can be obtained by considering an augmented dynamics in which the control input \mathbf{u} is part of an augmented vector state and its time derivative $\mathbf{v} = \dot{\mathbf{u}}$ is the actual control to be designed:

$$\begin{bmatrix} \dot{\hat{\mathbf{x}}} \\ \dot{z} \\ \dot{\mathbf{u}} \\ \dot{\hat{\mathbf{x}}} \end{bmatrix} = \begin{bmatrix} \hat{\mathbf{x}} \\ 1 \\ 0 \\ \frac{\partial}{\partial x_{n+1}} \mathbf{f}(\mathbf{x}, \mathbf{u}, t) + \frac{\partial}{\partial \mathbf{x}} \mathbf{f}(\mathbf{x}, \mathbf{u}, t) \cdot \hat{\mathbf{x}} \end{bmatrix} + \begin{bmatrix} 0 \\ 0 \\ 1 \\ \frac{\partial}{\partial \mathbf{u}} \mathbf{f}(\mathbf{x}, \mathbf{u}, t) \end{bmatrix} \cdot \mathbf{v} \quad (4.34)$$

in which $\partial \mathbf{f} / \partial \mathbf{u}$ is a full-rank matrix [Levant, 1993a]. Thus, when HOSM algorithms are

considered, it is common to refer to affine stationary nonlinear systems as

$$\dot{\mathbf{x}}(t) = \mathbf{f}(\mathbf{x}) + \mathbf{g}(\mathbf{x}) \cdot \mathbf{u}(t) \quad (4.35)$$

where $\mathbf{x} \in \mathbb{R}^n$ is the state vector (possibly augmented), $\mathbf{u} \in \mathbb{R}^q$ is the control input, possibly the time derivative of the plant input, $\mathbf{f} : \mathbb{R}^n \rightarrow \mathbb{R}^n$ and $\mathbf{g} : \mathbb{R}^n \rightarrow \mathbb{R}^n \times \mathbb{R}^q$ are sufficiently smooth vector fields and matrix, respectively, in the state space.

Remark 4.5. For many years the possibility of considering the time derivative of the plant input as the discontinuous control variable, given by the implementation of second-order sliding mode control systems, was considered an eligible approach to eliminate the chattering phenomenon in real control systems, since the plant input results to be continuous [Emelyanov, 1959, Levant, 1993a, Bartolini et al., 1998b]. Anyway, recently, it was proven that chattering in real applications can not be removed but only attenuated because it is associated to both nonideal/unmodeled actuator's dynamics and measurement devices that cause finite frequency switchings of the control command [Fridman, 2003, Boiko et al., 2004, Boiko et al., 2006, Pilloni et al., 2012a, Lee & Utkin, 2007]. ■

Proposition 4.1. Given the system dynamics (4.35), a r -SMC on the manifold (4.2) can be designed if $n = rq$, $L_g L_f^k \sigma = 0 \forall k = 1, 2, \dots, r-2$ and $L_g L_f^{r-1} \sigma$ has full rank. ■

As discussed in [Pisano & Usai, 2011], the simplest way to implement a high order sliding mode algorithm is to consider a proper linear combination of the functions defining \mathfrak{G}_r as the output for system (4.35) by resorting to the so-called Dynamical sliding mode control [Sira-Ramírez, 1993].

Theorem 4.5. [Pisano & Usai, 2011] Consider system (4.35) and the set (4.2). Define the system output as

$$\mathbf{s} = \sigma^{r-1} + \sum_{i=0}^{r-2} c_i \sigma^{(i)} \quad (4.36)$$

where $c_i \in \mathbb{R}^+$ are proper coefficients such that the polynomial $P(p) = p^{r-1} + \sum_{i=0}^{r-2} c_i p^i$ is Hurwitz. If the corresponding internal dynamics is BIBS stable and the system dynamics fulfill the following conditions:

$$\begin{aligned} \|L_g^k \sigma\| &\leq \Lambda_k(\mathbf{x}) & k = 1, 2, \dots, r \\ L_g L_f^k \sigma &= 0 & k = 0, 1, 2, \dots, r-2 \\ 0 < \Lambda_m &\leq \min \left\{ \lambda_i \left[L_g L_f^{r-1} \sigma \right] (\mathbf{x}, t); i = 1, \dots, q \right\} & \forall \mathbf{x} \in \mathfrak{X}_\varepsilon, \quad \forall t \end{aligned} \quad (4.37)$$

where $\Lambda_k(\mathbf{x}) : \mathbb{R}^n \rightarrow \mathbb{R}^+$ with $k = 1, 2, \dots, r$ are sufficiently smooth positive functions, and Λ_m is a constant lower bound for the eigenvalues of the matrix $L_g L_f^{r-1} \sigma$, then the control law

$$\mathbf{u}(t) = -\frac{\Lambda_r(\mathbf{x}) + \sum_{i=0}^{r-2} c_i \Lambda_{i+1}(\mathbf{x}) + \mathbf{v}}{\Lambda_m} \cdot \frac{\mathbf{s}}{\|\mathbf{s}\|_s} \quad (4.38)$$

with $\mathbf{v} > 0$, makes the integral manifold (4.33) asymptotically stable, and a r th-order sliding mode on the manifold \mathfrak{G} in (4.2) is established asymptotically. ■

Proof. Conditions (4.37) and (4.37) fulfill Theorem 4.4 and therefore $\mathbf{s} = 0$ is achieved in a finite time T_r . From that time instant on the internal dynamics of variables $\sigma^{(k)}$ with $k = 0, 1, \dots, r-1$, is characterized by a linear dynamics whose stable modes are defined by the Hurwitz polynomial $P(p)$, and therefore $\sigma^{(k)} \rightarrow \mathbf{0} \forall k = 0, 1, \dots, r-1$, asymptotically. ■

Notice that the above HOSM algorithm is, practically, an extension of classical first-order sliding mode. Indeed the system state is forced onto a linear manifold in a new space defined by the variable s and their $r - 1$ time derivatives, and on such a manifold the origin is reached asymptotically.

4.4.1 Second-order sliding mode control

In the following a brief presentation of the most used 2-SMC algorithms [Levant, 1993a], [Bartolini et al., 1999] respectively: the Generalized Sub-Optimal [Bartolini et al., 1999] and the Super-Twisting [Levant, 1993a] algorithm is provided. For the sake of brevity only the tuning rules will be provided without any proof. The reader is referred to [Pisano & Usai, 2011] and reference therein for further details.

4.4.2 The Generalized Sub-Optimal controller

Both the *twisting* [Levant, 1993a] and the *sub-optimal* algorithm [Bartolini et al., 1998b] can deal with relative-degree two constraint variables. They are, both, special cases of the general algorithm [Bartolini et al., 2003]

$$u(t) = -\alpha(t)U \operatorname{sign}(s - \beta s_M) \quad (4.39)$$

with

$$\alpha(t) = \begin{cases} 1 & , \text{ if } (s - s_M)s_M \geq 0 \\ \alpha^* & , \text{ if } (s - s_M)s_M < 0 \end{cases} \quad \beta \in [0, 1) \quad (4.40)$$

where U is the minimum control magnitude, α^* is called the *modulation factor*, β is the *anticipation factor*, and s_M is the value of the sliding variable s corresponding to the most recent local minimum, maximum or horizontal flex point (i.e., the value of s at the last time instant $t_{M,k}$ at which $\dot{s} = 0$ occurs). s_M can be evaluated either by checking $\operatorname{sign}(\dot{s})$ or, by inspection of the past values of $s(t)$, or, approximately, by inspection of the first-difference of $s(t)$; in last two cases no information about \dot{s} is needed. U , α^* , and β are the controller parameters, that must be tuned to assure the finite time convergence onto the sliding set \mathfrak{G}_2 in (4.32).

Theorem 4.6. Consider system (4.35) and define its output as (4.6) with $q = 1$. If the system dynamics fulfill the following conditions:

$$\begin{aligned} \|\Lambda_f^2 \sigma\| &\leq \Lambda \\ L_g \sigma &= 0 \\ 0 < \Gamma_m &\leq L_g L_f \sigma \leq \Gamma_M \end{aligned} \quad \forall \mathbf{x} \in \mathfrak{X}_\varepsilon \quad \forall t \quad (4.41)$$

where Λ , Γ_m , Γ_M are known positive constants, then the control law (4.39)-(4.40) with

$$U \geq \frac{\Lambda}{\Gamma_m} \quad , \quad \alpha^* \in [1, +\infty) \cap \left(\frac{2\Lambda + (1 - \beta)\Gamma_M U}{(1 + \beta)\Gamma_m U}, +\infty \right) \quad (4.42)$$

guarantees the finite time stability of the integral manifold (4.32), and a 2nd-order sliding mode is established on \mathfrak{G} . ■

Notice that by setting $\beta = 0$ the control law (4.39)-(4.40) causes the system to have the same trajectories of the well known twisting algorithm [Levant, 1993a] defined as follows:

$$u(t) = -\alpha_1 \text{sign}(s) - \alpha_2 \text{sign}(\dot{s}) \quad (4.43)$$

with $\alpha_2 = U$ and $\alpha_1 = \alpha^*U$. The convergence conditions for this 2-SMC are easily obtained by setting $\beta = 0$ in (4.42) and

$$U > \frac{\Lambda}{\Gamma_m}, \quad \alpha^* \geq \frac{2\Lambda + \Gamma_M U}{\Gamma_m U} \quad (4.44)$$

Whereas, by setting $\beta = 0.5$ the Sub-Optimal SMC algorithm takes place [Bartolini et al., 2003].

4.4.3 The Super-Twisting controller

The so-called Super-Twisting algorithm is conceptually different from the other 2-SMC algorithms, for two reasons: first, it depends only on the actual value of the sliding variable, while the others have more information demand. Second, it is effective only for chattering attenuation purposes as far as relative degree one constraints are dealt with. It is defined by the following dynamic controller [Levant, 1993a]:

$$\begin{aligned} u(t) &= v(t) - \lambda |s(t)|^{\frac{1}{2}} \text{sign}(s(t)) \\ \dot{v}(t) &= -\alpha \text{sign}(s(t)) \end{aligned} \quad (4.45)$$

where $u(t) \in \mathbb{R}$ is the input of system (4.35) with $q = 1$ and $s(t) \in \mathbb{R}$ is the sliding variable (i.e., the system output) (4.6) measuring the distance of the system from the sliding surface \mathfrak{S} in (4.2).

Theorem 4.7. Consider system (4.35), define its output as (4.6) with $q = 1$ and assume that its trajectories are infinitely extendible in time for any bounded feedback control. If the system dynamics fulfill the following conditions:

$$\begin{aligned} \left| L_f^2 \sigma + (L_f L_g \sigma + L_g L_f \sigma) u + L_g^2 \sigma u^2 \right| &\leq \Lambda \quad \forall x \in \mathfrak{X}_\varepsilon, \quad \forall t \\ 0 < \Gamma_m \leq L_g \sigma \leq \Gamma_M \end{aligned} \quad (4.46)$$

where $\Lambda, \Gamma_m, \Gamma_M$ are known positive constants, then the control law (4.45) with

$$\begin{aligned} \alpha &> \frac{\Lambda}{\Gamma_m} \\ \lambda^2 &> 2 \frac{\alpha \Gamma_M + \Lambda}{\Gamma_m} \end{aligned} \quad (4.47)$$

guarantees the finite time stability of the integral manifold (4.32), and a 2nd-order sliding mode is established on \mathfrak{S} . ■

4.4.4 Arbitrary order sliding mode controllers

Consider the problem of finite time stabilization of a r th-order sliding mode for system (4.35) satisfying Proposition 4.1 with $q = 1$. Because of the difficulties in defining r -sliding

controllers with $r = 3$ only recently some results are available for this case [Levant, 2005, Bartolini et al., 2002, Bartolini et al., 2007a, Kryachkov et al., 2010]. Worth of noting the work of Levant [Levant, 2005] where arbitrary order sliding mode controllers have been developed. The key idea was to recursively built, a r -order controller which embed its $(r - 1)$ -order one. The requirement of this approach is the availability of the sliding variable and its time derivatives up to the $(r - 1)$ th order.

Let m be the least common multiple of $1, 2, \dots, r$ and define the following quantities

$$N_{i,r} = \left(\sum_{k=0}^{i-1} |s^{(k)}|^{\frac{m}{r-k}} \right)^{\frac{r-i}{m}} \quad \text{with } i = 1, 2, \dots, r-1 \quad (4.48)$$

and

$$\begin{cases} \phi_{0,r} = s \\ \phi_{i,r} = s^{(i)} + \beta_i N_{i,r} \text{sign}(\phi_{i-1,r}) \quad \text{with } i = 1, 2, \dots, r-1 \end{cases} \quad (4.49)$$

The following Theorem provide conditions for achieving finite-time stability for an arbitrary relative degree system as in (4.35).

Theorem 4.8. [Levant, 2005] Consider system (4.35) (4.6), with $q = 1$, and assume that its trajectories are infinitely extendible in time for any Lebesgue-measurable bounded feedback control. Then, if the following conditions hold for some constants Λ_r , Λ_m and Λ_M

$$\begin{aligned} \|\Lambda_f^r \sigma\| &\leq \Lambda_r \\ L_g L_f^k \sigma &= 0 \quad k = 1, 2, \dots, r-2 \\ 0 < \Gamma_m &\leq L_g L_f^{r-1} \sigma \leq \Gamma_M \quad \forall x \in \mathfrak{X}_\varepsilon, \forall t \end{aligned} \quad (4.50)$$

then, with properly chosen positive parameters $\beta_1, \beta_2, \dots, \beta_{r-1}$, α , the controller

$$u = -\alpha \cdot \text{sign} \left(\phi_{r-1,r}(s, \dot{s}, \dots, s^{(r-1)}) \right) \quad (4.51)$$

where $\phi_{r-1,r}$ is defined in (4.48) and (4.49), makes the integral set (4.33) finite time stable and a r -sliding mode on the manifold \mathfrak{G} in (4.2) is established. ■

Proof. See [Levant, 2005]. ■

The above Theorem determines a controller family (4.51) applicable to all systems of the type (4.35) (4.6), with $q = 1$ and relative degree r , satisfying (4.50). Parameters $\beta_1, \beta_2, \dots, \beta_{r-1}$ affect the reaching time and are to be chosen sufficiently large in index order. Such a parameters β_i can be preliminarily chosen for each r in advance, while parameter α must be chosen specifically on the knowledge, or estimation, of the bounds Λ_r , Γ_m and Γ_M of the uncertain dynamics. The controller performance is insensitive to any system perturbation preserving these bounds. For complexness, in the following few examples of arbitrary order sliding controllers up to order $r = 3$ are provided:

$$r = 1 \quad u = -\alpha \cdot \text{sign}(s) \quad (4.52)$$

$$r = 2 \quad u = -\alpha \cdot \text{sign} \left(\dot{s} + |s|^{\frac{1}{2}} \text{sign}(s) \right) \quad (4.53)$$

$$r = 3 \quad u = -\alpha \cdot \text{sign} \left(\ddot{s} + 2 \left(|\dot{s}|^3 + |s|^2 \right)^{\frac{1}{6}} \text{sign}(s) \right) \quad (4.54)$$

4.5 Chattering Analysis in High-Order Sliding Mode

As well known, the main drawbacks of classical first-order Sliding Modes (1-SM) are principally related to the so-called chattering effect [Utkin & Guldner, 1999, Boiko, 2003]. The main cause of chattering has been identified as the presence of unmodeled parasitic dynamics in the switching devices [Gonçalves et al., 2001, Boiko, 2009]

Three main approaches to counteract the chattering phenomenon in SMC systems were proposed in the mid-eighties:

- the use of a continuous approximation of the relay [Burton & Zinober, 1986];
- the use of an asymptotic state-observer to confine chattering in the observer dynamics bypassing the plant [Bondarev & Utkin, 1985];
- the use of higher-order sliding mode control algorithms [Emelyanov, 1959]

The main drawbacks of the continuous approximations and of the observed-based approach are the deterioration of accuracy and system robustness [Boiko et al., 2006]. In recent papers [Fridman, 2003, Boiko, 2003, Boiko et al., 2006, Boiko et al., 2004, Piloni et al., 2012a] it has been shown that even the 2-SM algorithms suffer from chattering if parasitic dynamics are present increasing the system relative degree. In literature there are two main approaches to chattering analysis: the time-domain analysis of the system dynamics or the use of frequency-domain techniques. Preliminary results regarding the time-domain analysis of chattering in 2-SMC systems were presented in [Boiko et al., 2006].

Anyway, when linear plants are considered frequency-domain techniques can be used to assess the existence and stability of periodic solutions. The Tsytkin locus method [Tsytkin, 1984] and the recently proposed *Locus of a Perturbed Relay System* (LPRS) [Boiko, 2009] provides exact values of the amplitude and frequency of chattering. An approximate analysis method based on the Describing Function (DF) technique could be useful whenever the low-pass filtering condition is satisfied [Atherton, 1975]. The DF method has already been used to estimate the frequency and the amplitude of the periodic motions in the 1-SMC systems [Shtessel & Lee, 1996]. The results obtained via the use of exact frequency-domain techniques feature a satisfactory correspondence with those obtained via the approximate DF method [Boiko, 2003].

With the aim to support the treatment presented in Chapter 5, in which a systematic DF-based tuning procedure for mitigate the unavoidable oscillations in control loop controlled by the Super-Twisting Algorithm when the overall relative degree of the plant is greater than one; in the following some notes about the analysis in the frequency domain of the well known generalized sub-optimal 2-SMC algorithm [Bartolini et al., 1998a] are provided. Notice that, in order to take into account both the Twisting, the Sub-Optimal and even the classical first order SM the generalized sub-optimal 2-SMC algorithm in (4.39) has been considered.

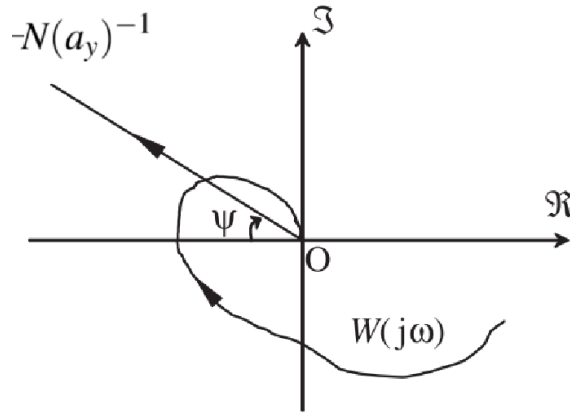


Figure 4.2: DF-analysis in the complex plane.

4.5.1 Describing-function analysis of the generalized sub-optimal algorithm

A way for evaluating self-sustained oscillation in SISO control loops controlled by the GSO algorithm (4.39) when the overall relative degree of the plant plus the actuator is three or more is presented in [Boiko et al., 2006]. The idea is to study the solution of the so-called *Harmonic Balance* [Vander Velde, 1968] presented below:

$$1 + N(a_y) \cdot W(j\omega) = 0 \quad (4.55)$$

where $W(j\omega) = Y(j\omega)/U(j\omega)$ is the transfer function of the plant, supposed to be stable and $N(a_y)$ is the DF of the GSO algorithm with a_y defined as the amplitude of the periodic motion.

The DF of the GSO algorithm is [Boiko et al., 2006] :

$$N(a_y) = \frac{2U}{\pi a_y} \left[(\alpha^* + 1) \sqrt{1 - \beta^2} + j \cdot [(\alpha^* + 1) + \beta(\alpha^* + 1)] \right] \quad (4.56)$$

As known, a periodic solution can appear if the negative reciprocal of the DF (4.56) intersects the Nyquist plot of the plant's harmonic response $W(j\omega)$. Therefore by substituting (4.56) into (4.55), and separating the resulting complex equation in its magnitude and phase, the following well-posed system takes place:

$$M = |W(j\Omega)| = \frac{\pi a_y}{2\sqrt{2}U \sqrt{\alpha^*(1 + \beta) + (1 - \beta)}} \quad (4.57)$$

$$\psi = \text{atan} \left(\frac{(\alpha^* - 1) + \beta(\alpha^* + 1)}{(\alpha^* + 1) \sqrt{1 - \beta^2}} \right) \quad (4.58)$$

from which it is possible to evaluate the amplitude a_y and the frequency Ω of the chattering. The resulting locus in the Nyquist Plane described by the system of equations (4.57)-(4.58) is depicted in Figure 4.2, where M and ψ are respectively the magnitude and the phase of the plant's transfer function $W(j\Omega)$ at the frequency of the steady-state periodic motion Ω . As shown in Figure 4.2, periodic oscillations can occur only if the overall relative degree of

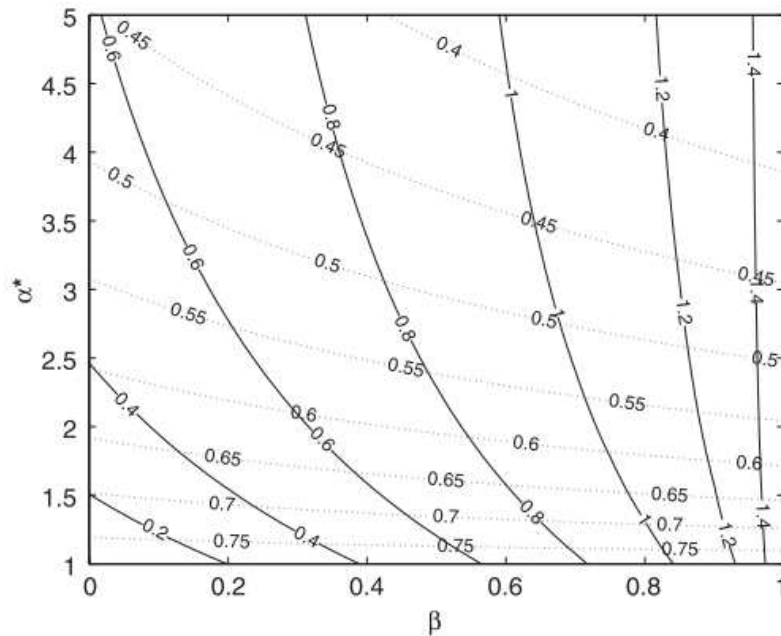


Figure 4.3: Level sets of (continuous lines) and MU/a_y (dotted lines) in the (β, α^*) plane.

the plant is three or more. Indeed only in this case the $-N(a_y)^{-1}$ in (4.56) and $W(j\omega)$ can present an intersection.

As discussed in [Boiko et al., 2006], equations (4.57)-(4.58) can be also employed to impose some prescribed constraints on the amplitude a_y and the frequency Ω of the steady-state periodic oscillation by choosing properly the parameter of the GSO α^* and β (see (4.35)). Notice that the direct use for design of the nonlinear formulas (4.57)-(4.58) can be avoided by using the chart depicted in Figure 4.3 and by applying the following three-step tuning procedure:

Procedure 4.1.

- A. Let $\omega_1 \leq \Omega \leq \omega_2$ be the desired range for the periodic solution frequency;
- B. Evaluate $\psi_1 = -\pi - \arg\{W(j\omega_1)\}$ and $\psi_2 = -\pi - \arg\{W(j\omega_2)\}$;
- C. Identify in the table reported in Fig. 4 proper values for the parameters α^* and β such that $\psi_1 \leq \psi \leq \psi_2$ while maximizing MU/a_y .

Notice that, maximizing MU/a_y means minimizing the oscillation amplitude a_y , is achieved by increasing β [Boiko et al., 2006].

4.6 Conclusion

In this Chapter a brief survey on Sliding Mode Control (SMC) Theory based on the work [Pisano & Usai, 2011] has been provided. Throughout the Chapter the basic notion on Sliding Modes Control Theory in dynamical systems with discontinuous right-hand side has been discussed with particular emphasis to the problem of robust stabilization of perturbed nonlinear systems. In particular, notion on Filippov Continuation and Equivalent Control

and Chattering Analysis have been introduced in order to provide to the reader the necessary notion for understanding the treatment presented in the following Chapters. Furthermore the main Higher-Order Sliding Modes algorithm such as the Super-Twisting [Levant, 1993a], the Twisting [Levant, 1993a, Orlov, 2008], Suboptimal [Bartolini et al., 1998b] and the Arbitrary order sliding mode algorithm [Levant, 2005] are presented.

Part II

Author's Contributions

Chapter 5

Chattering adjustment and Tuning of the Super-Twisting Algorithm

As discussed in Chapter 4 the chattering phenomenon is one of the main drawbacks in the area of sliding mode control and discontinuous-based control [Slotine et al., 1991].

Due to the extensive use of High Order Sliding Mode in all the remainder of the Thesis, the purpose of the present Chapter is to illustrate a systematic procedure for tuning the parameters of the Super-Twisting Algorithm when the plant's relative degree is higher than one, for example due to the presence of unmodeled parasitic dynamics [Pilloni et al., 2012a, Pilloni et al., 2012b]. Indeed in that case self-sustained periodic oscillation takes place in the feedback loop. Notice that the topic of this Chapter is not strictly related to the framework of distributed systems. Anyway, it is reasonable thinking that when discontinuous control actions are applied for controlling real networks of systems, due to the unavoidable presence of parasitic dynamics and the coupling among the systems operating over a network, complex phenomena such as chattering can appear [Ameri & Boiko, 2013].

The proposed methodology is based on the Describing Function (DF) and requires only the prior knowledge of the plant's Harmonic Response (magnitude and phase) at the desired chattering frequency. In the following, it will be theoretically illustrated and verified by means of, both, simulative results and experiments carried out by making references to a DC motor.

5.1 Introduction

The main drawbacks of classical relay-based SMC (also called "first-order" SMC, or 1-SMC) are principally related to the so-called chattering effect [Utkin & Guldner, 1999], i.e. undesired high-frequency steady-state vibrations affecting the variables of the plant. To mitigate the chattering effect, a possible solution is the use of higher-order sliding mode control algorithms (HOSM) [Bartolini et al., 1998b, Levant, 2003], a set of advanced algorithms that constitute the core of modern SMC theory [Bartolini et al., 2008].

In the literature there are two main approaches to chattering analysis that provide an exact solution in terms of magnitude and frequency of the periodic oscillation:

- time-domain analysis by Poincare Maps (see [Gonçalves et al., 2001]);
- frequency domain techniques as Tsypkin Locus (see [Tsypkin, 1984]), and LPRS Method (see [Boiko, 2009]).

Anyway, all these approaches require lengthy computations. Therefore, the application of approximate analysis methods has been found useful whenever the plant under analysis fulfill the filtering hypothesis [Atherton, 1975]. Under this hypothesis, the Described Function (DF) method is a well-established approach. In fact it has already been used to analyze periodic motions for both 1-SMC [Shtessel & Lee, 1996] and second order SMC (2-SMC) systems [Boiko et al., 2005, Boiko et al., 2004, Boiko et al., 2006], and the results obtained via the use of exact techniques often feature a satisfactory similarity with those obtained via the approximate DF method [Boiko, 2003].

In this Chapter the attention has been focused on one of the most popular second order sliding mode algorithms known as Super-Twisting algorithm (STW) [Levant, 1993a]. Among the reasons for the popularity of the STW algorithm, its similarity with the conventional PI and the fact that it gives rise to a continuous control law are worth to mention. Whenever applied to linear plants with relative greater than one, STW controlled systems always exhibit chattering [Boiko et al., 2005] in the form of periodic oscillations of the output variable.

In the following a DF-based procedure for selecting the algorithm parameters in order to assign prescribed values to the frequency and amplitude of chattering is presented. The ability to affect the frequency of the residual steady state oscillations may be useful, for example, to mitigate resonant behaviors.

This Chapter is organized as follows sections: Section 5.2 and 5.3 present the STW algorithm and recall its DF-Based analysis [Boiko et al., 2005]. Section 5.4 states the problem under investigation and presents the tuning procedure for setting the parameters of the STW algorithm in order to assign prescribed amplitude and frequency to the periodic chattering motion. In Sections 5.5 and 5.6 the proposed tuning procedure is verified by means of simulations and experimental tests. Section 5.7 provides some concluding remarks and hints for next research.

5.2 Motivations

Conventional Proportional-Integral (PI) controllers are undoubtedly the most employed controllers in industry. Main advantages of classical PIs are their simplicity, satisfactory performance for “slow” processes, and the availability of effective automatic tuning rules, such as the Ziegler-Nichols or Astrom-Hagglund methods [Astrom & Hagglund, 2005]. Internal model principle establishes their capability of providing the asymptotic rejection of constant disturbances and zero steady-state error for constant set-point signals. However, PI controllers may behave unsatisfactorily in presence of strong nonlinearity effects (i.e. friction, hysteresis, backlash) and/or rapidly varying set-point and disturbance signals.

Here performances of linear systems controlled by means of a nonlinear version of a PI known as “Super-Twisting” (STW) Algorithm (see [Levant, 1993a]) will be investigated.

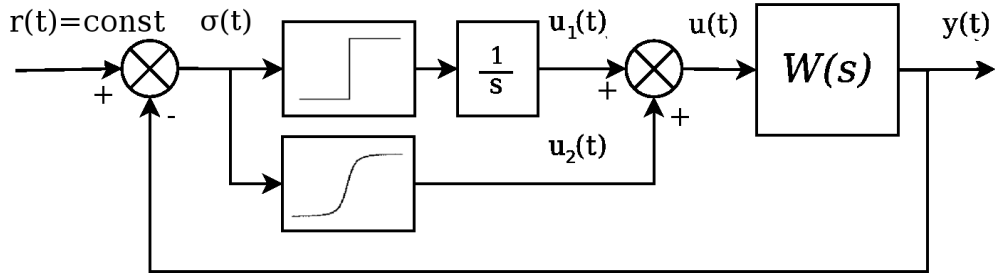


Figure 5.1: Block diagram of a linear plant with the Super-Twisting Algorithm.

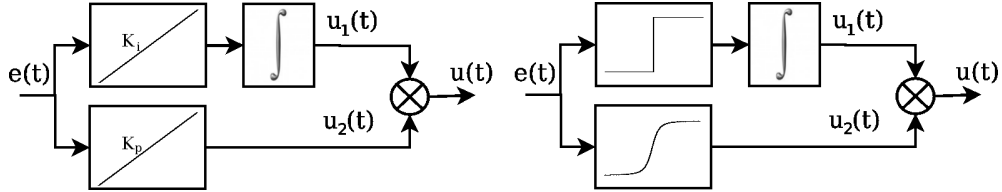


Figure 5.2: Architecture Comparison between linear (left) and nonlinear PI.

The considered controller is described as follows

$$u(t) = u_1(t) + u_2(t) , \quad (5.1)$$

$$\dot{u}_1 = -\gamma \text{sign}(\sigma) , \quad u_1(0) = 0 , \quad (5.2)$$

$$u_2 = -\lambda |\sigma|^{\frac{1}{2}} \text{sign}(\sigma) , \quad (5.3)$$

where λ , γ are positive design parameters. As known this algorithm belongs to the family of, so-called, *Second Order Sliding Mode* controllers. A block scheme representing its structure is depicted in Figure 5.1. As we can see, the similarity between the classical PI controller and the STW algorithm (5.1)-(5.3) are evident (see Figure 5.2) in that they both possess a static component (a constant proportional gain, for the PI, and a nonlinear gain with infinite slope at the origin for the nonlinear PI) and an integral action (error integration for the PI, and integration of the sign of the error variable for the nonlinear PI).

Particularity of the STW controller is that it gives rise to a continuous *non-smooth* control action which possesses significant robustness properties against nonlinearities, uncertainties and disturbances. In recent years it has become the most studied SMC algorithm and it has been applied to address control, estimation and fault detection tasks for some classes of linear and nonlinear processes (see [Fridman et al., 2007a, Fridman et al., 2008, Pilloni et al., 2012c]).

Whenever applied to systems (possibly nonlinear) having relative degree one, the STW algorithm provides:

- rejection of smooth disturbances of arbitrary shape;
- tracking of smooth references of arbitrary shape;
- finite-time convergence to the set-point.

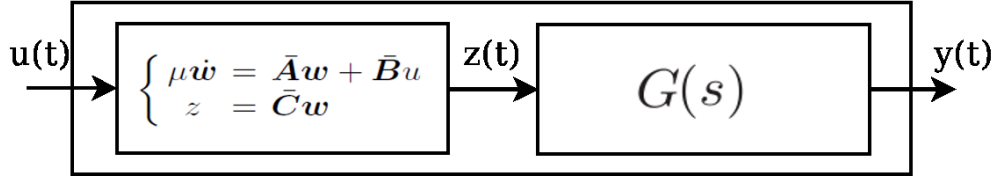


Figure 5.3: Decomposition of the arbitrary relative degree plant $W(s)$.

Although the STW algorithm guarantees the finite-time exact convergence for a rather limited class of plants having input-output relative degree one, it was proved its “practical stability” for a wider class of arbitrary relative degree systems admitting a certain decomposition (see [Levant & Fridman, 2010]). In particular, the following theorem holds once the considered dynamics is formed by the cascade of a stable actuator, of arbitrary relative degree, and a relative degree one dynamics.

Theorem 5.1. *Consider a LTI plant $W(s) = Y(s)/U(s)$, admitting the decomposition shown in Figure 5.3, where $H(s) = Z(s)/U(s)$ is an asymptotically stable dynamics with arbitrary relative degree, with the positive coefficient μ scaling its poles as an equivalent time constant, and $G(s)$ is of relative degree one. Then, the feedback control system in Figure 5.1 provides the following steady-state condition*

$$|\sigma| < O(\mu^2) . \quad (5.4)$$

■

Theorem 5.1 follows from [Levant & Fridman, 2010], Lemma 1. The motion within the $O(\mu^2)$ boundary layer (5.4), established in Theorem 5.1, proves to be periodic, thereby amenable to be investigated by means of the DF concept (see, e.g. [Atherton, 1975]).

5.3 Super-Twisting Algorithm and its DF Analysis

Consider a linear SISO system, described by the following state-space representation which comprises principal and parasitic dynamics:

$$\begin{cases} \dot{\mathbf{x}}(t) = \mathbf{A}\mathbf{x}(t) + \mathbf{B}u(t), & \mathbf{x} \in R^n, u \in R \\ y(t) = \mathbf{C}\mathbf{x}(t), & y \in R \end{cases}, \quad (5.5)$$

where \mathbf{A} , \mathbf{B} , \mathbf{C} are matrices of appropriate dimensions, \mathbf{x} is the state vector, u is the actuator input, and y the plant output. Consider the plant description in the form of transfer function as follows

$$W(s) = \frac{Y(s)}{U(s)} = \mathbf{C}(s\mathbf{I} - \mathbf{A})^{-1} \mathbf{B} . \quad (5.6)$$

Assuming that the plant transfer function satisfies the filtering hypothesis property. Using the STW algorithm (5.1)-(5.3), the control system under analysis can be represented in the form of the block diagram in Figure 5.1 where $\sigma(t) = r(t) - y(t)$ is the error variable. The DF of the nonlinear function (5.3) was derived in [Boiko et al., 2005] as follows:

$$N_2(a_y) = \frac{2\lambda}{\pi\sqrt{a_y}} \int_0^\pi (\sin \psi)^{\frac{3}{2}} d\psi = \frac{2\lambda}{\sqrt{\pi a_y}} \frac{\Gamma(1.25)}{\Gamma(1.75)} \approx 1.1128 \frac{\lambda}{\sqrt{a_y}}, \quad (5.7)$$

where a_y is the oscillation amplitude of the error variable σ , to be determined, and $\Gamma(\cdot)$ is the Euler's Gamma function. The DF of the nonlinear integral component (5.2) can be written as follows:

$$N_1(a_y, \omega) = \frac{4\gamma}{\pi a_y} \frac{1}{j\omega} , \quad (5.8)$$

which is the cascade connection of an ideal relay (with the DF equal to $4\gamma/\pi a_y$ (see [Atherton, 1975])), and an integrator with the frequency response $1/j\omega$. Taking into account both control components in (5.1), the DF of the STW algorithm (5.1)-(5.3) can be finally written as

$$N(a_y, \omega) = N_1(a_y, \omega) + N_2(a_y) = \frac{4\gamma}{\pi a_y} \frac{1}{j\omega} + 1.1128 \frac{\lambda}{\sqrt{a_y}} . \quad (5.9)$$

Let us note that the DF of the STW algorithm depends on, both, the amplitude a_y and frequency ω of the periodic solution.

In general, the parameters of the periodic limit cycle can be approximately found via the solution of the following complex equation

$$1 + W(j\omega) \cdot N(a_y, \omega) = 0 , \quad (5.10)$$

so-called, *harmonic balance* [Atherton, 1975]. The harmonic balance equation (5.10) can be rewritten as

$$W(j\omega) = -N^{-1}(a_y, \omega) , \quad (5.11)$$

and a periodic oscillation of frequency Ω and amplitude A_y exists when an intersection between the Nyquist plot of the plant $W(j\omega)$ and the negative reciprocal DF $N^{-1}(A_y, \omega)$ occurs at $\omega = \Omega$. Thus, the parameters of the limit cycle can be found via solution of (5.10) where the DF is given by (5.9). The negative reciprocal of the DF (5.9) can be written in explicit form as

$$-\frac{1}{N} = -\frac{0.8986 \frac{\sqrt{a_y}}{\lambda} + j1.0282 \frac{\gamma}{\omega \lambda^2}}{1 + \frac{1.3091}{a_y} \left(\frac{\gamma}{\omega \lambda}\right)^2} . \quad (5.12)$$

It is of interest to plot the negative reciprocal of the DF (5.12) in the complex plane. It depends on the two variables a_y and ω ; which are both nonnegative by construction. It is clear from (5.12) that with positive gains λ and γ the locus is entirely contained in the lower-left quadrant of the complex plane when the variables a_y and ω vary from zero to infinity. In Figure 5.4, the curves obtained for $\lambda = 0.6$ and $\gamma = 0.8$, some values $\omega = \omega_i$, and by letting a_y to vary from 0 to ∞ are displayed.

5.3.1 Existence of the Periodic Solution

Denoted A_y and Ω the amplitude and the and the frequency of the periodic oscillation which solves the harmonic balance, then (5.10) can be rewritten as

$$N(A_y, \Omega) = W^{-1}(j\Omega) , \quad (5.13)$$

which, considering (5.9), specializes to

$$\frac{4\gamma}{\pi A_y} \frac{1}{j\Omega} + 1.1128 \frac{\lambda}{\sqrt{A_y}} = -W^{-1}(j\Omega) . \quad (5.14)$$

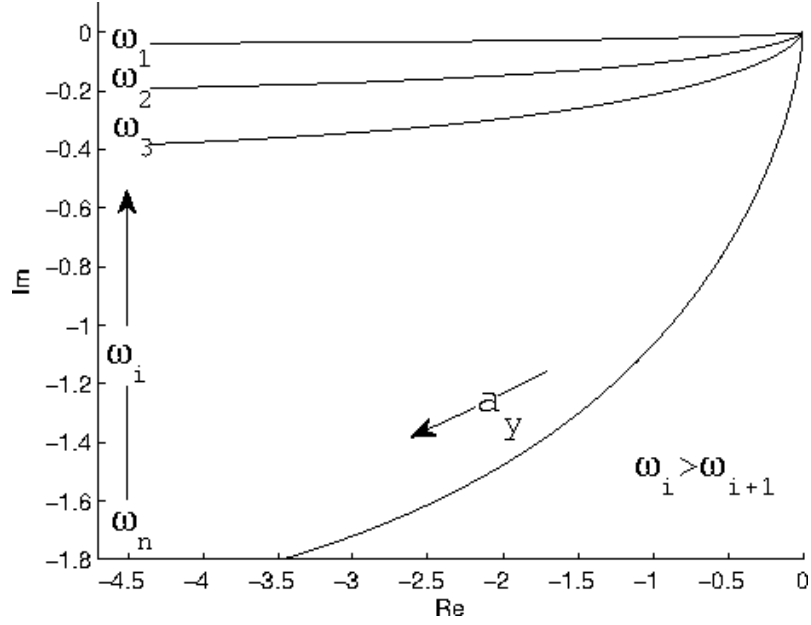


Figure 5.4: Plots of the negative reciprocal DF (5.12) for different values of ω .

Separating the complex equation (5.14) in its real and imaginary parts it yields

$$\begin{cases} 1.1128 \frac{\lambda}{\sqrt{A_y}} = -\Re W^{-1}(j\Omega) \\ \frac{4\gamma}{\pi\Omega} \frac{1}{A_y} = \Im W^{-1}(j\Omega) \end{cases} \quad (5.15)$$

Obtaining A_y from the first of (5.15) and substituting this value in the second equation of (5.15), it yields

$$\frac{4\gamma}{\pi\Omega} \frac{1}{\Im W^{-1}(j\Omega)} - \left(\frac{1.1128\lambda}{-\Re W^{-1}(j\Omega)} \right)^2 = 0, \quad (5.16)$$

which allows to compute the frequency Ω . Solution of (5.16) cannot be derived in closed form, and a numerical, or graphical, approach is mandatory.

Once obtained Ω , the amplitude of the periodic solution can be expressed as

$$A_y = \frac{4\gamma}{\pi\Omega} \frac{1}{\Im W^{-1}(j\Omega)}. \quad (5.17)$$

As noticed in [Boiko et al., 2005], a point of intersection between the Nyquist plot of the plant and the negative reciprocal of the STW DF (5.9) always exists if the relative degree of the plant transfer function is higher than one, and this point is located in the third quadrant of the complex plane. From Figure 5.4, it is also apparent that the frequency of the periodic solution induced by the STW is always lower than the frequency of the periodic motion for the system controlled by the conventional relay.

The orbital asymptotic stability of the periodic solution can be assessed using the *Loeb Criterion* (see [Atherton, 1975, Vander Velde, 1968]), that is not mentioned here for the sake of brevity.

5.4 Problem Formulation and Proposed Tuning Procedure

5.4.1 Problem Formulation

Consider the feedback control system in Figure 5.1, where the plant is modelled by an unknown transfer function $W(s)$ having relative degree greater than one. Given the steady-state performance requirements in terms of desired frequency Ω_d and amplitude A_{y_d} of the chattering motion, tuning procedure, based on the DF method, devoted to derive constructive controller tuning rules for the algorithm (5.1)-(5.3) will be defined.

To begin with, let us substitute (5.12) into (5.11) and rewrite the harmonic balance equation as

$$W(j\omega) = -\frac{c_1 \frac{a_y^{1.5}}{\lambda}}{a_y + c_3 \left(\frac{\gamma}{\omega\lambda}\right)^2} - j \frac{c_2 \frac{a_y \gamma}{\omega\lambda^2}}{a_y + c_3 \left(\frac{\gamma}{\omega\lambda}\right)^2}, \quad (5.18)$$

with $c_1 = 0.8986$, $c_2 = 1.0282$, $c_3 = 1.3091$. Let

$$K_1(\omega) = \frac{\gamma}{\omega}, \quad K_2(\omega) = \frac{\gamma}{\omega\lambda}. \quad (5.19)$$

Multiplying both sides of (5.18) by γ/ω , it results

$$K_1(\omega)W(j\omega) = -\frac{c_1 a_y^{1.5} K_2(\omega)}{a_y + c_3 K_2^2(\omega)} - j \frac{c_2 a_y K_2^2(\omega)}{a_y + c_3 K_2^2(\omega)}. \quad (5.20)$$

Once considered the design requirements $a_y = A_{y_d}$ and $\omega = \Omega_d$, separating the complex equation (5.20) in its magnitude and phase as follows

$$K_1(\Omega_d) |W(j\Omega_d)| = \sqrt{\frac{c_1^2 A_{y_d}^3 K_2(\Omega_d) + c_2^2 A_{y_d}^2 K_2(\Omega_d)}{(A_{y_d} + c_3 K_2^2(\Omega_d))^2}} \quad (5.21)$$

$$\arg\{W(j\Omega_d)\} = \operatorname{atan}\left\{\frac{c_2 K_2(\Omega_d)}{c_1 \sqrt{A_{y_d}}}\right\} \quad (5.22)$$

it results a well-posed system of equations, where $K_1^d = K_1(\Omega_d)$ and $K_2^d = K_2(\Omega_d)$ are the two unknowns. The magnitude and phase of $W(j\omega)$ at the desired chattering frequency Ω_d can be identified by a simple test on the plant. Therefore, solving (5.21)-(5.22), and then considering (5.19) with $\omega = \Omega_d$, the controller parameters λ and γ that guarantee a steady-state periodic motion with desired characteristics can be derived. Corresponding formulas are

$$\begin{cases} \gamma = \Omega_d K_1^d \\ \lambda = \frac{\gamma}{\Omega_d K_2^d} = \frac{K_1^d}{K_2^d} \end{cases} \quad (5.23)$$

Direct solution of the nonlinear equations (5.21)-(5.22) can be avoided. By following a graphical approach it is convenient to refer to the curves in Figure 5.5, where each curve represents a specific instance of the right-hand side of (5.20) in the complex plane, for different values of A_{y_d} , by letting K_2 to vary from 0 to ∞ . Drawing in the abacus a segment connecting

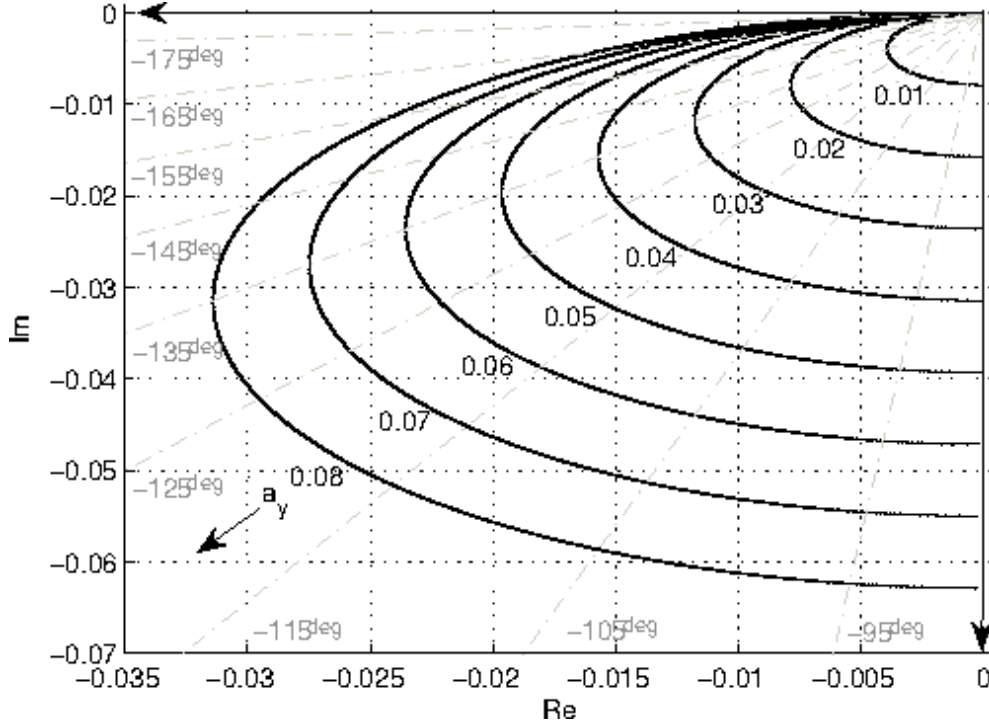


Figure 5.5: Level sets of the right-hand of (5.20) for different values of a_y .

the origin of the complex plane and the point P of the curve associated to A_{y_d} , with phase equal to $\arg\{W(j\Omega_d)\}$ (see Figure 5.8), the length of the segment \overline{OP} which corresponds to the right-hand side of (5.21) can be easily extrapolated. Then, once known \overline{OP} , K_1^d and K_2^d can be computed by the following relationship:

$$\begin{cases} K_1^d = \frac{\sqrt{\frac{c_1^2 A_{y_d}^3 K_2(\Omega_d) + c_2^2 A_{y_d}^2 K_2(\Omega_d)}{(A_{y_d} + c_3 K_2^2(\Omega_d))^2}}}{|W(j\Omega_d)|} = \frac{\overline{OP}}{|W(j\Omega_d)|} \\ K_2^d = \frac{c_1 \sqrt{A_{y_d}}}{c_2} \tan\{\arg\{W(j\Omega_d)\}\} \end{cases} \quad (5.24)$$

Remark 5.1. *It is important to underline that the intersection between the Nyquist plot of $W(j\omega)$ and $-N^{-1}(a_y, \omega)$ always lies in the lower-left quadrant of the complex plane, so the desired frequency of chattering oscillation Ω_d must satisfy the sector condition*

$$\Omega_1 < \Omega_d < \Omega_2 \quad (5.25)$$

where

$$\arg\{W(j\Omega_1)\} = \frac{\pi}{2}, \quad \arg\{W(j\Omega_2)\} = \pi \quad (5.26)$$

Remark 5.2. *The right-hand side of (5.20) is independent of the plant transfer function. Therefore the set of curves in Figure 5.5 represents an abacus, independent of the plant, too, hence very useful to simplify the solution of (5.20).*

5.4.2 Proposed Tuning Procedure

Given a *low-pass plant with relative degree greater than one*, the proposed procedure can be summarized as follows:

Procedure 5.1.

- A. Let A_{y_d} and Ω_d be the desired chattering characteristics;
- B. Evaluate by an harmonic response test on the plant the quantities $|W(j\Omega_d)|$ and $\arg\{W(j\Omega_d)\}$ and check if $\pi/2 < \arg\{W(j\Omega_d)\} < \pi$, otherwise chose a different value for Ω_d and go back to step A;
- C. Draw in the abacus a segment connecting the origin and the point P of the curve $a_y = A_{y_d}$ with phase equal to $\arg\{W(j\Omega_d)\}$;
- D. Use (5.23) to compute λ and γ .

5.5 Simulation Results

In order to outline the proposed methodology, consider the cascade connection of a linear plant $G(s)$ and a stable actuator $H(s)$, such that the relative degree of $W(s) = H(s) \cdot G(s)$ is greater than one, i.e.:

$$G(s) = \frac{s+1}{s^2+s+1} \quad , \quad H(s) = \frac{1}{(\mu s+1)^2} \quad , \quad (5.27)$$

$$W(s) = H(s) \cdot G(s) \quad , \quad \mu = 1/50 \quad .$$

Let us apply Procedure 5.1 to shape the steady-state permanent oscillation of the closed-loop system with the STW algorithm.

- A. Let $A_{y_d} = 0.05$ and $\Omega_d = 25$ rad/sec;
- B. By frequency response test it results:

$$|W(j\Omega_d)| \approx 0.032 \quad , \quad \arg\{W(j\Omega_d)\} \approx -143.14 \text{ deg} \quad ;$$

- C. Drawing the segment \overline{OP} in the abacus until it intersects the curve associated to a_{y_d} (see Figure 5.8), it results

$$\overline{OP} = \sqrt{(-0.01882)^2 + (-0.01414)^2} = 0.0235 \quad ;$$

- D. Using (5.24) and (5.19) obtain

$$\lambda = 5.0119 \quad , \quad \gamma = 18.3575 \quad . \quad (5.28)$$

In Figure 5.6, some simulation results are shown. Signal $y_1(t)$ represents the closed-loop unit-step response of the plant (5.27) with control parameters (5.28). Signal $y_2(t)$ represent the output signal obtained using the reduced value $\mu = 1/100$ for the actuator time constant parameter. The bottom left zoomed sub-plot confirms that the steady-state chattering motion fulfills the given specification of amplitude and frequency. The bottom right sub-plot shows that the chattering amplitude a_y is 4 times smaller, according to Theorem 5.1. The achieved results fully agree with the presented analysis.

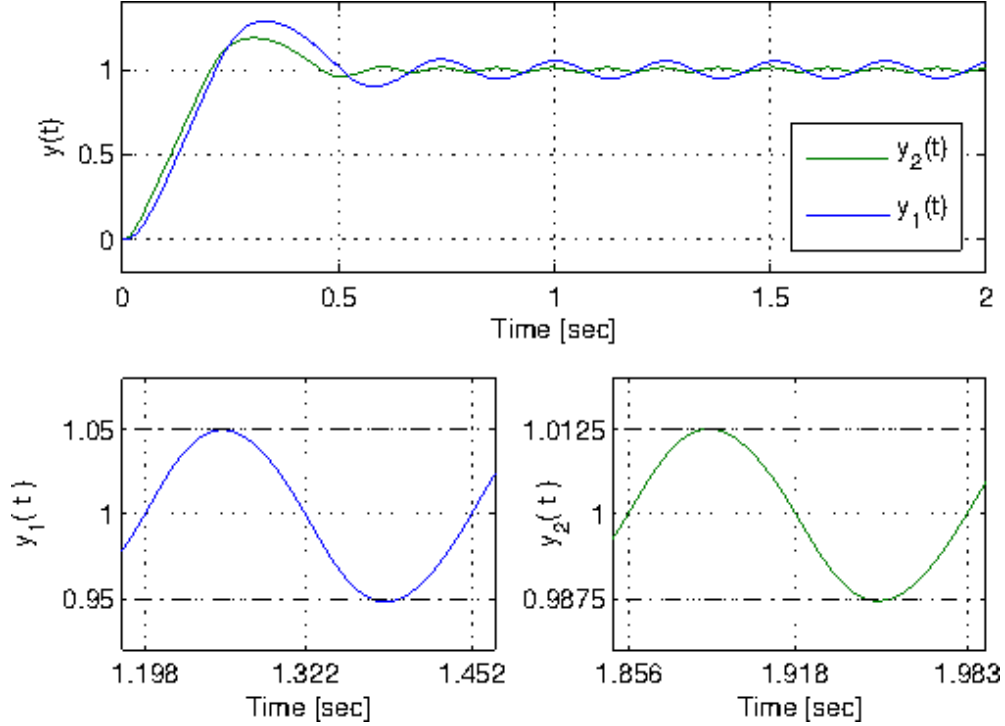


Figure 5.6: Step response of the plant $W(s)$ in closed-loop with STW parameters $\lambda = 5.0119$, $\gamma = 18.3575$.

5.6 Experimental Results

The proposed method has been experimentally tested with reference to the position control of a commercial DC Motor. In Figure 5.7 the experimental setup is shown.

As first step (Step A), the desired frequency and magnitude of the periodic oscillation were set as

$$A_{y_d} = 0.05 \quad , \quad \Omega_d = 50 \text{ rad/sec} \quad . \quad (5.29)$$

Then, by an harmonic test (Step B), the following values are obtained

$$|W(j\Omega_d)| \approx 0.0081 \quad , \quad \arg\{W(j\Omega_d)\} \approx -138.7 \text{ deg} \quad . \quad (5.30)$$

Afterwards, by the abacus in Figure 5.8 (Step C) results

$$\overline{OP} = \sqrt{(-0.0195)^2 + (-0.0171)^2} = 0.0259 \quad (5.31)$$

from which, (Step D) the designed gains for the nonlinear PI (5.1)-(5.3) are

$$\lambda = 18.64 \quad , \quad \gamma = 159.99 \quad . \quad (5.32)$$

In Figure 5.9, the closed-loop unit-step response of the motor with control parameters (5.32) is displayed. It can be checked that the actual amplitude and frequency of the oscillation closely match the desired ones. A second experiment has been made by evaluating the parameters giving rise to a periodic oscillations having the same frequency $\Omega_d = 50 \text{ rad/sec}$

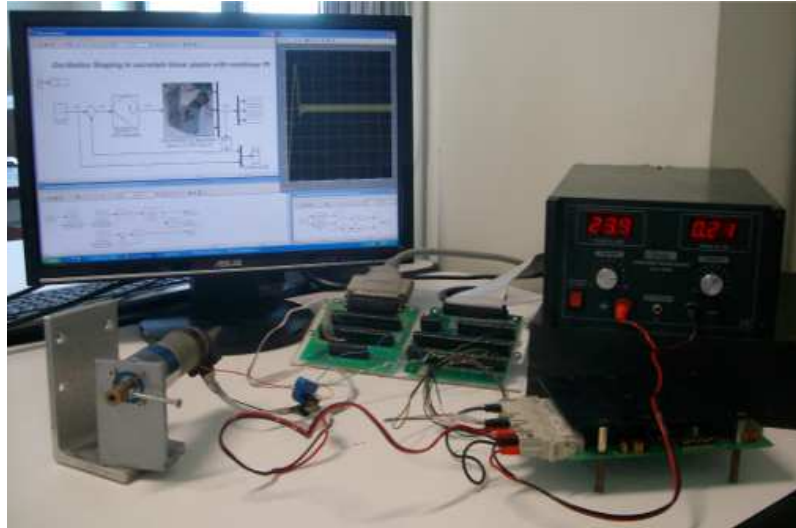


Figure 5.7: Experimental set-up with FAULHABER[®] DC Micromotor Series 3557 024 CS.

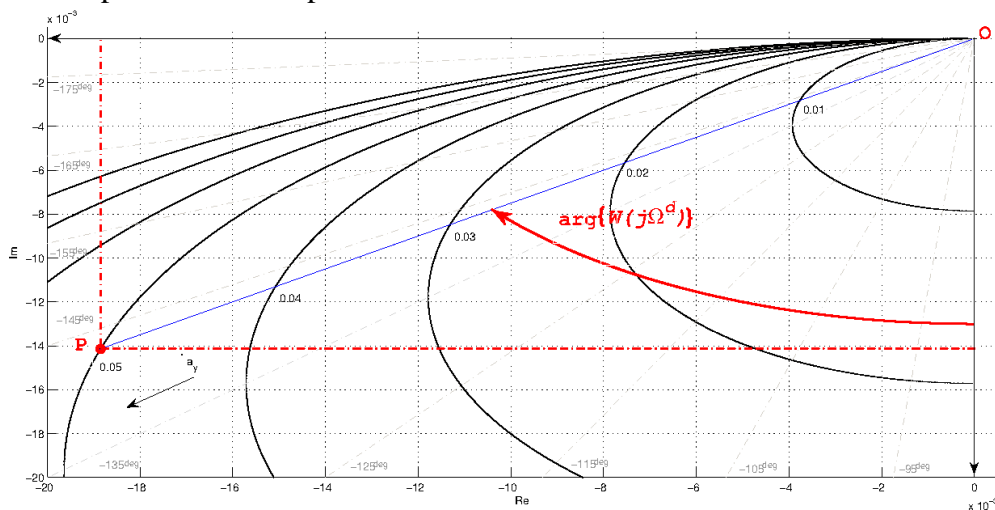


Figure 5.8: Example of abacus utilization for the system $W(s)$ (5.27).

and a different, bigger, amplitude $A_{y_d} = 0.07$. By repeating the suggested tuning procedure, the next controller parameters were obtained

$$\lambda = 20.05 \quad , \quad \gamma = 223.99 \quad . \quad (5.33)$$

The results of the corresponding experiment are shown in the Figure 5.10, which shows, again, an almost perfect matching between the actual and expected characteristics of the steady state oscillation.

5.7 Conclusions and Future Works

A describing function approach for tuning a feedback control system with a linear plant driven by STW algorithm has been presented. It allows to shape the characteristics of the chattering motion that occurs when the linear plant has a relative degree greater than one, for example due to the presence of parasitic unmodeled dynamics. A constructive procedure

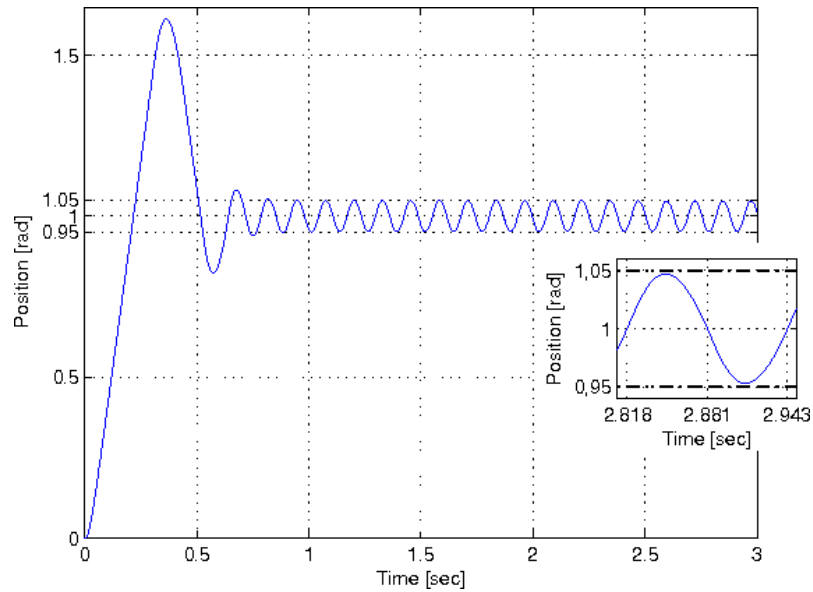


Figure 5.9: Experimental step response of the DC-Motor in closed-loop with $\lambda = 18.64$, $\gamma = 159.99$.

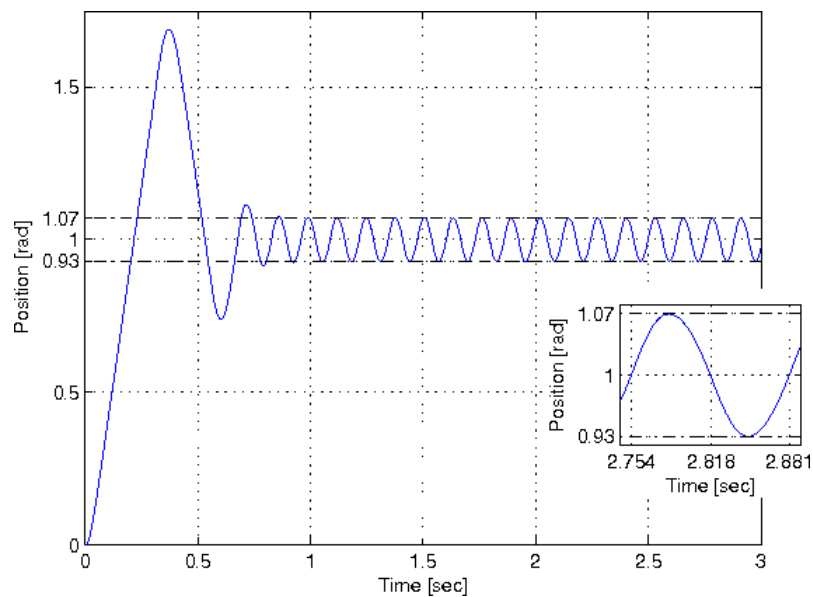


Figure 5.10: Experimental step response of the DC-Motor in closed-loop with $\lambda = 20.05$, $\gamma = 223.99$.

for determining in advance the periodic solution parameters (frequency and amplitude) has been developed and tested by means of both computer simulations and experiments. Among some interesting directions for improving the present result, the analysis, and shaping, of the transient oscillations is of special interest. The mathematical treatment presented in [Boiko, 2011] and the *dynamic harmonic balance* concept in particular, could be a possible starting point to this end.

Chapter 6

Decentralized Estimation in Complex Network

This Chapter considers the problem of state estimation and unknown input reconstruction of a class of connected heterogeneous perturbed LTI MIMO systems. Local high order sliding mode observers at each node of the network are designed for this purpose. The proposed method, under some network structural conditions, is inherently robust, nonlinear and totally independent of the time-varying network topology. Knowledge of the number of nodes that belong to the network is not required. At the supervisory level, decentralized control signals are computed based on the state estimates in order to operate the network-synchronization. By mean of simulation, the effectiveness of the proposal procedure is shown.

6.1 Introduction

Control applications in distributed and cooperative environments has been a subject growing interest in the last decades becoming one of the most important research fields in the control and decision theory (see [Šiljak, 1991]). Analysis and control of complex behaviors in large networks attracted the attention of researcher from different fields; an overview of the problems related to networks of dynamic systems is given in [Newman et al., 2006], and contribution in synchronization of networks and in cooperative control can be found in [Wu, 2007].

Complex networks are usually characterized by several distinctive properties including complexity, topological structure, dynamical evolution, time-varying coupling strengths and interactions between nodes. The first model of networks was proposed in [Erdős & Rényi, 1960] (ER-Model). In that model each pair of elements was randomly connected with the same probability. However in the real world, connectivity between each element is neither completely regular nor completely random. Thanks to Watts and Strogatzs (WS-Model) a more realistic representation has been given (see [Watts & Strogatz, 1998]). Another significant recent discovery in the field of complex networks is the observation that a number of large-scale and complex networks are scale-free, that is, their connectivity distributions have the power-law form (see [Barabási et al., 1999]). In this work, a scale-free dynamical

network representation, consistent with [Wang & Chen, 2002a], will be utilized.

The motivation for the present work is to increase the level of autonomy for a class of scale-free networks composed of heterogeneous systems created to perform synchronization on a common reference trajectory. Network of mobile robots, unmanned aerial vehicle, satellites and localization systems are just some examples of cooperative systems (see [Frew et al., 2005b]). It is noteworthy that in autonomous application, the agents are often monitored at a supervisory level, and in most cases a supervisory level node use to drive the systems (see [Frew et al., 2005b, Edwards & Menon, 2008]).

A great deal of attention has been paid to the problem of decentralized state-space estimation in complex networks. Motivated by a large amount of important practical problems, the estimation of uncertain systems has become an important area of research. Such problem arises in systems subject to disturbances or with inaccessible or unmeasurable inputs and in many applications such as fault detection isolation [Pilloni et al., 2012c, Pilloni et al., 2013c, Floquet et al., 2004, Edwards et al., 2000, Spurgeon, 2008, Fridman et al., 2008, Davila et al., 2009]. In the literature several approaches to deal with this class of problem has been proposed (see [Edwards & Menon, 2008, Stankovic et al., 2009, Pilloso et al., 2011]), however, recently, sliding mode control (SMC) theory has been further extended in the area of networked systems (see [Yan et al., 2006]). The main features of SMC are insensitivity to external disturbances, high accuracy and finite time convergence, which make it one of the useful tools in robust state estimation. The main drawbacks of classical SMC are principally related to the so-called chattering effect but this could be not a dramatic drawback in observation problems implemented in digital devices. High-order sliding modes (HOSM) have been suggested both to deal with high relative degree systems and to attenuate this phenomena whilst maintaining the mentioned robustness properties (see [Levant, 1993a, Levant, 2005, Bartolini et al., 2003]). Furthermore the combination of HOSM control algorithms and sliding mode differentiators ([Levant, 1998]) produces effective observers (see [Davila et al., 2009]).

In this Chapter, network structural conditions for designing local nonlinear observers independent from any topological changing are provided. Complete finite-time state estimation and the unknown input reconstruction of each system operating over a network are fulfilled. The estimated state variables of each node are then used to synchronize the whole network. The Chapter is organized as follows; in Section 6.2 a brief description of scale-free system is presented; Section 6.3 provides a reminder of the concepts of strong observability, and an approach based on the *observability indices* is presented; in Section 6.4 conditions for the design of a decentralized observer are given. The proposed framework is verified by means of simulations in Section 6.5. Section 6.6 provides some concluding remarks and hints for further research.

6.2 The Scale-Free Dynamical Network Model

Many real-world networks are scale-free. The main features of a scale-free network are "growth" and "preferential attachment". These refer to networks continuously evolving by the insertion/removal of nodes and changing interconnection. Such topological changes can be described using graph theory and the notation $\mathcal{G} = \{\mathcal{G}_1, \dots, \mathcal{G}_M\}$, where each \mathcal{G}_i represents

an interaction topology for a particular time period. For the graph \mathcal{G} the adjacency matrix $\mathcal{A}[\mathcal{G}](t) = [a_{ij}(t)]$ is a binary matrix whose entries depend on the current graph \mathcal{G}_i at time t , the entry $a_{ij}(t) = 1$ if the i -th and j -th node are adjacent at time t , and zero otherwise. Let $\Delta[\mathcal{G}](t) = [\delta_{ij}(t)]$ be a diagonal matrix which represents the in-degree matrix for the considered graph \mathcal{G}_i at time t , $\delta_{ii}(t)$ is the input-degree of the i -th vertex. The Laplacian matrix of \mathcal{G} , $\mathcal{L}[\mathcal{G}] = [\mathcal{L}_{ij}]$ is defined as the difference $\Delta[\mathcal{G}] - \mathcal{A}[\mathcal{G}]$.

Suppose that the scale-free network consists of N heterogenous, dynamical, linearly and diffusively coupled nodes. According to [Wang & Chen, 2002a, Edwards & Menon, 2008], each node Σ_i of the graph \mathcal{G} can be described as follow:

$$\dot{\mathbf{x}}_i = \mathbf{A}_i \mathbf{x}_i + \mathbf{B}_i \mathbf{u}_i + \mathbf{D}_i \mathbf{f}_i - c(t) \sum_{j=1}^N \mathcal{L}_{ij} \Gamma_{ij} \mathbf{x}_j \quad (6.1)$$

$$\mathbf{y}_i = \mathbf{C}_i \mathbf{x}_i \quad (6.2)$$

where $\mathbf{x}_i = [x_{i,1} \dots x_{i,n_i}]^T \in \mathbb{R}^{n_i}$ and $\mathbf{y}_i = [y_{i,1} \dots y_{i,p_i}]^T \in \mathbb{R}^{p_i}$ represent the n_i -dimensional state and output vectors of the i -th node of the network. Functions $\mathbf{u}_i(\mathbf{x}_i) \in \mathbb{R}^{m_i}$ and $\mathbf{f}_i \in \mathbb{R}^{q_i}$ represent respectively the control inputs and the unknown inputs of the i -th node. For the sake of simplicity it is assumed $q_i = 1$. The unknown term is assumed to satisfy certain sectors bounds which will be defined later. The term $c(t)$ is the time varying coupling strength between nodes and it is assumed to be for simplicity identical for all links between the nodes. The matrices $\mathbf{A}_i, \mathbf{B}_i, \mathbf{C}_i, \mathbf{D}_i$ describe the dynamics of node i and are assumed to be of appropriate dimensions. $\Gamma_{ij} \in \mathbb{R}^{n_i \times n_j}$ is a binary matrix and represents the node-to-node coupling configuration among the i -th and j -th node. The entries of Γ_{ij} are nonzero if a communication channel among different states of neighbors nodes exist.

Assumption 6.1. *Each node Σ_i is assumed to be observable.* ■

Assumption 6.2. *For achieving network synchronization, it is assumed each pair $(\mathbf{A}_i, \mathbf{B}_i)$ to be controllable.* ■

6.3 Strong Observability and Unknown Input Reconstruction

Consider a LTI system Σ :

$$\dot{\mathbf{x}} = \mathbf{A} \mathbf{x} + \mathbf{D} \mathbf{f} \quad (6.3)$$

$$\mathbf{y} = \mathbf{C} \mathbf{x} \quad (6.4)$$

where $\mathbf{x} \in \mathbb{R}^n$, $\mathbf{y} \in \mathbb{R}^p$ and $\mathbf{f} \in \mathbb{R}^q$ represent the state, the output and the unknown input vector of Σ . Generic well-known strong observability conditions for LTI systems with unknown inputs \mathbf{f} based on the study of the invariant zeros of the triple $(\mathbf{A}, \mathbf{D}, \mathbf{C})$ are summarized in [Trentelman et al., 2001].

Whereas in [Fridman et al., 2007b] necessary conditions for strong observability with respect to the unknown input \mathbf{f} , under the assumption that $q = p$, has been given.

In particular, let \mathbf{c}_i and \mathbf{d}_j be the rows of \mathbf{C} and the columns of \mathbf{D} . The output vector $\mathbf{y} = \mathbf{C} \mathbf{x}$ is said to have vector relative degree $\mathbf{r} = (r_1, \dots, r_p)$ with respect to the unknown

input \mathbf{f} if the following conditions hold:

$$\begin{aligned} \mathbf{c}_i \mathbf{A}^l \mathbf{D} &= \mathbf{0}_{(1 \times q)} & \text{with } & \begin{cases} i = 1, 2, \dots, p \\ l = 0, 1, \dots, r_i - 2 \end{cases} \end{aligned} \quad (6.5)$$

$$\det(\mathbf{Q}) \neq 0 \quad \text{with } \mathbf{Q} = \begin{pmatrix} \mathbf{c}_1 \mathbf{A}^{r_1-1} \mathbf{d}_1 & \dots & \mathbf{c}_1 \mathbf{A}^{r_1-1} \mathbf{d}_q \\ \vdots & & \vdots \\ \mathbf{c}_p \mathbf{A}^{r_p-1} \mathbf{d}_1 & \dots & \mathbf{c}_p \mathbf{A}^{r_p-1} \mathbf{d}_q \end{pmatrix} \quad (6.6)$$

The next lemma gives sufficient conditions for guarantee that the system (6.3)-(6.4) is strong observable:

Lemma 6.1. *Let the output \mathbf{y} of Σ have vector relative degree \mathbf{r} . Then the vectors*

$$\mathbf{c}_1, \dots, \mathbf{c}_1 \mathbf{A}^{r_1-1}, \dots, \mathbf{c}_p, \dots, \mathbf{c}_p \mathbf{A}^{r_p-1} \quad (6.7)$$

are linearly independent. Σ is strongly observable if the total relative degree of the system $\bar{\mathbf{r}} = \sum_{k=1}^p r_k$ is equal to n . ■

Remark 6.1. *Generalizing Lemma 6.1 to the the case of rectangular systems ($q < p$), it is obvious that $\mathbf{c}_1, \dots, \mathbf{c}_1 \mathbf{A}^{r_1-1}, \dots, \mathbf{c}_p, \dots, \mathbf{c}_p \mathbf{A}^{r_p-1}$ can not be linearly independent even if the system is strongly observable. This assertion can be easily proved applying the same procedure shown in [Fridman et al., 2007b] because \mathbf{Q} is a non-square matrix.* ■

Currently checking the strong observability property of a non-square LTI systems ($q < p$) by means of the relative degree vector is not a completely established matter. In the rest of this section, in order to define a possible approach for such class of systems, the concept of *observability index* is recalled.

Consider the system in (6.3)-(6.4), the observability index for the i -th output of Σ can be defined as follows:

Definition 6.1. *The maximum number (v_i) of successive linearly independent derivatives of the i -th output of Σ , it is called the observability index and represents the number of system state which can be reconstructed from y_i .* ■

The set $\mathcal{V} := \{v_1, \dots, v_p\}$ is called the *observability indices of the pair (\mathbf{A}, \mathbf{C})* . It is obvious that each entry v_i can not be greater then the order of the system n . Recalling the definition of relative degree r_i of the i -th output of the system with respect to an unknown input \mathbf{f} in (6.5), it can be asserted that if the following lemma holds, the system Σ is strongly observable and unknown input reconstruction (UIR) is practicable.

Lemma 6.2. *The system Σ is strongly observable if it is possible to define a set of positive integers $\mathcal{U} := \{\mu_1, \dots, \mu_h\}$ with $h \leq p$, in which each element is associated with one output's component, such that the following conditions are satisfied:*

$$\begin{cases} \mu_i \leq v_i & \mu_1 + \mu_2 + \dots + \mu_h = n \\ \mu_i \leq r_i & \text{with } i = 1, 2, \dots, h \end{cases} \quad (6.8)$$

$$\det\{\mathbf{M}\} \neq 0, \quad \mathbf{M} = \begin{pmatrix} M_1 \\ \vdots \\ M_i \\ \vdots \\ M_h \end{pmatrix}, \quad M_i = \begin{pmatrix} \mathbf{c}_i \\ \mathbf{c}_i \mathbf{A} \\ \mathbf{c}_i \mathbf{A}^2 \\ \vdots \\ \mathbf{c}_i \mathbf{A}^{\mu_i-1} \end{pmatrix} \in \mathbb{R}^{\mu_i \times n} \quad (6.9)$$

■

Proof. Suppose the pair (\mathbf{A}, \mathbf{C}) is observable, \mathcal{O} has n linearly independent rows. After choosing a set \mathcal{U} which satisfies the conditions (6.8)-(6.9), it is obvious that the matrix \mathbf{M} is full-rank because it is obtained combining linear independent block like $\mathbf{c}_i, \mathbf{c}_i \mathbf{A}, \dots, \mathbf{c}_i \mathbf{A}^{\mu_i-1}$ linearly independent each other. Then, applying the following bijection mapping $\mathbf{x} = \mathbf{M} \mathbf{x}_o$ the following canonical observable representation is obtained:

$$\begin{aligned}\dot{\mathbf{x}}_o &= \mathbf{A}_o \mathbf{x}_o + \mathbf{D}_o \mathbf{f} \\ \mathbf{y}_o &= \mathbf{C}_o \mathbf{x}_o\end{aligned}\quad (6.10)$$

where

$$\mathbf{A}_o = \begin{pmatrix} \mathbf{A}_{11} & \cdots & \mathbf{A}_{1h} \\ \vdots & \ddots & \vdots \\ \mathbf{A}_{h1} & \cdots & \mathbf{A}_{hh} \end{pmatrix}, \quad \mathbf{C}_o = \begin{pmatrix} \mathbf{c}_{11} & \cdots & \mathbf{c}_{1h} \\ \vdots & \ddots & \vdots \\ \mathbf{c}_{h1} & \cdots & \mathbf{c}_{hh} \end{pmatrix}\quad (6.11)$$

$$\mathbf{A}_{ii} = \begin{pmatrix} 0 & 1 & \cdots & 0 \\ \vdots & \vdots & \ddots & \vdots \\ 0 & 0 & \cdots & 1 \\ a_{ii,1} & a_{ii,2} & \cdots & a_{ii,\mu_i} \end{pmatrix}, \quad \mathbf{A}_{ij} = \begin{pmatrix} 0 & \cdots & 0 \\ \vdots & & \vdots \\ 0 & \cdots & 0 \\ a_{ij,1} & \cdots & a_{ij,\mu_j} \end{pmatrix}\quad (6.12)$$

$$\mathbf{D}_o = \mathbf{M} \mathbf{D} = \begin{pmatrix} \delta_1 \\ \vdots \\ \delta_h \end{pmatrix}, \quad \delta_i = \begin{pmatrix} 0 \\ \vdots \\ 0 \\ \mathbf{c}_i \mathbf{A}^{\mu_i-1} \mathbf{D} \end{pmatrix} \in \mathbb{R}^{\mu_i \times q}\quad (6.13)$$

$$\mathbf{c}_{ii} = (1 \ 0 \ \cdots \ 0) \in \mathbb{R}^{1 \times \mu_i}, \quad \mathbf{c}_{ij} = (0 \ \cdots \ 0) \in \mathbb{R}^{1 \times \mu_j}\quad (6.14)$$

Note that the previous mapping emphasized the strong observability property of Σ . Since the condition $\mathbf{y} \equiv \mathbf{0}$ implies $\mathbf{x} = \mathbf{0}$ for any unknown input \mathbf{f} , if μ_i is chosen lower than r_i the entries $\mathbf{c}_i \mathbf{A}^{\mu_i-1} \mathbf{D}$ in δ_i are zero, then \mathbf{f} has no effect on the linear combination \mathbf{M}_i obtained by the i -th component of \mathbf{y} . ■

Corollary 6.1. If Lemma 6.2 is satisfied and

$$\text{rank} \left\{ (\mathbf{D}^T \mathbf{D})^{-1} \mathbf{D}^T \mathbf{M}^{-1} \mathbf{T} \right\} = q\quad (6.15)$$

with $\mathbf{T} = \text{diag}(\mathbf{t}_1, \dots, \mathbf{t}_i, \dots, \mathbf{t}_h)$ and $\mathbf{t}_i = (0 \ \cdots \ 0 \ 1)^T \in \mathbb{R}^{\mu_i \times 1}$, it is possible to reconstruct completely the unknown vector $\mathbf{f} = [f_1, \dots, f_q]^T$ by a suitable robust observer. ■

Proof. Consider the system (6.10) and the following observer:

$$\begin{aligned}\dot{\hat{\mathbf{x}}}_o &= \mathbf{A}_o \hat{\mathbf{x}}_o + \mathbf{T} \zeta \\ \hat{\mathbf{y}}_o &= \mathbf{C}_o \hat{\mathbf{x}}_o\end{aligned}\quad (6.16)$$

where $\hat{\mathbf{x}}_o$, $\hat{\mathbf{y}}_o$ and ζ represent the estimated states, the observed output and the injection term. If condition (6.15) holds, it is obvious that the mapping $\mathbf{x} = \mathbf{M} \mathbf{x}_o$ implies that the matrix $\text{rank}\{\mathbf{D}_o\} = \text{rank}\{\mathbf{D}\} = q$. Let $\mathbf{e}_o = \hat{\mathbf{x}}_o - \mathbf{x}_o$ be the state observation error, its dynamic takes the following form:

$$\dot{\mathbf{e}}_o = \mathbf{A}_o \mathbf{e}_o + \mathbf{T} \zeta - \mathbf{D}_o \mathbf{f}\quad (6.17)$$

Let $\mathbf{F} = [F_1, \dots, F_q]^T$ be a constant vector which constitutes an upper bound on the input \mathbf{f} so that $|f_i| < F_i$, then it can be designed an algorithm which drives to zero the observation error dynamic $(\mathbf{e}, \dot{\mathbf{e}}) \rightarrow (\mathbf{0}, \mathbf{0})$, allowing us to reconstruct \mathbf{f} as follows:

$$\mathbf{f} = \mathbf{D}_o^+ \mathbf{T} \zeta = \mathbf{D}^+ \mathbf{M}^{-1} \mathbf{T} \zeta\quad (6.18)$$

where the index $+$ indicates the Moore-Penrose pseudo-inverse of the matrix. It is obvious that by construction, the solution of system (6.18) gives an unique solution with respect to the unknown input \mathbf{f} if and only if the condition (6.15) is satisfied. ■

Remark 6.2. Consider the observer structure (6.16). Applying the inverse mapping $\mathbf{x}_o = \mathbf{M}^{-1}\mathbf{x}$, it can be obtained a completely equivalent representation for the observer (6.16) which dispenses with the need to work in a transformed domain. In the rest of the Chapter will be used this observer representation. ■

6.4 Local Network Observer design

Consider the scale-free network of N heterogeneous dynamical, coupled, nodes in (6.1)-(6.2). Hereinafter is presented a framework for designing local nonlinear observers for the complete finite-time state estimation and the UIR of each node Σ_i of the network. This is an extension of the strategy for SISO systems presented in [Davila et al., 2009], for networks of MIMO systems. Conditions to achieve this goal will be discussed below in details. Consider the following observer structure:

$$\dot{\hat{\mathbf{x}}}_i = \mathbf{A}_i \hat{\mathbf{x}}_i + \mathbf{B}_i \mathbf{u}_i + \mathbf{G}_i \zeta_i \quad (6.19)$$

$$\hat{\mathbf{y}}_i = \mathbf{C}_i \hat{\mathbf{x}}_i \quad (6.20)$$

where $\hat{\mathbf{x}}_i \in \mathbb{R}^{n_i}$ and $\hat{\mathbf{y}}_i \in \mathbb{R}^{p_i}$ represent the estimated state and the observed output for the node Σ_i . In order to capitalize on the advantages of the sliding mode algorithms, all the equations will be understood in a Filippov sense. Filippov's solution coincides with the classical one for ODEs with continuous right-hand side ([Filippov, 1960]). \mathbf{G}_i and the injection term $\zeta_i = [\zeta_{i,1}, \dots, \zeta_{i,h}] \in \mathbb{R}^{h_i}$ will be designed in the sequel, in such a way that each component of the node's outputs has a suitable preassigned relative degree with respect to the associated injection term. Observing the structure of the scale-free dynamical network in (6.1)-(6.2), due to the presences of the coupling term related to the i -th node with its neighbors, Lemma 6.2 is not applicable in the present form. Before presenting the conditions under which the state estimation and the UIR are practicable, the concept of relative degree of the k -th output of the i -th node $y_{i,k}$ with respect to the local unknown input signal ($r_{i,k}$) and the coupling terms with the j -th neighbor ($w_{i,k}$) need to be defined. Let $\mathbf{c}_{i,k}$ be the k -th row of the output matrix \mathbf{C}_i , in accordance with the definition of relative degree in (6.5), for each output component of Σ_i the following indices are defined:

$$\begin{aligned} \mathbf{c}_{i,k} \mathbf{A}_i^l \mathbf{D}_i &= \mathbf{0}_{(1 \times q_i)} \\ \mathbf{c}_{i,k} \mathbf{A}_i^{r_{i,k}-1} \mathbf{D}_i &\neq \mathbf{0}_{(1 \times q_i)} \end{aligned} \quad \text{with} \quad \begin{cases} k = 1, 2, \dots, p_i \\ i = 1, 2, \dots, N \\ l = 0, 1, \dots, r_{i,k} - 2 \end{cases} \quad (6.21)$$

$$\begin{aligned} \mathbf{c}_{i,k} \mathbf{A}_i^l \Gamma_{ij} &= \mathbf{0}_{(1 \times q_i)} \\ \mathbf{c}_{i,k} \mathbf{A}_i^{w_{i,k}-1} \Gamma_{ij} &\neq \mathbf{0}_{(1 \times n_j)} \end{aligned} \quad \text{with} \quad \begin{cases} k = 1, 2, \dots, p_i \\ l = 0, 1, \dots, w_{i,k} - 2 \end{cases} \quad (6.22)$$

Then in order to adapt Lemma 6.2 for the class of connected systems in (6.1)-(6.2), it can be reformulated as follows:

Lemma 6.3. The scale-free network of N heterogeneous dynamical, coupled nodes in (6.1)-(6.2) is strongly observable, if it is possible to find a set of integer $\mathcal{U}_i := \{\mu_{i,1}, \dots, \mu_{i,h}\}$ with

$h \leq p$ in which each element is associated to one output's component and such that the following conditions are satisfied:

$$\begin{cases} \mu_{i,k} \leq v_{i,k} \\ \mu_{i,k} \leq \min \{r_{i,k}, w_{i,k}\} \end{cases}, \quad \mu_{i,1} + \dots + \mu_{i,h_i} = n_i \quad \text{with } k = 1, 2, \dots, h_i \quad (6.23)$$

$$\det \{M_i\} \neq 0, M_i = \begin{pmatrix} M_{i,1} \\ \vdots \\ M_{i,k} \\ \vdots \\ M_{i,h} \end{pmatrix}, M_{i,k} = \begin{pmatrix} c_{i,k} \\ c_{i,k} A_i \\ c_{i,k} A_i^2 \\ \vdots \\ c_{i,k} A_i^{\mu_{i,k}-1} \end{pmatrix} \quad (6.24)$$

Proof. The proof of this lemma can be obtained in a similar manner to Lemma 6.2 by inspection of the canonical observable representation obtained by the following mapping $x_i = M_i x_{o,i}$. ■

In light of Lemma 6.3, in the following it is analyzed how to design an observer which allows to achieve the state space estimation for the complex network in (6.1)-(6.2) and are provided additional structural conditions for the UIR. Supposing Lemma 6.3 is satisfied. Let $T_i = \text{diag} (t_{i,1}, \dots, t_{i,k}, \dots, t_{i,h_i}) \in \mathbb{R}^{n_i \times h_i}$ be a block-diagonal matrix with each k-th block designed as follows:

$$t_{i,k} = \begin{pmatrix} 0 & \dots & 0 & 1 \end{pmatrix}^T \in \mathbb{R}^{\mu_{i,k} \times 1} \quad (6.25)$$

The matrix G_i in (6.19) can be selected as follows

$$M_i G_i = T_i \rightarrow G_i = M_i^{-1} T_i \quad (6.26)$$

In light of (6.23)-(6.26), taking a generic observer output $\hat{y}_{i,k}$ and differentiating it $\mu_{i,k}$ times, the following I/O dynamic results:

$$\frac{d}{dt} \begin{pmatrix} \hat{y}_{i,k} \\ \hat{y}_{i,k} \\ \vdots \\ \hat{y}_{i,k}^{(\mu_{i,k}-1)} \end{pmatrix} = \begin{pmatrix} c_{i,k} A_i \\ c_{i,k} A_i^2 \\ \vdots \\ c_{i,k} A_i^{\mu_{i,k}} \end{pmatrix} \hat{x}_i + \begin{pmatrix} c_{i,k} B_i \\ c_{i,k} A_i B_i \\ \vdots \\ c_{i,k} A_i^{\mu_{i,k}-1} B_i \end{pmatrix} u_i + \begin{pmatrix} 0 \\ \vdots \\ 0 \\ 1 \end{pmatrix} \zeta_{i,k} \quad (6.27)$$

which can be rewritten as

$$\dot{\hat{y}}_{i,k} = M_{i,k} A_i \hat{x}_i + M_{i,k} B_i u_i + t_k \zeta_{i,k} \quad (6.28)$$

where the matrix $M_{i,k} A_i$ takes the following form:

$$M_{i,k} A_i = \left(\begin{array}{cccc|cccc} 0 & 1 & \dots & 0 & 0 & \dots & 0 & \\ 0 & \vdots & \ddots & \vdots & \vdots & & \vdots & \\ 0 & 0 & \dots & 1 & 0 & \dots & 0 & \\ \hline * & * & \dots & * & * & \dots & * & \end{array} \right) \in \mathbb{R}^{\mu_{i,k} \times n_i} \quad (6.29)$$

It is easy to see that the k-th observer's output $\hat{y}_{i,k}$ has relative degree $\mu_{i,k}$ with respect to the injection term $\zeta_{i,k}$. Let $e_i = \hat{x}_i - x_i$ be the state error for the agent Σ_i , it can be defined the output error dynamic for the k-th output $\hat{y}_{i,k}$ as follows:

$$e_{i,y_k} = \hat{y}_{i,k} - y_{i,k} = c_{i,k} e_i \quad \text{for } k = 1, 2, \dots, h \quad (6.30)$$

$$\Phi_{i,k} = \left(\varphi_{i,k,1} \quad \cdots \quad \varphi_{i,k,\mu_{i,k}} \right)^T = \left(e_{i,y_k} \quad \dot{e}_{i,y_k} \quad \cdots \quad e_{i,k}^{(\mu_{i,k}-1)} \right)^T \quad (6.31)$$

$$\begin{cases} \dot{\varphi}_{i,k,1} &= \varphi_{i,k,2} \\ \dot{\varphi}_{i,k,2} &= \varphi_{i,k,3} \\ \vdots & \vdots \\ \dot{\varphi}_{i,k,\mu_{i,k}} &= \tilde{\varphi}_{i,k,(\mu_{i,k}+1)} + \zeta_{i,k} \end{cases} \quad (6.32)$$

with

$$\tilde{\varphi}_{i,k,(\mu_{i,k}+1)} = c_{i,k} A_i^{\mu_{i,k}} e_i + \varrho_{i,k} f_i + \sum_{j=1}^N \eta_{i,k}(t) x_j \quad (6.33)$$

$$\varrho_{i,k} = c_{i,k} A_i^{\mu_{i,k}-1} D_i \quad (6.34)$$

$$\eta_{i,k}(t) = c(t) \mathcal{L}_{ij} c_{i,k} A_i^{\mu_{i,k}-1} \Gamma_{ij} \quad (6.35)$$

where the I/O dynamic (6.32) has the so-called Brunovsky chain-of-integrator canonical form. Note that the presence of $\varrho_{i,k}$ and $\eta_{i,k}$ is strictly related to the choice of the differentiation index $\mu_{i,k}$. The following cases list explain all the possible scenarios:

- 1) if $\mu_{i,k} = r_{i,k} = w_{i,k}$, from (6.21)-(6.22), both terms $\varrho_{i,k}$ and $\eta_{i,k}$ appear in (6.33);
- 2) if $\mu_{i,k} = r_{i,k} < w_{i,k}$, $\eta_{i,k} = 0$, thus only the *Unknown Input Term* $\varrho_{i,k}$ appears in (6.33);
- 3) if $\mu_{i,k} = w_{i,k} < r_{i,k}$, $\varrho_{i,k} = 0$ thus only the *Dynamical Coupling Term* $\eta_{i,k}$ appears in (6.33);
- 4) if $\mu_{i,k}$ is smaller than both $r_{i,k}$ and $w_{i,k}$ according to (6.21)-(6.22) these terms are both $\varrho_{i,k}$ and $\eta_{i,k}$ equal to zero.

Following similar reasoning, the complete observation error dynamic $\Phi_i = [\Phi_{i,1}, \dots, \Phi_{i,h_i}]^T$ can be obtained by putting in columns the h_i Brunovsky canonical blocks (6.32) calculated at the time. Note that each sub-dynamic has relative degree $\mu_{i,k}$. In order to estimate the whole state space of each node Σ_i , a suitable injections signals able to drive to zero the error $e_i = [e_{i,1}, \dots, e_{i,n_i}]^T$ is needed. Since $\Phi_i = M_i e_i$ with M_i invertible, it is obvious that $\Phi_i = 0$ implies $e_i = 0$. Thus if it is possible to drive to zero all the h_i sub-dynamics expressed by (6.32), automatically the whole observation error e_i goes to zero. Make the following boundedness assumption:

Assumption 6.3. *There are known constants $F_{i,k}$ such that the function $\tilde{\varphi}_{i,k,(\mu_{i,k}+1)}$ satisfies:*

$$|\tilde{\varphi}_{i,k,(\mu_{i,k}+1)}| < F_{i,k} \quad \forall \quad k = 1, 2, \dots, h_i \quad (6.36)$$

■

Under this assumption the finite-time convergence to zero of Φ_i by a properly designed HOSM can be guaranteed. The choice of the most suitable HOSM algorithm is strictly related to the relative degree $\mu_{i,k}$ of each sub-block (6.32). Table 6.1 shows the best choices depending on $\mu_{i,k}$. Note that the so-called *quasi-continuous arbitrary-order* (QCAO) SMC

is able to provide finite-time stabilization of arbitrary relative degree dynamics. For relative degree one or two systems, the best choices are respectively the *Super-Twisting* (STW) algorithm and the *Generalized Sub-Optimal* algorithm (GSO). In particular STW gives rise to a continuous control action which possesses significant robustness properties against nonlinearities and disturbances, whilst the GSO algorithm stabilizes second order dynamics without any derivative estimation, simplifying the complexity of the algorithm (see [Bartolini et al., 2003]). However the GSO has a discontinuous behavior, whereas the QCAO SMC has discontinuities only during the sliding motion $\varphi_{i,k} = \dot{\varphi}_{i,k} = \dots = \varphi_{i,k}^{\mu_{i,k}-1}$ (see [Levant, 2005]).

Taking into account the case list presented earlier, Corollary 6.1 can be adjusted in order that UIR becomes practicable.

Corollary 6.2. *If Lemma 6.3 is satisfied along with*

$$\text{rank} \{ \mathbf{D}_i^+ \mathbf{M}_i^{-1} \mathbf{T}_i \} = q_i \quad (6.37)$$

where $\mathbf{T}_i = \text{diag} (t_{i,1}, \dots, t_{i,h_i})$, $t_{i,k} = (0, \dots, 0, 1) \in \mathbb{R}^{\mu_{i,k} \times 1}$

$$\mathbf{M}_i \mathbf{D}_i = \begin{pmatrix} \delta_{i,1} \\ \vdots \\ \delta_{i,h} \end{pmatrix}, \delta_{i,k} = \begin{pmatrix} 0 \\ \vdots \\ c_{i,k} \mathbf{A}_i^{\mu_{i,k}-1} \mathbf{D}_i \end{pmatrix} \in \mathbb{R}^{\mu_{i,k} \times n_i} \quad (6.38)$$

and each sub-block $\delta_{i,k}$ has its index $\mu_{i,k}$ which satisfies

$$\mu_{i,k} = r_{i,k} < w_{i,k} \quad (6.39)$$

then it is possible to reconstruct completely the unknown vector $\mathbf{f}_i = [f_{i,1}, \dots, f_{i,q}]^T$ by a suitable robust observer. ■

Proof. *The proof of this corollary can be obtained similarly to Corollary 6.1 by inspection of the following error dynamic:*

$$\dot{\mathbf{e}}_i = \mathbf{A}_i \mathbf{e}_i + \mathbf{G}_i \zeta_i - \mathbf{D}_i \mathbf{f}_i + c(t) \sum_{i=1}^N \mathcal{L}_{ij} \Gamma_{ij} \mathbf{x}_j \quad (6.40)$$

Since the error dynamic (6.40) can be driven to zero in finite time, once $(\mathbf{e}_i, \dot{\mathbf{e}}_i) = (\mathbf{0}, \mathbf{0})$ UIR can be achieved as follows

$$\mathbf{f}_i = \mathbf{D}^+ \mathbf{M}^{-1} \mathbf{T}_i \zeta_i - c(t) \sum_{i=1}^N \mathcal{L}_{ij} \mathbf{D}^+ \Gamma_{ij} \mathbf{x}_j \quad (6.41)$$

If the state \mathbf{x}_j is accessible only at the supervisory level, it would be impossible to locally reconstruct \mathbf{f}_i without the knowledge of the neighbors states. However, if both conditions (6.37) and (6.39) hold, $\mathbf{D}^+ \Gamma_{ij} = \mathbf{0}$ and the complete information of \mathbf{f}_i is contained in ζ_i . UIR can be obtained as the unique solution of the following equalities $\mathbf{f}_i = (\mathbf{D}^T \mathbf{D})^{-1} \mathbf{D}^T \mathbf{M}^{-1} \mathbf{T}_i \zeta_i$. ■

6.5 Numerical Example

6.5.1 Observer design

Before presenting results for a scale-free network, for the sake of completeness an application of the design strategy shown in Lemma 6.2 for an rectangular unstable system in

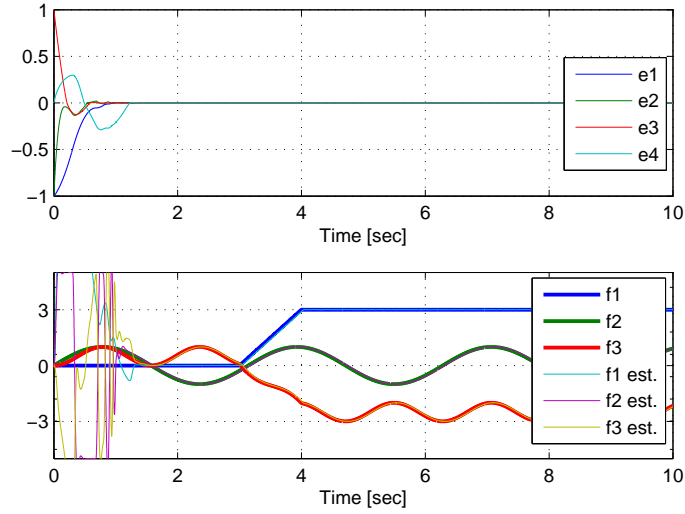


Figure 6.1: Estimation errors and UIR after proper filtering.

form (6.3)-(6.4) is presented. The following matrices describes the system:

$$\begin{aligned}
 \mathbf{A} &= \begin{pmatrix} 0 & -1 & -1 & 0 & 0 \\ 1 & 0.2 & 0 & 0 & 0 \\ 0 & 0 & -6 & 1 & 0 \\ 0 & 0 & 0 & 0 & 1 \\ 1 & 0 & 0 & -1 & -2 \end{pmatrix}, \mathbf{D} = \begin{pmatrix} 0 & 1 & 0 \\ 0 & 0 & 0 \\ 1 & 1 & 0 \\ 0 & 0 & 0 \\ 0 & 0 & 1 \end{pmatrix}, \mathbf{C} = \begin{pmatrix} 0 & 1 & 0 & 0 & 0 \\ 0 & 0 & 1 & 1 & 1 \\ 0 & 0 & 0 & 1 & 0 \\ 1 & 1 & 0 & 1 & 1 \end{pmatrix} \\
 \mathbf{f} &= \begin{pmatrix} f_1 \\ f_2 \\ f_3 \end{pmatrix} = \begin{pmatrix} 3(\delta_{-2}(t-3) - \delta_{-2}(t-4)) \\ \cos(2t) \\ \cos^2(2t) - 3(\delta_{-2}(t-3) - \delta_{-2}(t-4)) \end{pmatrix}
 \end{aligned} \tag{6.42}$$

From Definition 6.1 the set of observability indices is $\mathcal{V} = \{5, 5, 5, 5\}$, while the vector relative degree is $\mathbf{r} = \{2, 1, 2, 1\}$. By means of Lemma 6.2 and Corollary 6.1, the observer matrices \mathbf{M} and \mathbf{T} can be easily derived by the following possible set of indices $\mathcal{U} = \{\mu_i\}_{i=1,\dots,4} = \{2, 1, 1, 1\}$. Then in order to reduce the need of sliding differentiators needed for the injection term $\zeta = [\zeta_1, \dots, \zeta_4]^T$, in accordance with Table 6.1, STW and GSO algorithms for the relative degree one and two dynamics, respectively are designed. For further details on these algorithms refer to Chapter 4 or references in Table 6.1. In Figure 6.1 the estimation errors (upper plot) and the comparison between the \mathbf{f} components and the reconstructed unknown input vector (lower plot) as in (6.18) after proper low-pass Butterworth filtering are shown.

6.5.2 Observer design for agents networks

To demonstrate the theory developed in this Chapter, the time-varying network \mathcal{G} of six heterogeneous chaotic circuits show in Figure 6.2 is considered. In light of (6.1)-(6.2), hereinafter the dynamics of each node Σ_i of the complex network are presented:

- Nodes Σ_i with $i = 1, 2, 3$ and $j = 1, 2, \dots, 6$ are represented by a Rössler dynamic as follows:

$$\mathbf{A}_i = \begin{pmatrix} 0 & -1 & -1 \\ 1 & 0.2 & 0 \\ 0 & 0 & -6 \end{pmatrix}, \mathbf{D}_i = \begin{pmatrix} 0 \\ 0 \\ 1 \end{pmatrix}, \mathbf{\Gamma}_{ij} = \begin{pmatrix} 1 & \dots & 1 \\ 0 & \dots & 0 \\ 0 & \dots & 0 \end{pmatrix} \tag{6.43}$$

Table 6.1: Sliding mode and relative degree

Relative Degree	HOSM Algorithm
1	Super-Twisting SMC ([Levant, 1993a])
2	Generalized Sub-Optimal SMC ([Bartolini et al., 2003])
≥ 2	Quasi-Continuous Arbitr. Order SMC ([Levant, 2005])

$$\mathbf{B}_i = \mathcal{I}_{3 \times 3}, \mathbf{C}_i = \begin{pmatrix} 0 & 1 & 0 \\ 0 & 0 & 1 \end{pmatrix}, f_i(x_i) = (0.2 + x_{i,1}x_{i,3}) \quad (6.44)$$

- Nodes Σ_i with $i = 4, 5, 6$ and $j = 1, 2, \dots, 6$ are represented by an Hyper-chaotic Rössler dynamic as follows:

$$\mathbf{A}_i = \begin{pmatrix} 0 & -1 & -1 & 0 \\ 1 & 0.25 & 0 & 1 \\ 0 & 0 & 0 & 0 \\ 0 & 0 & -0.5 & 0.05 \end{pmatrix}, \mathbf{D}_i = \begin{pmatrix} 0 \\ 0 \\ 1 \\ 0 \end{pmatrix}, \mathbf{\Gamma}_{ij} = \begin{pmatrix} 0 & \dots & 0 \\ 0 & \dots & 0 \\ 1 & \dots & 1 \\ 1 & \dots & 1 \end{pmatrix} \quad (6.45)$$

$$\mathbf{B}_i = \mathcal{I}_{4 \times 4}, \mathbf{C}_i = \begin{pmatrix} 1 & 0 & 0 & 0 \\ 0 & 1 & 0 & 0 \end{pmatrix}, f_i(\mathbf{x}_i) = (3 + x_{i,1}x_{i,3}) \quad (6.46)$$

Note that for both circuits, the coefficients are such that Rössler chaotic and hyper-chaotic attractors dynamic are presented. A window of 100 seconds of simulation is considered. The time varying coupling strength is $c(t) = \sin(2\pi 50t)$.

Full static state error feedback synchronization

Consistent with [Suykens et al., 1999], the control strategy adopted in the supervisory level for synchronization in the network is a full static feedback rule as $\mathbf{u}_i = \mathbf{F}_i(\mathbf{z} - \hat{\mathbf{x}}_i)$, where \mathbf{z} and $\hat{\mathbf{x}}_i$ are the master state vector and the estimated state of the i -th node. \mathbf{F}_i has been constructed with the intention to synchronize each node with the following unstable limit cycle:

$$\begin{cases} z_1 = \cos(\xi) (a \cos(\omega t) + c \sin(2\omega t)) + \\ \quad - \sin(\xi) (b \sin(\omega t) + c \sin(2\omega t)) \\ z_2 = 0.6 \cdot [a \sin(\xi) \cos(\omega t) - b \cos(\xi) \sin(\omega t)] + \\ \quad + 0.3 \cdot [c \sin(\xi) \cos(2\omega t) - c \cos(\xi) \sin(2\omega t)] \\ z_3 = z_3(0) \exp^{-t} - \int_0^t \exp^{-(t-\tau)} \tilde{z}_2 d\tau, \quad z_4 = 0 \end{cases} \quad (6.47)$$

where $a = 2.6$, $b = 1.2$, $c = 0.2$, $\xi = \pi/18$, $\omega = 1.7$. Note that the fourth control involve only the nodes $\Sigma_4, \Sigma_5, \Sigma_6$.

State Estimation and Unknown Input Reconstruction

The objective is to demonstrate the robustness of the presented framework to time varying coupling strengths and varying network topologies at different time intervals (see Figure 6.2). Note that it is not necessary to have any a prior knowledge of the number of nodes,

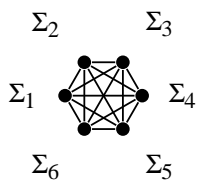
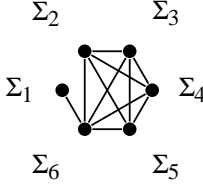
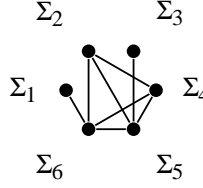
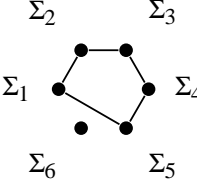
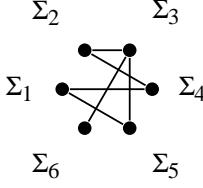
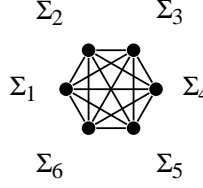
		
Time [0 to 12 sec.]	Time [12 to 24 sec.]	Time [24 to 36 sec.]
		
Time [36 to 50 sec.]	Time [50 to 65 sec.]	Time [65 to 100 sec.]

Figure 6.2: Time-Varying network topology.

but only the knowledge of the matrix Γ_{ij} of each node part of the network or of a new potential one.

Recalling Definition 6.1, and the definitions of relative degree with respect to the unknown input and the coupling terms with the j -th neighbor, (in (6.21) and (6.22)), and Lemma 6.3, the only combination of the designing indices $\mu_{i,k}$ which satisfy for each node conditions in (6.23) and (6.24), is the following one:

- for the first three nodes Σ_i with $i = 1, 2, 3$:

$$\left(v_{i,1} = 3, r_{i,1} = 3, w_{i,1} = 2 \right) \mapsto \mu_{i,1} = 2 \quad (6.48)$$

$$\left(v_{i,2} = 1, r_{i,2} = 1, w_{i,2} = \infty \right) \mapsto \mu_{i,2} = 1 \quad (6.49)$$

- for the remaining nodes Σ_i with $i = 4, 5, 6$:

$$\left(v_{i,1} = 3, r_{i,1} = 2, w_{i,1} = 2 \right) \mapsto \mu_{i,1} = 2 \quad (6.50)$$

$$\left(v_{i,2} = 2, r_{i,2} = 3, w_{i,2} = 2 \right) \mapsto \mu_{i,2} = 2 \quad (6.51)$$

Thus from equations (6.24) and (6.26), the design matrices M_i and G_i for each observer (6.19)-(6.20) can be derived. Then in accordance with Table 6.1, and in light of (6.48)-(6.51), the following sliding mode algorithms as injection terms has been chosen:

- for the first three nodes Σ_i with $i = 1, 2, 3$:

$$\zeta_i = \left(\zeta_{i,1} \quad \zeta_{i,2} \right)^T = \left(\zeta_{\text{GSO}_{i,1}} \quad \zeta_{\text{STW}_{i,2}} \right)^T \quad (6.52)$$

- for the last three nodes Σ_i with $i = 4, 5, 6$:

$$\zeta_i = \left(\zeta_{i,1} \quad \zeta_{i,2} \right)^T = \left(\zeta_{\text{GSO}_{i,1}} \quad \zeta_{\text{GSO}_{i,2}} \right)^T \quad (6.53)$$

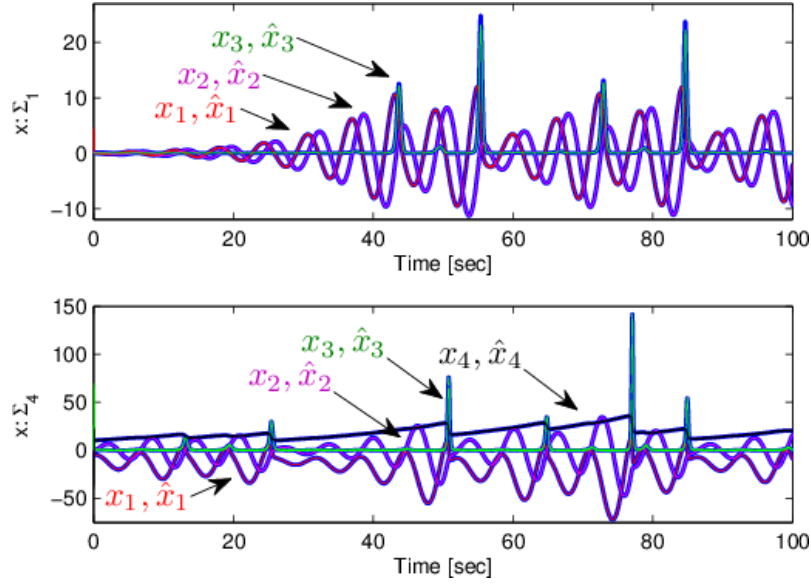


Figure 6.3: State reconstruction process in Σ_1 (top) and Σ_4 (down).

where $\zeta_{\text{GSO}_{i,k}}$ and $\zeta_{\text{STW}_{i,k}}$ are

$$\zeta_{\text{GSO}_{i,k}} = -U_{i,k} \text{sign}(\varphi_{i,k,2} - \beta_{i,k} \varphi_{M_{i,k,2}}) \quad (6.54)$$

$$\zeta_{\text{STW}_{i,k}} = \zeta_{i,k_1} + \zeta_{i,k_2} \text{ with } \begin{cases} \zeta_{i,k_1} = -\lambda_{i,k_1} |\varphi_{i,k,1}|^{1/2} \text{sign}(\varphi_{i,k,1}) \\ \zeta_{i,k_2} = -\lambda_{i,k_2} \text{sign}(\varphi_{i,k,1}), \zeta_{i,k_2}(0) = 0 \end{cases} \quad (6.55)$$

where $U_{i,k} > F_{i,k}$ is the control magnitude, $\beta_{i,k} = 0.5$ the anticipation parameter, $\varphi_{M_{i,k,2}}$ is the "latest singular" point of the sliding surface $\varphi_{i,k,2}$, while $\lambda_{i,k_1} > 2\sqrt{F_{i,k}}$ and $\lambda_{i,k_2} > F_{i,k}$ are suitable constant gains. For further details on these algorithms refer to the references in Table 6.1. The good performances of the estimation process are shown in Figure 6.3. The actual and estimated states of Σ_1 and Σ_4 are depicted. No synchronization has been applied ($\mathbf{u}_i = \mathbf{0} \forall i$).

From Corollary 6.2 and the chosen indices in (6.48)-(6.51), due to the structure of the coupling matrix Γ_{ij} for the last three nodes it is possible to assert that UIR is practicable only in $\Sigma_1, \Sigma_2, \Sigma_3$, because $\mu_{i,2} = r_{i,2} < w_{i,2}$ and $\text{rank}\{D_i^+ M_i T_i\} = 1$. However if the third row of Γ_{ij} in (6.46) was all zero, taking $\mu_{i,1} = \mu_{i,2} = 2$ the UIR either for the last three nodes would have been possible. Figure 6.4 (top) shows the convergence of the six nodes to the reference trajectory, whereas in the bottom, the UIR of the signal f_1 obtained by means of $\zeta_{1,2} = \zeta_{\text{STW}_{1,2}}$ is shown.

6.6 Conclusion

A new approach for designing HOSM observers based on the concept of observability indices for rectangular MIMO systems affected by multiple unknown input signals has been proposed. The framework has been extended to the problem of decentralized state estimation and unknown input reconstruction from a class of connected heterogeneous systems. Conditions for complete finite-time state estimation and the UIR in each system operating over

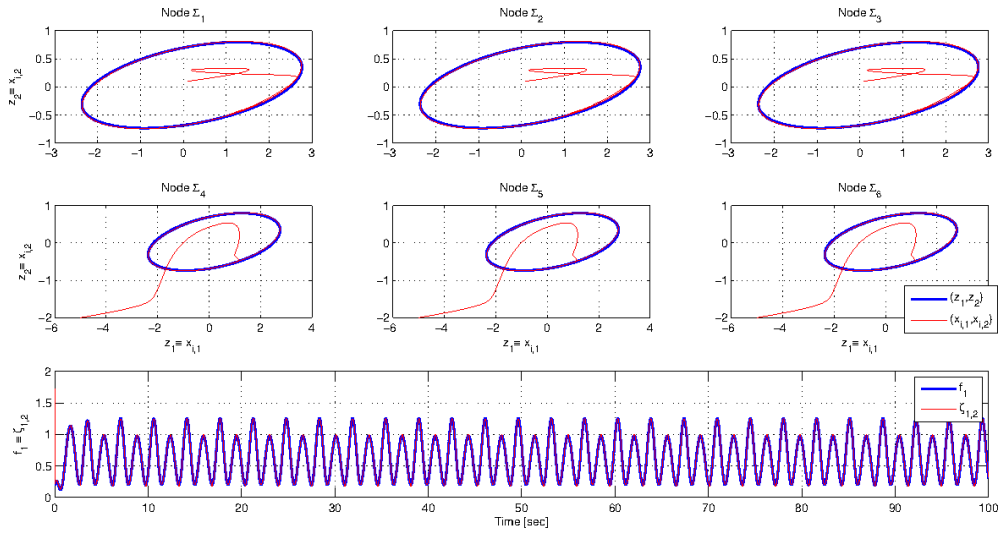


Figure 6.4: Convergence to the references trajectory and UIR.

a network are fulfilled. The proposed framework is inherently robust and is totally independent to the network configuration or to the number of nodes. Simulation results confirmed the effectiveness of the presented methods.

Chapter 7

Sliding Mode Strong Observer as a tool for FDI: An application to Induction Motor

As mentioned in Chapter 4 SMC algorithms has found a rich soil in the area of robust state-estimation and fault detection and isolation. The reasons of this trend are multiples. The first one is obviously related to their properties of robustness. An example has been shown in Chapter 6 where thanks to these properties tasks like complete state-estimation and unknown input reconstruction have been easily achieved combining SMC algorithm along with suitable diffeomorphic transformation. The second one is that software-based applications due to their high bandwidth suffer less from the chattering phenomenon [[Spurgeon, 2008](#), [Utkin & Guldner, 1999](#)].

In this Chapter, strictly related to the task of designing strong observers in MIMO systems (see Chapter 4 and 6), HOSM observers are employed as a tool for detecting certain abnormal operating conditions in squirrel cage induction motors (SCIMs) [[Pilloni et al., 2013c](#), [Pilloni et al., 2012c](#)].

To justifying the presented treatment, a mathematical characterization of the faulty operating mode in SCIM is derived in which rotor broken bars faults and the rotor eccentricity are taken into account. The performances of the proposed scheme have been analyzed by Lyapunov methods and verified by real implementation tests using measurements taken from certain commercial three-phase SCIMs intentionally damaged in order to reproduce the fault scenarios of concern.

7.1 Motivations

Nowadays three-phase Squirrel Cage Induction Motors (SCIMs) are used in a variety of industrial applications due to their cheapness, ruggedness and low maintenance [[Bonnett & Albers, 2000a](#)]. Voltage stresses, caused by the modern high frequency power converters, along with the corrosive and dusty industry environments where motors operate can reduce the motor lifetime considerably. The rotor has always been considered the Achilles heel

of SCIMs. In fact, although the stator windings' design has achieved remarkable improvements in the last decades, cage rotor's design has undergone little change [Bonnett & Albers, 2000a].

Technical surveys have shown that a remarkable percentage of total SCIM failures is found in the rotor. Broken bars, end-ring faults, and eccentricity result the most common failures [Benbouzid & Kliman, 2003, Bonnett & Albers, 2000b, Bonnett & Soukup, 1986, Kliman et al., 1988, Puche-Panadero et al., 2009]. Anyway a prompt detection of these abnormal conditions can avoid costly disservice, and potentially catastrophic breakdowns if the fault remains undetected.

Even though temperature and vibration monitoring devices have been utilized for decades, recent research efforts have been directed towards the inspection of the motor currents, which is more convenient from the practical implementation point of view. Up to now *Motor Current Signature Analysis* (MCSA) methods are the most popular approaches for SCIM diagnostics [El Hachemi Benbouzid, 2000]. When broken cage bars, end-ring faults, or abnormal levels of eccentricity occur, asymmetry in the rotor air-gap appear and spurious harmonics at well defined characteristic frequencies coming out in the stator current spectrum [Kliman et al., 1988, Puche-Panadero et al., 2009, El Hachemi Benbouzid, 2000, Didier et al., 2006, Thomson & Fenger, 2001]. MCSA is an online diagnosis family of methods which requires just the measurement of a single stator phase current and, at least under constant load condition, allows to correctly classify simultaneous failures. MCSA has the advantage of dispensing with the knowledge of the electromechanical motor parameters, and it can be inexpensively implemented by utilizing a current transformer or current clamp already in place in most industrial applications. As a result, MCSA has become the current standard for online motor diagnosis [El Hachemi Benbouzid, 2000]. Modern MCSA methodologies based on advanced processing techniques such as Hilbert, Wavelet transforms or Transient MCSA (T-MCSA) are continuously developed to enhance the reliability of the diagnosis process [Puche-Panadero et al., 2009].

There are, however, some inherent drawbacks of MCSA, such as its sensitivity to the spectral leakage caused by the finite-time measurement window, the need for high frequency resolution (i.e., small sampling intervals), and its sensitivity to varying load conditions and to the presence of additional spurious harmonics caused by mechanical devices, such as gearboxes, that can often overwhelm the frequency pattern associated to the fault [Puche-Panadero et al., 2009, El Hachemi Benbouzid, 2000]. Furthermore MCSA methodologies have to be periodically activated due to their inability to identify the occurrence of the faults.

In recent years model-based approach to fault detection and isolation (FDI) are receiving a growing interest [Simani et al., 2003, Petkovic M. & A., 2012, Orani et al., 2010]. For these reasons a novel model-based approach for detecting the occurrence of incipient rotor fault like broken bar fault or eccentricity conditions is here discussed.

Requirements of the proposed method are respectively measurement taken from: stator currents, voltages, shaft speed, and a priory knowledge of the nominal motor's electromechanical parameters. Notice that to overcome the uncertainties in the load torque, strong observation approach, robust to the presence of exogenous input terms, are employed.

The framework of design relies on the so-called high-order sliding mode observers [Orani et al., 2010, Pisano & Usai, 2011, Piloni et al., 2013a, Fridman et al., 2007a, Floquet

et al., 2004, Pillosu et al., 2011, Bejarano & Pisano, 2011, Bejarano et al., 2011]. Suitable residuals are computed and processed by a threshold based FDI logic for achieving a quick and computationally simple detection of the faulty conditions. Once the occurrence of a fault is detected, additional information about the nature of the fault occurred can be recovered by performing a spectral analysis of the "faulty" residuals. The main advantage of the method, as compared to the MCSA approaches, is that the need of continuous spectral or transform-based analysis is dispensed with, which reduces the computational effort of the diagnosis algorithm.

The Chapter is organized as follows. In Section 7.2 a mathematical model of a SCIM under faulty conditions is presented along with a brief description of the effects of each faults in terms of characteristic frequencies. In Section 7.3 the proposed FDI observer is outlined. Convergence and estimation properties are demonstrated, then the suggested FDI logic is illustrated. Section 7.4 discusses some experimental results obtained, whilst Section 7.5 presents some concluding remarks and possible lines of investigation for future research.

7.2 Faulty SCIM Model

As it is well known, the equations representative of the nominal (i.e., healthy) operation of a three-phase induction motor mathematical model (both Wound or Squirrel-Cage Rotor) in (α, β) reference frame (or stator reference frame) are (see for example [Krause & Thomas, 1965, Marino et al., 1993]):

$$\begin{cases} \dot{x}_1 = a_1(x_3x_4 - x_2x_5) - a_2x_1 + a_3T_L \\ \dot{x}_2 = b_1x_4 - b_2x_2 + b_3x_1x_3 + b_4u_{s\alpha} \\ \dot{x}_3 = b_1x_5 - b_2x_3 - b_3x_1x_2 + b_4u_{s\beta} \\ \dot{x}_4 = c_1x_2 - c_2x_4 - n_p x_1x_5 \\ \dot{x}_5 = c_1x_3 - c_2x_5 + n_p x_1x_4 \end{cases} \quad (7.1)$$

where a_i , b_i and c_i are coefficients dependent on the machine parameters which take the following form:

$$\begin{aligned} a_1 &= \frac{n_p L_m}{J L_r} & a_2 &= \frac{f_p}{J} \\ a_3 &= -\frac{1}{J} & \sigma &= 1 - \frac{L_m^2}{L_r L_s} \\ b_1 &= \frac{L_m R_r}{\sigma L_s L_r^2} & b_2 &= \frac{L_m^2 R_r + L_r^2 R_s}{\sigma L_s L_r^2} \\ b_3 &= \frac{n_p L_m}{\sigma L_s L_r} & b_4 &= \frac{1}{\sigma L_s} \\ c_1 &= \frac{R_r}{L_r} L_m & c_2 &= \frac{R_r}{L_r} \end{aligned} \quad (7.2)$$

The state-space variables x_i with $i = 1, \dots, 5$ and the electromechanical parameters in (7.1)-(7.2) are in Table 7.1. In order to find out a mathematical representation of the machine in faulty operating condition, in the following the main effects of broken bar and eccentricity faults, are briefly discussed.

Table 7.1: Nomenclature of SCIM Model

State Variables:		
Shaft speed	x_1	[rad/sec]
(α, β) Stator Currents	$x_{2,3}$	[A]
(α, β) Rotor Fluxes	$x_{4,5}$	[Wb]
Input Signals:		
(α, β) Stator Voltage Supply	$u_{\alpha, \beta}$	[V]
Load Torque	T_L	[N · m]
Model Parameters:		
Pole pairs number	n_p	-
Rotor and stator resistance	$R_{r,s}$	[Ω]
Rotor, stator and mutual inductance	$L_{r,s,m}$	[H]
Viscous friction coefficient	f_v	[Kg · m ² /s]
Rotor inertia	J	[Kg · m ²]

7.2.1 Air-Gap Eccentricity Fault

Eccentricity manifests in two different versions, referred to as static and dynamic eccentricity. *Static eccentricity* takes place when the angular position of the minimum radial air-gap length is fixed in space. It can be caused by stator-core ovality or incorrect positioning of the rotor in the stator. For these reasons an inherent level of static eccentricity always occurs due to manufacturing tolerances or specific design features. *Dynamic eccentricity* corresponds to the case where the minimum air-gap revolves with the rotor and is a function of space and time. This can be caused by a non-concentric outer rotor diameter or rotor thermal bowing. Static and dynamic eccentricity generate an electromagnetic force called *unbalanced magnetic pull* (UMP), respectively of "steady" and "rotating" type in the two cases, that in some cases can bring rotor and stator in contact [Puche-Panadero et al., 2009, El Hachemi Benbouzid, 2000]. The air-gap eccentricity specified by manufacturers is the *radial air-gap eccentricity* (static plus dynamic) and is normally given as a percentage of the nominal air-gap length. Levels of air-gap eccentricity should be kept within a maximum of 10% in three-phase SCIMs to avoid their catastrophic damage. Static plus dynamic eccentricity is also known as *mixed eccentricity*. The sideband spurious frequencies associated with the eccentricity are given by:

$$f_{ecc} = |f_s \pm k \cdot f_r|, \quad k = 1, 2, 3 \dots \quad (7.3)$$

where f_s and f_r are the electrical and mechanical frequencies of the machine. From (7.3) it is clear that these specific sideband frequencies do not depend on the machine parameters.

7.2.2 Broken Bars Fault

Breakages in the rotor cage introduce anomalies in the air-gap magnetic field, and consequently sideband harmonics appear in the stator currents [Benbouzid & Kliman, 2003, El Hachemi Benbouzid, 2000]. These harmonics of fault have well-defined frequencies located respectively at:

$$f_{brb} = f_s \cdot [1 \pm 2 k \cdot s], \quad k = 1, 2, 3 \dots \quad (7.4)$$

where $s = 1 - \omega_r / \omega_s$ is the *motor slip*, $\omega_r = 2\pi f_r$ and $\omega_s = 2\pi f_s$ represent respectively the mechanical speed and the synchronous speed of magnetic field. Although broken bar faults do not cause immediate disservice, they can imply serious secondary effects (i.e. overheating, bar hitting, damaging of motor insulation and consequent winding failure) and hence prompt detection is mandatory.

7.2.3 Faulty machine model

From the above considerations regarding the considered fault scenarios, it is possible to assert that the insertion of additional exogenous voltages $f_{s\alpha}, f_{s\beta}$ in the current equations of (7.1) might be a reasonable approach for modeling faulty SCIM drives. The following

mathematical model intends to represent a *Faulty SCIM*:

$$\begin{cases} \dot{x}_1 = a_1(x_3x_4 - x_2x_5) - a_2x_1 + a_3T_L \\ \dot{x}_2 = b_1x_4 - b_2x_2 + b_3x_1x_3 + b_4(u_{s\alpha} + f_{s\alpha}) \\ \dot{x}_3 = b_1x_5 - b_2x_3 - b_3x_1x_2 + b_4(u_{s\beta} + f_{s\beta}) \\ \dot{x}_4 = c_1x_2 - c_2x_4 - n_px_1x_5 \\ \dot{x}_5 = c_1x_3 - c_2x_5 + n_px_1x_4 \end{cases} \quad (7.5)$$

where in absence of fault conditions, the additional entries $f_{s\alpha}$ and $f_{s\beta}$ are identically zero, otherwise when some fault occurs they became nonzero and inject the appropriate pattern frequencies in the model. The load torque T_L being generally not available for measurements in applications, it is deemed as an "unknown input" within the observer design problem using the presented model.

It is worth noting by inspection of (7.3) and (7.4) that an accurate estimation of the speed ω_r is a prerequisite for reliable MCSA diagnosis.

7.3 Second order sliding mode FDI observer for SCIMs

An algorithm for FDI in SCIMs, supported by the theory of model-based FDI [Simani et al., 2003] shall be presented hereinafter. Model-based FDI is built upon a number of idealized assumptions, one of which is that the mathematical model used is a faithful replica of the plant dynamics. This is, of course, unreasonable in practice. For these reasons a major objective of model-based FDI is to maximize the fault detection coverage and at the same time minimize the effect of modeling errors and disturbances [Simani et al., 2003].

The approach taken in this Chapter relies upon the use of a robust observer based on the sliding mode theory. In particular, the desirable feature of the sliding mode to reconstruct, in some cases, the unknown inputs acting on the observed system is exploited [Bejarano & Fridman, 2010]. It is clear that the fault signals $f_{s\alpha}$ and $f_{s\beta}$ contain useful information (symptoms) about the faults, and their estimation would be extremely useful for FDI purposes. In the following a scheme that can reconstruct both the unknown exogenous fault signals $f_{s\alpha}$ and $f_{s\beta}$ in (7.5) while mitigating the effect of modeling errors by relying on the inherent robustness properties of sliding mode observers is devised. The detection of faults will be achieved by a non conventional, threshold based residual evaluation procedure applied to the reconstructed fault signals.

Hereinafter will be explored the two main stages of the FDI scheme design for the considered case of study, respectively *residual generation* and *residual evaluation*.

7.3.1 Residual Generation

The aims of *residual generation* is to reconstruct fault symptoms using available inputs and outputs token from the monitored system. The structure of the suggested *Unknown-Input*

Observer (UIO) is the following:

$$\begin{cases} \dot{\hat{x}}_1 = a_1 (x_3 \hat{x}_4 - x_2 \hat{x}_5) - a_2 x_1 + a_3 v_1 \\ \dot{\hat{x}}_2 = b_1 \hat{x}_4 - b_2 x_2 + b_3 x_1 \hat{x}_5 + b_4 (u_{s\alpha} + v_2) \\ \dot{\hat{x}}_3 = b_1 \hat{x}_5 - b_2 x_3 - b_3 x_1 \hat{x}_4 + b_4 (u_{s\beta} + v_3) \\ \dot{\hat{x}}_4 = c_1 x_2 - c_2 \hat{x}_4 - n_p x_1 \hat{x}_5 \\ \dot{\hat{x}}_5 = c_1 x_3 - c_2 \hat{x}_5 + n_p x_1 \hat{x}_4 \end{cases} \quad (7.6)$$

Note that the observer equations (7.6) represent a replica of the faulty motor model (7.5) with suitable injection terms v_1 , v_2 and v_3 in place of the unknown inputs $f_{s\alpha}$, $f_{s\beta}$ and T_L . Shaft speed x_1 and stator currents (x_2, x_3) are supposed to be available for measurements whereas \hat{x}_i with $i = 1, \dots, 5$ represent the estimated state variables. The observation error variables are defined as follow

$$e_i(t) = \hat{x}_i(t) - x_i(t) \quad \text{with } i = 1, \dots, 5, \quad (7.7)$$

where e_1 , e_2 and e_3 are accessible for measurements, while e_4 and e_5 are unknown.

The assumption on the considered exogenous fault signals are specified as follows.

Assumption 1: Let F_s and F_L be a-priory known constants, such that, at any $t \geq 0$, the time derivatives of the unknown inputs $f_{s\alpha}$, $f_{s\beta}$ and T_L satisfy the next inequalities

$$\left| \frac{d}{dt} f_{s_i}(t) \right|_{i \in \{\alpha, \beta\}} \leq F_s \quad , \quad \left| \frac{d}{dt} T_L(t) \right| \leq F_L \quad (7.8)$$

■

The observer injection terms are built according to the following algorithm:

$$v_i(t) = v_{i_1}(t) + v_{i_2}(t) \quad i = 1, 2, 3 \quad (7.9)$$

where v_{i_1} and v_{i_2} are defined as

$$\begin{cases} v_{i_1}(t) = -k_i \cdot \sqrt{|e_i(t)|} \cdot \text{sign}(e_i(t)) \\ \dot{v}_{i_2}(t) = -w_i \cdot \text{sign}(e_i(t)) \quad , \quad v_{i_2}(0) = 0 \end{cases} \quad (7.10)$$

and k_i and w_i are constants (see [Levant, 1993b]).

The next theorem sets the underlying tuning rules of the considered observer and establishes the associated convergence properties.

Theorem 1 Consider the faulty SCIM model (7.5) and let Assumption 1 be satisfied. Then, the observer (7.6), (7.9), (7.10) with the tuning parameters chosen according to

$$w_i > F_i \quad , \quad k_i^2 > 4F_i \cdot \frac{w_i + F_i}{w_i - F_i} \quad i = 1, 2, 3, \quad (7.11)$$

$$F_1 = F_L \quad , \quad F_2 = F_3 = F_s, \quad (7.12)$$

guarantees the achievement of the next condition starting from a finite moment T^*

$$v_1(t) = T_L(t) + \xi_1(t) \quad (7.13)$$

$$v_2(t) = f_{s\alpha}(t) + \xi_2(t), \quad t \geq T^* \quad (7.14)$$

$$v_3(t) = f_{s\beta}(t) + \xi_3(t) \quad (7.15)$$

where $\xi_1(t)$, $\xi_2(t)$ and $\xi_3(t)$ are exponentially vanishing signals. \blacksquare

Proof of Theorem 1: The observation error dynamics can be easily obtained by (7.5) and (7.6) as follows:

$$\dot{e}_1 = a_1x_3e_4 - a_1x_2e_5 + a_3(v_1 - T_L) \quad (7.16)$$

$$\dot{e}_2 = b_1e_4 + b_3x_1e_5 + b_4(v_2 - f_{s\alpha}) \quad (7.17)$$

$$\dot{e}_3 = b_1e_5 - b_3x_1e_4 + b_4(v_3 - f_{s\beta}) \quad (7.18)$$

$$\dot{e}_4 = -c_2e_4 - n_px_1e_5 \quad (7.19)$$

$$\dot{e}_5 = -c_2e_5 + n_px_1e_4 \quad (7.20)$$

It is easy to see that the flux estimation errors (e_4, e_5) are decoupled from the other ones. Introducing the next Lyapunov Function

$$V = \frac{1}{2} \cdot (e_4^2 + e_5^2) \quad (7.21)$$

by trivial manipulations, its time derivative along the trajectories of (7.19)-(7.20) is

$$\dot{V} = e_4\dot{e}_4 + e_5\dot{e}_5 = -c_2 \cdot V \quad (7.22)$$

which establish the exponential convergence to zero of the errors (e_4, e_5) .

Consider now equation (7.16), rewriting it as follows

$$\dot{z} = K(\phi(t) + u(t) - f(t)) \quad (7.23)$$

with $z(t) = e_1(t)$, $\phi(t) = (a_1x_3e_4 - a_1x_2e_5)/a_3$ is an exponentially vanishing term (as implied by (7.21) and (7.22)), $K = a_3$ is a positive constant, $u(t) = v_1(t)$ is the adjustable control input and $f(t) = T_L(t)$ is an uncertain term fulfilling the inequality

$$\left| \frac{d}{dt}f(t) \right| \leq F_D. \quad (7.24)$$

Taking into account the control algorithm (7.9)-(7.10), the control signal $u(t)$ is taken as

$$u(t) = u_1(t) + u_2(t), \quad (7.25)$$

$$\begin{cases} u_1(t) = -k \sqrt{|z(t)|} \text{sign}(z(t)) \\ \dot{u}_2(t) = -w \text{sign}(z(t)), u_2(0) = 0 \end{cases}, \quad (7.26)$$

where k and w are chosen, in accordance with the tuning rules (7.11) and the assumption (7.24), as follows

$$w > F_D, \quad k^2 > 4F_D \cdot \frac{w + F_D}{w - F_D}. \quad (7.27)$$

The control law (7.25)-(7.26) in question is known in the literature as the Super-Twisting algorithm, and it belongs to the family of second order sliding mode controllers. Its stability properties were analyzed, e.g., in [Levant, 1993b]. It was proven that both $z(t)$ and $\dot{z}(t)$ tend to zero in finite time. In particular, once the following condition is achieved

$$\dot{z}(t) = 0, \quad t \geq T^* \quad (7.28)$$

since $\phi(t) \rightarrow 0$ as $t \rightarrow \infty$, it directly follows from (7.23) that $u(t)$ reconstructs the unknown input $f(t)$ with a convergence rate strictly related to the vanishing property of $\phi(t)$. Similarly, identical considerations might be derived for the equations (7.14) and (7.15). Theorem 1 is proven. ■

The injection signals (v_2, v_3) will be used as residuals in the next analysis, as they provide asymptotically converging estimates of the fault signals ($f_{s\alpha}, f_{s\beta}$). Signal v_1 represent an asymptotically exact estimation of the unknown load torque T_L , which may useful in *Direct Torque Control* (DTC) applications (see for example [La et al., 2000, Youb & Craciunescu, 2007]). The suggested FDI observer also provides an exponentially converging estimate of the rotor flux components as well.

7.3.2 Residual Evaluation

Residual evaluation exploits the relations (7.14) and (7.15). The squared sum of the two residuals is taken as a scalar measurement of the fault occurrence

$$r(t) = v_2^2(t) + v_3^2(t). \quad (7.29)$$

The simplest fault detection strategy could be sought as follows [Simani et al., 2003]:

$$\begin{cases} \text{if } r(t) \leq \varepsilon & \text{then machine is healthy} \\ \text{if } r(t) > \varepsilon & \text{then BBF or EF is active} \end{cases} \quad (7.30)$$

where ε is a suitably chosen constant threshold. However, the above FDI logic would be rather sensitive against the measurement noise. For this reason the next signal is considered

$$E(t) = \sqrt{\int_{t-\Delta T}^t r(\tau) d\tau}, \quad (7.31)$$

where ΔT is the width of the receding horizon time window. The corresponding FDI logic becomes:

$$\begin{cases} \text{if } E(t) \leq \varepsilon & \text{then machine is healthy} \\ \text{if } E(t) > \varepsilon & \text{then BBF or EF is active} \end{cases} \quad (7.32)$$

Once the fault is detected, dedicated methods such as FFT and T-MCSA, or modern approaches like Hilbert or Wavelet transform applied to the output-injection signals v_2 and v_3 , can be employed to classify the nature of occurred fault.

Table 7.2: Siemens 1LA7090 { 2AA10 , 4AA10 } Ratings

Rated terminal supply voltage:	230 V – Δ	400 V – Y
Rated frequency/full-load speed:	50 Hz	1410 rpm 2860 rpm
Rated power :	1.5 kW	$\cos \phi = 0.85$
	1.1 kW	$\cos \phi = 0.80$
Rated supply current with full load:	4.60 A – Δ	2.70 A – Y
	5.65 A – Δ	3.25 A – Y

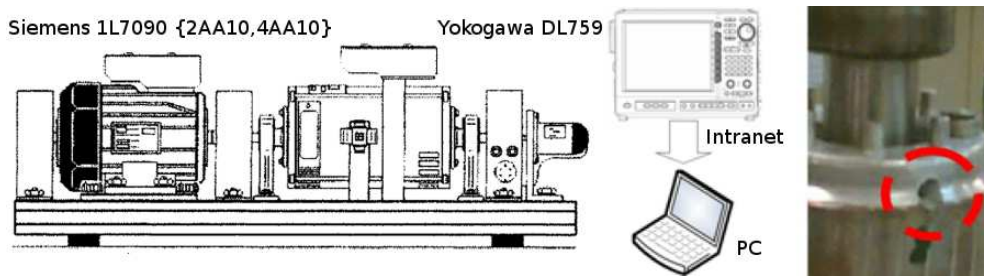


Figure 7.1: Experimental set-up (left) and a drilled rotor cage bar (right).

7.4 Experimental Results

The suggested methodology has been tested offline by using real measurements acquired from several healthy and faulty commercial three-phase SCIMs intentionally damaged in order to reproduce a broken bar fault and the two considered types of eccentricity. The broken bar faulty machine has been realized by drilling a single rotor bar (see right picture in Figure 7.1). The eccentricity faults have been reproduced by suitable hardware modification. Respectively, it has been tested a machine with 0.2mm of static eccentricity, and a second one with 0.07mm of dynamic eccentricity, too.

The left plot of Figure 7.1 depicts the structure of the experimental set-up, where a DC motor is mechanically coupled to the SCIM under diagnosis in order to apply a controlled torque. The experimental tests have been performed using several commercial SCIM drives in healthy and faulty condition. Two 2-pole drives for broken bar tests, and three 4-pole motors for eccentricity test fed, respectively, at (230V- Δ , 50Hz) and (400V-Y, 50Hz). Rating parameters of both SCIMs are reported in the Table 7.2.

The electromechanical motor parameters needed for the observer implementation are derived from the motor's data sheet. After few trial and error tests, devoted to guarantee an accurate convergence to zero of the measurable estimation errors e_1, e_2 , and e_3 in healthy

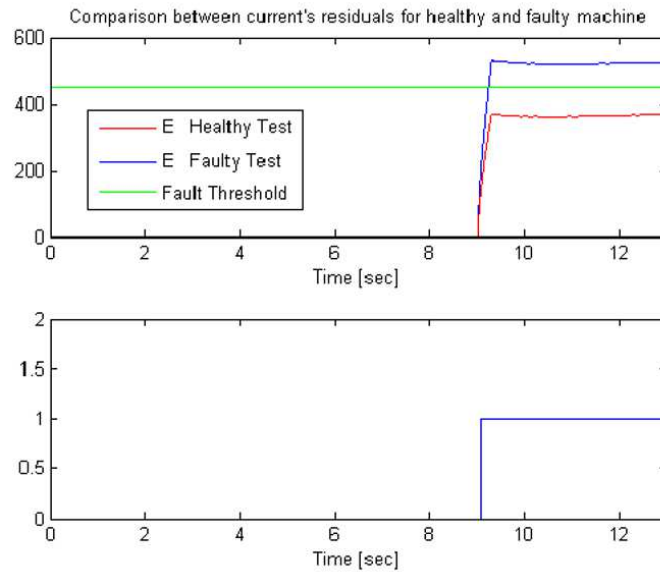


Figure 7.2: Residuals and chosen threshold (upper plot) and diagnosis signal (lower plot) for the broken bar tests.

operating condition, the observer gains for both tests have been set as follows:

$$\begin{aligned} w_1 = 14 \quad w_2 = 22 \quad w_3 = 22 \\ k_1 = 80 \quad k_2 = 200 \quad k_3 = 200 \end{aligned} \quad (7.33)$$

A suitable value for the time window size ΔT in (7.31) has been found as

$$\Delta T = 0.3 \text{ s} . \quad (7.34)$$

The choice of ΔT turned out to be not critical, satisfactory performance has been obtained with different values as well.

The observer (7.6) has been activated at start-up whereas the residual evaluation logic (7.31) is activated after 9 seconds, to let the machine reach the sinusoidal steady state under the applied three-phase input voltage.

Figure 7.2 and Figure 7.3 show, respectively, the $E(t)$ residual profiles obtained using measurements from an healthy and a faulty motor. These figures show that the healthy and faulty residuals are appreciably different, and a suitable threshold value ε , to be used in the fault detection logic (7.32) for achieving an accurate detection of the fault occurrence, can be found.

Actually, to perform an affective tuning of the threshold few experiments with healthy measurements are sufficient, by selecting the corresponding threshold sufficiently bigger than the steady state values of $E(t)$. It is apparent from the Figure 7.2 and Figure 7.3 that the faulty conditions are diagnosed almost instantaneously after that the FDI algorithm is activated.

Finally, to validate the suggested faulty motor model (7.5), and to simultaneously show the effectiveness of the observer (7.6) as well, the spectrum of a faulty stator current and one of the associated injection signal, are compared.

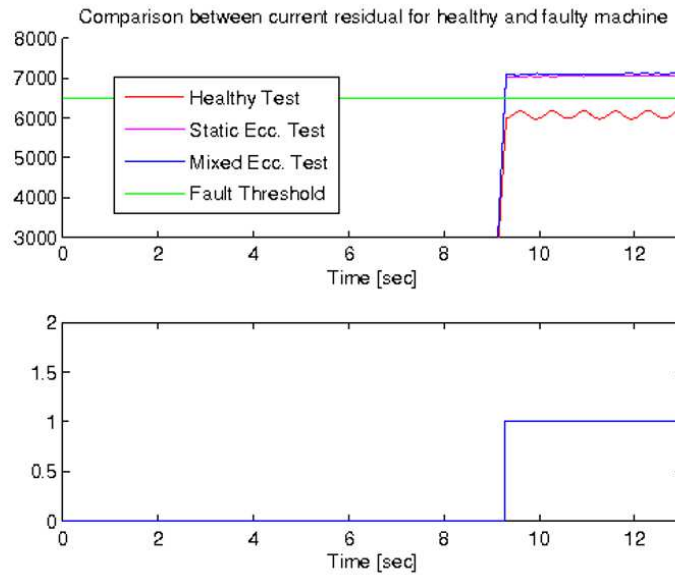


Figure 7.3: Residuals and chosen threshold (upper plot) and diagnosis signal (lower plot) for the eccentricity tests.

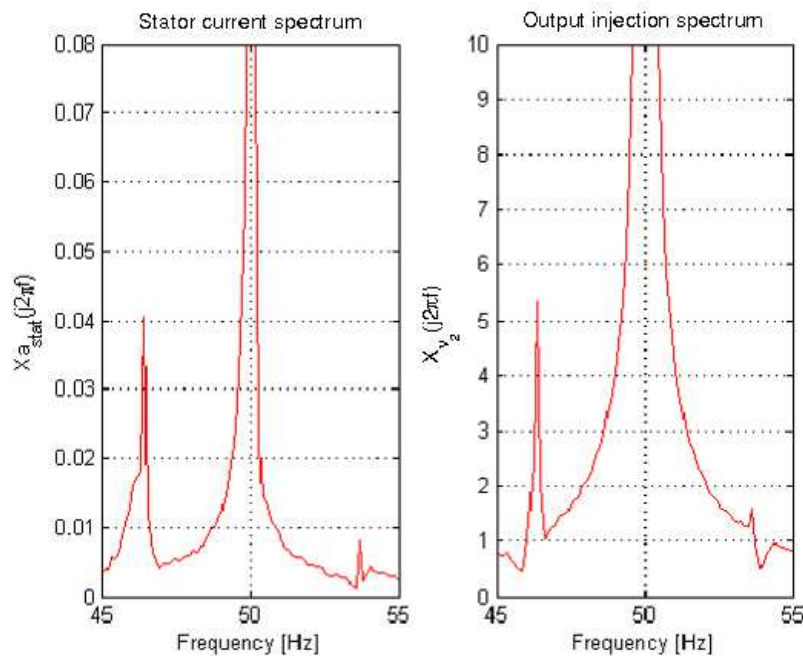


Figure 7.4: Comparison between the normalized spectra of the faulty motor stator currents (left plot) and that of the observer injection signal v_2 (right plot) for the broken bar test.

Figures 7.4 and 7.5 show that the normalized spectrum of a stator current (left side) and the spectrum of an injection signal, e.g. $v_2(t)$, (right side) contains the same frequencies for broken bar and static eccentricity test respectively. The satisfactory performances of the suggested FDI observer have been demonstrated in both the faulty scenarios investigated.

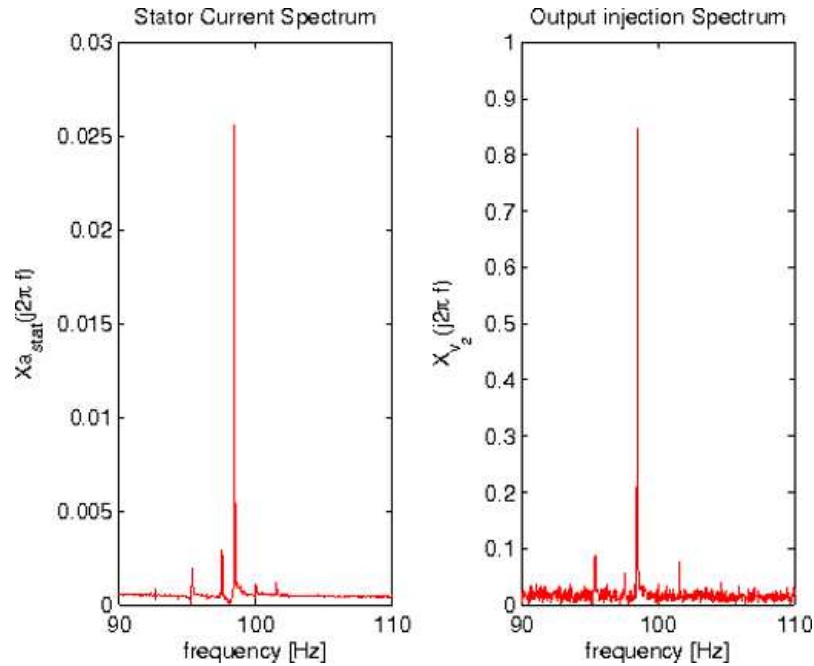


Figure 7.5: Comparison between the normalized spectra of the faulty motor stator currents (left plot) and that of the observer injection signal v_2 (right plot) for the eccentricity test.

7.5 Conclusions and Future Works

This Chapter has explored a novel approach for fault detection in squirrel cage induction motors based on second order sliding mode observers. The stability of proposed unknown input observer has been theoretically proven. Its effectiveness in detecting the presence of broken cage bars or eccentricity conditions has been experimentally tested by offline processing of real motor data taken from several different commercial 1.1kW and 1.5kW drives.

The computational load of the method is limited, which makes its online implementation easily feasible with cheap hardware. The method has provided good performance with real motor data, which certifies a certain degree of robustness. Noteworthy, the proposed observer allows to reconstruct, both, the load torque and the direct and quadrature rotor fluxes.

Among the most interesting directions for next research, combination of the tested methodology with modern classification approaches appears particularly promising.

Chapter 8

Robust Consensus Algorithms for First-integrator Dynamics

In this Chapter is proposed a novel decentralized consensus algorithm for a network of continuous-time integrators subjected to persistent disturbances and communication changes. Notice that, although the network during its evolution is not always connected, it is proved that under certain restrictions on the directed switching policy, after a finite transient time, the agents achieve an approximated consensus condition by attenuating the destabilizing effect of the disturbances. A Lyapunov-based analysis confirm the effectiveness of the suggested algorithm. To confirm the effectiveness of the proposed protocol, simulative results are illustrated and discussed.

8.1 Introduction

The problem of reaching consensus, i.e., driving the state of a set of interconnected dynamical systems towards the same value, has received much attention due to its many applications in, both, the modeling of natural phenomena such as flocking (see e.g. [Reynolds, 1987, Jadbabaie et al., 2003, Toner & Tu, 1998]) and in the solution of several control problems involving synchronization or agreement between dynamical systems (see [Olfati-Saber et al., 2007, Ren & Beard, 2005, Dorfler & Bullo, 2010, Arcak, 2007]).

In this Chapter, it is discussed an approach to reach consensus in a network of interacting agents whose dynamics are modeled by first order continuous time integrators subjected to unknown-but-bounded persistent perturbations. The approach is based on a local interaction rule which combines linear and nonlinear terms. The linear terms, as usual, feed each agent with the difference between the current agent's state and the states of its neighbors, while the nonlinear terms consider the sign of those differences yielding a discontinuous local interaction rule involving sliding mode control concepts (see [Utkin, 1992]).

Discontinuous local interaction rules have been already exploited in the framework of consensus or agreement algorithms to exploit the underlying finite-time convergence and robustness against disturbances and unmodeled dynamics. Several examples of applications to flocking or synchronization problems can be found in the literature (see e.g. [Gazi et al.,

2007]). Discontinuous local interactions were studied in [Cortés, 2006a], within a general framework of gradient flows, and several examples of discontinuous consensus protocols were analyzed.

In [Khoo et al., 2009], a finite-time consensus algorithm is proposed to address the leader-follower tracking problem in multi-robot systems with static topology but varying leader. In [Wang & Xiao, 2010], [Menon & Edwards, 2010] and [Rao & Ghose, 2011], finite-time consensus algorithms are provided for networks of unperturbed integrators by exploiting discontinuous local interaction rules under time varying (both undirected and directed) network topologies.

The consensus problem in presence of measurement errors is studied in [Garulli & Giannitrapani, 2011], in a discrete-time setting, with reference to linear consensus protocols with constant or vanishing weights. The authors derive explicit upper bounds to the maximum disagreement error as function of the bounds on the noise magnitude and of the smallest non-zero singular value of the network's state update matrix.

In [Bauso et al., 2009] the authors suggest a class of non-linear continuous protocols that are able to achieve the so-called " ϵ -consensus", namely an approximate agreement condition where all agents converge towards a set, in spite of the presence of additive disturbances. The work presented in this Chapter differs from the one in [Bauso et al., 2009] in that here it is considered a discontinuous protocol, as opposed to continuous, that is able to achieve almost complete disturbance rejection up to an arbitrarily small error if the network is always connected.

An approach that shares some technical issues with the protocol proposed here, is the continuous-time consensus problem in presence of quantization errors. In [Frasca, 2012] the continuous-time consensus problem is studied in the case of quantized information exchange between agents, and this leads to an instance of discontinuous protocol where the effect of quantization can be regarded as a disturbance.

The approach illustrated in this Chapter further differs from the above mentioned literature works in that, here the analysis of the practical stability and disturbance attenuation properties of finite-time consensus under the effect of unknown perturbations and, additionally, with a switching and directed communication topology is addressed. Furthermore, the finite time transient to reach consensus can be made arbitrarily small by properly selecting the algorithm parameters. The disturbance rejection performance will primarily depend on the time-varying network connectivity properties. To the best of my knowledge, the above aspects were never simultaneously addressed and characterized in the existing literature.

The main result of the present work, outlined in Theorem 8.1, consists in proposing a feasible local interaction rule which provides finite time convergence of the network to a condition of approximate agreement, by attenuating the effect of the disturbances. This result is subjected to the requirement that the time varying graph defining the network switching interaction topology has a directed spanning tree, at least, a certain "minimal percentage" of time.

This Chapter generalizes the preliminary results presented in [Franceschelli et al., 2012a] by extending the analysis to cover directed switching topologies that were not dealt with in the original paper. The key factor enabling such an extension is a modification of the underlying Lyapunov analysis, which, in the present Chapter, involves a max function considering

the maximal difference between the agents' states. This new approach considerably relaxes the conservatism of the tuning inequalities guaranteeing convergence to the approximate consensus condition using lower values of the control gains. Additionally, here are considered both continuous and discontinuous terms in the local interaction rule in such a way that the convergence to consensus can be accelerated by increasing the weight of the linear continuous terms, rather than those of the nonlinear discontinuous terms, thereby mitigating the chattering effect.

The structure of the Chapter is as follows. In Section 8.2 are recalled some basic definitions and formulate the problem under investigation. In Section 8.3 is described the proposed local interaction rule and are investigated the associated convergence properties by stating the main result. In Section 8.4 some simulation results are presented, and, finally, in Section 8.5 conclusions are drawn and possible future research directions are discussed.

8.2 Preliminaries and Problem Statement

Let us consider a network consisting of N interacting agents whose communication topology, is modeled by a directed graph $\mathcal{G} = (\mathcal{V}, \mathcal{E})$, where $\mathcal{V} = \{1, \dots, N\}$ and $\mathcal{E} \subseteq \mathcal{V}^2$ denote, respectively, the collection of agents and the edge set. An edge, denoted as (i, j) , belongs to \mathcal{E} if the agent i is able to obtain information from its neighbor j . As a consequence, the set of neighbors of the agent i is denoted by $\mathcal{N}_i = \{j \in \mathcal{V} / \{i\} : (j, i) \in \mathcal{E}\}$. By assumption the presence of self-loops in \mathcal{G} is not allowed. Each agent is modeled as a continuous-time perturbed integrator

$$\dot{x}_i(t) = \vartheta_i(t) + u_i(t), \quad x_i(0) = x_{i0}, \quad i \in \mathcal{V} \quad (8.1)$$

where $x_i(t) \in \mathbb{R}$ and x_{i0} are respectively the state of the i -th agent and its initial value, $u_i(t) \in \mathbb{R}$ is the local control input, and $\vartheta_i(t)$ is a bounded unknown perturbation

The only assumption made on the unknown perturbations $\vartheta_i(t)$ is:

$$\exists \Pi \in \mathbb{R}^+ : \forall i \in \mathcal{V}, \quad |\vartheta_i(t)| \leq \Pi \quad (8.2)$$

Assuming that at each time instant, only a subset of the available communication edges in \mathcal{G} is active for information exchange, it is defined $\hat{\mathcal{G}}(t) = (\mathcal{V}, \mathcal{E}(t))$ as a time-varying graph representative of the active instantaneous topology, where $\mathcal{E}(t) \subseteq \mathcal{E}$ is the subset of active edges at time t . Accordingly, it can be defined the instantaneous neighbors set of the i -th agent as follows:

$$\mathcal{N}_i(t) = \{j \in \mathcal{V} : (j, i) \in \mathcal{E}(t)\} \subseteq \mathcal{N}_i \quad (8.3)$$

Let Γ and t_r be two positive constants, the task of the present Chapter is to design a local interaction rule $u_i(t)$, compatible with $\hat{\mathcal{G}}(t)$, which can guarantee, under suitable assumptions on the time-varying topology, the achievement of the next *practical finite-time consensus* condition

$$\exists \Gamma, t_r \in \mathbb{R}^+ : \forall t > t_r, \forall i, j \in \mathcal{V}, \quad |x_i(t) - x_j(t)| \leq \Gamma \quad (8.4)$$

8.3 Main result and Convergence Analysis

The proposed local interaction protocol is defined as follows:

$$u_i(t) = u_{i,1}(t) + u_{i,2}(t), \quad i \in \mathcal{V} \quad (8.5)$$

with

$$u_{i,1}(t) = -\lambda_1 \sum_{k \in \mathcal{N}_i(t)} (x_i(t) - x_k(t)), \quad (8.6)$$

$$u_{i,2}(t) = -\lambda_2 \sum_{k \in \mathcal{N}_i(t)} \text{sign}(x_i(t) - x_k(t)), \quad (8.7)$$

where λ_1 and λ_2 are the nonnegative tuning constants of the algorithm and the $\text{sign}(\cdot)$ function is defined as follows

$$\text{sign}(\mathfrak{S}) = \begin{cases} 1 & \text{if } \mathfrak{S} > 0 \\ 0 & \text{if } \mathfrak{S} = 0 \\ -1 & \text{if } \mathfrak{S} < 0 \end{cases} \quad (8.8)$$

Let $r_{ik}(t)$ be a binary variable, representative of the presence or not of a directed communication channel coming from agent i to agent k at time t , denoted as:

$$r_{ik}(t) = \begin{cases} 1 & \text{if } k \in \mathcal{N}_i(t) \\ 0 & \text{otherwise} \end{cases} \quad (8.9)$$

Then, it can be rewritten the linear and nonlinear control components $u_{i,1}(t)$ and $u_{i,2}(t)$ in (8.6) and (8.7) as follows:

$$u_{i,1}(t) = -\lambda_1 \sum_{k \in \mathcal{V}, k \neq i} r_{ik}(t) \cdot (x_i(t) - x_k(t)), \quad \lambda_1 \geq 0. \quad (8.10)$$

$$u_{i,2}(t) = -\lambda_2 \sum_{k \in \mathcal{V}, k \neq i} r_{ik}(t) \cdot \text{sign}(x_i(t) - x_k(t)), \quad \lambda_2 > 0. \quad (8.11)$$

Remark 8.1. *Due to the concurrent effect of the suggested discontinuous local interaction rule (8.11), the switching network topology $\hat{\mathcal{G}}(t)$, and the possibly discontinuous nature of the external disturbances (supposed to be only uniformly bounded), the closed loop network dynamics (8.1) will be discontinuous and the resulting solution notion needs to be discussed and clarified. For a differential equation with discontinuous right-hand side, following [Filippov, 1988], the resulting solution in the so-called Filippov Sense can be understood as the solution of an appropriate differential inclusion, whose existence is guaranteed (owing on certain properties of the associated set-valued map) and for which noticeable properties, such as absolute continuity, are in force. The reader is referred to [Cortes, 2008] for a comprehensive account of the notions of solution for discontinuous dynamical systems. ■*

From now on the conditions under which the local interaction protocol (8.5)-(8.7) can achieve the approximate consensus conditions (8.4) are investigated. Define a set of error variables for each edge in the network as follows

$$\delta_{ij}(t) = x_i(t) - x_j(t) \quad \text{with } (i, j) \in \mathcal{E}. \quad (8.12)$$

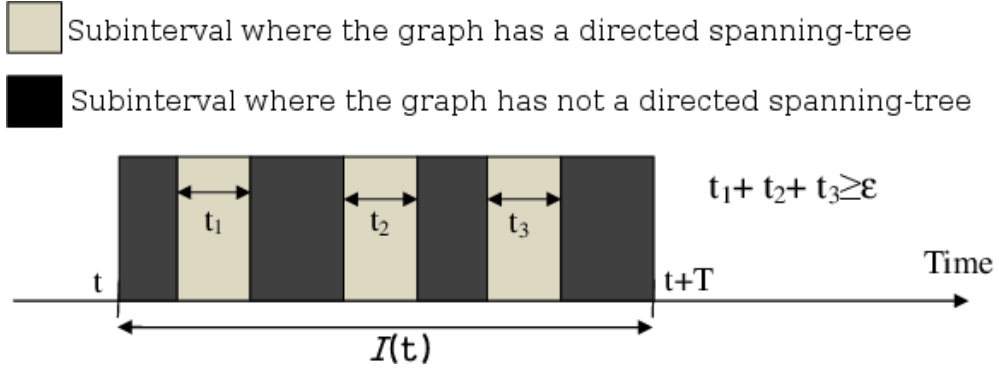


Figure 8.1: Changes in network topology and communication constraints.

The dynamics of $\delta_{ij}(t)$ are easily obtained by differentiating (8.12), and considering the closed loop dynamics of each agents

$$\dot{x}_i = \vartheta_i - \lambda_1 \sum_{k \in \mathcal{V}, k \neq i} r_{ik} \delta_{ik} - \lambda_2 \sum_{k \in \mathcal{V}, k \neq i} r_{ik} \cdot \text{sign}(\delta_{ik}) \quad (8.13)$$

Trivial manipulations yield

$$\begin{aligned} \dot{\delta}_{ij} = & \vartheta_i - \vartheta_j - \lambda_1 \left[\sum_{k \in \mathcal{V}, k \neq i} r_{ik} \delta_{ik} - \sum_{k \in \mathcal{V}, k \neq j} r_{jk} \delta_{jk} \right] + \\ & - \lambda_2 \left[\sum_{k \in \mathcal{V}, k \neq i} r_{ik} \cdot \text{sign}(\delta_{ik}) - \sum_{k \in \mathcal{V}, k \neq j} r_{jk} \cdot \text{sign}(\delta_{jk}) \right] \end{aligned} \quad (8.14)$$

The requirement concerning the switching communication topology is that the time varying graph $\hat{\mathcal{G}}(t)$ has a directed spanning-tree, at least, a certain “minimal percentage” of time. This is formalized by the next Assumption.

Assumption 8.1. *There are positive constants ε and T , with $\varepsilon \leq T$, such that during the receding horizon time interval $\mathcal{I}(t) = (t, t+T)$, $\hat{\mathcal{G}}(t)$ has a directed spanning tree along a subinterval $\mathcal{S}(t) \subseteq \mathcal{I}(t)$, possibly formed by the union of disjoint subintervals, whose overall length is at least equal to ε . ■*

The meaning of Assumption 8.1 is clarified by the Figure 8.1, namely the overall duration of the disjoint grey subintervals during which the instantaneous digraph $\hat{\mathcal{G}}(t)$ has a directed spanning-tree should be not less than the constant ε . Now it is possible to state the main result of the Chapter.

Theorem 8.1. *Consider the agents’ dynamics (8.1), which satisfies (8.2), and let Assumption 8.1 be in force. Then, the discontinuous local interaction rule (8.5), (8.9)-(8.11) with tuning parameters selected according to*

$$\lambda_1 \geq 0 \quad , \quad \lambda_2 \geq \frac{2T \cdot \Pi}{\varepsilon} + \mu^2 \quad , \quad \mu \neq 0, \quad (8.15)$$

provides the approximate consensus condition (8.4) where

$$\Gamma = [2 \cdot (T - \varepsilon) + \xi] \cdot \Pi, \quad (8.16)$$

where $\xi > 0$ is an arbitrary infinitesimally small positive parameter and the transient time t_r is upper bounded as follows

$$t_r \leq \left(\frac{T}{\varepsilon \mu^2} \right) \cdot \max_{i,j \in \mathcal{V} \times \mathcal{V}} |x_i(0) - x_j(0)| \quad (8.17)$$

■

Proof. Consider

$$V(t) = |\delta_{ij}(t)| \quad (8.18)$$

as a candidate Lyapunov function, where

$$(i,j) = \operatorname{argmax}_{(i,j) \in \mathcal{V} \times \mathcal{V}} |\delta_{ij}(t)| \quad (8.19)$$

in such a way that, without loss of generality, index i will correspond to an agent carrying the maximal value at time t among all the agents in the network, and, dually, index j will correspond to an agent carrying the minimal value, i.e.

$$x_i(t) = \sup_{h \in \mathcal{V}} x_h(t), \quad x_j(t) = \inf_{h \in \mathcal{V}} x_h(t) \quad (8.20)$$

Let us preliminarily address the case $\varepsilon < T$. It is worth to emphasize that the chosen Lyapunov function (8.18) is continuous at those time instants at which either i or j will change its value. Clearly, the vanishing of $V(t)$ implies the exact consensus condition among the agents of the network, while small values for $V(t)$ correspond to a practical consensus condition as in (8.4). Note that the considered Lyapunov function is locally Lipschitz and it is not differentiable when $\delta_{ij}(t) = 0$. Thus, the treatment refers for stability analysis to the *Lyapunov Generalized Theorem* for non-smooth analysis reported in [Paden & Sastry, 1987], which makes use of the *Clarke's Generalized Gradient* [Clarke, 1983]. However, it can be observed that $\delta_{ij}(t) = 0$ only when the exact consensus condition is in force, which will bring some useful simplification in the stability analysis.

In the remainder, the computation method illustrated in [Paden & Sastry, 1987] is referred to as, where a Lyapunov analysis based on an analogous sum-of-absolute-value Lyapunov function was dealt with. All the necessary technicalities justifying the correctness of adopting the chain rule to compute the time derivative of $V(t)$, which exists almost everywhere in the form of a suitable set-valued map, are not reported here, and the reader is referred, e.g., to [Cortés, 2006a, Paden & Sastry, 1987, Shevitz & Paden, 1994] where discontinuous systems and non-smooth Lyapunov tools analogous to those involved in the present analysis were discussed in detail.

The time-derivative of $V(t)$ along the solutions of the deviation error dynamics (8.14) takes the following set-valued form

$$\begin{aligned} \dot{V}(t) &= \operatorname{SIGN}(\delta_{ij}(t)) \cdot \dot{\delta}_{ij}(t) = \\ &= \operatorname{SIGN}(\delta_{ij}) \cdot (\vartheta_i - \vartheta_j) \\ &\quad - \lambda_1 \cdot \operatorname{SIGN}(\delta_{ij}) \sum_{k \in \mathcal{V}, k \neq i} r_{ik} \cdot \delta_{ik} \\ &\quad + \lambda_1 \cdot \operatorname{SIGN}(\delta_{ij}) \sum_{k \in \mathcal{V}, k \neq j} r_{jk} \cdot \delta_{jk} \\ &\quad - \lambda_2 \cdot \operatorname{SIGN}(\delta_{ij}) \sum_{k \in \mathcal{V}, k \neq i} r_{ik} \cdot \operatorname{sign}(\delta_{ik}) \\ &\quad + \lambda_2 \cdot \operatorname{SIGN}(\delta_{ij}) \sum_{k \in \mathcal{V}, k \neq j} r_{jk} \cdot \operatorname{sign}(\delta_{jk}) \end{aligned} \quad (8.21)$$

where $\text{SIGN}(\delta_{ij}(t))$, the generalized gradient of $V(t)$ (see [Paden & Sastry, 1987]), is the multi-valued function

$$\text{SIGN}(\delta_{ij}(t)) = \begin{cases} 1 & \text{if } \delta_{ij}(t) > 0 \\ [-1, 1] & \text{if } \delta_{ij}(t) = 0 \\ -1 & \text{if } \delta_{ij}(t) < 0 \end{cases} \quad (8.22)$$

Note that by definition, and considering (8.20), as long as $V(t) \neq 0$, it results that $\text{SIGN}(\delta_{ij}(t)) = 1$. Furthermore due to the uniform boundedness of the disturbance (8.2), the next estimation is in force

$$|\vartheta_i - \vartheta_j| \leq 2\Pi \quad (8.23)$$

Thus, (8.21) can be manipulated so as to obtain

$$\begin{aligned} \dot{V}(t) &\leq 2 \cdot \Pi - \lambda_1 \sum_{k \in \mathcal{V}, k \neq i} r_{ik} \cdot \delta_{ik} + \\ &\quad + \lambda_1 \sum_{k \in \mathcal{V}, k \neq j} r_{jk} \cdot \delta_{jk} + \\ &\quad - \lambda_2 \sum_{k \in \mathcal{V}, k \neq i} r_{ik} \cdot \text{sign}(\delta_{ik}) + \\ &\quad + \lambda_2 \sum_{k \in \mathcal{V}, k \neq j} r_{jk} \cdot \text{sign}(\delta_{jk}) \end{aligned} \quad (8.24)$$

Note that, in light of (8.20), irrespectively of the instantaneous current graph topology, all the state-dependent feedback terms in the right hand side of (8.24) are positive, i.e.

$$\begin{aligned} &-\lambda_1 \sum_{k \in \mathcal{V}, k \neq i} r_{ik} \cdot \delta_{ik} + \lambda_1 \sum_{k \in \mathcal{V}, k \neq j} r_{jk} \cdot \delta_{jk} + \\ &\quad - \lambda_2 \sum_{k \in \mathcal{V}, k \neq i} r_{ik} \cdot \text{sign}(\delta_{ik}) + \\ &\quad + \lambda_2 \sum_{k \in \mathcal{V}, k \neq j} r_{jk} \cdot \text{sign}(\delta_{jk}) \leq 0 \end{aligned} \quad (8.25)$$

The receding horizon time interval $\mathcal{I}(t) = (t, t + T)$ is divided into the union between subinterval $\mathcal{S}(t)$, along which the graph is guaranteed to has a directed spanning-tree, and the complementary interval $\mathcal{I}(t) \setminus \mathcal{S}(t)$ during which nothing can be said about the connectivity properties of the switching graph. By virtue of (8.24) and (8.25) one can conclude that

$$\dot{V}(t) \leq 2 \cdot \Pi, \quad t \in \mathcal{I}(t) \setminus \mathcal{S}(t). \quad (8.26)$$

It shall be noted that the pair (i, j) is not uniquely defined and there can be multiple agents carrying the maximal or minimal values x_i and x_j at time t . At those time instants when $\hat{\mathcal{G}}(t)$ has a directed spanning tree, however, at least **one of the following conditions holds**:

1. among all agents carrying the maximal value, there is at least one of them which admits, among its neighbors, one agent with state value strictly less than x_i ;

2. among all agents carrying the minimal value, there is at least one of them which admits, among its neighbors, one agent with state value strictly greater than x_j ;

Suppose “i” (resp., “j”) is the agent for which the maximum (resp., minimum) is achieved at time t . If there are many such agents, we choose one, if any, which share an active edge with a neighbor having state value strictly less (resp., greater) than x_i (resp., x_j). If there are still many of such agents we choose any one of those, but commit to that until a new agent holds the maximum (resp., minimum) value. As a consequence of the previous developments, at those time instants when $\hat{\mathcal{G}}(t)$ has a directed spanning tree there exists at least an agent index \bar{k} , $\bar{k} \neq i$, $\bar{k} \neq j$, which satisfies at least one of the following conditions:

$$r_{i\bar{k}}(t) = 1 \quad , \quad \delta_{i\bar{k}} > 0 \quad (8.27)$$

$$r_{j\bar{k}}(t) = 1 \quad , \quad \delta_{j\bar{k}} < 0 \quad (8.28)$$

When either of (8.27) and (8.28) is in force, it follows that the right hand side of (8.24) can be upper-estimated as follows. Whenever $t \in \mathcal{S}(t)$ and $V(t) \neq 0$

$$\dot{V}(t) \leq 2 \cdot \Pi - \lambda_2 \quad t \in \mathcal{S}(t) \quad (8.29)$$

By construction, the next relation holds:

$$V(t+T) - V(t) = \int_{\mathcal{S}(t)} \dot{V}(\tau) d\tau + \int_{\mathcal{I}(t) \setminus \mathcal{S}(t)} \dot{V}(\tau) d\tau \quad (8.30)$$

where the length of the subinterval $\mathcal{S}(t)$ is at least ε , then according to Assumption 1, it follows that the length of the interval $\mathcal{I}(t) \setminus \mathcal{S}(t)$ will not exceed the value of $T - \varepsilon$.

Thus, in light of (8.26) and (8.29), from (8.30) it yields:

$$\begin{aligned} V(t+T) - V(t) &\leq \varepsilon(2\Pi - \lambda_2) + (T - \varepsilon)2 \cdot \Pi = \\ &= -\varepsilon\lambda_2 + 2T \cdot \Pi \end{aligned} \quad (8.31)$$

By plugging (8.15) into (8.31) one obtains the next condition

$$V(t+T) - V(t) \leq -\mu^2 \varepsilon \quad (8.32)$$

which will be satisfied as long as $V(\tau) \neq 0 \forall \tau \in (t, t+T)$, thereby guaranteeing the existence of a finite transient time t_r such that $V(t_r) = 0$. To evaluate an upper bound of t_r , denoted $V_\kappa = V(\kappa T)$, with $\kappa = 0, 1, 2, \dots$, (8.32) can be expressed in the first-order finite difference form as follows

$$V_{\kappa+1} = V_\kappa - \mu^2 \varepsilon \quad (8.33)$$

from which the following recursive solution is in force

$$V_\kappa = V(0) - \kappa \cdot \mu^2 \varepsilon \quad (8.34)$$

Thereby, accordingly to (8.17), it can be readily concluded that

$$t_r \leq \kappa T = \frac{V(0)}{\varepsilon \mu^2} \cdot T = \left(\frac{T}{\varepsilon \mu^2} \right) \cdot \max_{i,j \in \mathcal{V} \times \mathcal{V}} |x_i(0) - x_j(0)| \quad (8.35)$$

We now prove that, at $t \geq t_r$, the Lyapunov function $V(t)$ undergoes bounded fluctuations preserving the consensus accuracy established by (8.4) and (8.16). Define

$$V_S = \sup_{t \geq t_r} V(t) \quad (8.36)$$

which sets the ultimate precision of the approximate consensus condition. If, at any time t' one has that $V(t') = 0$ then along the time interval $t \in (t', t' + T)$ the Lyapunov function $V(t)$ may deviate from zero, at most, by a quantity $2(T - \varepsilon)\Pi$, which is obtained by integrating (8.26) for a time $T - \varepsilon$ (the maximal consecutive time interval in which the graph is disconnected, according to the Assumption 1 starting from the zero initial condition. Thereby, the domain

$$V(t) \leq 2(T - \varepsilon)\Pi. \quad (8.37)$$

is positively invariant at any $t \geq t_r$.

Now let us address the case in which $\varepsilon = T$, i.e. the time varying graph has a directed spanning tree at all times. The previous analysis has shown that there exists a finite time t_r , satisfying (8.17), at which exact consensus is achieved, i.e. $V(t_r) = 0$. Unfortunately, $V(t) = 0$ cannot be an equilibrium state at $t \geq t_r$ due to the fact that all the local control laws $u_i(t)$ are identically zero when $V(t) = 0$ (as a consequence of all δ_{ij} 's in (8.12) being zero and in view of the adopted definition (8.8) of the sign function) while the disturbances $\vartheta_i(t)$ are not. On the other hand, an infinitesimal deviation of $V(t)$ from zero will restore the convergence features of the algorithm, steering immediately $V(t)$ back to zero. This phenomenon, local instability of the ideal consensus condition $V(t) = 0$ when the disturbances are acting, can be characterized by an infinitesimal increase of Γ as follows:

$$\Gamma \leq [2(T - \varepsilon) + \xi]\Pi \quad (8.38)$$

where ξ is an arbitrarily small positive real number. Theorem 8.1 is proven. \square

Remark 8.2. Note that the transient time, which satisfies (8.35), can be made arbitrarily small by taking the design parameter μ in (8.15) large enough. It can be defined a μ -dependent majorant curve, illustrated in Figure 8.2, such that

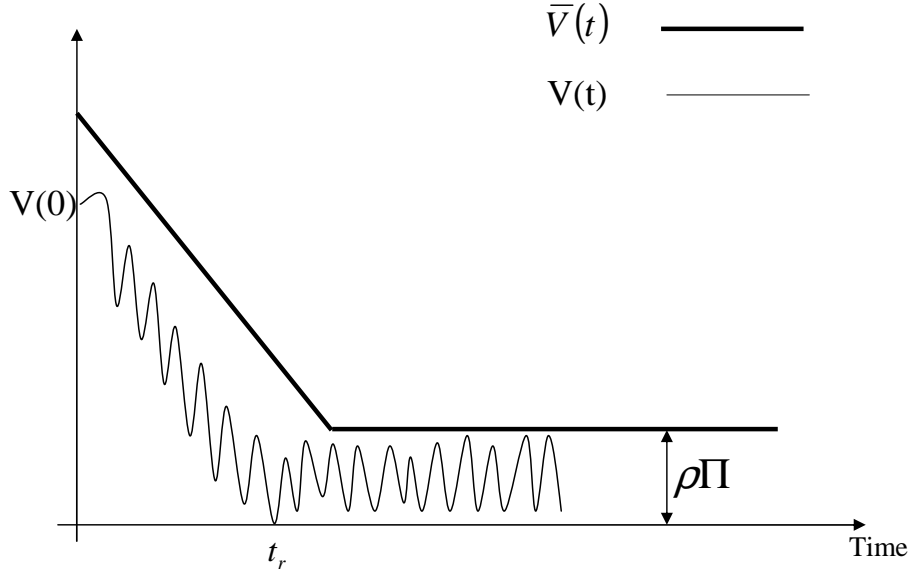
$$V(t) \leq \bar{V}(t) = \max \left\{ V(0) - \mu^2 \varepsilon \frac{t}{T} + \Gamma, \Gamma \right\}, \quad (8.39)$$

It is also worth to remark that the λ_2 tuning does not require the perfect knowledge of the time varying network topology, and it can be carried out on the basis of an upper bound to the noise magnitude and an upper bound to the ratio T/ε that sets the relative amount of time during which the network has a directed spanning tree.

8.4 Numerical Simulations

To demonstrate the effectiveness of the proposed local interaction protocol, a network of 20 agents is considered, which interact through a randomly chosen directed communication network with switching topology. Each agent, modeled as in (8.1), has a randomly chosen initial state $x_{i0} \in [0, 5]$. The disturbances are selected according to

$$\vartheta_i(t) = \eta_i(t) + \alpha_i + \beta_i \cdot \sin(20 \cdot t + \phi_i), \quad i = 1, \dots, 20 \quad (8.40)$$

Figure 8.2: Actual and majorant curves of $V(t)$

where $\eta_i(t)$ is a bounded uniformly distributed random signal, α_i is a random constant, and the pair β_i, ϕ_i are the characteristic parameter of the harmonic part of the disturbance. All the underlying disturbance parameters have been randomly chosen in such a way to guarantee the bound $|\vartheta_i(t)| \leq \Pi = 2.5 \forall i$.

The communication topology is set by a randomly chosen time-varying graph $\mathcal{G}(t)$ such that at most $|\mathcal{E}| = 30$ edges can be simultaneously active. The random edge selection policy is implemented in such a way that the requirement of Assumption 1 is met. The value $T = 0.01s$ is used in all tests while different choices for ε have been considered for the sake of comparison.

Four tests, using different values of ε and of the control gains λ_1, λ_2 have been considered, according to the next tabular representation.

TEST1 :	$\varepsilon = T,$	$\lambda_1 = 0,$	$\lambda_2 = 6$
TEST2 :	$\varepsilon = 0.5T,$	$\lambda_1 = 0,$	$\lambda_2 = 11$
TEST3 :	$\varepsilon = 0.1T,$	$\lambda_1 = 0,$	$\lambda_2 = 51$
TEST4 :	$\varepsilon = 0.5T,$	$\lambda_1 = 5,$	$\lambda_2 = 11$

The chosen control gains are always according to the design inequalities (8.15). The continuous time network (8.1) has been simulated numerically by using the Euler fixed-step solver with sampling time $T_s = 10^{-4}$. Figure 8.3 and Figure 8.4 display, respectively, the time evolutions of the agents state variables, and of the corresponding Lyapunov function $V(t)$, relative to the first three tests. It can be verified that in all tests agents become synchronized after a finite transient time. Particularly, Figure 8.4 shows the negative impact of an increasing difference $T - \varepsilon$ on the steady state accuracy, in accordance with conditions (8.4) and (8.16).

With reference to TEST2 and TEST4, Figure 8.5 shows how the introduction of the linear control component in the consensus protocol (8.5)-(8.7) speeds up the achievement of

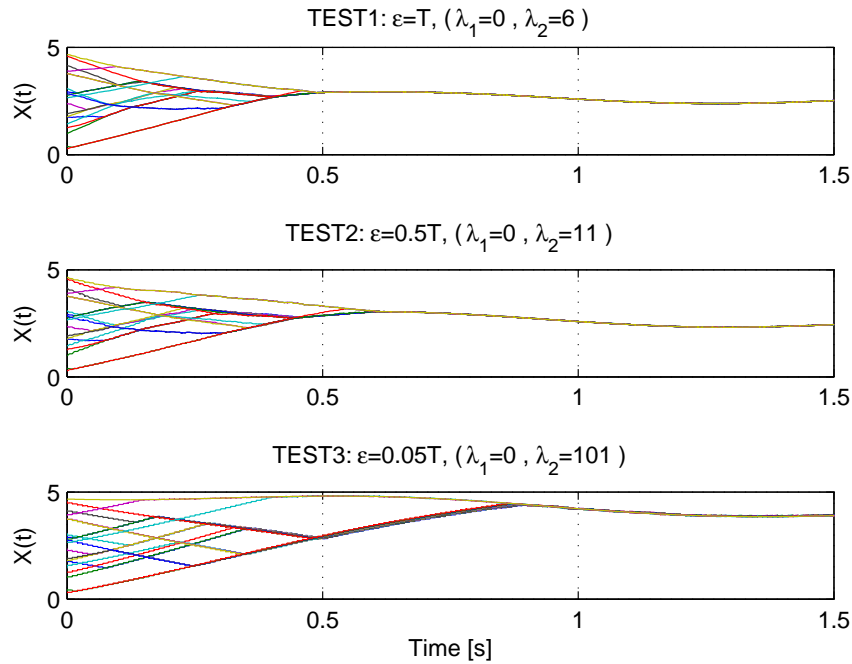


Figure 8.3: Time evolution of the clock variables for TEST1-3 (right).

consensus without causing chattering, as it would be the case by increasing the parameter λ_2 instead.

Figure 8.6 shows the Lyapunov function relative to an additional conclusive test (TEST 5) where, under the same conditions of TEST 1, the external perturbations have been removed ($\vartheta_i(t) = \Pi = 0$). A small residual synchronization error is still present, even if the achievement of a theoretically-exact consensus condition would be expected in this condition due to (8.16). The source of this error is, however, of purely numerical nature and the size of the residual set tends to zero while the sampling-time T_s is progressively reduced.

8.5 Conclusion and Future Works

In this Chapter a distributed algorithm, based on the mixed use of continuous and discontinuous local interaction rules, is suggested to solve the finite-time consensus problem in a network of continuous time integrators with additive disturbances. It has been proven that the network converges in finite time to an approximate consensus condition. Numerical simulations have been provided to corroborate the analytical results. Among the most interesting directions for next research, more complex agent's dynamics are currently under investigation along with the possibility to consider more general switching communication policy are actually under investigation. Furthermore, discrete time implementation of the proposed interaction rule is under study as well.

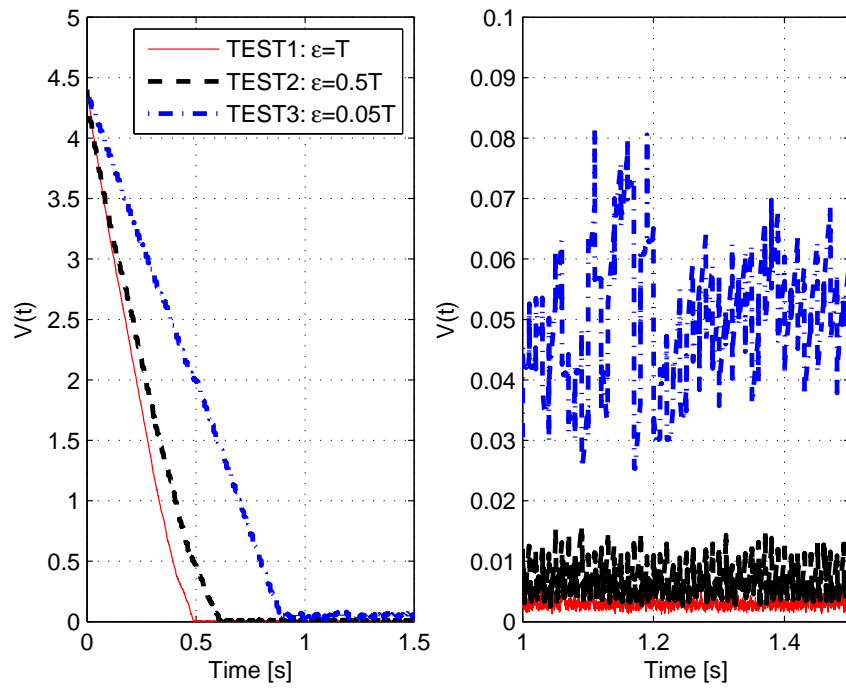


Figure 8.4: Transient evolution (left) and steady state accuracy (right) of the Lyapunov function $V(t)$.

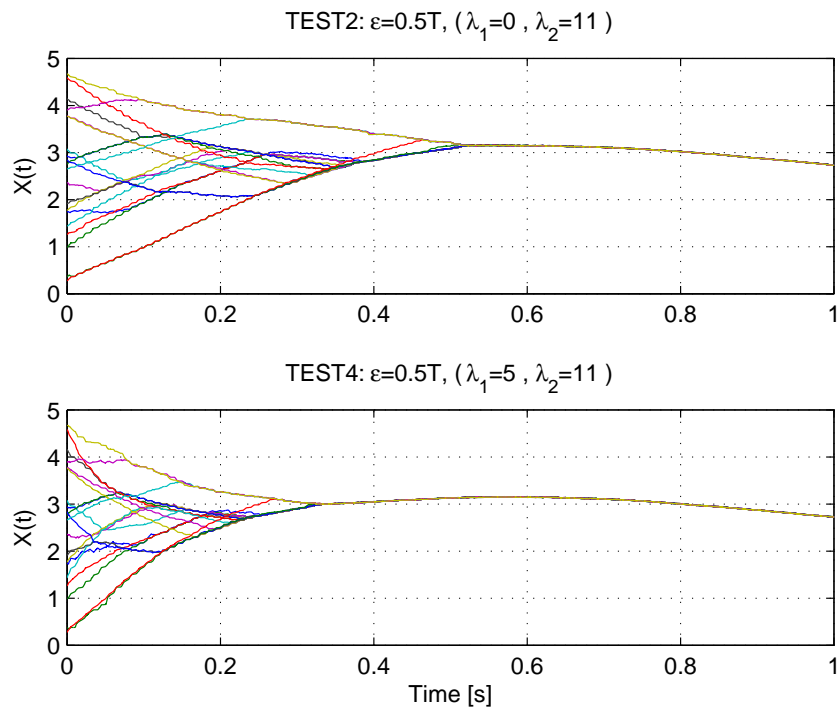


Figure 8.5: Transient evolution of the agent states in TEST2 and TEST4.

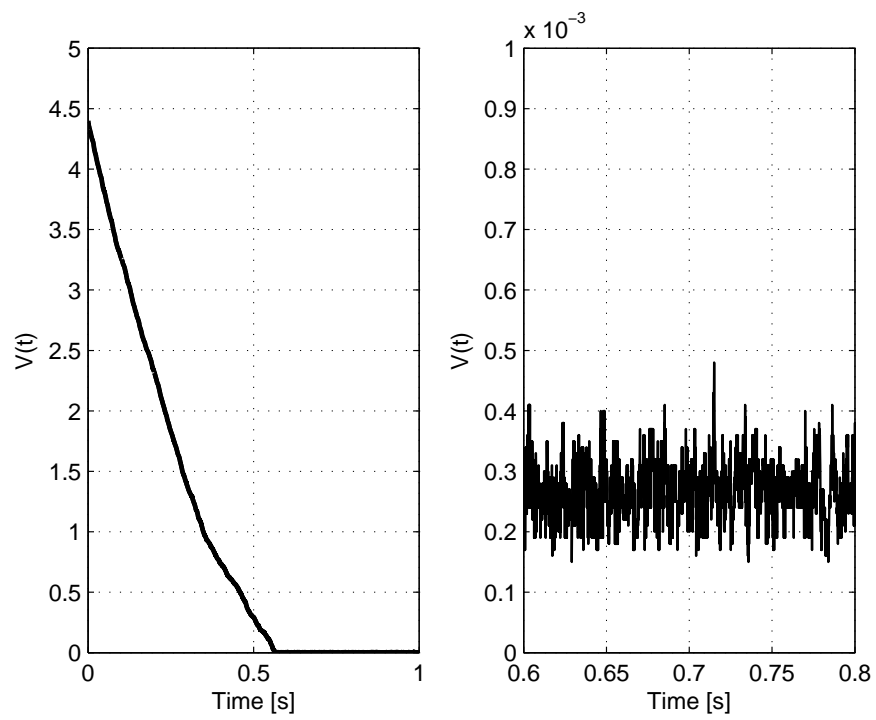


Figure 8.6: Transient evolution (left) and steady state accuracy (right) of the Lyapunov function $V(t)$ in TEST 5.

Chapter 9

Robust Consensus Algorithms for Double-integrator Dynamics

9.1 Introduction

This work focuses on a consensus algorithm for perturbed double integrator dynamics. Since these systems are suitable to model networks of point-mass vehicles, they are of higher interest as compared to the single integrator dynamics due to the possible applications in rendezvous, formation control, flocking and sensor networks [Ren et al., 2007a, Deshpande et al., 2011, Ren, 2008, Olfati-Saber & Shamma, 2005, Cortés, 2006b, Li et al., 2013].

With reference to an undirected topology, asymptotic consensus for double integrators dynamics is presented in [Ren, 2008, Xie & Wang, 2007]. In [Ren, 2008] several nonlinear protocols have been presented, while in [Xie & Wang, 2007] linear interaction rules were dealt with by including in the analysis the effect of measurement delays. Sufficient conditions for achieving asymptotic consensus in presence of nonlinear second-order agents' dynamics is considered in [Yu et al., 2010]. More recently, the finite-time consensus problem for a network of double integrators is studied in [Cao & Ren, 2012] for an undirected static topology and in [Cortés, 2006b] for an undirected static or switching topology using non-smooth protocols. However, none of the above works takes into account the presence of perturbation terms in the agents' dynamics by studying "ideal" double integrators only.

In [Franceschelli et al., 2013a] finite time consensus with perturbation terms is investigated in the case of single integrators with undirected and switching network topology.

Here, it is proposed a discontinuous consensus algorithm for achieving finite-time agreement in a network of perturbed agents with a static and undirected communication graph while completely rejecting the effect of the disturbances. The class of perturbations considered in the present work only assume them to be bounded, in magnitude, by a-priori known constants. Complete rejection of such a wide class of disturbance was never achieved in the existing literature quoted above. The proposed local interaction rule can be thought as a distributed version of the well-known *Twisting Second Order Sliding Mode Algorithm* [Levant, 1993a, Orlov, 2004, Bartolini et al., 2003] with a non-trivial function of the neighbors states used as sliding manifold. All significant robustness properties against uncertainties and dis-

turbances typical of Variable Structure Control Theory are inherited [Bartolini et al., 2008].

The performance of the proposed protocol is investigated by Lyapunov-based analysis, and simple tuning rules to adjust the algorithm parameters are provided.

The Chapter is organized as follows: in Section 2 preliminaries of graph theory and multi-agent systems are provided to clarify the notation that will be used in the Chapter. The problem statement and the proposed local interaction rule are presented in Section 3. Section 4 presents a constructive Lyapunov analysis which demonstrates that the proposed discontinuous protocol solves the finite-time consensus problem for a network of double integrators affected by bounded unknown perturbations. To corroborate the theoretical results, simulation results are shown in Section 5. Section 6 provides some concluding remarks and hints for further investigation.

9.2 Preliminaries and Notation

With reference to a network of N agents, the associated undirected communication graph $\mathcal{G} = (\mathcal{V}, \mathcal{E})$ is considered, where $\mathcal{V} = \{1, \dots, N\}$ is the set of agents and $\mathcal{E} \subseteq \mathcal{V}^2$ represent the set of edges. The set of neighbors of the i -th agent is defined as $\mathcal{N}_i^- = \{j \in \mathcal{V} / \{i\} : (i, j) \in \mathcal{E}\}$. Topological information associated with graph \mathcal{G} is encoded in the *Laplacian Matrix* $\mathcal{L} = [\mathcal{L}_{ij}] \in \mathbb{R}^{N \times N}$ where

$$\mathcal{L}_{ij} := \begin{cases} |\mathcal{N}_i^-| & \text{if } i = j \\ -1 & \text{if } (i, j) \in \mathcal{E} \\ 0 & \text{otherwise} \end{cases} \quad (9.1)$$

and $|\mathcal{N}_i^-|$ is the cardinality of the i -th agent neighbor set.

For an undirected graph, \mathcal{L} is a symmetric and positive semi-definite matrix [Garin & Schenato, 2011, Olfati-Saber et al., 2007, Godsil et al., 2001]. In addition, \mathcal{L} has real eigenvalues that can be ordered sequentially as follows $0 = \lambda_1 \leq \dots \leq \lambda_N$.

The null eigenvalue λ_1 has multiplicity equal to the number of connected components of \mathcal{G} and the corresponding left and right eigenvectors are respectively $\mathbf{1}_N = \text{col}(1, \dots, 1) \in \mathbb{R}^N$ and $\mathbf{1}_N^T$, where the expression $\text{col}(\cdot)$ denotes a column vector. Thus, the following identities hold:

$$\mathcal{L} \cdot \mathbf{1}_N = \mathbf{0}_N \quad , \quad \mathbf{1}_N^T \cdot \mathcal{L} = \mathbf{0}_N^T \quad (9.2)$$

In addition, the next property holds [Horn & Johnson, 1990]

$$\|\mathcal{L}\zeta\|_1 \geq \|\mathcal{L}\zeta\|_2 = \sqrt{\zeta^T \mathcal{L}^2 \zeta} \geq \lambda_2 \cdot \|\zeta\|_2 \quad (9.3)$$

where λ_2 is the smallest nonzero eigenvalue of \mathcal{L} , known as *algebraic connectivity* [Pereira, 2011], and $\zeta \in \mathbb{R}^N$ is any vector such that $\mathbf{1}_N^T \zeta = 0$.

9.3 Problem Statement

Let us consider a connected network consisting of N agents where each agent is governed by the following perturbed double-integrator dynamics:

$$\dot{\mathbf{x}}_i(t) = \mathbf{A}\mathbf{x}_i(t) + \mathbf{B}(u_i(t) + \vartheta_i(t)), \quad i \in \mathcal{V}, \quad (9.4)$$

with

$$\mathbf{A} = \begin{pmatrix} 0 & 1 \\ 0 & 0 \end{pmatrix}, \quad \mathbf{B} = \begin{pmatrix} 0 \\ 1 \end{pmatrix}, \quad (9.5)$$

where $\mathbf{x}_i = \text{col}(x_{i,1}, x_{i,2}) \in \mathbb{R}^2$ represents the state of the i -th agent, $u_i(t) \in \mathbb{R}$ is the control input, and $\vartheta_i(t) \in \mathbb{R}$ is an unknown perturbation which corrupts the agent's dynamics. A compact representation of the collective network dynamics can be expressed as follows:

$$\dot{X} = (\mathbf{I}_{N \times N} \otimes \mathbf{A})X + (\mathbf{I}_{N \times N} \otimes \mathbf{B})(U + \Theta) \quad (9.6)$$

where \otimes denotes the *Kronecker Product*, $\mathbf{I}_{N \times N} \in \mathbb{R}^{N \times N}$ is the identity matrix of order N , and

$$\begin{aligned} X &= \text{col}(\mathbf{x}_1, \dots, \mathbf{x}_N) \in \mathbb{R}^{2N} \\ U &= \text{col}(u_1, \dots, u_N) \in \mathbb{R}^N \\ \Theta &= \text{col}(\vartheta_1, \dots, \vartheta_N) \in \mathbb{R}^N \end{aligned} \quad (9.7)$$

Then, let

$$\begin{aligned} Z_1 &= \text{col}(x_{1,1}, \dots, x_{N,1}) \in \mathbb{R}^N \\ Z_2 &= \text{col}(x_{1,2}, \dots, x_{N,2}) \in \mathbb{R}^N \end{aligned} \quad (9.8)$$

be two vectors which stack together, respectively, the position and velocity of each agents. The collective dynamics (9.6) can be expressed in the following regular form:

$$\begin{aligned} \dot{Z}_1 &= Z_2 \\ \dot{Z}_2 &= U + \Theta \end{aligned} \quad (9.9)$$

The next assumption has been done

Assumption 9.1. \mathcal{G} is a connected undirected graph and the disturbance vector Θ is bounded in accordance with:

$$|\vartheta_i(t)| \leq \Pi_i \leq \Pi \quad \text{with} \quad \Pi = \max_{i \in \mathcal{V}} \{\Pi_i\} = \|\Theta\|_\infty < \infty \quad (9.10)$$

■

The objective of the present work is to present a novel discontinuous local interaction rule guaranteeing the achievement of the next finite-time consensus conditions:

$$\begin{aligned} |z_{i,1}(t) - z_{j,1}(t)| &= 0 \\ |z_{i,2}(t) - z_{j,2}(t)| &= 0 \end{aligned}, \quad t \geq T, \quad T < \infty, \quad \forall i, j \in \mathcal{V} \quad (9.11)$$

The next local interaction rule is suggested:

$$u_i(t) = -a \cdot \text{sign}(\mathcal{L}_i Z_1) - b \cdot \text{sign}(\mathcal{L}_i Z_2), \quad i \in \mathcal{V} \quad (9.12)$$

where a and b are positive tuning constants, \mathcal{L}_i is the i -th row of the Laplacian Matrix and $\text{sign}(\cdot)$ is defined as follows:

$$\text{sign}(\mathfrak{S}) = \begin{cases} 1 & \text{if } \mathfrak{S} > 0 \\ [-1, 1] & \text{if } \mathfrak{S} = 0 \\ -1 & \text{if } \mathfrak{S} < 0 \end{cases} \quad (9.13)$$

The proposed discontinuous protocol in (9.12) can be thought as a distributed version of the "Twisting" second order sliding mode algorithm [Levant, 1993a], where a non-trivial function of the neighbors states is used as sliding manifold. The arguments of the sign functions take the next explicit form:

$$\mathcal{L}_i Z_k = \sum_{j \in \mathcal{N}_i^-} (z_{i,k} - z_{j,k}), \quad i \in \mathcal{V}, \quad k = 1, 2 \quad (9.14)$$

Define

$$\sigma(\mathcal{L}Z_k) = \text{col}(\text{sign}(\mathcal{L}_1 Z_k), \dots, \text{sign}(\mathcal{L}_N Z_k)), \quad k = 1, 2 \quad (9.15)$$

the local interaction protocol (9.12) can be rewritten at the network level in the following compact form:

$$U(t) = -a \cdot \sigma(\mathcal{L}Z_1) - b \cdot \sigma(\mathcal{L}Z_2) \quad (9.16)$$

Remark 9.1. *Due to the proposed discontinuous local interaction rule, and the possibly discontinuous nature of the external disturbances (which are only supposed to be uniformly bounded), the closed loop network dynamics will be discontinuous and the resulting solution notion needs to be discussed and clarified. For a differential equation with discontinuous right-hand side, following [Filippov,], the resulting solution in the so-called Filippov sense as the solution of an appropriate differential inclusion is considered, the existence of which is guaranteed (owing on certain properties of the associated set-valued map) and for which noticeable properties, such as absolute continuity, are in force. The reader is referred to [Cortes, 2008] for a comprehensive account of the notions of solution for discontinuous dynamical systems. ■*

9.4 Convergence Analysis

In this section, the performance of protocol (9.16) are investigated by means of Lyapunov-Based Analysis. Simple tuning rules for the control gains a and b will be derived.

Common approach adopted to deal with the consensus problem for network of simple integrator agents is to study the convergence to zero of the disagreement vector dynamics [Franceschelli et al., 2012b], which imply the convergence to the consensus value $\mathbf{1}_N^T \cdot Z_1 / N$ of each agents. Since second-order agents are considered, the following disagreement vectors take place:

$$\delta_k(t) = Z_k(t) - \frac{\mathbf{1}_N \cdot \mathbf{1}_N^T}{N} \cdot Z_k(t), \quad k = 1, 2 \quad (9.17)$$

The achievement of the consensus condition (9.11) corresponds to the annihilation of vectors $\delta_1(t)$ and $\delta_2(t)$ in finite time. It is worth noting that both the disagreement vectors satisfy the

following conditions [Olfati-Saber et al., 2007]:

$$\mathbf{1}_N^T \cdot \delta_k = 0, \quad \mathcal{L}\delta_k = \mathcal{L}Z_k \quad k = 1, 2 \quad (9.18)$$

along with the property (9.3), which can be rewritten as:

$$\delta_k^T \mathcal{L}\delta_k \geq \lambda_2 \|\delta_k\|_2^2, \quad k = 1, 2 \quad (9.19)$$

The dynamics of δ_1 and δ_2 can be easily derived by differentiating (9.17) and considering (9.9), (9.16) and (9.18) as follows:

$$\begin{aligned} \dot{\delta}_1 &= \delta_2 \\ \dot{\delta}_2 &= -a \cdot \sigma(\mathcal{L}\delta_1) - b \cdot \sigma(\mathcal{L}\delta_2) + \hat{\Theta}(t) + \Omega(t) \cdot \mathbf{1}_N \end{aligned} \quad (9.20)$$

where

$$\hat{\Theta}(t) = \Theta(t) - \frac{\mathbf{1}_N \cdot \mathbf{1}_N^T}{N} \Theta(t) \quad (9.21)$$

$$\Omega(t) = \frac{a \cdot \mathbf{1}_N^T \sigma(\mathcal{L}\delta_1) + b \cdot \mathbf{1}_N^T \sigma(\mathcal{L}\delta_2)}{N} \quad (9.22)$$

The main result of the Chapter can be now presented.

Theorem 9.1. *Consider the collective dynamics (9.9) and let Assumption 9.1 be satisfied. Consider the local interaction rule (9.16) and let tuning parameters be selected according to*

$$a > b + \Pi, \quad b > \Pi. \quad (9.23)$$

Then, the finite-time consensus property (9.11) is achieved. ■

Proof: The proof is broken into three simple consecutive steps.

▷ Equi-uniform stability

Consider the following candidate Lyapunov function:

$$V(t) = a \cdot \|\mathcal{L}\delta_1\|_1 + \frac{1}{2} \cdot \delta_2^T \mathcal{L}\delta_2 \quad (9.24)$$

The considered Lyapunov function is a locally Lipschitz function and it is not differentiable when any entry of vector $\mathcal{L}\delta_1$ is zero. Thus, the following treatment refers for stability analysis to the Lyapunov Generalized Theorem for non-smooth analysis reported in [Paden & Sastry, 1987], which makes use of Clarke's generalized gradient [Clarke, 1983] and involves a set-valued form for the resulting Lyapunov function time derivative. In the remainder, the computation method illustrated in [Paden & Sastry, 1987], where a Lyapunov analysis involving an analogous sum-of-absolute-value Lyapunov function term was dealt with is considered. For the sake of brevity, here all the necessary technicalities justifying the correctness of adopting the chain rule to compute the time derivative $V(t)$, which exists almost everywhere in the form of an appropriate set valued map are omitted. The reader is referred to the works [Cortes, 2008, Paden & Sastry, 1987, Shevitz & Paden, 1994] where discontinuous systems and non-smooth Lyapunov tools analogous to those involved in the present analysis were discussed in detail.

The corresponding time derivative takes the form

$$\dot{V}(t) = a\delta_1^T \mathcal{L}\sigma(\mathcal{L}\delta_1) + \delta_2^T \mathcal{L}\dot{\delta}_2 \quad (9.25)$$

Considering (9.20) into (9.25), and taking into account that $\Omega(t)$ is a scalar and that $\mathbf{1}_N^T \cdot \mathcal{L} = 0$, the next simplification can be made after evaluating its time-derivative along the trajectory of the perturbed dynamic (9.20)-(9.22)

$$\begin{aligned} \dot{V}(t) &= a\delta_2^T \mathcal{L}\sigma(\mathcal{L}\delta_1) - a\delta_2^T \mathcal{L}\sigma(\mathcal{L}\delta_1) - b \cdot \delta_2^T \mathcal{L}\sigma(\mathcal{L}\delta_2) \\ &+ \delta_2^T \mathcal{L}\hat{\Theta}(t) + \Omega(t)\delta_2^T \mathcal{L} \cdot \mathbf{1}_N \\ &= -b \cdot \delta_2^T \mathcal{L}\sigma(\mathcal{L}\delta_2) + \delta_2^T \mathcal{L}\hat{\Theta} \\ &= -b \cdot \|\mathcal{L}\delta_2\|_1 + \delta_2^T \mathcal{L}\hat{\Theta} \end{aligned} \quad (9.26)$$

Applying the *Hölder's Inequality* and taking into account (9.10), the next estimation, involving the last sign-undefined term in the right hand side of (9.26), can be made

$$|\delta_2^T \mathcal{L}\hat{\Theta}| \leq \|\mathcal{L}\delta_2\|_1 \|\hat{\Theta}\|_\infty \leq \Pi \cdot \|\mathcal{L}\delta_2\|_1 \quad (9.27)$$

on the basis of which it yields

$$\dot{V}(t) \leq -(b - \Pi) \cdot \|\mathcal{L}\delta_2\|_1 \quad (9.28)$$

It follows by (9.23) that $\dot{V}(t) \leq 0$, therefore the uncertain system (9.20)-(9.22) is equi-uniformly stable [Orlov, 2008]. Indeed, initializing the system in an arbitrarily vicinity of the origin such that $V(0) \leq R_0$, the uncertain system (9.20)-(9.22) cannot leave this vicinity, regardless of whichever admissible uncertainty $\hat{\Theta}$ affects the system. In other words, inequality (9.28) guarantees the boundedness of the perturbed disagreement vector's state trajectories in (9.20)-(9.22).

▷ Global equi-uniform asymptotic stability

To begin with, let us note that by virtue of (9.28) all possible solutions of (9.20)-(9.22), initialized at $t_0 \in \mathbb{R}$ within the invariant compact set

$$\mathcal{D}_R = \{(\delta_1, \delta_2) \in \mathbb{R}^{2N} : V(\delta_1, \delta_2) \leq R\} \quad (9.29)$$

are a priori estimated by

$$\sup_{t \in [t_0, \infty]} V(\delta_1, \delta_2) \leq R \quad (9.30)$$

which, considering the Lyapunov function definition (9.24), implies the following relations:

$$\|\mathcal{L}\delta_1\|_1 \leq R/a \quad , \quad \delta_2^T \mathcal{L}\delta_2 \leq 2R \quad (9.31)$$

Furthermore, by virtue of (9.19), the following chain of inequalities holds:

$$\lambda_2 \|\delta_2\|_2^2 \leq \delta_2^T \mathcal{L}\delta_2 \leq \lambda_N \|\delta_2\|_2^2 \quad (9.32)$$

which allows to manipulate (9.31) as

$$\|\mathcal{L}\delta_1\|_1 \leq R/a \quad , \quad \|\delta_2\|_2 \leq \sqrt{2R/\lambda_2} \quad (9.33)$$

The idea behind the remainder of the proof is inspired by the Extended Invariance Principle [Orlov, 2008] and it is based on constructing a parameterized family of local Lyapunov function $V_R(\delta_1, \delta_2)$, $R > 0$ such that each $V_R(\delta_1, \delta_2)$ is well posed on the corresponding compact set \mathcal{D}_R and its time derivative, initialized within \mathcal{D}_R is negative definite and yields the desired stability and convergence properties. A parameterized Lyapunov function $V_R(\delta_1, \delta_2)$, $R > 0$ with the properties above, can be obtained by augmenting the Lyapunov function (9.24) as follows:

$$V_R(t) = V(t) + \kappa_R \cdot U(t) \quad (9.34)$$

where $U(t)$ is the sign-indefinite function

$$U(t) = \delta_1^T \mathcal{L} \delta_2 \quad (9.35)$$

and κ_R is a proper positive constant. By Young's inequality and taking into account (9.33), then it follows that

$$\begin{aligned} U(t) &= \delta_1^T \mathcal{L} \delta_2 \geq -\frac{1}{2} (\|\mathcal{L} \delta_1\|_2^2 + \|\delta_2\|_2^2) \geq \\ &\geq -\frac{1}{2} \left(\frac{R}{a} \cdot \|\mathcal{L} \delta_1\|_1 + \|\delta_2\|_2^2 \right) \end{aligned} \quad (9.36)$$

Taking into account (9.34), (9.36), and the left inequality in (9.32), it follows that

$$V_R \geq \left[a - \frac{\kappa_R R}{2a} \right] \cdot \|\mathcal{L} \delta_1\|_1 + \frac{1}{2} [\lambda_2 - \kappa_R] \cdot \|\delta_2\|_2^2 \quad (9.37)$$

which, in accordance with the following restriction:

$$\kappa_R < \min \left\{ \frac{2a^2}{R}, \lambda_2 \right\} \quad (9.38)$$

guarantees that $V_R(t)$ is not negative in spite of having added the sign indefinite term $U(t)$.

In turns, by differentiating (9.35) along the trajectory of the uncertain dynamic (9.20)-(9.22), it results:

$$\dot{U} = \delta_2^T \mathcal{L} \delta_2 - a \cdot \|\mathcal{L} \delta_1\|_1 - b \cdot \delta_1^T \mathcal{L} \sigma(\mathcal{L} \delta_2) + \delta_1^T \mathcal{L} \hat{\Theta} \quad (9.39)$$

In the right hand side of (9.39) there is a negative definite term (the second one) and three positive or sign-indefinite terms. Bounds to the latter de-stabilizing terms are now derived. As for the first entry, by the Hölder inequality and the right inequality in (9.33), it derives that

$$|\delta_2^T \mathcal{L} \delta_2| \leq \|\mathcal{L} \delta_2\|_2 \|\delta_2\|_2 \leq \sqrt{\frac{2 \cdot R}{\lambda_2}} \cdot \|\mathcal{L} \delta_2\|_1 \quad (9.40)$$

As for the term $-b \cdot \delta_1^T \mathcal{L} \sigma(\mathcal{L} \delta_2)$ one can exploit once more the Hölder inequality, taking into account that $\|\sigma(\mathcal{L} \delta_2)\|_\infty = 1$. to assess that

$$|b \cdot \delta_1^T \mathcal{L} \sigma(\mathcal{L} \delta_2)| \leq b \|\mathcal{L} \delta_1\|_1 \|\sigma(\mathcal{L} \delta_2)\|_\infty \leq b \|\mathcal{L} \delta_1\|_1 \quad (9.41)$$

The last term in the right hand side of (9.39) satisfies the inequality

$$|\delta_1^T \mathcal{L} \hat{\Theta}| \leq \|\mathcal{L} \delta_1\|_1 \|\hat{\Theta}\|_\infty \leq \Pi \cdot \|\mathcal{L} \delta_1\|_1 \quad (9.42)$$

Therefore relation (9.39) can be estimated as

$$\begin{aligned} \dot{U} &\leq \sqrt{\frac{2R}{\lambda_2}} \cdot \|\mathcal{L}\delta_2\|_1 - a \cdot \|\mathcal{L}\delta_1\|_1 + b \cdot \|\mathcal{L}\delta_1\|_1 + \\ &\quad + \Pi \cdot \|\mathcal{L}\delta_1\|_1 \end{aligned} \quad (9.43)$$

Then, by combining (9.28) and (9.43), the time derivative of (9.34) can be upper-estimated as follows:

$$\begin{aligned} \dot{V}_R &\leq -c_1 \cdot \|\mathcal{L}\delta_1\|_1 - c_2 \cdot \|\mathcal{L}\delta_2\|_1 \leq \\ &\leq -c_R \cdot (\|\mathcal{L}\delta_1\|_1 + \|\mathcal{L}\delta_2\|_1) \end{aligned} \quad (9.44)$$

where

$$c_1 = \kappa_R (a - b - \Pi) , \quad c_2 = b - \Pi - \kappa_R \sqrt{2R/\lambda_2} \quad (9.45)$$

$$c_R = \min \{c_1, c_2\} \quad (9.46)$$

and with the coefficient κ_R subject to the next inequality which is stricter than (9.38)

$$\kappa_R < \min \left\{ \frac{2a^2}{R}, \lambda_2, \sqrt{\frac{\lambda_2}{2R}} \cdot (b - \Pi) \right\} \quad (9.47)$$

The exponential convergence towards the manifold $\mathcal{L}\delta_1 = \mathcal{L}\delta_2 = \mathbf{0}$, can be shown taking into account the following

$$\begin{aligned} V_R &\leq a \cdot \|\mathcal{L}\delta_1\|_1 + \frac{1}{2} |\delta_2^T \mathcal{L}\delta_2| + \kappa_R \cdot |\delta_1^T \mathcal{L}\delta_2| \leq \\ &\leq \bar{c}_1 \cdot \|\mathcal{L}\delta_1\|_1 + \bar{c}_2 \cdot \|\mathcal{L}\delta_2\|_1 \leq \\ &\leq \bar{c}_R \cdot (\|\mathcal{L}\delta_1\|_1 + \|\mathcal{L}\delta_2\|_1) \end{aligned} \quad (9.48)$$

with

$$\bar{c}_1 = a + \kappa_R \sqrt{\frac{2R}{\lambda_2}} , \quad \bar{c}_2 = \frac{1}{2} \sqrt{\frac{2R}{\lambda_2}} , \quad \bar{c}_R = \max \{ \bar{c}_1, \bar{c}_2 \} \quad (9.49)$$

which can be derived applying the Hölder Inequalities and substituting the bounds in (9.33), along with (9.44) which leads to

$$\dot{V}_R(\delta_1, \delta_2) \leq -\rho_R \cdot V_R(\delta_1, \delta_2) \quad (9.50)$$

with

$$\rho_R \leq \frac{c_R}{\bar{c}_R} = \frac{\min \left\{ \kappa_R (a - b - \Pi), b - \Pi - \kappa_R \sqrt{2R/\lambda_2} \right\}}{\max \left\{ a + \kappa_R \sqrt{2R/\lambda_2}, \sqrt{R/2\lambda_2} \right\}} \quad (9.51)$$

which implies the exponential decay of $V_R(t)$.

▷ Global equi-uniform finite-time stability

Consider the uncertain disagreement vector dynamics (9.20)-(9.22) rewritten in the following compact form:

$$\dot{\delta} = \Phi(\delta) + \Psi(t) \quad , \quad \delta = \text{col}(\delta_1, \delta_2) \in \mathbb{R}^{2N} \quad (9.52)$$

where

$$\Psi(t) = \text{col}(\mathbf{0}_N, \hat{\Theta} + \Omega \cdot \mathbf{1}_N) = \text{col}(\psi_1, \dots, \psi_{2N}) \in \mathbb{R}^{2N} \quad (9.53)$$

is an uncertain vector of uniformly bounded functions, according to

$$|\psi_i(t)| \leq M_i, \quad M_i = \begin{cases} 0, & i = 1, \dots, N \\ \Pi + a + b, & i = N + 1, \dots, 2N \end{cases} \quad (9.54)$$

and

$$\begin{aligned} \Phi(\delta) &= \text{col}(\delta_2, -a \cdot \sigma(\mathcal{L}\delta_1) - b \cdot \sigma(\mathcal{L}\delta_2)) = \\ &= \text{col}(\phi_1, \dots, \phi_{2N}) \in \mathbb{R}^{2N} \end{aligned} \quad (9.55)$$

is a vector of piece-wise continuous functions.

Since the proof of finite-time convergence will be based on the properties of homogeneous systems, in the following it is introduced the definition of *local homogeneity* and the *Quasi-homogeneity Principle*, both taken from [Orlov, 2004], upon which the presented reasoning will rely on. Homogeneity concepts were applied for finite-time stability analysis of consensus protocols for first-order agents in, e.g, [Wang & Hong, 2010].

Definition 9.1. A piece-wise continuous vector field

$$\mathbf{f}(t) = \text{col}(f_1(\mathbf{x}), \dots, f_n(\mathbf{x})) \in \mathbb{R}^n \quad \text{with} \quad \mathbf{x} \in \mathbb{R}^n \quad (9.56)$$

is called *locally homogeneous of degree* $q \in \mathbb{R}$ with respect to the dilation vector $\mathbf{r} = (r_1, \dots, r_n)$, $r_i > 0$, if for all $\varepsilon > 0$

$$f_i(\varepsilon^{r_1}x_1, \dots, \varepsilon^{r_n}x_n, \varepsilon^{-q}t) = \varepsilon^{q+r_i}f_i(\mathbf{x}, t), \quad i = 1, \dots, n \quad (9.57)$$

■

Theorem 9.2. [Orlov, 2004] *Quasi-homogeneity Principle.* The uncertain system (9.52) is globally equi-uniformly finite-time stable if the following conditions are satisfied:

1. The right-hand side of (9.52) consists of a locally homogeneous piece-wise continuous function $\Phi(\delta)$ of degree $q < 0$ with respect to dilation \mathbf{r} and a piece-wise continuous function $\Psi(t)$ whose components ψ_i , $i = 1, \dots, n$ are locally uniformly bounded by constants $M_i \geq 0$ within a homogeneity ball;
2. $M_i = 0$ whenever $q + r_i > 0$;
3. The uncertain system (9.52) is globally equi-uniformly asymptotically stable around the origin.

■

In accordance with the Definition 9.1, it is possible to observe that $\Phi(\delta)$ is locally homogeneous of degree $q = -1$ with respect to the dilation vector $\mathbf{r} = [r_i] \in \mathbb{R}^{2N}$ taking the form

$$r_i = \begin{cases} r_i = 2, & \text{with } i = 1, \dots, N \\ r_i = 1, & \text{with } i = N + 1, \dots, 2N \end{cases} \quad (9.58)$$

Then, since system (9.52) is globally equi-uniformly asymptotically stable, and the following conditions hold:

$$\begin{aligned} q + r_i > 0 \quad \forall i : M_i = 0 &\Rightarrow i = 1, \dots, N \\ q + r_i \leq 0 \quad \forall i : M_i \neq 0 &\Rightarrow i = N + 1, \dots, 2N \end{aligned} \quad (9.59)$$

all the conditions of Theorem 9.2 are satisfied, and the proposed local interaction rule (9.12) guarantees the finite-time stability of system (9.52). As a consequence, the consensus problem (9.11) is solved in finite-time. The proof of Theorem 9.1 is completed. \square

Remark 9.2. *It is worth to remark that protocol (9.12) can be extended to the task of “distributed leader-tracking” [Khoo et al., 2009] for multi-robot networks (9.4) [Pilloni et al., 2014a, Pilloni et al., 2014c]. Indeed, let agent $i = 1$ be a autonomous leader with bounded acceleration i.e. $|\dot{x}_{1,2}| < \Lambda$, able to communicate by with only a subset of followers ($\mathcal{V}/\{1\}$); according to \mathcal{G} , protocol (9.12) ensures the finite-time tracking of the leader position by its followers, i.e. $x_{i,k} - x_{1,k} = 0 \quad \forall i = 2, \dots, N, k = 1, 2$. This can be proven by non-smooth Lyapunov analysis considering the following candidate Lyapunov function:*

$$V(t) = a \cdot \|\mathcal{M}\tilde{\delta}_1\|_1 + \frac{1}{2} \cdot \tilde{\delta}_2^T \mathcal{M}\tilde{\delta}_2 \quad (9.60)$$

where $\tilde{\delta}_{i,k} = x_{i,k} - x_{1,k}$ is the distributed tracking error and $\mathcal{M} = \mathcal{L}_f - \text{diag}\{\ell_{21}, \dots, \ell_{N1}\}$, with \mathcal{L}_f the Laplacian associated to the subgraph of \mathcal{G} composed only by followers (see i.e. [Khoo et al., 2009]).

The same results can be extended to the case of multi-dimensional state trajectories for each agent by exploiting straightforwardly the Kronecker product. \blacksquare

Remark 9.3. *Remarkably, the proposed controller, can provide the global achievement of consensus by using a control authority that remains always bounded, thereby addressing issues of actuator saturation [Ren, 2009, Roy et al., 2004, Ren, 2008]. This is not the case, e.g., with more classical consensus protocols, either linear [Ren et al., 2007a] or nonlinear [Cao & Ren, 2012], which imply an unbounded control effort when the discrepancy between agent’s initial conditions tends to infinity.* \blacksquare

Remark 9.4. *Denoting $\delta = \text{col}(\delta_1, \delta_2) = [d_i] \in \mathbb{R}^{2N}$, as discussed in Section 3 of [Orlov, 2004], an upper bound on the settling-time function after which the network of agents will be synchronized (i.e., $\delta_1 = \delta_2 = \mathbf{0}$) is*

$$T(t_0, \delta(t_0)) \leq \tau(\delta(0), E_R) + \frac{1}{1 - 2^q} (\zeta R^{-1})^q s(\zeta) \quad (9.61)$$

where

$$\tau(\delta(0), E_R) = \sup_{\delta(\cdot, t_0, \delta(0))} \inf \{T \geq 0 : \delta(t, t_0, \delta(0)) \in E_R\} \quad (9.62)$$

for all $t_0 \in \mathbb{R}$, $t \geq t_0 + T$, and

$$s(\zeta) = \sup \tau\left(\delta(0), E_{\frac{1}{2}\zeta}\right) \quad (9.63)$$

are respectively the reaching-time functions and its upper-bound. E_R denotes an ellipsoid of the form

$$E_R = \left\{ \delta \in \mathbb{R}^{2N} : \sqrt{\sum_{i=1}^{2N} \left(\frac{d_i}{R^i}\right)^2} \leq 1 \right\} \quad (9.64)$$

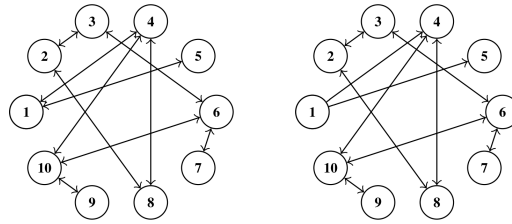


Figure 9.1: Communication topologies respectively for the second-order consensus task (left) and the distributed-tracking task (right).

located within a homogeneity ball $\zeta \geq \varepsilon_0 R$, and $\varepsilon_0 \leq \varepsilon$ is a positive constant called lower estimate of the homogeneity parameter ε . For further details see ([Orlov, 2004], Section 3).

■

9.5 Numerical Simulations

To demonstrate the efficacy of the proposed protocol consider the network on the left-side of Figure 9.1, consisting of 10 perturbed agents. Agents' dynamics are governed by equations (9.4)-(9.5). Disturbances $\vartheta_i(t)$ are selected as harmonic signals with randomly time-varying chosen coefficients guaranteeing that the upper-bound Π in (9.10) is $\Pi = 2$. The initial states are chosen as $x_{i,1}(0) = i$, $x_{i,2}(0) = -5.5 + i$ with $i = 1, \dots, 10$. For the computation of the control gains, according to the tuning rule (9.23), the values $a = 15$ and $b = 10$ were chosen. The continuous time network dynamics (9.9) has been simulated by using the Runge-Kutta 4-th order integration method with fixed step size equal to $10^{-3}s$.

Figure 9.2 shows the time evolutions of the disagreement vectors (9.17). It can be seen that consensus is achieved after a transient of about 4 seconds. Figure 9.3 depicts a comparison between the time evolution of the Lyapunov Function (9.34) during three tests where different control gain pairs (a, b) were adopted, according to the legend inserted in the plot. Comparing those curves it is seen how higher values of the control gains a and b can reduce the settling time to reach consensus. Overall, the collective network's dynamics behaves as expected and the disturbance effect is rejected in the sense that exact consensus is achieved in spite of the presence of unknown perturbations corrupting the agents' dynamics.

With reference to the extension of the consensus problem (9.11) to the task of distributed leader-tracking for multi-robot perturbed networks as in (9.4), consider the right network on Figure 9.1. Let agent 1 to be a perturbed leader with a sinusoidal reference trajectory $x_{1,0} = 2 \sin(t)$ in Figure 9.4 it can be appreciated how after a transient finite-time all followers reach the leader's position in spite of the presence of unknown but bounded perturbations.

9.6 Conclusion and Future Works

This Chapter proposed a discontinuous distributed local interaction rule for achieving finite-time consensus in a network of double integrators agents affected by bounded disturbances. Agents are supposed to interact through an indirected, static and connected, com-

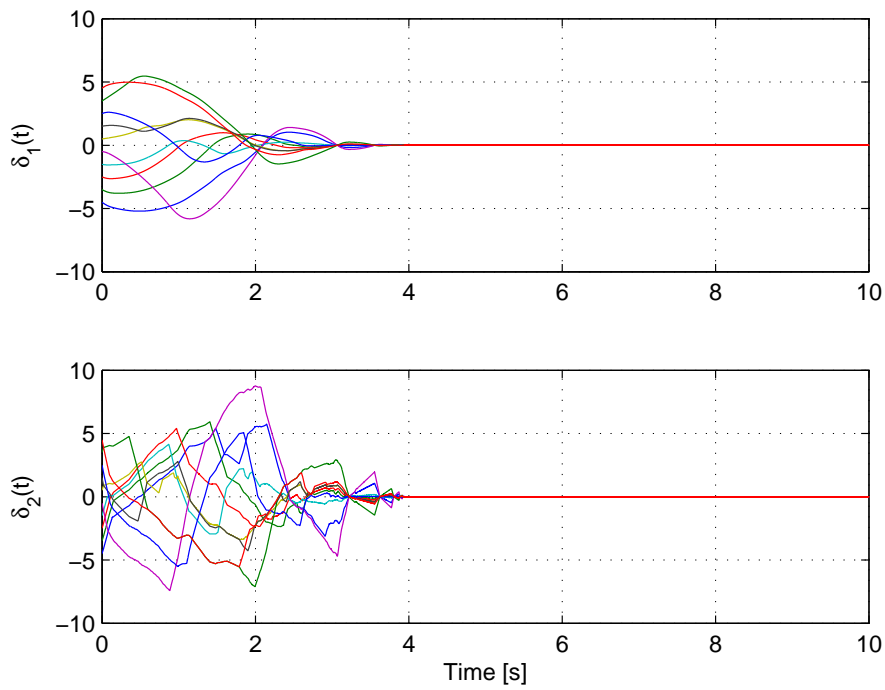


Figure 9.2: Trajectories of the disagreement vectors $\delta_1(t)$ and $\delta_2(t)$.

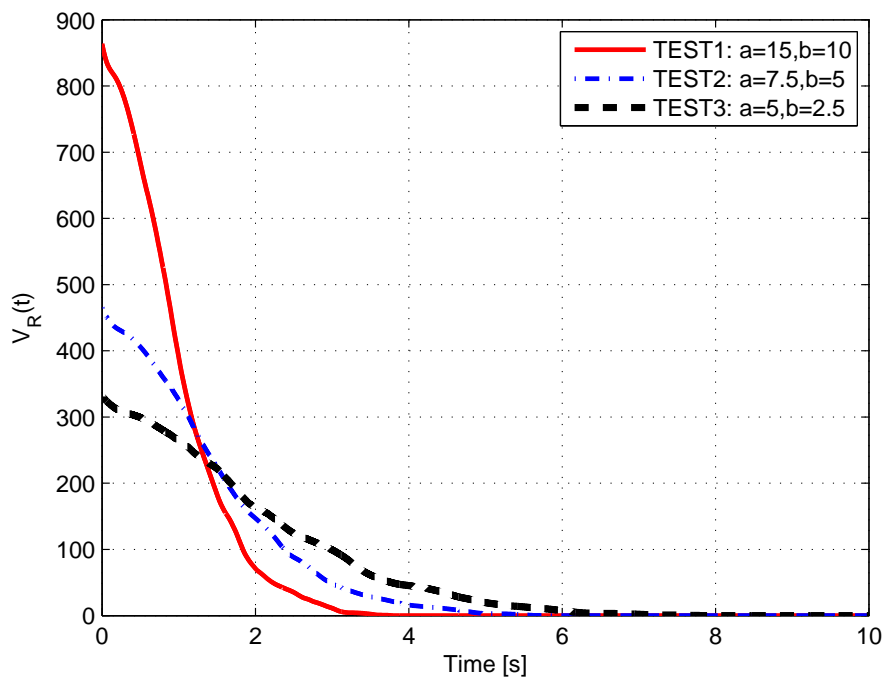


Figure 9.3: Transient evolution of the Lyapunov Function $V_R(t)$.

munication topology. A Lyapunov-Based analysis confirm effectiveness of the proposed algorithm to solve the finite-time consensus problem and provides a very simple set of tuning rules for adjusting the algorithm parameters. Complete disturbance rejection has been provided. Numerical simulations confirm the theory developed.

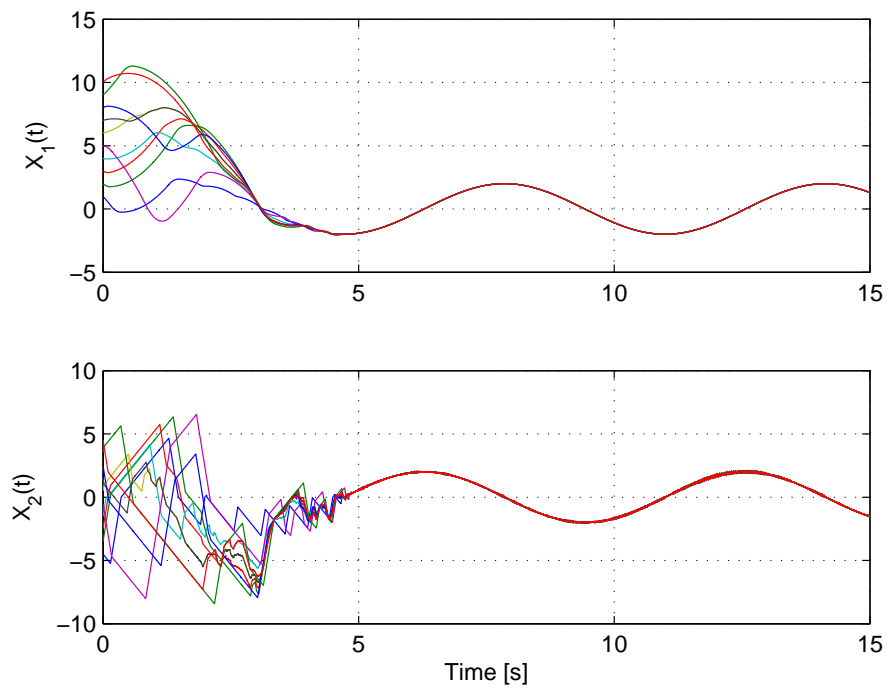


Figure 9.4: Transient evolution of the state-space vectors $X_1(t)$ and $X_2(t)$ for the distributed tracking task.

Chapter 10

Robust Consensus Algorithms in Infinite-Dimensional Networked Systems

In this Chapter the problem of driving a group of perturbed infinite-dimensional agents communicating through an undirected topology towards a common temperature's consensus value is considered. Since agents communicate by exchanging only information acquired at the boundary of the spatial domain, the proposed consensus algorithm can be considered as a boundary cooperative control. Each agent is modeled as 1D rod, described by the well-known heat diffusion equation, whereas perturbations are supposed to be only bounded in derivative and acting at the boundary of each rod too. Performances of the proposed local interaction rule in terms of robustness and rate of convergence are investigated by Lyapunov-Based approach from which simple tuning rules for achieving the consensus condition are developed. Simulative results demonstrate the effectiveness of the suggested scheme.

10.1 Introduction

Although a lot of practical engineering applications involves concepts of partial differential equations (PDEs) [Krstic & Smyshlyaev, 2008], the consensus problem for this class of system or more generally for infinite dimensional system has not yet received the same level of attention with respect to its finite-dimensional counterpart [Demetriou, 2013]. Some recent, but precursors works in this area are listed here [Chao et al., 2007, Tricaud & Chen, 2009, Demetriou, 2010, Demetriou, 2009]. These works treat different aspects of consensus in the framework of PDEs. With regards to the existing literature in this area, Demetriou has extensively studied the problem of designing adaptive consensus filters for state estimation in order to integrate local information coming from a spatial domain [Demetriou, 2009, Demetriou, 2010, Demetriou, 2012]. Whereas in [Chao et al., 2007, Tricaud & Chen, 2009] applications of consensus for controlling mobile actuators in diffusion processes are discussed.

The aims of the present Chapter is to consider the problem of synchronization or consensus of the states of systems governed by a class of parabolic PDEs. In particular, the problem of driving the states of a group of perturbed infinite-dimensional agents communicating through an undirected topology towards a common consensus value is considered.

In literature, one of the first attempts to tackle this problem is presented in [Bliman & Ferrari-Trecate, 2008], where starting from the classical finite-dimensional consensus theory [Olfati-Saber & Murray, 2004], the authors provide conditions for achieving average consensus in the framework of delayed MAS and partial difference equations. Afterwards in [Galbusera et al., 2007] a control scheme based on the wave equation for consensus in MAS with double integrator dynamics is presented. More recently, a similar statement to the one here discussed can be found in [Demetriou, 2013], where the consensus problem for a network of agents modeled by parabolic PDEs communicating by an undirected communication topology is treated.

Nevertheless, all these works propose protocols in which the control action acts in the whole spatial domain of each agent, but it is commonly considered to be more realistic to have actuation and sensing nonintrusive (think, for example, of a fluid flow where actuation would normally be from the walls of the flow domain) [Krstic & Smyshlyaev, 2008, Pisano & Orlov, 2012].

Therefore, in this Chapter the communication policy limited only at the boundary of the agents has been considered. This means that agents can exchange information acquired only at the boundary of their domain. For this reasons, the proposed consensus algorithm can be considered as a *boundary cooperative protocol* [Krstic & Smyshlyaev, 2008].

Furthermore, in order to consider a more realistic scenario, each agent is modeled as 1D rod, described by the well-known heat diffusion equation perturbed by some unknown disturbances. The class of perturbations here considered only assume them, to be bounded in derivative and acting at the boundary of each rod too.

The major contribution of this work is to enforce a robust asymptotic agreement amongst the agent's states and thus the nullification of their disagreement, only sharing information captured at the boundary of each rod and even in presence of perturbation or sensing disturbances.

The complete rejection of such a wide class of perturbation was firstly discussed in [Pisano & Orlov, 2012] for classic local boundary control but was never achieved in the framework of infinite-dimensional MAS. The protocol that will be discussed later extends the results obtained by the authors in [Pilloni et al., 2013b] in the finite-dimensional MAS framework. A further novelty with respect to [Pilloni et al., 2013b], is that this protocol is born to be discontinuous, but by augmenting the system state with its derivative and applying it to the augmented dynamic it result to be continuous. In other words, the discontinuous protocol passing through a first-order dynamical filter is smoothed-out, which implies a lot of benefits but the most important is the attenuation of the possible undesired phenomenon known as *chattering*, common in discontinuous control theory (see [Boiko et al., 2008, Pilloni et al., 2012a] and references therein).

The Chapter is organized as follows: in Section 10.2 some useful norm's properties are reminded to provide the reader with necessary context and background. The problem statement and the proposed boundary consensus protocol are presented in Section 10.3. Section 10.4 discusses the performances of the proposed algorithm in terms of robustness and rate of convergence by a Lyapunov-Based approach from which simple tuning rules for achieving the consensus condition are provided. To corroborate the theoretical results, simulation results are shown in Section 10.5. Conclusion and hints for further investigation in

Section 10.6 close the Chapter.

10.2 Mathematical Preliminaries and Notations

10.2.1 Useful Norm Properties

With reference to real spaces, let $\mathbf{x} = \text{col}(x_1, \dots, x_N)$ be a column vector in \mathbb{R}^N , the L^p -norm and the L^∞ -norm of \mathbf{x} are defined respectively as

$$\|\mathbf{x}\|_p = (|x_1|^p + \dots + |x_N|^p)^{1/p}, \quad p = 1, 2, \dots \quad (10.1)$$

$$\|\mathbf{x}\|_\infty = \lim_{p \rightarrow \infty} \|\mathbf{x}\|_p = \max\{|x_1|, \dots, |x_N|\} \quad (10.2)$$

Let's considering L^1 -, L^2 - and L^∞ -norm of any given vector \mathbf{x} , the following inequality is always satisfied [Khalil, 2002]:

$$\|\mathbf{x}\|_\infty \leq \|\mathbf{x}\|_2 \leq \|\mathbf{x}\|_1 \quad (10.3)$$

Useful inequalities concerning the scalar product of two vectors \mathbf{x} and $\mathbf{y} \in \mathbb{R}^N$ are, respectively, the Hölder's Inequality

$$|\mathbf{x}^T \cdot \mathbf{y}| \leq \|\mathbf{x}\|_p \cdot \|\mathbf{y}\|_q, \quad \frac{1}{p} + \frac{1}{q} = 1 \quad (10.4)$$

and straight from the Young's Inequality

$$|\mathbf{x}^T \cdot \mathbf{y}| \leq \frac{\|\mathbf{x}\|_p^p}{p} + \frac{\|\mathbf{y}\|_q^q}{q}, \quad \frac{1}{p} + \frac{1}{q} = 1 \quad (10.5)$$

With reference to norms of regular quadratic forms, let $\mathbf{M} \in \mathbb{R}^{N \times N}$ be a symmetric positive semi-definite matrix with ordered eigenvalues $\gamma_1 \leq \dots \leq \gamma_N$, it yields:

$$\gamma_1 \|\mathbf{x}\|_2^2 \leq \mathbf{x}^T \mathbf{M} \mathbf{x} \leq \gamma_N \|\mathbf{x}\|_2^2 \quad (10.6)$$

In the end, let $H^l(0, 1)$, with $l = 0, 1, 2, \dots$, be the Sobolev Space of absolutely continuous scalar functions $z_i(\zeta)$ with square integrable derivatives $z_i^{(k)}(\zeta)$ up to order l , it can be now presented the extension of the concept of norm for vectors $\mathbf{z}(\zeta) = \text{col}(z_1(\zeta), \dots, z_N(\zeta))$ of infinite dimensional functions as follows:

$$\|\mathbf{z}(\cdot)\|_l = \left(\int_0^1 \sum_{k=0}^l \|\mathbf{z}^{(k)}(\xi)\|_2^2 d\xi \right)^{\frac{1}{2}} \quad (10.7)$$

where $\|\mathbf{z}^{(k)}(\xi)\|_2 = (\int_0^1 \mathbf{z}^{(k)}(\mu)^T \cdot \mathbf{z}^{(k)}(\mu) d\mu)^{\frac{1}{2}}$ is the L^2 -norm of the k -th derivative of $\mathbf{z}(\xi)$. Throughout the Chapter it shall also utilize the standard notation $H^0(0, 1) = L^2(0, 1)$. Lastly, generalizing Lemma 1 in [Pisano & Orlov, 2012] for vectors of infinite dimensional functions the following result yields:

Lemma 10.1. *Let $w(\zeta) \in H^1(0,1)$ and $w_\zeta(\zeta)$ its derivative with respect to ζ , then the following upper-estimation holds:*

$$\|w(\cdot)\|_0^2 \leq 2(\|w(\tau)\|_2^2 + \|w_\zeta(\cdot)\|_0^2) \quad \text{with } \tau = 0,1 \quad (10.8)$$

■

10.3 Problem Statements

Let us to consider a connected network of N agents. Each agent's is modeled by a thermally conducting rod spatially distributed on mono-dimensional (1D) domain and whose temperature fields $Q^i(\zeta, t)$ with $i = 1, \dots, N$, are functions of the normalized spatial variable $\zeta \in (0, 1)$ and time $t \in \mathbb{R}^+$.

The evolution of the agent's temperature profile is governed by the parabolic PDE commonly referred to as "Heat Equation":

$$Q_t^i(\zeta, t) = \theta \cdot Q_{\zeta\zeta}^i(\zeta, t) \quad i \in \mathcal{V} \quad (10.9)$$

where $Q_t^i(\zeta, t)$ and $Q_{\zeta\zeta}^i(\zeta, t)$ denote the temporal and the second-order spatial derivatives, and θ refers to the "diffusivity coefficient" supposed to be identical $\forall i$ but unknown a priori.

Here, the realistic scenario that each agent "i" is supposed to be perturbed at the boundary by a sufficiently smooth thermal unknown input $\psi^i(t)$, and controlled by a matched boundary control $u^i(t)$ is investigated [Pisano & Orlov, 2012, Krstic & Smyshlyaev, 2008]. It follows that the following Neumann-type boundary conditions (BCs) are considered:

$$Q_\zeta^i(0, t) = 0 \quad , \quad Q_\zeta^i(1, t) = u^i(t) + \psi^i(t) \quad (10.10)$$

Whereas the initial conditions (ICs) are

$$Q^i(\zeta, 0) \in H^4(0, 1) \quad (10.11)$$

The class of boundary conditions under analysis are specified by the next assumption.

Assumption 10.1. *The initial temperatures $Q^i(\zeta, 0)$ in (10.11) are consistent to the next perturbed heat fluxes:*

$$Q_\zeta^i(0, 0) = 0 \quad , \quad Q_\zeta^i(1, 0) = \psi^i(0) \quad \forall i \in \mathcal{V} \quad (10.12)$$

where the disturbance, supposed to be unknown, are once continuously differentiable $\psi^i(t) \in \mathcal{C}^1(\mathbb{R})$, and there exist an a priori known positive constant Π such that

$$|\psi_t^i(t)| = |\dot{\psi}^i(t)| \leq \Pi \quad \text{with} \quad \Pi = \max_{i \in \mathcal{V}} \Pi_i < \infty \quad (10.13)$$

■

Remark 10.1. *It is worth mentioning that at the boundary $\zeta = 1$, constraints (10.10) and (10.12) implies that $u^i(0) = 0$. Furthermore, by Assumption 10.1, the stability of the each agent's heat dynamics are studied in a proper Sobolev Space denoted as $H^2(0, 1)$. As a consequence, the domain of the infinitesimal operator $\partial^2 / \partial \zeta^2$ in the boundary problem (10.9)-(10.11) is confined into a Sobolev Space $H^4(0, 1)$.* ■

The objective of the present work is to present a novel continuous local interaction rule for achieving global asymptotic temperature synchronization in a network of thermal spatially distributed process. More formally, the problem statement can be represented by the following consensus condition [Olfati-Saber et al., 2007]

$$\lim_{t \rightarrow \infty} |Q^i(\zeta, t) - Q^j(\zeta, t)| = 0, \quad \forall i, j \in \mathcal{V} \quad (10.14)$$

It is worth to note that the proposed interaction rule can be assimilated to a boundary control [Krstic & Smyshlyaev, 2008] such that temperatures along the entire rod's profiles being actuated to steer towards a common temperature profile enforced by the network topology even in presence of heterogeneous sufficiently smooth perturbation at the boundary.

To achieve the control goal, the agents' state is augmented through a *dynamic input extension* by inserting an integrator at the agent input $u^i(t)$. It follows that the control derivative $u_t^i(t) = \dot{u}^i(t)$ is then regarded to as a fictitious control variable returned by suitable feedback mechanism. Thus, the following boundary interaction protocol is suggested

$$\dot{u}^i(t) = \dot{u}_1^i(t) + \dot{u}_2^i(t) + \dot{u}_3^i(t), \quad i \in \mathcal{V} \quad (10.15)$$

with

$$\dot{u}_1^i(t) = -a \cdot \text{sign}(\mathcal{L}^i Q(1, t)) - b \cdot \text{sign}(\mathcal{L}^i Q_t(1, t)) \quad (10.16)$$

$$\dot{u}_2^i(t) = -W_1 \cdot \mathcal{L}^i Q(1, t) - W_2 \cdot \mathcal{L}^i Q_t(1, t) \quad (10.17)$$

$$\dot{u}_3^i(t) = -W_3 \cdot Q_t(1, t) \quad (10.18)$$

where a , b , W_1 , W_2 and W_3 are nonnegative tuning constants, the $\text{sign}(\cdot)$ stands for the multi-valued function such that

$$\text{sign}(\mathfrak{S}) = \begin{cases} 1 & \text{if } \mathfrak{S} > 0 \\ [-1, 1] & \text{if } \mathfrak{S} = 0 \\ -1 & \text{if } \mathfrak{S} < 0 \end{cases} \quad (10.19)$$

Whereas \mathcal{L}^i is the i -th row of the Laplacian Matrix and $Q(\zeta, t) \in H^4(0, 1) \times \mathbb{R}^N$ and its time-derivative $Q_t(\zeta, t)$ are vector-valued function, which stack together, respectively, the temperature and the heat flux of each rod

$$Q(\zeta, t) = \text{col}\left(Q^1(\zeta, t), \dots, Q^N(\zeta, t)\right) \quad (10.20)$$

$$Q_t(\zeta, t) = \text{col}\left(Q_t^1(\zeta, t), \dots, Q_t^N(\zeta, t)\right) \quad (10.21)$$

For completeness, according to (9.1), an explicit representation of the sign's arguments are [Pilloni et al., 2013b]:

$$\mathcal{L}^i Q(1, t) = \sum_{j \in \mathcal{N}_i^-} (Q^i(1, t) - Q^j(1, t)), \quad i \in \mathcal{V} \quad (10.22)$$

$$\mathcal{L}^i Q_t(1, t) = \sum_{j \in \mathcal{N}_i^-} (Q_t^i(1, t) - Q_t^j(1, t)), \quad i \in \mathcal{V} \quad (10.23)$$

The proposed boundary dynamic protocol (10.15) is composed by three components. The contribution (10.16) can be thought as a distributed version of the ‘‘Twisting’’ HOSM algorithm [Levant, 1993a], where a non-trivial function of the boundary neighbors states (at $\zeta = 1$) is used as sliding manifold (10.23) (see i.e. [Pilloni et al., 2013b]), and two linear parts, (10.17), being a PD-based consensus algorithm [Franceschelli et al., 2013b], and lastly (10.18) which has the only role to filter and then keep bounded the control input $u^i(t)$. Infact, differentiating (10.10) and substituting (10.18), at the boundary of each rod it yields:

$$\dot{Q}_t^i(1,t) + W_3 \cdot Q_t^i(1,t) = \dot{u}_1^i(t) + \dot{u}_2^i(t) + \dot{\Psi}^i(t) \quad \forall i \in \mathcal{V} \quad (10.24)$$

Remark 10.2. *Note that, despite state derivative is normally not permitted in the synthesis task (i.e. it generally induces algebraic loops), its use becomes acceptable when dynamic input extension is performed. Similar analysis is discussed in [Pisano & Orlov, 2012]. As a consequence, this statement can be viewed as a second-order consensus problem [Pilloni et al., 2013b]. In the following, it will be shown that the temperature’s consensus (10.14) will be achieved asymptotically in terms of both agent’s temperature $Q(\zeta,t)$ and its time-derivative, which physically corresponds to the heat fluxes $Q_t(\zeta,t)$.* ■

Remark 10.3. *Since at the boundary $\zeta = 1$, the proposed dynamic control input is governed by the ODE (10.24) with discontinuous right-hand side, the solution of the resulting distributed parameter agent’s dynamic will be understood, in the so-called Filippov Sense [Filippov,]. Extensions of the Filippov concepts towards infinite dimensional setting can be found in [Levaggi, 2002, Orlov, 2008], where as in the finite-dimensional scenario, a motion along discontinuity manifolds, is referred to as Sliding Mode. It is worth to note that the existence of a solution for the class of equations under analysis is always guaranteed (owing on certain properties of the associated set-valued map) and from which noticeable properties, such as absolute continuity, are in force. The reader is referred to [Cortes, 2008] for a comprehensive account of the notions of solution for discontinuous dynamical systems.* ■

The present work focuses on the solution of the consensus problem (10.14) for a network of infinite-dimensional agents, whereas the rigorous demonstration of the well-posedness of the network dynamic (10.9)-(10.11), (10.15)-(10.18) goes beyond the Chapter’s aims. Anyway the well-posedness of the system in question, under the assumption imposed on the ICs and BCs, can be verified in accordance with Theorem 3.3.3. in [Curtain & Zwart, 1995] by the taking into account that the consensus protocol (10.15)-(10.18) is twice piece-wise continuously differentiable along the state trajectories (see e.g. [Pisano & Orlov, 2012]).

Let’s say that, designed the following column wise vectors

$$\dot{\Psi} = \text{col}(\dot{\psi}^1(t), \dots, \dot{\psi}^N) \quad (10.25)$$

$$\sigma(\mathcal{L}Q) = \text{col}(\text{sign}(\mathcal{L}_1 Q), \dots, \text{sign}(\mathcal{L}_N Q)) \quad (10.26)$$

and given the next representation, at the network level, for the vector of fictitious boundary local interaction protocols (10.15)

$$\begin{aligned} \dot{U}(t) &= \text{col}(\dot{u}^1(t), \dots, \dot{u}^N(t)) \\ &= -a \cdot \sigma(\mathcal{L}Q(1,t)) - b \cdot \sigma(\mathcal{L}Q_t(1,t)) + \\ &\quad - W_1 \cdot \mathcal{L}Q(1,t) - W_2 \cdot \mathcal{L}Q_t(1,t) - W_3 \cdot Q_t(1,t) \end{aligned} \quad (10.27)$$

in the reminder, denoted $Q(\cdot, t) = Z_1(\cdot, t)$, and $Q_t(\cdot, t) = Z_2(\cdot, t)$, it is simply assumed the following.

Assumption 10.2. *The networked system (10.9)-(10.11), (10.16)-(10.18) always possesses a unique Filippov solution $Z_1(\cdot, t) \in H^4(0, 1) \times \mathbb{R}^N$ and its time derivative $Z_2(\cdot, t) \in H^2(0, 1) \times \mathbb{R}^N$ verifies the following auxiliary boundary-valued problem:*

$$\begin{aligned} \dot{Z}_1(\zeta, t) &= Z_2(\zeta, t) \\ \dot{Z}_2(\zeta, t) &= \theta \cdot Z_{2,\zeta\zeta}(\zeta, t) \end{aligned} \quad (10.28)$$

$$\text{BCs: } \begin{cases} Z_{2,\zeta}(0, t) = 0_N \\ Z_{2,\zeta}(1, t) = \dot{U}(t) + \dot{\Psi}(t) \end{cases} \quad (10.29)$$

$$\text{ICs: } Z_2(\zeta, 0) = \theta \cdot Q_{\zeta\zeta}(\zeta, 0) \in H^2(0, 1) \times \mathbb{R}^N \quad (10.30)$$

■

Notice that the auxiliary problem (10.28)-(10.30) is obtained by differentiating (10.9)-(10.11) and (10.16)-(10.18) in the time variable, whereas the ICs are straight derived from (10.9) and (10.12).

As discussed in [Pisano & Orlov, 2012], it should be pointed out that the solution's meaning of the auxiliary boundary-value problem (10.28)-(10.30) has to be viewed in the mild sense (see e.g. [Curtain & Zwart, 1995]). Furthermore, from [Butkovskii, 1982], it should be noted that the mild solution of (10.28)-(10.30) coincides to the corresponding weak solution of the so-called standardizing PDE in distributions

$$\begin{aligned} \dot{Z}_1(\zeta, t) &= Z_2(\zeta, t) \\ \dot{Z}_2(\zeta, t) &= \theta \cdot Z_{2,\zeta\zeta} + \theta \cdot (\dot{U}(t) + \dot{\Psi}(t)) \cdot \hat{\delta}(\zeta - 1) \end{aligned} \quad (10.31)$$

subject to the following homogeneous BCs:

$$Z_{2,\zeta}(0, t) = 0_N \quad , \quad Z_{2,\zeta}(1, t) = 0_N \quad (10.32)$$

and to the same ICs in (10.30), where $\hat{\delta}(\zeta - 1)$ is the *Dirac's sampling function* at $\zeta = 1$. It's worth to mentioning that, according to [Pisano & Orlov, 2012], $Z_2(\cdot, t) \in L^2(0, 1) \times \mathbb{R}^N$ is a vector of continuous functions which solves the boundary problem (10.31)-(10.32) on $t \in [0, \tau) \in \mathbb{R}^+$ in the weak sense (see Definition 1 in [Pisano & Orlov, 2012] for further details).

10.4 Convergence Analysis

In this Section the performance of the proposed consensus protocol (10.15)-(10.18) are investigate by means of Lyapunov-Based Analysis, from which simple tuning rules for the control gains will be straightforward derived. Referring to Remark 1, this statement can be viewed as a second order consensus problem [Cao & Ren, 2012, Piloni et al., 2013b].

As it is well-known in standard consensus theory [Olfati-Saber et al., 2007], the achievement of the consensus condition (10.14) simply implies the annihilation of the so-called

disagreement vector (see e.g [Pilloni et al., 2013b]). Extending those concepts to infinite-dimensional multi-agent systems, it can be straight derived the following definition for the *infinite-dimensional disagreement vectors*:

$$\delta_k(\cdot, t) = \left(\mathcal{I}_{N \times N} - \frac{\mathbf{1}_N \cdot \mathbf{1}_N^T}{N} \right) \cdot Z_k(\cdot, t) = \mathcal{L}_c \cdot Z_k(\cdot, t) \quad (10.33)$$

which obviously still preserve their own properties [Olfati-Saber et al., 2007]

$$\mathbf{1}_N^T \cdot \delta_k(\cdot, t) = 0, \quad \mathcal{L} \cdot \delta_k(\cdot, t) = \mathcal{L} \cdot Z_k(\cdot, t), \quad k = 1, 2 \quad (10.34)$$

and following from (9.3), it even yields:

$$\int_0^1 \delta_k^T(\zeta, t) \mathcal{L} \delta_k(\zeta, t) d\zeta \geq \lambda_2 \cdot \|\delta_k(\cdot, t)\|_0^2, \quad k = 1, 2 \quad (10.35)$$

In the remainder of the Chapter, it will be demonstrated the achieving of the consensus condition (10.14) even in presence of disturbances acting at the boundary of each rod, showing the exponential convergence to zero in the space $H^2(0, 1) \times \mathbb{R}^N$ of the disagreement vector dynamic. To do this, manipulating the boundary problem (10.31)-(10.32) according to (10.33), derives the following *disagreement vector boundary-problem*:

$$\begin{aligned} \dot{\delta}_1(\zeta, t) &= \delta_2(\zeta, t) \\ \dot{\delta}_2(\zeta, t) &= \theta \cdot \delta_{2,\zeta\zeta}(\zeta, t) + \theta \mathcal{L}_c [\dot{U} + \dot{\Psi}] \cdot \hat{\delta}(\zeta - 1) \end{aligned} \quad (10.36)$$

$$\text{BCs: } \begin{cases} \delta_{1,\zeta}(0, t) = \delta_{2,\zeta}(0, t) = 0 \\ \delta_{1,\zeta}(1, t) = \delta_{2,\zeta}(1, t) = 0 \end{cases} \quad (10.37)$$

$$\text{ICs: } \delta_2(\zeta, 0) = \theta \cdot \mathcal{L}_c Z_2(\zeta, 0) \in H^2(0, 1) \times \mathbb{R}^N \quad (10.38)$$

Theorem 10.1. Consider the perturbed collective infinite-dimensional multi-agents system (10.9)-(10.11) and let Assumption 10.1 and 10.2 be satisfied, with the boundary local interaction protocol (10.15)-(10.18) applied and tuning parameters selected according to

$$a > b + \Pi, \quad b > \Pi, \quad W_1 > 0, \quad W_2 > 0, \quad W_3 > 0 \quad (10.39)$$

then, the consensus condition (10.14) is globally asymptotically achieved in the space $H^2(0, 1)$. ■

Proof of Theorem 1: The proof has been broken into two simple consecutive steps.

▷ Equi-uniform stability

Consider as candidate Lyapunov function the following positive definite functional

$$\begin{aligned} V(\delta_1, \delta_2) &= \theta a \cdot \|\mathcal{L} \delta_1(1, t)\|_1 + \frac{1}{2} \theta W_1 \cdot \|\mathcal{L} \delta_1(1, t)\|_2^2 + \\ &+ \frac{1}{2} \int_0^1 \delta_2(\zeta, t)^T \mathcal{L} \delta_2(\zeta, t) d\zeta \end{aligned} \quad (10.40)$$

computed on the solutions $\delta_1(\cdot, t)$ of the boundary-valued problem (10.36)-(10.38)

Since (10.40) is locally Lipschitz and not differentiable at $\zeta = 1$ when any entry vector $\mathcal{L}\delta_1(1, t)$ is zero then, as mentioned in Remark 10.3, the following treatment refers for stability analysis to the Lyapunov Generalized Theorem for non-smooth analysis reported in [Paden & Sastry, 1987], which makes use of Clarke's Generalized Gradient [Clarke, 1983] and involves a set-valued form for the resulting Lyapunov function time derivative. A similar analysis to the one here presented, involving a sum-of-absolute-value Lyapunov function, can be found in [Paden & Sastry, 1987]. The reader is referred to [Paden & Sastry, 1987, Clarke, 1983, Shevitz & Paden, 1994] for a more detailed analysis of the correctness of adopting the chain rule to compute the time-derivative of $V(t)$ for non-smooth Lyapunov analysis.

By (10.34) it results that $\mathcal{L} \cdot \mathcal{L}c = \mathcal{L}$, then the time derivative of (10.40) on the solution of the boundary problem (10.36)-(10.38) is

$$\begin{aligned} \dot{V}(t) &= \theta a \delta_2(1, t)^T \mathcal{L} \sigma(\mathcal{L} \delta_1(1, t)) + \theta W_1 \delta_2(1, t)^T \mathcal{L}^2 \delta_1(1, t) + \\ &\quad + \int_0^1 \delta_2(\zeta, t)^T \mathcal{L} \delta_{2,t}(\zeta, t) d\zeta = \\ &= \theta a \delta_1(2, t)^T \mathcal{L} \sigma(\mathcal{L} \delta_1(1, t)) + \theta W_1 \delta_2(1, t)^T \mathcal{L}^2 \delta_1(1, t) + \\ &\quad + \theta \int_0^1 \delta_2(\zeta, t)^T \mathcal{L} \delta_{2,\zeta\zeta}(1, t) d\zeta + \\ &\quad + \theta \delta_2(1, t)^T \mathcal{L} [\dot{U} + \dot{\Psi}(t)] \end{aligned} \quad (10.41)$$

where the integral term in the right hand side of (10.41) can be integrated by parts under the homogeneous BCs (10.37) and upper estimated as follows:

$$\begin{aligned} &\int_0^1 \delta_2(\zeta, t)^T \mathcal{L} \theta \delta_{2,\zeta\zeta}(\zeta, t) d\zeta = \\ &= \theta [\delta_2(1, t)^T \mathcal{L} \delta_{2,\zeta}(1, t) - \delta_2(0, t)^T \mathcal{L} \delta_{2,\zeta}(0, t)] + \\ &\quad - \theta \int_0^1 \delta_{2,\zeta}(\zeta, t)^T \mathcal{L} \delta_{2,\zeta}(\zeta, t) d\zeta \leq \\ &\leq -\theta \lambda_2 \int_0^1 \delta_{2,\zeta}(\zeta, t)^T \delta_{2,\zeta}(\zeta, t) d\zeta = -\theta \lambda_2 \|\delta_{2,\zeta}(\cdot, t)\|_2^2 \end{aligned} \quad (10.42)$$

Then, replacing the closed-loop controller (10.27) into the latter term of (10.41), it yields

$$\begin{aligned} \theta \cdot \delta_2(1, t)^T \mathcal{L} [\dot{U} + \dot{\Psi}(t)] &= -\theta a \cdot \delta_2(\zeta, t)^T \mathcal{L} \sigma(\mathcal{L} \delta_1(1, t)) + \\ &\quad - \theta b \cdot \|\mathcal{L} \delta_2(1, t)\|_1 - \theta W_1 \cdot \delta_2(1, t)^T \mathcal{L}^2 \delta_1(1, t) + \\ &\quad - \theta W_2 \cdot \|\mathcal{L} \delta_2(1, t)\|_2^2 - \theta W_3 \cdot \delta_2(1, t)^T \mathcal{L} \delta_2(1, t) + \\ &\quad + \theta \cdot \delta_2(\zeta, t)^T \mathcal{L} \dot{\Psi}(t) \end{aligned} \quad (10.43)$$

Substituting (10.42) and (10.43) into (10.41) and invoking the Hölder's Inequality (10.4) combined with (9.3), it can be demonstrated the boundedness of the solution of the perturbed *infinite-dimensional disagreement vector* boundary-valued problem (10.36)-(10.38)

as follows:

$$\begin{aligned} \dot{V}(t) \leq & -\theta \cdot (b - \|\dot{\Psi}(t)\|_\infty) \cdot \|\mathcal{L}\delta_2(1, t)\|_1 + \\ & -\theta\lambda_2 \cdot \|\delta_{2,\zeta}(\cdot, t)\|_0^2 - \theta W_2 \lambda_2^2 \cdot \|\delta_2(1, t)\|_2^2 + \\ & -\theta W_3 \lambda_2 \cdot \|\delta_2(1, t)\|_2^2 \end{aligned} \quad (10.44)$$

where gains b , W_2 and W_3 must be selected according to the next constraints:

$$b \geq \|\dot{\Psi}\|_\infty = \Pi \quad , \quad W_2 \geq 0 \quad , \quad W_3 \geq 0 \quad (10.45)$$

From (10.44) it has been shown that, initializing the system in an arbitrarily vicinity of the origin $V(\zeta, 0) \leq R_0$, the uncertain system (10.36)-(10.38) cannot leave this vicinity, regardless of whichever admissible uncertainty $\dot{\Psi}(t)$ affects the network.

▷ Global equi-uniform asymptotic stability

To begin with, as discussed in [Pisano & Orlov, 2012] for infinite dimensional systems, let us note that by virtue of (10.44) all possible solutions of the disagreement vector boundary-problem (10.36)-(10.38), initialized at $t_0 \in \mathbb{R}^+$ within the invariant compact set

$$\begin{aligned} \mathcal{D}_R^V = \{ & (\delta_1(\zeta, t), \delta_2(\zeta, t)) \in H(0, 1) \times L^2(0, 1) \times \mathbb{R}^N : \\ & V(\delta_1, \delta_2) \leq R \} \end{aligned} \quad (10.46)$$

there always remain confined

$$\sup_{t \in [t_0, \infty]} V(\delta_1, \delta_2) \leq R \quad (10.47)$$

By (10.40) combined with (10.47) and (9.3), the following upper-bounds can be easily derived:

$$\|\mathcal{L}\delta_1(1, t)\|_1 \leq R/\theta a \quad (10.48)$$

$$\|\delta_1(1, t)\|_2^2 \leq 2R/\theta W_1 \lambda_2 \quad (10.49)$$

$$\|\delta_2(\cdot, t)\|_0^2 \leq 2R/\lambda_2 \quad (10.50)$$

Remark 10.4. *The idea behind the remainder of the proof is inspired by the Extended Invariance Principle [Orlov, 2008] and it is based on constructing a parameterized family of local Lyapunov function $V_R(\delta_1, \delta_2)$, $R > 0$ such that, each $V_R(\delta_1, \delta_2)$ is well posed on the corresponding compact set \mathcal{D}_R^V and its time derivative, initialized within \mathcal{D}_R^V , is negative definite and yields the desired stability and convergence properties. ■*

A parameterized Lyapunov function $V_R(\delta_1, \delta_2)$, $R > 0$ with the properties above, can be obtained by augmenting the Lyapunov function (10.40) as follows:

$$V_R(t) = V(t) + \kappa_R \cdot \bar{V}(t) \quad (10.51)$$

where $\bar{V}(t)$ is a sign-indefinite function defined below

$$\bar{V}(t) = \frac{1}{2} \theta W_2 \cdot \|\mathcal{L}\delta_1(1, t)\|_2^2 + \int_0^1 \delta_1(1, t)^T \mathcal{L}\delta_2(\zeta, t) d\zeta \quad (10.52)$$

and κ_R is a proper small enough positive constant.

In order to demonstrate the positive definitiveness of the functional (10.51), the lower estimation of $\bar{V}(t)$ is first computed. By the generalization for vectors of the Young's Inequality in (10.5), along with (10.48), it simply results that the integral term in (10.52) can be lower bounded as follows

$$\begin{aligned} \int_0^1 \delta_1(1,t)^T \mathcal{L} \delta_2(\zeta,t) d\zeta &\geq -\frac{1}{2} (\|\mathcal{L} \delta_1(1,t)\|_2^2 + \|\delta_2(\cdot,t)\|_0^2) \geq \\ &\geq -\frac{1}{2} \left(\frac{R}{\theta a} \cdot \|\mathcal{L} \delta_1(1,t)\|_1 + \|\delta_2(\cdot,t)\|_0^2 \right) \end{aligned} \quad (10.53)$$

whereas by the Laplacian's property in (9.3), the lower bound of the second term of (10.52) is

$$\frac{1}{2} \theta W_2 \cdot \|\mathcal{L} \delta_1(1,t)\|_2^2 \geq \frac{1}{2} \theta W_2 \lambda_2^2 \cdot \|\delta_1(1,t)\|_2^2 \quad (10.54)$$

Therefore, combining results (10.53) and (10.54), along with the lower estimation of $V(t)$, which can be easily computed by analogous considerations, the positive definitiveness of $V_R(t)$ is guaranteed if and only if the positive constant κ_R satisfies the following constraint:

$$\kappa_R \leq \min \left\{ \frac{2\theta^2 a^2}{R}, \lambda_2 \right\} \quad (10.55)$$

To confirm what has been already said, hereinafter the complete lower estimation of the augmented function (10.51) is reported:

$$\begin{aligned} V_R(t) &\geq \left[\theta a - \frac{\kappa_R R}{2\theta a} \right] \cdot \|\mathcal{L} \delta_1(1,t)\|_1 + \\ &\quad + \frac{1}{2} (\lambda_2 - \kappa_R) \cdot \|\delta_2(\cdot,t)\|_0^2 + \\ &\quad + \frac{1}{2} \theta \lambda_2^2 (W_1 + \kappa_R W_2) \cdot \|\delta_1(1,t)\|_2^2 \end{aligned} \quad (10.56)$$

where the restriction (10.55) confirms the positiveness of $V_R(t)$.

In turns, reminding that $\mathcal{L} \cdot \mathcal{L} = \mathcal{L}$ and differentiating (10.51) along the trajectories of the uncertain boundary-problem (10.36)-(10.38), it results:

$$\begin{aligned} \dot{V}_R(t) &= \dot{V}(t) + \kappa_R \theta W_2 \cdot \delta_2(1,t) \mathcal{L}^2 \delta_1(1,t) + \\ &\quad + \kappa_R \cdot \frac{d}{dt} \left\{ \int_0^1 \delta_1(1,t)^T \mathcal{L} \delta_2(\zeta,t) d\zeta \right\} = \\ &= \dot{V}(t) + \kappa_R \cdot \theta W_2 \delta_2(1,t) \mathcal{L}^2 \delta_1(1,t) + \\ &\quad + \kappa_R \cdot \int_0^1 \theta \delta_1(1,t)^T \mathcal{L} \delta_{2,\zeta\zeta}(\zeta,t) d\zeta + \\ &\quad + \kappa_R \cdot \int_0^1 \theta \delta_1(1,t)^T \mathcal{L} [\dot{U}(t) + \dot{\Psi}(t)] \delta(\zeta-1) d\zeta + \\ &\quad + \kappa_R \cdot \int_0^1 \delta_2(1,t)^T \mathcal{L} \delta_2(\zeta,t) d\zeta \end{aligned} \quad (10.57)$$

where due to the boundary conditions (10.37), the first integral in (10.57) has not contribution

$$\begin{aligned} & \int_0^1 \delta_1(1,t)^T \mathcal{L} \delta_{2,\zeta\zeta}(\zeta,t) d\zeta = \\ & = \delta_1(1,t) \mathcal{L} \cdot (\delta_{2,\zeta}(1,t) - \delta_{2,\zeta}(0,t)) = 0 \end{aligned} \quad (10.58)$$

Substituting (10.27) in the second integral term of (10.57), it can be compute its upper-estimation as follows:

$$\begin{aligned} & \theta \cdot \int_0^1 \delta_1(1,t)^T \mathcal{L} [\dot{U}(t) + \dot{\Psi}(t)] \delta(\zeta - 1) d\zeta = \\ & = \theta \cdot \delta_1(1,t)^T \mathcal{L} [\dot{U}(t) + \dot{\Psi}(t)] = \\ & = -\theta a \cdot \|\mathcal{L} \delta_1(1,t)\|_1 - \theta b \cdot \delta_1(1,t) \mathcal{L} \sigma(\mathcal{L} \delta_2(1,t)) + \\ & \quad - \theta W_1 \cdot \|\mathcal{L} \delta_1(1,t)\|_2^2 - \theta W_2 \cdot \delta_1(1,t)^T \mathcal{L}^2 \delta_2(1,t) + \\ & \quad - \theta W_3 \cdot \delta_1(1,t)^T \mathcal{L} \delta_2(1,t) + \theta \cdot \delta_1(1,t)^T \mathcal{L} \dot{\Psi}(t) \end{aligned} \quad (10.59)$$

Following this line, by the Hölder's Inequality (10.4), also the magnitude of the last integral term in the right-hand side of (10.57) can be upper estimated as follows:

$$\begin{aligned} \left| \int_0^1 \delta_2(1,t)^T \mathcal{L} \delta_2(\zeta,t) d\zeta \right| & \leq \|\mathcal{L} \delta_2(1,t)\|_2 \cdot \|\delta_2(\cdot,t)\|_0 \leq \\ & \leq \|\delta_2(\cdot,t)\|_0 \cdot \|\mathcal{L} \delta_2(1,t)\|_1 \end{aligned} \quad (10.60)$$

where $\|\cdot\|_0$ represents the H^0 -norm defined as in (10.7). Finally by the bounds (10.58)-(10.60), the (10.57) can be upper-estimated as

$$\begin{aligned} \dot{V}_R(t) & \leq \dot{V}(t) - \kappa_R \theta (a - b - \|\dot{\Psi}(t)\|_\infty) \cdot \|\mathcal{L} \delta_1(1,t)\|_1 + \\ & \quad - \kappa_R \theta W_1 \lambda_2^2 \cdot \|\delta_1(1,t)\|_2^2 + \\ & \quad + \kappa_R \theta \cdot \|\delta_2(\cdot,t)\|_0 \|\mathcal{L} \delta_2(1,t)\|_1 + \\ & \quad + \kappa_R \theta W_3 \cdot |\delta_1(1,t)^T \mathcal{L} \delta_2(1,t)| \end{aligned} \quad (10.61)$$

from which, applying (10.4) and (10.49) at the last term of (10.61)

$$\begin{aligned} |\delta_1(1,t)^T \mathcal{L} \delta_2(1,t)| & \leq \|\delta_1(1,t)\|_2 \|\mathcal{L} \delta_2(1,t)\|_2 \leq \\ & \leq \|\delta_1(1,t)\|_2 \|\mathcal{L} \delta_2(1,t)\|_1 \leq \sqrt{\frac{R}{\theta a \lambda_2}} \cdot \|\mathcal{L} \delta_2(1,t)\|_1 \end{aligned} \quad (10.62)$$

and substituting (10.44) and (10.50), it results:

$$\begin{aligned} \dot{V}_R(t) & \leq -\theta \left(b - \|\dot{\Psi}(t)\|_\infty - \kappa_R \sqrt{2R/\lambda_2} \right) \cdot \|\mathcal{L} \delta_2(1,t)\|_1 + \\ & \quad + \kappa_R W_3 \sqrt{R/\theta a \lambda_2} \cdot \|\mathcal{L} \delta_2(1,t)\|_1 + \\ & \quad - \kappa_R \theta (a - b - \|\dot{\Psi}(t)\|_\infty) \cdot \|\mathcal{L} \delta_1(1,t)\|_1 + \\ & \quad - \theta (W_2 \lambda_2^2 + W_3 \lambda_2) \cdot \|\delta_2(1,t)\|_2^2 - \theta \lambda_2 \cdot \|\delta_{2,\zeta}(\cdot,t)\|_0^2 + \\ & \quad - \kappa_R \theta W_1 \lambda_2^2 \cdot \|\delta_1(1,t)\|_2^2 \end{aligned} \quad (10.63)$$

As closure, in light of Lemma 10.1 it is possible to write the next inequality

$$-\alpha_1 \cdot \|\delta_2(1, t)\|_2^2 - \alpha_2 \cdot \|\delta_{2, \zeta}(\cdot, t)\|_2^2 \leq -c_4 \|\delta_2(\cdot, t)\|_0^2 \quad (10.64)$$

with

$$\alpha_1 = \theta(W_2\lambda_2^2 + W_3\lambda_2) \quad , \quad \alpha_2 = \theta\lambda_2 \quad (10.65)$$

from which, by the next upper-estimation the negative definitiveness of $\dot{V}_R(t)$ and then, the convergence towards the consensus condition (10.14) of the agent's temperatures can be demonstrated:

$$\begin{aligned} \dot{V}_R(t) \leq & -c_1 \cdot \|\mathcal{L}\delta_1(1, t)\|_1 - c_2 \cdot \|\mathcal{L}\delta_2(1, t)\|_1 + \\ & -c_3 \cdot \|\delta_1(1, t)\|_2^2 - c_4 \cdot \|\delta_2(\cdot, t)\|_0^2 \end{aligned} \quad (10.66)$$

with coefficients $c_i \in \mathbb{R}^+$ with $i = 1, \dots, 4$ defined as follows

$$c_1 = \kappa_R \theta (a - b - \|\dot{\Psi}\|_\infty) \quad (10.67)$$

$$c_2 = \theta \left(b - \|\dot{\Psi}\|_\infty - \kappa_R \sqrt{2R/\lambda_2} - \kappa_R W_3 \sqrt{R/\theta a \lambda_2} \right) \quad (10.68)$$

$$c_3 = \kappa_R \theta W_1 \lambda_2^2 \quad (10.69)$$

$$c_4 = \min \{ \theta \lambda_2, \theta \lambda_2 (W_2 \lambda_2 + W_3) \} \quad (10.70)$$

tuning parameter selected according to (10.39) and the constant κ_R stricter than

$$\kappa_R = \min \left\{ \frac{2\theta^2 a^2}{R}, \lambda_2, \frac{b - \Pi}{\sqrt{2R\lambda_2} + \sqrt{R/\theta a \lambda_2}} \right\} \quad (10.71)$$

To complete the proof and thus demonstrate the exponential decay of $V_R(t)$ initialized within any invariant set \mathcal{D}_R^V defined as in (10.46), the lower estimation of $V_R(t)$ in (10.56) can be rewritten in the following form

$$\begin{aligned} V_R(t) \geq & \bar{c}_1 \cdot \|\mathcal{L}\delta_1(1, t)\|_1 + \bar{c}_3 \cdot \|\delta_2(1, t)\|_2^2 + \\ & + \bar{c}_4 \cdot \|\delta_2(\cdot, t)\|_0^2 \end{aligned} \quad (10.72)$$

with

$$\bar{c}_1 = \theta a - \kappa_R / 2\theta a \quad (10.73)$$

$$\bar{c}_3 = (\lambda_2 - \kappa_R) / 2 \quad (10.74)$$

$$\bar{c}_4 = \theta (W_1 + \kappa_R W_2) / 2 \quad (10.75)$$

from which, it can be readily derived that

$$\dot{V}_R(t) \leq -\rho_R \cdot V_R(t) \quad \text{with} \quad \rho_R = \frac{\min\{c_1, c_2, c_3, c_4\}}{\min\{\bar{c}_1, \bar{c}_2, \bar{c}_3\}} \quad (10.76)$$

It remains to note that, since $V_R(t) > V(t)$ holds, then the functional $V(t)$ exponentially decays too, which implies the synchronization of the agents' temperatures and so, the achievement of the consensus condition (10.14). The proof of Theorem 10.1 is now completed.

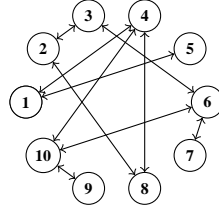


Figure 10.1: Graph representation $\mathcal{G} = (\mathcal{V}, \mathcal{E})$ of the network under test.

10.5 Simulation Results

To demonstrate the efficacy of the proposed consensus protocol (10.15)-(10.18) a connected network of $N = 10$ rods, displayed in Figure 10.1 has been considered. It is worth to note that each agent $i \in \mathcal{V} = \{1, \dots, N\}$, needs to know the temperatures and their time-derivatives, computed at the boundary $\zeta = 1$, just of the agents belonging to its neighbor set $\mathcal{N}_i^- = \{j \in \mathcal{V} / \{i\} : (i, j) \in \mathcal{E}\} \subseteq \mathcal{V}$.

With regard to the agents dynamic, these are governed by the heat equation (10.9), with diffusivity parameter $\theta = 1$ and homogeneous Neumann-type BC's as in (10.10). The uncertain disturbance has been set as

$$\psi^i(t) = \sin(k^i \pi t) \quad \text{with} \quad k^i \in [0, 2] \Rightarrow \Pi = \|\dot{\Psi}(t)\|_\infty = 2\pi$$

whereas the initial conditions at $t = 0$ are set to

$$Q^i(\zeta, 0) = 10 + \bar{k}^i \cdot \cos(4\pi\zeta) \quad \text{with} \quad \bar{k}^i = -4.5 + i$$

For solving the networked boundary-problem (10.9)-(10.11), a standard finite-difference approximation method has been used. Each spatial domain $\zeta \in [0, 1]$ has been discretized into $n = 30$ uniformly spaced nodes. The resulting temporal dynamic of order 300 is then solved by Runge-Kutta 4-th order with fixed step size equal to 10^{-4} .

The consensus protocol's parameters have been selected in accordance with Theorem 10.1 as next:

$$a = 32 \quad , \quad b = 16 \quad , \quad W_1 = W_2 = W_3 = 5$$

The attainment of the temperature's synchronization and then the achievement of the consensus condition (10.14) can be appreciate respectively by Figure 10.2 and Figure 10.3, where the spatiotemporal temperature distribution for the 5-th and 10-th agent are depicted. In confirmation of what has been presented, according with (10.76), in Figure 10.4 and Figure 10.5 is shown the exponential convergence to zero of the temperature *distributed disagreement vector* $\delta_1(\zeta, t)$ which implies the achievement of condition (10.14). More precisely Figure 10.4 shows the spatiotemporal evolution of $\delta_1(\zeta, t) \in L^2(0, 1) \times \mathbb{R}^N$ for the whole spatial distribution, whereas Figure 10.5 shows the temporal evolution of $\delta_1(\zeta, t)$ computed at the boundaries $\zeta = 1$ and $\zeta = 0$ and at the central node (node 15-th) corresponding to $\zeta = 0.4828$.

Overall, the collective network's state evolution behaves as expected in the sense that robust exponential consensus is achieved in spite of the presence of unknown perturbation acting at the boundary of each rod.

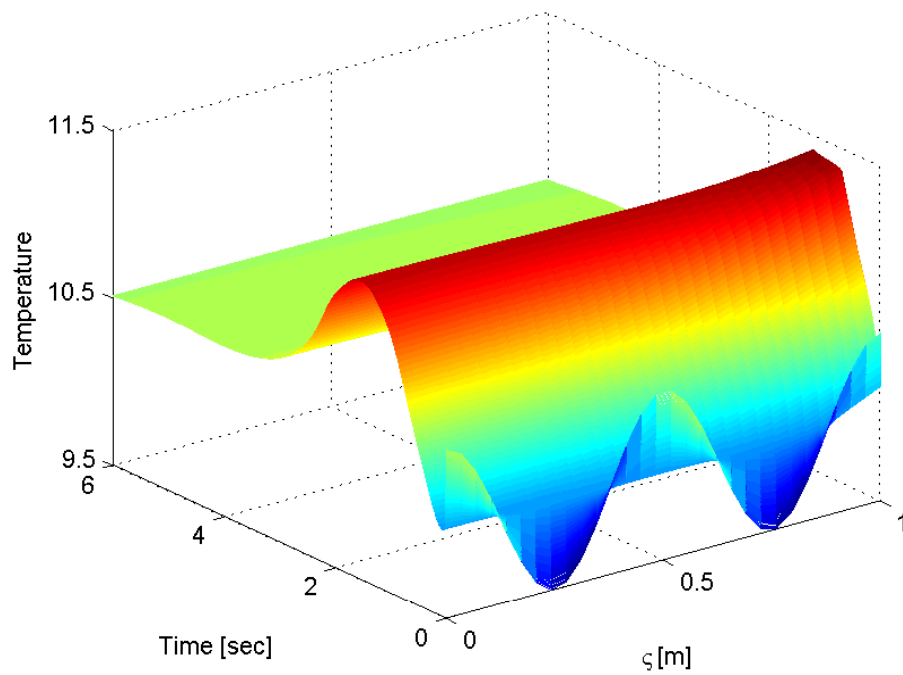


Figure 10.2: Spatial distribution of temperature of the 5-st Rod $Q^5(\zeta, t)$.

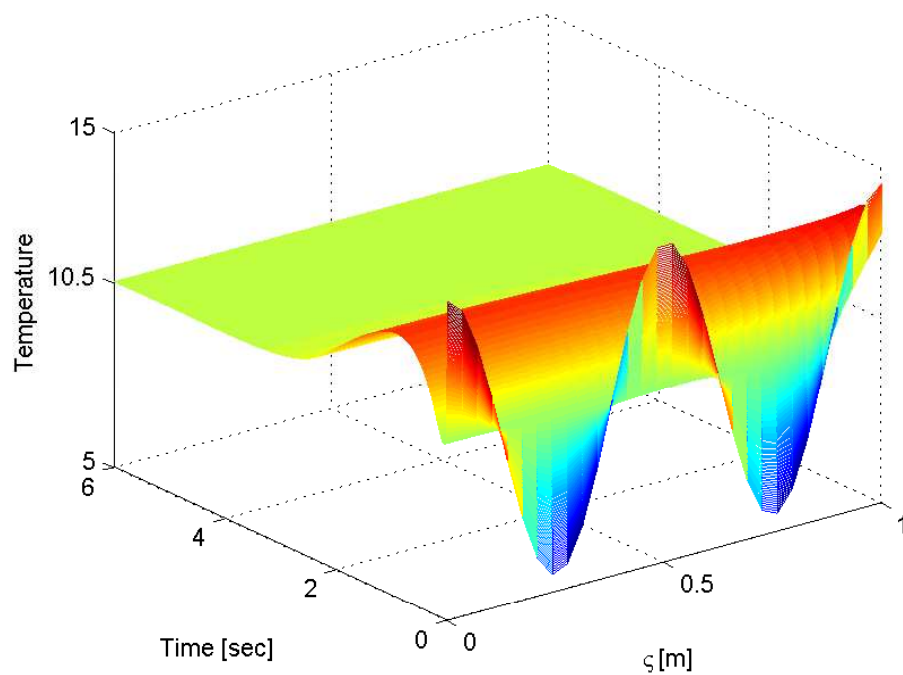


Figure 10.3: Spatial distribution of temperature of the 10-th Rod $Q^{10}(\zeta, t)$.

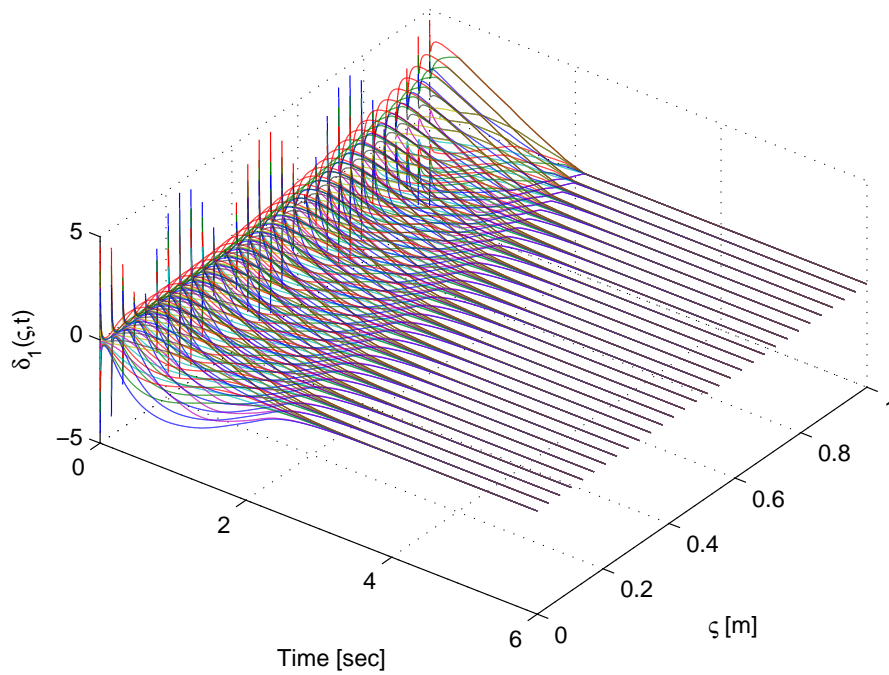


Figure 10.4: Spatial distribution of temperature disagreement vector $\delta_1(\zeta, t)$ computed for all the 30 discretization's nodes.

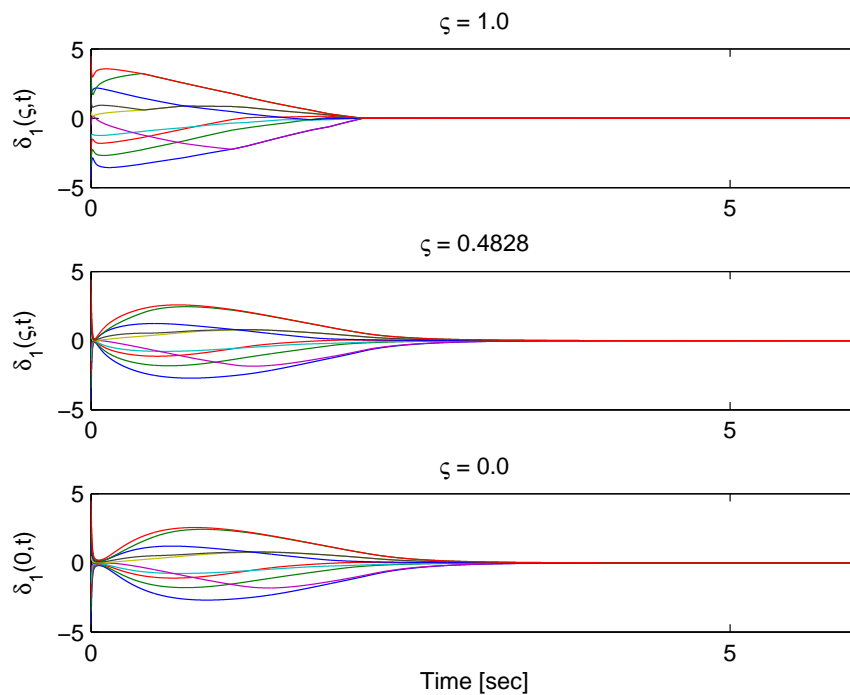


Figure 10.5: Temperature disagreement vector $\delta_1(\zeta, t)$ behavior computed at boundaries $\zeta = 1$, $\zeta = 0$ and in the middle node of the spatial discretization $\zeta = 0.4828$.

10.6 Conclusion

In this Chapter it has been considered the problem of driving a group of perturbed infinite-dimensional agents communicating through an undirected topology towards a com-

mon temperature's consensus value.

The major contribution of this work is to enforce a robust asymptotic agreement amongst the agent's states and thus the nullification of their disagreement, only sharing information captured at the boundary of each rod and even in presence of perturbation or sensing disturbances. Among the most challenging directions for next researches, further investigations focused on relaxing the topological restrictions for directed topologies, possibly switching and the consideration of different classes of PDEs are mandatory.

Chapter 11

Conclusion

In this Thesis several approaches for dealing with the problem of observation and control in both the framework of multi-agents and complex systems have been presented. These techniques, based on concepts of discontinuous sliding-mode and high-order sliding mode control, have been employed for solving, in a finite-time, problems such as robust state estimation, unknown input reconstruction and consensus-based synchronization. Both directed and undirected topologies have been taken into account.

Those algorithms present improvements with respect to the State of the Art in the exploitation of new approaches for dealing with perturbed complex systems. Hereinafter a summary of the main part of the Thesis along with some comments and hints about the potential future research directions for the contribution of each Chapter are discussed below:

- In Chapter 5 it has been theoretically illustrated and experimentally tested a systematic procedure for tuning the parameters of the Super-Twisting Algorithm when unmodeled parasitic dynamics such as sensors or actuators are taken into account in the control loop. It is worth to mention, as discussed in [Ameri & Boiko, 2013], that the treatment here discussed was probably one of the few works in literature which consider this kind of problem. Infact, the vast majority of publications related on STW control loops consider only principal dynamics of relative degree one. Among the some interesting directions for improving the present result, the analysis, and shaping, of the transient oscillations is of special interest;
- In Chapter 6 a new approach for designing decentralized strong observers has been presented. The approach illustrated defines sufficiently conditions for achieving the full state-estimation and unknown-input reconstruction in the framework of MIMO rectangular systems and then designing strong observers. The approach has been easily extend to networks of perturbed, diffusively coupled heterogeneous dynamical systems. Worth of noting that the proposed approach result inherently robust to disturbances and totally independent to the network configuration or to the number of nodes. An extension of this work might be the generalization to generic nonlinear systems;
- In Chapter 7, strictly related to the task of designing strong observers in MIMO systems, HOSM observers are employed as a tool for detecting

certain abnormal operating conditions in squirrel cage induction motors (SCIMs). Major contribution of this work is a novel mathematical characterization of the faulty operating mode in SCIMs and the design of a suitable observer capable of detecting rotor faults such as broken bar faults and eccentricity conditions by relying on stator current and shaft speed measurements. Experiments carried out on commercial motor drives confirm the effectiveness of the proposed approach;

- In Chapter 8 is proposed a novel decentralized consensus algorithm for networks of continuous-time integrators subjected to persistent disturbances and topological changes. This algorithm is superior in the sense that is able to perform the achievement of the approximated consensus condition even in presence of persistent disturbances and not permanently connected communication topologies. It results that under certain restrictions on the directed switching topology, after a finite transient time, the agents achieve consensus condition by attenuating the destabilizing effect of the disturbances. Among the most interesting directions for next research, more general switching communication policy are actually under investigation along with the discrete-time implementation of the proposed interaction rule as well;
- In Chapter 9 a novel robust local interaction rule for achieving finite-time consensus in a network of double integrators agents affected by bounded disturbances is presented. It is worth to mention that in the literature the problem of consensus for second order agents was always treated studying *ideal* double integrators only, whereas here the perturbed case has been solved. Further investigations will focus on relaxing the topological restriction for directed, possibly switching topologies;
- In Chapter 10 it is considered the problem of driving a group of perturbed infinite-dimensional agents communicating through an undirected topology towards a common temperature's consensus value. It is worth to mention that the problem of achieving consensus by exchanging only information acquired at the boundary of the spatial domain was never treated in the literature. Among the most challenging directions for next researches, further investigations focused on relaxing the topological restrictions and the consideration of different classes of PDEs are mandatory.

Bibliography

- [Albert & Barabási, 2000] Albert, R. & Barabási, A.-L. (2000). Topology of evolving networks: local events and universality. *Physical review letters*, 85(24), 5234.
- [Ameri & Boiko, 2013] Ameri, O. A. & Boiko, I. (2013). Analysis of performance of a liquid level process controlled by the super-twisting algorithm. In *Control Conference (ECC), 2013 European* (pp. 3222–3227).: IEEE.
- [Arcak, 2007] Arcak, M. (2007). Passivity as a design tool for group coordination. *IEEE Trans. on Automatic Control*, 52(8), 1380–1390.
- [Astrom & Hagglund, 2005] Astrom, K. J. & Hagglund, T. (2005). Advanced pid control. *ISA-The Instrumentation, Systems, and Automation Society*.
- [Atherton, 1975] Atherton, D. (1975). Nonlinear control engineering-describing function analysis and design. *Workingham Berks, U.K.*
- [Barabási et al., 1999] Barabási, A., Albert, R., & Jeong, H. (1999). Mean-field theory for scale-free random networks. *Physica A: Statistical Mechanics and its Applications*, 272(1), 173–187.
- [Barabási et al., 2002] Barabási, A.-L., Jeong, H., Néda, Z., Ravasz, E., Schubert, A., & Vicsek, T. (2002). Evolution of the social network of scientific collaborations. *Physica A: Statistical Mechanics and its Applications*, 311(3), 590–614.
- [Barnes & Harary, 1983] Barnes, J. A. & Harary, F. (1983). Graph theory in network analysis. *Social Networks*, 5(2), 235–244.
- [Barrat & Weigt, 2000] Barrat, A. & Weigt, M. (2000). On the properties of small-world network models. *The European Physical Journal B-Condensed Matter and Complex Systems*, 13(3), 547–560.
- [Bartolini, 1989] Bartolini, G. (1989). Chattering phenomena in discontinuous control systems. *International journal of systems science*, 20(12), 2471–2481.
- [Bartolini et al., 1999] Bartolini, G., Ferrara, A., Levant, A., & Usai, E. (1999). On second order sliding mode controllers. *Variable structure systems, sliding mode and nonlinear control*, (pp. 329–350).
- [Bartolini et al., 1998a] Bartolini, G., Ferrara, A., & Usai, E. (1998a). Chattering avoidance by second-order sliding mode control. *Automatic control, IEEE Transactions on*, 43(2), 241–246.
- [Bartolini et al., 1998b] Bartolini, G., Ferrara, A., & Usai, E. (1998b). Chattering avoidance by second-order sliding mode control. *Automatic control, IEEE Transactions on*, 43(2), 241–246.
- [Bartolini et al., 2008] Bartolini, G., Fridman, L., Pisano, A., & Usai, E. (2008). *Modern sliding mode control theory: New perspectives and applications*, volume 375. Springer.
- [Bartolini et al., 2002] Bartolini, G., Pilloso, S., Pisano, A., & Usai, E. (2002). Time-optimal stabilization for a third-order integrator: a robust state-feedback implementation. In *Dynamics, Bifurcations, and Control* (pp. 131–144). Springer.
- [Bartolini et al., 2003] Bartolini, G., Pisano, A., Punta, E., & Usai, E. (2003). A survey of applications of second-order slid-

- ing mode control to mechanical systems. *Int. J. of Control*, 76(9-10), 875–892.
- [Bartolini et al., 2007a] Bartolini, G., Pisano, A., & Usai, E. (2007a). On the finite-time stabilization of uncertain nonlinear systems with relative degree three. *Automatic Control, IEEE Transactions on*, 52(11), 2134–2141.
- [Bartolini et al., 2004] Bartolini, G., Punta, E., & Zolezzi, T. (2004). Simplex methods for nonlinear uncertain sliding-mode control. *Automatic Control, IEEE Transactions on*, 49(6), 922–933.
- [Bartolini et al., 2007b] Bartolini, G., Punta, E., & Zolezzi, T. (2007b). Approximability properties for second-order sliding mode control systems. *Automatic Control, IEEE Transactions on*, 52(10), 1813–1825.
- [Bartolini & Zolezzi, 1985] Bartolini, G. & Zolezzi, T. (1985). Variable structure systems nonlinear in the control law. *Automatic Control, IEEE Transactions on*, 30(7), 681–684.
- [Bauso et al., 2009] Bauso, D., Giarré, L., & Pesenti, R. (2009). Consensus for networks with unknown but bounded disturbances. *Siam Journal on Control and Optimization*, 48, 1756–1770.
- [Bejarano & Fridman, 2010] Bejarano, F. & Fridman, L. (2010). High order sliding mode observer for linear systems with unbounded unknown inputs. *International Journal of Control*, 83(9), 1920–1929.
- [Bejarano & Pisano, 2011] Bejarano, F. & Pisano, A. (2011). Switched observers for switched linear systems with unknown inputs. *Automatic Control, IEEE Transactions on*, (99), 1–1.
- [Bejarano et al., 2011] Bejarano, F., Pisano, A., & Usai, E. (2011). Finite-time converging jump observer for switched linear systems with unknown inputs. *Nonlinear Analysis: Hybrid Systems*, 5(2), 174–188.
- [Benbouzid & Kliman, 2003] Benbouzid, M. & Kliman, G. (2003). What stator current processing-based technique to use for induction motor rotor faults diagnosis? *Energy Conversion, IEEE Transactions on*, 18(2), 238–244.
- [Berman & Plemmons, 1979] Berman, A. & Plemmons, R. J. (1979). Nonnegative matrices. *The Mathematical Sciences, Classics in Applied Mathematics*, 9.
- [Bhatia, 1997] Bhatia, R. (1997). *Matrix analysis*, volume 169. Springer.
- [Biggs, 1993] Biggs, N. (1993). *Algebraic graph theory*. Cambridge University Press.
- [Bliman & Ferrari-Trecate, 2008] Bliman, P.-A. & Ferrari-Trecate, G. (2008). Average consensus problems in networks of agents with delayed communications. *Automatica*, 44(8), 1985–1995.
- [Boiko, 2003] Boiko, I. (2003). Analysis of sliding mode control systems in the frequency domain. In *American Control Conference, 2003. Proceedings of the 2003*, volume 1 (pp. 186–191).: IEEE.
- [Boiko, 2009] Boiko, I. (2009). *Discontinuous control systems: Frequency-domain analysis and design*. Springer.
- [Boiko et al., 2004] Boiko, I., Fridman, L., & Castellanos, M. (2004). Analysis of second-order sliding-mode algorithms in the frequency domain. *Automatic Control, IEEE Transactions on*, 49(6), 946–950.
- [Boiko et al., 2005] Boiko, I., Fridman, L., & Iriarte, R. (2005). Analysis of chattering in continuous sliding mode control. In *American Control Conference, 2005. Proceedings of the 2005* (pp. 2439–2444).: IEEE.

- [Boiko et al., 2006] Boiko, I., Fridman, L., Iriarte, R., Pisano, A., & Usai, E. (2006). Parameter tuning of second-order sliding mode controllers for linear plants with dynamic actuators. *Automatica*, 42(5), 833–839.
- [Boiko et al., 2008] Boiko, I., Fridman, L., Pisano, A., & Usai, E. (2008). A comprehensive analysis of chattering in second order sliding mode control systems. In *Modern Sliding Mode Control Theory* (pp. 23–49). Springer.
- [Boiko, 2011] Boiko, I. M. (2011). Dynamic harmonic balance and its application to analysis of convergence of second-order sliding mode control algorithms. In *American Control Conference (ACC), 2011* (pp. 208–213).: IEEE.
- [Bondarev & Utkin, 1985] Bondarev, A. G., B. S. A. K. N. Y. & Utkin, V. I. (1985). Sliding modes in systems with asymptotic state observers. *Automatica i telemechanica (Automation and Remote Control)*, 46(5), 679–684.
- [Bonnett & Albers, 2000a] Bonnett, A. & Albers, T. (2000a). Squirrel cage rotor options for ac induction motors. In *Pulp and Paper Industry Technical Conference, 2000. Conference Record of 2000 Annual* (pp. 54–67).: IEEE.
- [Bonnett & Albers, 2000b] Bonnett, A. & Albers, T. (2000b). Squirrel cage rotor options for ac induction motors. In *Pulp and Paper Industry Technical Conference, 2000. Conference Record of 2000 Annual* (pp. 54–67).: IEEE.
- [Bonnett & Soukup, 1986] Bonnett, A. & Soukup, G. (1986). Rotor failures in squirrel cage induction motors. *Industry Applications, IEEE Transactions on*, (6), 1165–1173.
- [Borkar & Varaiya, 1982] Borkar, V. & Varaiya, P. (1982). Asymptotic agreement in distributed estimation. *Automatic Control, IEEE Transactions on*, 27(3), 650–655.
- [Bullo et al., 2009] Bullo, F., Cortés, J., & Martinez, S. (2009). *Distributed control of robotic networks: a mathematical approach to motion coordination algorithms*. Princeton University Press.
- [Burton & Zinober, 1986] Burton, J. & Zinober, A. S. (1986). Continuous approximation of variable structure control. *International journal of systems science*, 17(6), 875–885.
- [Butkovskii, 1982] Butkovskii, A. G. (1982). *Greenšs functions and transfer functions handbook*. Halsted.
- [Cao & Ren, 2012] Cao, Y. & Ren, W. (2012). Finite-time consensus for second-order systems with unknown inherent nonlinear dynamics under an undirected switching graph. In *American Control Conference* (pp. 26–31).: IEEE.
- [Chang et al., 2003] Chang, C., Kuusilinna, K., Richards, B., & Brodersen, R. W. (2003). Implementation of bee: a real-time large-scale hardware emulation engine. In *Proceedings of the 2003 ACM/SIGDA eleventh international symposium on Field programmable gate arrays* (pp. 91–99).: ACM.
- [Chao et al., 2007] Chao, H., Chen, Y., & Ren, W. (2007). Consensus of information in distributed control of a diffusion process using centroidal voronoi tessellations. In *Decision and Control, 2007 46th IEEE Conference on* (pp. 1441–1446).: IEEE.
- [Chatterjee & Seneta, 1977] Chatterjee, S. & Seneta, E. (1977). Towards consensus: Some convergence theorems on repeated averaging. *Journal of Applied Probability*, (pp. 89–97).

- [Chua, 1998] Chua, L. O. (1998). *CNN: A paradigm for complexity*, volume 31. World Scientific.
- [Clarke, 1983] Clarke, F. (1983). *Optimization and Nonsmooth Analysis*. Wiley & Sons, New York.
- [Corless & Leitmann, 1981] Corless, M. & Leitmann, G. (1981). Continuous state feedback guaranteeing uniform ultimate boundedness for uncertain dynamic systems. *Automatic Control, IEEE Transactions on*, 26(5), 1139–1144.
- [Cortés, 2006a] Cortés, J. (2006a). Finite-time convergent gradient flows with applications to network consensus. *Automatica*, 42(11).
- [Cortés, 2006b] Cortés, J. (2006b). Finite-time convergent gradient flows with applications to network consensus. *Automatica*, 42(11), 1993–2000.
- [Cortés, 2008] Cortés, J. (2008). Discontinuous dynamical systems. *IEEE Control Systems Magazine*, 28(3), 36–73.
- [Curtain & Zwart, 1995] Curtain, R. F. & Zwart, H. (1995). *An introduction to infinite-dimensional linear systems theory*, volume 21. Springer.
- [Davila et al., 2009] Davila, J., Fridman, L., Pisano, A., & Usai, E. (2009). Finite-time state observation for non-linear uncertain systems via hoshm. *Int. Journal of Control*, 82(8), 1564–1574.
- [DeGroot, 1974] DeGroot, M. H. (1974). Reaching a consensus. *Journal of the American Statistical Association*, 69(345), 118–121.
- [Demetriou, 2009] Demetriou, M. A. (2009). Natural consensus filters for second order infinite dimensional systems. *Systems & Control Letters*, 58(12), 826–833.
- [Demetriou, 2010] Demetriou, M. A. (2010). Design of consensus and adaptive consensus filters for distributed parameter systems. *Automatica*, 46(2), 300–311.
- [Demetriou, 2012] Demetriou, M. A. (2012). Enforcing consensus on adaptive parameter estimation of structurally perturbed infinite dimensional systems.
- [Demetriou, 2013] Demetriou, M. A. (2013). Synchronization and consensus controllers for a class of parabolic distributed parameter systems. *Systems & Control Letters*, 62(1), 70–76.
- [Deshpande et al., 2011] Deshpande, P., Menon, P., Edwards, C., & Postlethwaite, I. (2011). Formation control of multi-agent systems with double integrator dynamics using delayed static output feedback. In *Decision and Control and European Control Conference (CDC-ECC), 2011 50th IEEE Conference on* (pp. 3446–3451).: IEEE.
- [Didier et al., 2006] Didier, G., Ternisien, E., Caspary, O., & Razik, H. (2006). Fault detection of broken rotor bars in induction motor using a global fault index. *Industry Applications, IEEE Transactions on*, 42(1), 79–88.
- [Dieci & Lopez, 2009] Dieci, L. & Lopez, L. (2009). Sliding motion in filippov differential systems: Theoretical results and a computational approach. *SIAM Journal on Numerical Analysis*, 47(3), 2023–2051.
- [Diestel, 1997] Diestel, R. (1997). *Graph theory, graduate texts in mathematics*, vol. 173.
- [Dorfler & Bullo, 2010] Dorfler, F. & Bullo, F. (2010). Synchronization and transient stability in power networks and non-uniform kuramoto oscillators. In *IEEE American Control Conference* (pp. 930–937).

- [Edwards & Menon, 2008] Edwards, C. & Menon, P. (2008). State reconstruction in complex networks using sliding mode observers. In *In Proc. of the CDC 2008* (pp. 2832–2837).: IEEE.
- [Edwards & Spurgeon, 1998] Edwards, C. & Spurgeon, S. (1998). *Sliding mode control: theory and applications*, volume 7. CRC.
- [Edwards et al., 2000] Edwards, C., Spurgeon, S., & Patton, R. (2000). Sliding mode observers for fault detection and isolation. *Automatica*, 36(4), 541–553.
- [El Hachemi Benbouzid, 2000] El Hachemi Benbouzid, M. (2000). A review of induction motors signature analysis as a medium for faults detection. *Industrial Electronics, IEEE Transactions on*, 47(5), 984–993.
- [Emelyanov, 1959] Emelyanov, S. (1959). Control of first order delay systems by means of an astatic controller and nonlinear corrections. *Proceedings of the IEEE*, 8(1), 983–991.
- [Erdős & Rényi, 1960] Erdős, P. & Rényi, A. (1960). *On the evolution of random graphs*. Akad. Kiadó.
- [Fadakar et al., 2013] Fadakar, I., Fidan, B., & Huissoon, J. (2013). Robust adaptive attitude synchronization of rigid body networks with unknown inertias. In *Control Conference (ASCC), 2013 9th Asian* (pp. 1–6).: IEEE.
- [Fax & Murray, 2004] Fax, J. A. & Murray, R. M. (2004). Information flow and cooperative control of vehicle formations. *IEEE Transactions on Automatic Control*, 49(9), 1465–1476.
- [Filippov,] Filippov, A. *Differential Equations with Discontinuous Righthand Sides: Control Systems*.
- [Filippov, 1960] Filippov, A. (1960). Differential equations with discontinuous righthand side. *Matematicheskii sbornik*, 93(1), 99–128.
- [Filippov, 1988] Filippov, A. (1988). *Differential Equations with Discontinuous Righthand Sides*. Kluwer Academic Publishers, Dordrecht (NLD).
- [Floquet et al., 2004] Floquet, T., Barbot, J., Perruquetti, W., & Djemai, M. (2004). On the robust fault detection via a sliding mode disturbance observer. *International Journal of control*, 77(7), 622–629.
- [Franceschelli et al., 2013a] Franceschelli, M., Giua, A., Pisano, A., & Usai, E. (2013a). Finite-time consensus for switching network topologies with disturbances. *Nonlinear Analysis: Hybrid Systems*, 10(1), 83–93.
- [Franceschelli et al., 2013b] Franceschelli, M., Pilloni, A., Pisano, A., Giua, A., & Usai, E. (2013b). Finite-time consensus with disturbance attenuation for directed switching network topologies by discontinuous local interactions. In *Decision and Control (CDC), 2013 IEEE 52nd Annual Conference on*: IEEE.
- [Franceschelli et al., 2012a] Franceschelli, M., Pisano, A., Giua, A., & Usai, E. (2012a). Finite-time consensus based clock synchronization by discontinuous control. In *4th IFAC Conference on Analysis and Design of Hybrid Systems*.
- [Franceschelli et al., 2012b] Franceschelli, M., Pisano, A., Giua, A., & Usai, E. (2012b). Finite-time consensus based clock synchronization by discontinuous control. In *Analysis and Design of Hybrid Systems, ADHS 2012. Proceedings. 4th IFAC Conference on* (pp. 172–177).
- [Frasca, 2012] Frasca, P. (2012). Continuous-time quantized consensus: Convergence of krasovskii solutions.

- Systems & Control Letters*, 61(2), 273 – 278.
- [Frew et al., 2005a] Frew, E. W., Dixon, C., Argrow, B., & Brown, T. (2005a). Radio source localization by a cooperating uav team. *Infotech@ Aerospace*, (pp. 1–11).
- [Frew et al., 2005b] Frew, E. W., Dixon, C., Argrow, B., & Brown, T. (2005b). Radio source localization by a cooperating uav team.
- [Fridman et al., 2007a] Fridman, L., Davila, J., & Levant, A. (2007a). High-order sliding-mode observation and fault detection. In *Decision and Control, 2007 46th IEEE Conference on* (pp. 4317–4322).: IEEE.
- [Fridman & Levant, 1996] Fridman, L. & Levant, A. (1996). Higher order sliding modes as a natural phenomenon in control theory. In *Robust control via variable structure and Lyapunov techniques* (pp. 107–133). Springer.
- [Fridman et al., 2007b] Fridman, L., Levant, A., & Davila, J. (2007b). Observation of linear systems with unknown inputs via high-order sliding-modes. *Int. Journal of Systems Science*, 38(10), 773–791.
- [Fridman et al., 2008] Fridman, L., Shtessel, Y., Edwards, C., & Yan, X.-G. (2008). Higher-order sliding-mode observer for state estimation and input reconstruction in nonlinear systems. *International Journal of Robust and Nonlinear Control*, 18(4-5), 399–412.
- [Fridman, 2003] Fridman, L. M. (2003). Chattering analysis in sliding mode systems with inertial sensors. *International Journal of Control*, 76(9-10), 906–912.
- [Galbusera et al., 2007] Galbusera, L., Marciandi, M. P. E., Bolzern, P., & Ferrari-Trecate, G. (2007). Control schemes based on the wave equation for consensus in multi-agent systems with double-integrator dynamics. In *Decision and Control, 2007 46th IEEE Conference on* (pp. 1498–1503).: IEEE.
- [Garin & Schenato, 2011] Garin, F. & Schenato, L. (2011). *Networked Control Systems*, volume 406 of *Lecture Notes in Control and Information Sciences*, chapter A survey on distributed estimation and control applications using linear consensus algorithms, (pp. 75–107). Springer.
- [Garulli & Giannitrapani, 2011] Garulli, A. & Giannitrapani, A. (2011). Analysis of consensus protocols with bounded measurement errors. *Systems & Control Letters*, 60(1), 44–52.
- [Gazi et al., 2007] Gazi, V., Fidan, B., Hanay, Y., & Köksal, M. (2007). Aggregation, foraging, and formation control of swarms with non-holonomic agents using potential functions and sliding mode techniques. *Turk J Elec Engin*, 15(2), 149–168.
- [Godsil et al., 2001] Godsil, C., Royle, G., & Godsil, C. (2001). *Algebraic graph theory*, volume 8. Springer New York.
- [Gonçalves et al., 2001] Gonçalves, J. M., Megretski, A., & Dahleh, M. A. (2001). Global stability of relay feedback systems. *Automatic Control, IEEE Transactions on*, 46(4), 550–562.
- [Hansen, 1998] Hansen, P. C. (1998). *Rank-deficient and discrete ill-posed problems: numerical aspects of linear inversion*, volume 4. Siam.
- [Hargrove et al., 2000] Hargrove, W. W., Gardner, R., Turner, M., Romme, W., & Despain, D. (2000). Simulating fire patterns in heterogeneous landscapes. *Ecological modelling*, 135(2), 243–263.

- [Hautus, 1983] Hautus, M. (1983). Strong detectability and observers. *Linear Algebra and its applications*, 50, 353–368.
- [Horn & Johnson, 1990] Horn, R. A. & Johnson, C. R. (1990). *Matrix analysis*. Cambridge university press.
- [Isidori, 1995] Isidori, A. (1995). *Nonlinear control systems*, volume 1. Springer Verlag.
- [Jadbabaie et al., 2003] Jadbabaie, A., Lin, J., & Morse, A. (2003). Coordination of groups of mobile autonomous agents using nearest neighbor rules. *IEEE Transactions on Automatic Control*, 48(6), 988–1001.
- [Jeong et al., 2000] Jeong, H., Tombor, B., Albert, R., Oltvai, Z. N., & Barabási, A.-L. (2000). The large-scale organization of metabolic networks. *Nature*, 407(6804), 651–654.
- [Khalil, 2002] Khalil, H. (2002). *Nonlinear Systems*. Prentice Hall.
- [Khoo et al., 2009] Khoo, S., Xie, L., & Man, Z. (2009). Robust finite-time consensus tracking algorithm for multirobot systems. *IEEE/ASME Transactions on Mechatronics*, 14(2), 219–228.
- [Kliman et al., 1988] Kliman, G., Koegl, R., Stein, J., Endicott, R., & Madden, M. (1988). Noninvasive detection of broken rotor bars in operating induction motors. *Energy Conversion, IEEE Transactions on*, 3(4), 873–879.
- [Krause & Thomas, 1965] Krause, P. & Thomas, C. (1965). Simulation of symmetrical induction machinery. *Power Apparatus and Systems, IEEE Transactions on*, 84(11), 1038–1053.
- [Krstic & Smyshlyaev, 2008] Krstic, M. & Smyshlyaev, A. (2008). *Boundary control of PDEs: A course on backstepping designs*, volume 16. SIAM.
- [Kryachkov et al., 2010] Kryachkov, M., Polyakov, A., & Strygin, V. (2010). Finite-time stabilization of an integrator chain using only signs of the state variables. In *Variable Structure Systems (VSS), 2010 11th International Workshop on* (pp. 510–515).: IEEE.
- [Kuramoto, 2003] Kuramoto, Y. (2003). *Chemical oscillations, waves, and turbulence*. Courier Dover Publications.
- [La et al., 2000] La, K., Shin, M., & Hyun, D. (2000). Direct torque control of induction motor with reduction of torque ripple. In *Industrial Electronics Society, 2000. IECON 2000. 26th Annual Conference of the IEEE*, volume 2 (pp. 1087–1092).: IEEE.
- [Lago-Fernández et al., 2000] Lago-Fernández, L. F., Huerta, R., Corbacho, F., & Sigüenza, J. A. (2000). Fast response and temporal coherent oscillations in small-world networks. *Physical Review Letters*, 84(12), 2758.
- [Lee & Utkin, 2007] Lee, H. & Utkin, V. I. (2007). Chattering suppression methods in sliding mode control systems. *Annual Reviews in Control*, 31(2), 179–188.
- [Levaggi, 2002] Levaggi, L. (2002). Sliding modes in banach spaces. *Differential and Integral Equations*, 15(2), 167–189.
- [Levaggi & Villa, 2007] Levaggi, L. & Villa, S. (2007). On the regularization of sliding modes. *SIAM Journal on Optimization*, 18(3), 878–894.
- [Levant, 1993a] Levant, A. (1993a). Sliding order and sliding accuracy in sliding mode control. *International journal of control*, 58(6), 1247–1263.
- [Levant, 1993b] Levant, A. (1993b). Sliding order and sliding accuracy in sliding mode control. *International journal of control*, 58(6), 1247–1263.

- [Levant, 1998] Levant, A. (1998). Robust exact differentiation via sliding mode technique. *Automatica*, 34(3), 379–384.
- [Levant, 2003] Levant, A. (2003). Higher-order sliding modes, differentiation and output-feedback control. *International journal of Control*, 76(9-10), 924–941.
- [Levant, 2005] Levant, A. (2005). Quasi-continuous high-order sliding-mode controllers. *Aut. Contr., IEEE Transaction on*, 50(11).
- [Levant & Fridman, 2010] Levant, A. & Fridman, L. M. (2010). Accuracy of homogeneous sliding modes in the presence of fast actuators. *Automatic Control, IEEE Transactions on*, 55(3), 810–814.
- [Li & Chen, 2003] Li, X. & Chen, G. (2003). Synchronization and desynchronization of complex dynamical networks: an engineering viewpoint. *Circuits and Systems I: Fundamental Theory and Applications, IEEE Transactions on*, 50(11), 1381–1390.
- [Li et al., 2013] Li, Z., Liu, X., Ren, W., & Xie, L. (2013). Distributed tracking control for linear multiagent systems with a leader of bounded unknown input. *IEEE Transactions on Automatic Control*, 58(2), 518–523.
- [Lin, 2006] Lin, Z. (2006). *Coupled dynamic systems: from structure towards stability and stabilizability*. PhD thesis, University of Toronto.
- [Lin et al., 2004] Lin, Z., Broucke, M., & Francis, B. (2004). Local control strategies for groups of mobile autonomous agents. *Automatic Control, IEEE Transactions on*, 49(4), 622–629.
- [Marino et al., 1993] Marino, R., Peresada, S., & Valigi, P. (1993). Adaptive input-output linearizing control of induction motors. *Automatic Control, IEEE Transactions on*, 38(2), 208–221.
- [Menon & Edwards, 2010] Menon, P. & Edwards, C. (2010). A discontinuous protocol design for finite-time average consensus. In *IEEE Conference on Control Applications* (pp. 2029–2034).
- [Molinari, 1976] Molinari, B. (1976). A strong controllability and observability in linear multivariable control. *Automatic Control, IEEE Transactions on*, 21(5), 761–764.
- [Newman et al., 2006] Newman, M., Barabasi, A., & Watts, D. (2006). *The structure and dynamics of networks*. Princeton Univ Pr.
- [Ni et al., 2013] Ni, W., Wang, X., & Xiong, C. (2013). Consensus controllability, observability and robust design for leader-following linear multi-agent systems. *Automatica*.
- [Oh & Khalil, 1997] Oh, S. & Khalil, H. K. (1997). Nonlinear output-feedback tracking using high-gain observer and variable structure control. *Automatica*, 33(10), 1845–1856.
- [Olfati-Saber et al., 2007] Olfati-Saber, R., Fax, J., & Murray, R. (2007). Consensus and cooperation in networked multi-agent systems. *Proceedings of the IEEE*, 95(1), 215–233.
- [Olfati-Saber & Murray, 2004] Olfati-Saber, R. & Murray, R. (2004). Consensus problems in networks of agents with switching topology and time-delays. *IEEE Transactions on Automatic Control*, 49(9), 1520–1533.
- [Olfati-Saber & Shamma, 2005] Olfati-Saber, R. & Shamma, J. S. (2005). Consensus filters for sensor networks and distributed sensor fusion. In *Proceedings of the 44th IEEE Conference on Decision and Control* (pp. 6698–6703).: IEEE.

- [Orani et al., 2010] Orani, N., Pisano, A., & Usai, E. (2010). Fault diagnosis for the vertical three-tank system via high-order sliding-mode observation. *Journal of the Franklin Institute*, 347(6), 923–939.
- [Orlov, 2004] Orlov, Y. (2004). Finite time stability and robust control synthesis of uncertain switched systems. *SIAM Journal on Control and Optimization*, 43(4), 1253–1271.
- [Orlov, 2008] Orlov, Y. (2008). *Discontinuous systems: Lyapunov analysis and robust synthesis under uncertainty conditions*. Springer.
- [Paden & Sastry, 1987] Paden, B. & Sastry, S. (1987). A calculus for computing filippov's differential inclusion with application to the variable structure control of robot manipulators. *IEEE Transactions on Circuits and Systems*, 34(1), 73–82.
- [Pereira, 2011] Pereira, T. (2011). Stability of Synchronized Motion in Complex Networks. *ArXiv e-prints*.
- [Petkovic M. & A., 2012] Petkovic M., Rapaić M., J. Z. & A., P. (2012). On-line adaptive clustering for process monitoring and fault detection. *Expert Systems With Applications*, 39(11), 10226–10235.
- [Pilloni et al., 2013a] Pilloni, A., Pisano, A., Edwards, C., & Menon, P. (2013a). Decentralized state estimation in connected systems. In *Proc. 5th IFAC Symposium on Systems, Structure and Control SSC 2013, Grenoble, France*.
- [Pilloni et al., 2013b] Pilloni, A., Pisano, A., Franceschelli, M., & Usai, E. (2013b). Finite-time consensus for a network of perturbed double integrators by second-order sliding mode technique. In *IEEE Conference on Decision and Control*.
- [Pilloni et al., 2014a] Pilloni, A., Pisano, A., Franceschelli, M., & Usai, E. (2014a). Distributed tracking for a network of perturbed double integrators by second-order sliding mode technique. *Under revision for submission on: Automatic Control, IEEE Transactions on*.
- [Pilloni et al., 2014b] Pilloni, A., Pisano, A., Orlov, Y., & Usai, E. (2014b). On boundary consensus protocol for a network of perturbed parabolic infinite dimensional processes. *Under revision for submission on: Automatic Control, IEEE Transactions on*.
- [Pilloni et al., 2013c] Pilloni, A., Pisano, A., Riera-Guasp, M., Puche-Panadero, R., & Pineda-Sanchez, M. (2013c). Chapter 14. fault detection in induction motors. *AC Electric Motors Control: Advanced Design Techniques and Applications*, (pp. 275–309).
- [Pilloni et al., 2012a] Pilloni, A., Pisano, A., & Usai, E. (2012a). Oscillation shaping in uncertain linear plants with nonlinear pi control: analysis and experimental results. In *Advances in PID Control (PID'12), Conference on: IFAC*.
- [Pilloni et al., 2012b] Pilloni, A., Pisano, A., & Usai, E. (2012b). Parameter tuning and chattering adjustment of super-twisting sliding mode control system for linear plants. In *Variable Structure Systems (VSS), 2012 12th International Workshop on* (pp. 479–484).: IEEE.
- [Pilloni et al., 2012c] Pilloni, A., Pisano, A., & Usai, E. (2012c). Robust fdi in induction motors via second order sliding mode technique. In *Variable Structure Systems (VSS), 2012 12th International Workshop on* (pp. 467–472).: IEEE.
- [Pilloni et al., 2014c] Pilloni, A., Pisano, A., & Usai, E. (2014c). Robust fdi in induction motors via second order sliding mode technique. In *Under revision for proceeding on: Variable Structure Systems*

- (VSS), 2014 13th International Workshop on: IEEE.
- [Pilloni et al., 2012d] Pilloni, A., Pisano, A., Usai, E., & Puche-Panadero, R. (2012d). Detection of rotor broken bar and eccentricity faults in induction motors via second order sliding mode observer. In *Decision and Control (CDC), 2012 IEEE 51st Annual Conference on* (pp. 7614–7619): IEEE.
- [Pillosu et al., 2011] Pillosu, S., Pisano, A., & Usai, E. (2011). Decentralised state estimation for linear systems with unknown inputs: a consensus-based approach. *Control Theory & App., IET*.
- [Pisano & Orlov, 2012] Pisano, A. & Orlov, Y. (2012). Boundary second-order sliding-mode control of an uncertain heat process with unbounded matched perturbation. *Automatica*, 48(8), 1768–1775.
- [Pisano & Usai, 2011] Pisano, A. & Usai, E. (2011). Sliding mode control: A survey with applications in math. *Mathematics and Computers in Simulation*, 81(5), 954–979.
- [Puche-Panadero et al., 2009] Puche-Panadero, R., Pineda-Sanchez, M., Riera-Guasp, M., Roger-Folch, J., Hurtado-Perez, E., & Perez-Cruz, J. (2009). Improved resolution of the mcsa method via hilbert transform, enabling the diagnosis of rotor asymmetries at very low slip. *Energy Conversion, IEEE Transactions on*, 24(1), 52–59.
- [Rao & Ghose, 2011] Rao, S. & Ghose, D. (2011). Sliding mode control-based algorithms for consensus in connected swarms. *International Journal of Control*, 84(9), 1477–1490.
- [Raudys & Mitasiunas, 2007] Raudys, S. & Mitasiunas, A. (2007). Multi-agent system approach to react to sudden environmental changes. In *Machine Learning and Data Mining in Pattern Recognition* (pp. 810–823). Springer.
- [Ren, 2007] Ren, W. (2007). Consensus strategies for cooperative control of vehicle formations. *Control Theory & Applications, IET*, 1(2), 505–512.
- [Ren, 2008] Ren, W. (2008). On consensus algorithms for double-integrator dynamics. *IEEE Transactions on Automatic Control*, 53(6), 1503–1509.
- [Ren, 2009] Ren, W. (2009). Distributed leaderless consensus algorithms for networked euler–lagrange systems. *International Journal of Control*, 82(11), 2137–2149.
- [Ren & Atkins, 2007] Ren, W. & Atkins, E. (2007). Distributed multi-vehicle coordinated control via local information exchange. *International Journal of Robust and Nonlinear Control*, 17(10-11), 1002–1033.
- [Ren & Beard, 2005] Ren, W. & Beard, R. (2005). Consensus seeking in multiagent systems under dynamically changing interaction topologies. *IEEE Transactions on Automatic Control*, 50(5), 655–661.
- [Ren & Beard, 2008] Ren, W. & Beard, R. (2008). *Distributed consensus in multi-vehicle cooperative control: theory and applications*.
- [Ren et al., 2007a] Ren, W., Beard, R. W., & Atkins, E. M. (2007a). Information consensus in multivehicle cooperative control. *Control Systems, IEEE*, 27(2), 71–82.
- [Ren et al., 2007b] Ren, W., Moore, K. L., & Chen, Y. (2007b). High-order and model reference consensus algorithms in cooperative control of multivehicle systems. *TRANSACTIONS-AMERICAN SOCIETY OF MECHANICAL ENGINEERS JOURNAL OF DYNAMIC SYSTEMS MEASUREMENT AND CONTROL*, 129(5), 678.

- [Reynolds, 1987] Reynolds, C. (1987). Flocks, herds and schools: A distributed behavioral model. In *ACM SIGGRAPH Computer Graphics*, volume 21 (pp. 25–34).
- [Rosenfeld, 2013] Rosenfeld, S. (2013). Global consensus theorem and self-organized criticality: Unifying principles for understanding self-organization, swarm intelligence and mechanisms of carcinogenesis. *Gene regulation and systems biology*, 7, 23.
- [Roy et al., 2004] Roy, S., Saberi, A., & Herlugson, K. (2004). Formation and alignment of distributed sensing agents with double-integrator dynamics and actuator saturation. *Sensor Network Applications*.
- [Schenato & Fiorentin, 2009] Schenato, L. & Fiorentin, F. (2009). Average timesync: A consensus-based protocol for time synchronization in wireless sensor networks. In *Estimation and Control of Networked Systems*, volume 1 (pp. 30–35).
- [Shevitz & Paden, 1994] Shevitz, D. & Paden, B. (1994). Lyapunov stability theory of nonsmooth systems. *IEEE Transactions on Automatic Control*, 39(9), 1910–1914.
- [Shtessel & Lee, 1996] Shtessel, Y. B. & Lee, Y.-J. (1996). New approach to chattering analysis in systems with sliding modes. In *Decision and Control, 1996., Proceedings of the 35th IEEE*, volume 4 (pp. 4014–4019).: IEEE.
- [Siganos et al., 2003] Siganos, G., Faloutsos, M., Faloutsos, P., & Faloutsos, C. (2003). Power laws and the as-level internet topology. *IEEE/ACM Transactions on Networking (TON)*, 11(4), 514–524.
- [Šiljak, 1991] Šiljak, D. (1991). *Decentralized Control of Complex Systems*, volume 184 of *Mathematics in Science and Engineering Series*. Acad. Press.
- [Simani et al., 2003] Simani, S., Fantuzzi, C., & Patton, R. (2003). Model-based fault diagnosis in dynamic systems using identification techniques. *Recherche*, 67, 02.
- [Sira-Ramírez, 1993] Sira-Ramírez, H. (1993). On the dynamical sliding mode control of nonlinear systems. *International Journal of Control*, 57(5), 1039–1061.
- [Slotine et al., 1991] Slotine, J.-J. E., Li, W., et al. (1991). *Applied nonlinear control*, volume 199. Prentice hall New Jersey.
- [Spurgeon, 2008] Spurgeon, S. K. (2008). Sliding mode observers: a survey. *International Journal of Systems Science*, 39(8), 751–764.
- [Stankovic et al., 2009] Stankovic, S., Stankovic, M., & Stipanovic, D. (2009). Consensus based overlapping decentralized estimator. *Automatic Control, IEEE Transactions on*, 54(2), 410–415.
- [Stankovic et al., 2011] Stankovic, S. S., Stankovic, M. S., & Stipanovic, D. M. (2011). Decentralized parameter estimation by consensus based stochastic approximation. *Automatic Control, IEEE Transactions on*, 56(3), 531–543.
- [Suykens et al., 1999] Suykens, J. A. K., Curran, P. F., & Chua, L. O. (1999). Robust synthesis for master-slave synchronization of lur'e systems. *IEEE Trans. on Circuits and Systems-I*, 46(7), 841–850.
- [Thomson & Fenger, 2001] Thomson, W. & Fenger, M. (2001). Current signature analysis to detect induction motor faults. *Industry Applications Magazine, IEEE*, 7(4), 26–34.
- [Toner & Tu, 1998] Toner, J. & Tu, Y. (1998). Flocks, herds, and schools: A quantitative theory of flocking. *Physical Review E*, 58(4), 4828.

- [Trentelman et al., 2001] Trentelman, H., Stoorvogel, A., & Hautus, M. (2001). *Control theory for linear systems*. Springer Verlag.
- [Tricaud & Chen, 2009] Tricaud, C. & Chen, Y. (2009). Optimal mobile actuator/sensor network motion strategy for parameter estimation in a class of cyber physical systems. In *American Control Conference, 2009. ACC'09*. (pp. 367–372).: IEEE.
- [Tsypkin, 1984] Tsypkin, Y. Z. (1984). *Relay control systems*. CUP Archive.
- [Utkin, 1977] Utkin, V. (1977). Variable structure systems with sliding modes. *Automatic Control, IEEE Transactions on*, 22(2), 212–222.
- [Utkin, 1992] Utkin, V. (1992). *Sliding modes in control and optimization*. Springer-Verlag Berlin.
- [Utkin & Guldner, 1999] Utkin, V. & Guldner, J. (1999). *Sliding mode control in electromechanical systems*. Taylor and Francis.
- [Vander Velde, 1968] Vander Velde, W. E. (1968). *Multiple-input describing functions and nonlinear system design*. New York: McGraw-Hill.
- [Wang & Xiao, 2010] Wang, L. & Xiao, F. (2010). Finite-time consensus problems for networks of dynamic agents. *IEEE Transactions on Automatic Control*, 55(4), 950–955.
- [Wang & Chen, 2002a] Wang, X. & Chen, G. (2002a). Pinning control of scale-free dynamical networks. *Physica A: Statistical Mechanics and its Applications*, 310(3), 521–531.
- [Wang & Hong, 2010] Wang, X. & Hong, Y. (2010). Distributed finite-time χ -consensus algorithms for multi-agent systems with variable coupling topology. *Journal of Systems Science and Complexity*, 23(2), 209–218.
- [Wang & Chen, 2002b] Wang, X. F. & Chen, G. (2002b). Synchronization in scale-free dynamical networks: robustness and fragility. *Circuits and Systems I: Fundamental Theory and Applications, IEEE Transactions on*, 49(1), 54–62.
- [Wang & Chen, 2003] Wang, X. F. & Chen, G. (2003). Complex networks: small-world, scale-free and beyond. *Circuits and Systems Magazine, IEEE*, 3(1), 6–20.
- [Wang & Wen, 2008] Wang, Y.-W. & Wen, C. (2008). A survey on pinning control of complex dynamical networks. In *Control, Automation, Robotics and Vision, 2008. ICARCV 2008. 10th International Conference on* (pp. 64–67).: IEEE.
- [Warshall, 1962] Warshall, S. (1962). A theorem on boolean matrices. *Journal of the ACM (JACM)*, 9(1), 11–12.
- [Wasserman, 1994] Wasserman, S. (1994). *Social network analysis: Methods and applications*, volume 8. Cambridge university press.
- [Watts & Strogatz, 1998] Watts, D. & Strogatz, S. (1998). Collective dynamics of 'small-world' networks. *nature*, 393(6684), 440–442.
- [Wu, 2007] Wu, C. (2007). *Synchronization in complex networks of nonlinear dynamical systems*. World Scientific Pub Co Inc.
- [Wu, 2008] Wu, C. W. (2008). Localization of effective pinning control in complex networks of dynamical systems. In *Circuits and Systems, 2008. ISCAS 2008. IEEE International Symposium on* (pp. 2530–2533).: IEEE.
- [Xie & Wang, 2007] Xie, G. & Wang, L. (2007). Consensus control for a class of networks of dynamic agents. *International Journal of Robust and Nonlinear Control*, 17(10-11), 941–959.

- [Yan et al., 2006] Yan, J., Hung, M., Chiang, T., & Yang, Y. (2006). Robust synchronization of chaotic systems via adaptive sliding mode control. *Physics letters A*, 356(3), 220–225.
- [Yang et al., 2003] Yang, R., Welch, G., & Bishop, G. (2003). Real-time consensus-based scene reconstruction using commodity graphics hardware. In *Computer Graphics Forum*, volume 22 (pp. 207–216).: Wiley Online Library.
- [Youb & Craciunescu, 2007] Youb, L. & Craciunescu, A. (2007). A comparison of various strategies for direct torque control of induction motors. In *Electrical Machines and Power Electronics, 2007. ACEMP'07. International Aegean Conference on* (pp. 403–408).: IEEE.
- [Young et al., 1996] Young, K. D., Utkin, V. I., & Ozguner, U. (1996). A control engineer's guide to sliding mode control. In *Variable Structure Systems, 1996. VSS'96. Proceedings., 1996 IEEE International Workshop on* (pp. 1–14).: IEEE.
- [Yu et al., 2010] Yu, W., Chen, G., & Cao, M. (2010). Some necessary and sufficient conditions for second-order consensus in multi-agent dynamical systems. *Automatica*, 46(6), 1089–1095.
- [Zampieri, 2008] Zampieri, S. (2008). Trends in networked control systems. In *17th IFAC World Congress* (pp. 2886–2894).